2010-11-09

Effectiveness of Compacted Fill and Rammed Aggregate Piers for Increasing Lateral Resistance of Pile Foundations

Nathan A. Lemme
Brigham Young University - Provo

Effectiveness of Compacted Fill and Rammed Aggregate Piers for Increasing Lateral Resistance of Pile Foundations

Nathan A. Lemme

A thesis submitted to the faculty of
Brigham Young University
in partial fulfillment of the requirements for the degree of

Master of Science

Kyle M. Rollins, Chair
Travis M. Gerber
Norman L. Jones

Department of Civil and Environmental Engineering

Brigham Young University

December 2010

ABSTRACT

Effectiveness of Compacted Fill and Rammed Aggregate Piers for

Increasing Lateral Resistance of Pile Foundations

Nathan A. Lemme

Department of Civil and Environmental Engineering

Master of Science

Compacted fill and rammed aggregate piers (RAPs) were separately installed adjacent to a 9-ft by 9-ft by 2.5-ft driven pile foundation founded in soft clay. The compacted fill used to laterally reinforce an area of 11 ft by 5 ft by 6 ft deep adjacent to the pile cap was clean concrete sand. The thirty-inch diameter RAPs were installed in three staggered rows to a depth of 12.5 ft below the ground surface adjacent to the pile cap to test the increase in lateral resistance afforded by their installation. The foundation was laterally loaded and load, displacement, and strain readings were recorded. The results of this testing were compared with similar tests performed with virgin soil conditions. The total lateral capacity of the pile foundation increased by 5 percent or14 kips due to compacted fill placement against the face of the pile cap. The passive force acting only on the pile cap decreased from 54 kips in the virgin case to 30 kips after installation of the compacted fill, a decrease of about 45 percent. The total lateral capacity of the pile foundation that was retrofit with RAPs was increased by 18 percent or 52 kips as compared to an identical pile cap in virgin clay. The passive force acting on the pile cap at 1.5 inches of pile cap displacement was determined to be approximately 50 kips, showing a slight decrease in passive resistance as compared to the tests performed on virgin soil. Both reinforcement techniques reduced pile head rotation and the bending moments in the shallow portions of the piles.

Keywords: Nathan Lemme, lateral, pile group, compacted fill, rammed aggregate pier, ground improvement, soil, reinforcement

ACKNOWLEDGMENTS

I wish to thank Dr. Kyle M. Rollins for allowing me the opportunity to be involved in such a ground-breaking project, and for all of his technical expertise and assistance. I could not have completed this incredible undertaking without the help, expertise, and mentoring of Dr. Travis M. Gerber, for which I am deeply grateful. Thanks to Dr. Norman L. Jones as well. I would also like to acknowledge the financial contributions of the National Cooperative Highway Research Program (NCHRP) and the donation of time and services provided by Geopier, Inc. I could not have accomplished any of this without the help of my fellow students, Matthew Adsero and Mark Herbst. My wife, Karissa, was a great support and motivator throughout the entire process of research and analysis. I would also like to mention Dave Anderson, Luke Heiner, Rodney Mayo, Dustin Minor, and Dave Halgren who from a construction and testing standpoint, made the project happen.

TABLE OF CONTENTS

LIST OF TABLES ..... **ix**

LIST OF FIGURES ..... **xi**

1 Introduction **1**

1.1 Project Objectives 3

1.2 Scope of Investigation 4

2 Literature Review **7**

2.1 Excavation and Replacement with Compacted Imported Natural Soil Backfill 7

2.2 Rammed Aggregate Piers 15

3 Geotechnical Site Characterization **21**

3.1 Field Investigations 21

3.2 Soil Profile, Classifications, and Shear Strengths 21

3.3 Cone Penetration and Seismic Cone Testing 25

4 Test Layout and Procedure **33**

4.1 Construction, Layout, and Materials 33

4.2 Actuator Layout 39

4.3 Instrumentation 41

4.4 Test Procedure 44

5 Soil Improvement Installation Procedures **47**

5.1 Compacted Fill Installation Procedure 47

5.2 RAP Installation Procedure 50

6 Test Results Introduction **59**

6.1 Baseline Selection and Test Numbering 60

6.2 Bending Moment Curve Construction 61

7 Virgin Clay Test Results 67

7.1 Virgin Clay – Test 1 67

7.1.1 Load versus Pile Cap Displacement 69

7.1.2 Pile Head Rotation versus Load 72

7.1.3 Pile Deflection versus Depth 74

7.1.4 Pile Bending Moment versus Depth 79

7.1.5 Moment versus Load Results 86

7.2 Virgin Clay without Passive Resistance – Test 2 91

7.2.1 Load versus Pile Cap Displacement 91

7.2.2 Load versus Pile Head Rotation 95

7.2.3 Pile Deflection versus Depth 96

7.2.4 Pile Bending Moment versus Depth 98

7.2.5 Moment versus Load Results 106

8 Compacted Fill Test Results 107

8.1 Virgin Clay Underlain with Compacted Fill – Test 5 107

8.1.1 Load versus Pile Cap Displacement 109

8.1.2 Load versus Pile Head Rotation 111

8.1.3 Pile Deflection versus Depth 112

8.1.4 Pile Bending Moment versus Depth 114

8.1.5 Moment versus Load Results 118

8.2 Compacted Fill Without Passive Resistance – Test 3 119

8.2.1 Load versus Pile Cap Displacement 122

8.2.2 Load versus Pile Head Rotation 125

8.2.3 Pile Deflection versus Depth 126

8.2.1 Pile Bending Moment versus Depth 126

8.2.2 Moment versus Load Results....132
8.3 Compacted Fill – Test 4....135
8.3.1 Load versus Pile Cap Displacement....136
8.3.2 Load versus Pile Head Rotation....136
8.3.3 Pile Deflection versus Depth....140
8.3.4 Pile Bending Moment versus Depth....142
8.3.5 Moment versus Load Results....145
9 RAP Test Results....149
9.1 RAPs – Test 6....149
9.1.1 Load versus Pile Cap Displacement....151
9.1.2 Load versus Pile Head Rotation....153
9.1.3 Pile Deflection versus Depth....154
9.1.4 Pile Bending Moment versus Depth....155
9.1.5 Moment versus Load Results....162
9.2 RAPs without Passive Resistance – Test 7....162
9.2.1 Load versus Pile Cap Displacement....164
9.2.2 Load versus Pile Head Rotation....166
9.2.3 Pile Deflection versus Depth....167
9.2.4 Pile Bending Moment versus Depth....169
9.2.1 Moment versus Load Results....172
10 Test Comparisons....177
10.1 Virgin Test Comparisons....177
10.1.1 Pile Head Load versus Displacement....178
10.1.2 Load versus Pile Head Rotation Comparison....180
10.1.3 Moment versus Load Comparisons....181

10.2 Compacted Fill Test Comparisons 184
10.2.1 Load versus Pile Head Rotation Comparison 189
10.2.2 Moment versus Load Comparisons 192
10.3 Rammed Aggregate Piers Comparisons 196
10.3.1 Load versus Pile Cap Displacement Comparisons 196
10.3.2 Load versus Pile Head Rotation Comparison 201
10.3.3 Moment versus Load Comparisons 202
10.4 Cost Comparisons 206
11 Conclusions 211
References 215
Appendix A Corbel Design 217
A.1 Corbel Specifications and Design Values 217
Appendix B PYCAP analysis of Compacted Fill 221

LIST OF TABLES

Table 3-1 Summary of laboratory results 25

Table 3-2 Seismic site class definitions from the IBC 2006 code 28

Table 5-1 Nuclear density gauge test results for compacted fill in front of cap 4 49

Table 10-1 Summary of ultimate passive resistance from clay adjacent to the pile cap assuming variable undrained shear strength 188

Table 10-2 Summary of costs associated with retrofitting the existing foundation in this project with compacted fill 207

Table 10-3 Summary of costs associated with retrofitting the existing foundation in this project with Rammed Aggregate Piers 208

Table 10-4 Summary of costs associated with structurally retrofitting the existing foundation for this project to achieve a comparable strength gain with compacted fill or RAPs 209

Table 11-1 Summary of maximum resistance results and quantified improvements 211

LIST OF FIGURES

Figure 2-1 Pile group interaction effect 8

Figure 2-2 Load versus deflection curves for 9 pile group in stiff clay and dense sand based on Brown et al (1987) (1988) 11

Figure 2-3 Load versus deflection curves for 15 pile group in medium stiff clay and dense sand based on Rollins et al (2005) and Walsh (2005) 11

Figure 2-4 Comparison of passive force provided by stiff partially saturated clay and compacted sandy gravel against 1.1m deep x 1.9 m wide cap block (Mokwa and Duncan 2001) 12

Figure 2-5 Measured passive force versus deflection relationships for two full-scale tests with silty sand compacted to 88 percent and 98 percent of the modified Proctor maximum unit weight (Rollins, Kwon, and Gerber 2008) 13

Figure 2-6 Passive force versus deflection curves for loose silty sand against a 17 ft wide by 3.67 ft high pile cap and after excavation and replacement with 3 ft and 6 ft zones of compacted gravel backfill against the cap (Rollins, Kwon, and Gerber 2008) 14

Figure 2-7 Plan view of crack patterns behind a pile cap after excavation and replacement of loose silty sand with (a) a 3-ft and (b) a 6-ft zone of compacted sandy gravel behind the pile cap (Rollins, Kwon, and Gerber 2008) 14

Figure 2-8 Plan view of “improvement areas” around abutments at a bridge site on the Legacy Parkway project north of Salt Lake City, Utah (Higbee 2007) 15

Figure 2-9 RAP installation process (Fitzpatrick 2002) 16

Figure 2-10 Typical RAP installation (Fitzpatrick 2002) 17

Figure 2-11 I-15 lateral load test schematic (*Figure courtesy of Evert Lawton)* 18

Figure 3-1 Aerial view of the test site and surrounding area 22

Figure 3-2 Plan view showing location of boring, CPT soundings relative to pile caps 23

Figure 3-3 Plot of (a) soil profile, (b) Atterberg limits and natural water content versus depth, and (c) undrained shear strength versus depth 27

Figure 3-4 Plot of (a) soil profile, (b) cone tip resistance versus depth, (c) friction ratio versus depth, and (d) pore pressure versus depth curves from cone penetration test (CPT) sounding 2 near the center of the site 30

Figure 3-5 Plot (a) soil profile, (b) cone tip resistance versus depth, (c) friction ratio versus depth and, (d) pore pressure versus depth from all four cone penetration test (CPT) soundings 31

Figure 3-6 Plot of (a) soil profile, (b) cone tip resistance versus depth, and (c) shear wave velocity versus depth from seismic cone testing.....32

Figure 4-1 Plan and profile drawings of pile caps 1 and 2 during Test 1 35

Figure 4-2 Three by three driven pile group, all 3ft OC in both directions (strain gauge instrumented piles circled with dotted line).....36

Figure 4-3 Driven pile layout prior to cap construction 37

Figure 4-4 Cross-section of piles within the pile groups 37

Figure 4-5 Bottom reinforcing mat layout for the test pile groups 38

Figure 4-6 Top reinforcing mat layout for the test pile groups.....38

Figure 4-7 Corbel steel layout for caps 1 and 4. 40

Figure 4-8 Corbel steel layout for caps 2 and 3. 40

Figure 4-9 Photo of actuator setup between caps 1 & 2 41

Figure 4-10 Typical instrumentation layout for pile caps with (a) a partial length and (b) a full length corbel 43

Figure 5-1 Compaction of fill under future pile cap 4 using a hydraulic plate compactor attached to the arm of a track hoe 48

Figure 5-2 Grain size distribution curve including upper and lower limits (Walsh 2005) 48

Figure 5-3 Passive resistance region of compacted sand fill being compacted.....50

Figure 5-4 RAP installation configuration.....53

Figure 5-5 Plan and profile of compacted fill treated area for Test 3 (diagonal hatching).....51

Figure 5-6 Plan and profile of compacted fill treated area for Tests 4 & 5 (diagonal hatching and spotted hatch) 52

Figure 5-7 Excavation for RAP installation.....54

Figure 5-8 Ramming of base material into bottom of excavated RAP hole 54

Figure 5-9 Placement of 1 ft lift for compaction of main body of RAP 56

Figure 5-10 Quality control table for RAPs....56

Figure 5-11 Photos of excavating of top layer of RAPs and of the excavation showing the difference between the clay and the material from the RAPs....57

Figure 5-12 Plan and profile for Tests 6 and 7 on RAPs: diamond hatching representing RAPs and dashed line representing soil excavated for Test 7 55

Figure 5-13 Photo of finished excavation with the RAP columns highlighted 57

Figure 7-1 Schematic plan view of Test 1 68

Figure 7-2 Plot of continuous pile cap displacement versus applied load for pile cap 1 during the virgin clay test (Test 1)....70

Figure 7-3 Plot of continuous pile cap displacement versus applied load for pile cap 2 during the virgin clay test (Test 1)....70

Figure 7-4 Plot of pile cap displacement versus peak applied load for each increment of the virgin clay test (Test 1) 71

Figure 7-5 Peak pile cap load versus pile head rotation for pile cap 1 during the virgin clay test (Test 1) obtained from string potentiometer and shape array measurements....73

Figure 7-6 Peak pile cap load versus pile head rotation for pile cap 2 during the virgin clay test (Test 1) obtained from string potentiometer and shape array measurements....73

Figure 7-7 Deflection versus depth curves for pile cap 1 for each increment of the virgin clay test (Test 1), with pile head displacements from the string potentiometers also shown 75

Figure 7-8 Deflection versus depth curves for pile cap 2 for each increment of the virgin clay test (Test 1), with pile head displacements from the string potentiometers also shown 76

Figure 7-9 Comparison of depth versus deflection curves for the piles in pile cap 1 from the north and south inclinometers, and shape array 104 and shape array 106 in the virgin clay test (Test 1)....78

Figure 7-10 Comparison of depth versus deflection curves for the piles in pile cap 2 from the north and south inclinometers, and shape array 115 and shape array 134 in the virgin clay test (Test 1) 79

Figure 7-11 Moment versus depth curve for the middle center pile of pile cap 1 (1-M) based on incremental deflection versus depth curves measured from shape array 104 during the virgin clay test (Test 1), with point moments measured from strain gauges at various depths also shown 80

Figure 7-12 Moment versus depth curve for the north center pile of pile cap 1 (1-N) based on incremental deflection versus depth curves measured from shape array 106 during the virgin clay test (Test 1), with point moments measured from strain gauges at various depths also shown 81

Figure 7-13 Moment versus depth comparison for the piles in pile cap 2 based on deflections measured from the north and south inclinometers, shape array 104 and shape array 106 during the virgin clay test (Test 1).....82

Figure 7-14 Moment versus depth curve for the middle center pile of pile cap 1 (1-M) based on incremental deflection versus depth curves measured from shape array 104 during the virgin clay test (Test 1) 84

Figure 7-15 Moment versus depth curve for the north center pile of pile cap 2 (2-N) based on incremental deflection versus depth curves measured from shape array 134 during the virgin clay test (Test 1) with point moments measured from strain gauges at various depths also shown 84

Figure 7-16 Moment versus depth comparison for the piles in pile cap 2 based on deflections measured from the north and south inclinometers, shape array 104 and shape array 134 during the virgin clay test (Test 1).....85

Figure 7-17 Maximum negative moment (base of cap) versus total pile cap load for piles (a) 1-N, (b) 1-M, and (c) 1-S in cap 1 during the virgin clay test (Test 1).....87

Figure 7-18 Maximum positive moment versus total pile cap load for piles (a) 1-N, (b) 1-M, and (c) 1-S in cap 1 during the virgin clay test (Test 1).....88

Figure 7-19 Maximum negative moment versus total pile cap load for piles (a) 2-N, (b) 2-M, and (c) 2-S in cap 2 during the virgin clay test (Test 1).....89

Figure 7-20 Maximum positive moment versus total pile cap load for piles (a) 2-N, (b) 2-M, and (c) 2-S in cap 2 during the virgin clay test (Test 1).....90

Figure 7-21 Schematic plan view of Test 2 92

Figure 7-22 Plot of continuous pile cap displacement versus applied load for pile cap 1 during Test 2 93

Figure 7-23 Plot of continuous pile cap displacement versus applied load for pile cap 2 during Test 2 94

Figure 7-24 Plot of pile cap displacement versus peak applied load for each increment of the virgin clay test after excavation (Test 2).....94

Figure 7-25 Peak pile cap load versus pile head rotation for cap 1 during the virgin clay test after excavation (Test 2) obtained from string potentiometer and shape array measurements.....95

Figure 7-26 Peak pile cap load versus pile head rotation for pile cap 2 during the virgin clay test after excavation (Test 2) obtained from string potentiometer and shape array measurements 96

Figure 7-27 Comparison of depth versus deflection curves for the piles in pile cap 1 from the north and south inclinometers, and shape array 104 and shape array 106 in the virgin clay test after excavation (Test 2) 97

Figure 7-28 Deflection versus depth curves for pile cap 1 for each increment of the virgin clay test after excavation (Test 2), with pile head displacements from the string potentiometers also shown 97

Figure 7-29 Moment versus depth curve for the middle center pile of pile cap 1 (1-M) based on incremental deflection versus depth curves measured from shape array 104 during the virgin clay test after excavation (Test 2), with point moments measured from strain gauges at various depths also shown 98

Figure 7-30 Moment versus depth curve for the north center pile of pile cap 1 (1-N) based on incremental deflection versus depth curves measured from shape array 106 during the virgin clay test after excavation (Test 2), with point moments measured from strain gauges at various depths also shown 99

Figure 7-31 Moment versus depth comparison for the piles in pile cap 1 based on deflections measured from the north and south inclinometers, shape array 104 and shape array 106 during the virgin clay test after excavation (Test 2) 101

Figure 7-32 Maximum negative moment (base of cap) versus total pile cap load for piles (a) 1-N, (b) 1-M, and (c) 1-S in cap 1 during the virgin clay test after excavation (Test 2) 102

Figure 7-33 Maximum positive moment versus total pile cap load for piles (a) 1-N, (b) 1-M, and (c) 1-S in cap 1 during the virgin clay test after excavation (Test 2) 103

Figure 7-34 Maximum negative moment versus total pile cap load for piles (a) 2-N, (b) 2-M, and (c) 2-S in cap 2 during the virgin clay test (Test 2) 104

Figure 7-35 Maximum positive moment versus total pile cap load for piles (a) 2-N, (b) 2-M, and (c) 2-S in cap 2 during the virgin clay test (Test 2) 105

Figure 8-1 Schematic plan view of Test 5 (See Figure 5-6 for dimensions) 108

Figure 8-2 Plot of continuous pile cap displacement versus applied load for pile cap 4 during testing of compacted fill under the cap (Test 5) 110

Figure 8-3 Plot of pile cap displacement versus peak applied load for each increment of testing of compacted fill under the cap (Test 5) with the final displacement data from the compacted fill test (Test 4) 110

Figure 8-4 Peak pile cap load versus pile head rotation for cap 4 during testing of compacted fill under the cap (Test 5) obtained from string potentiometer and shape array measurements.....111

Figure 8-5 Comparison of depth versus deflection curves for the piles in pile cap 4 from the north inclinometer with shape array 104 and the north and south inclinometers with shape array 106 for testing of compacted fill under the cap (Test 5).....112

Figure 8-6 Deflection versus depth curves for pile cap 4 for each increment of testing of compacted fill under the cap (Test 5), with pile head displacements from the string potentiometers also shown.....113

Figure 8-7 Moment versus depth curve for the north center pile of pile cap 4 (4-N) based on incremental deflection versus depth curves measured from shape array 104 during testing of compacted fill under the cap (Test 5), with point moments measured from strain gauges at various depths also shown.....115

Figure 8-8 Moment versus depth curve for the center pile of pile cap 4 (4-M) based on incremental deflection versus depth curves measured from shape array 106 during testing of compacted fill under the cap (Test 5).....116

Figure 8-9 Moment versus depth curve for the south pile of pile cap 4 (4-S) based on incremental deflection versus depth curves measured from strain gauges during testing of compacted fill under the cap (Test 5).....117

Figure 8-10 Moment versus depth comparison for the piles in pile cap 4 based on deflections measured from the north and south inclinometers, shape array 104 and shape array 106 during testing of compacted fill under the cap (Test 5).....118

Figure 8-11 Maximum negative moment (base of cap) versus total pile cap load for piles (a) 4-N, (b) 4-M, and (c) 4-S in cap 4 during testing of compacted fill under the cap (Test 5).....120

Figure 8-12 Maximum positive moment versus total pile cap load for piles (a) 4-N, (b) 4-M, and (c) 4-S in cap 4 during testing of compacted fill under the cap (Test 5).....121

Figure 8-13 Schematic plan view of Test 3 (See Figure 5-5 for dimensions).....123

Figure 8-14 Plot of continuous pile cap displacement versus applied load for pile cap 4 during the compacted fill test with no soil adjacent to the cap (Test 3).....124

Figure 8-15 Plot of pile cap displacement versus peak applied load for each increment of the compacted fill test with no soil adjacent to the cap (Test 3).....124

Figure 8-16 Peak pile cap load versus pile head rotation for cap 4 during the compacted fill test with no soil adjacent to the cap (Test 3) obtained from string potentiometer and shape array measurements.....125

Figure 8-17 Comparison of depth versus deflection curves for the piles in pile cap 4 from the north inclinometer with shape array 104 and the north and south inclinometers with shape array 106 for the compacted fill test with no soil adjacent to the cap (Test 3).....127

Figure 8-18 Deflection versus depth curves for pile cap 4 for each increment of the compacted fill test with no soil adjacent to the cap (Test 3), with pile head displacements from the string potentiometers also shown.....127

Figure 8-19 Moment versus depth curve for the north center pile of pile cap 4 (4-N) based on incremental deflection versus depth curves measured from shape array 104 during the compacted fill test with no soil adjacent to the cap (Test 3), with point moments measured from strain gauges at various depths also shown (Dashed lines are extrapolations).....129

Figure 8-20 Moment versus depth curve for the center pile of pile cap 4 (4-M) based on incremental deflection versus depth curves measured from shape array 106 during the compacted fill test with no soil adjacent to the cap (Test 3).....129

Figure 8-21 Moment versus depth comparison for the piles in pile cap 4 based on deflections measured from the north and south inclinometers, shape array 104 and shape array 106 during the compacted fill test with no soil adjacent to the cap (Test 3) 130

Figure 8-22 Pile cap rotation and resulting loading mechanisms 131

Figure 8-23 Maximum negative moment (base of cap) versus total pile cap load for piles (a) 4-N, (b) 4-M, and (c) 4-S in cap 4 during the compacted fill test with no soil adjacent to the cap (Test 3) 133

Figure 8-24 Maximum positive moment versus total pile cap load for piles (a) 4-N, (b) 4-M, and (c) 4-S in cap 4 during the compacted fill test with no soil adjacent to the cap (Test 3) 134

Figure 8-25 Schematic plan view of Test 4 (See Figure 5-2 for dimensions) 137

Figure 8-26 Plot of continuous pile cap displacement versus applied load for pile cap 4 during the compacted fill test with compacted fill adjacent to the cap (Test 4) 138

Figure 8-27 Plot of pile cap displacement versus peak applied load for each increment of the compacted fill test with compacted fill adjacent to the cap (Test 4).....138

Figure 8-28 Peak pile cap load versus pile head rotation for cap 4 during the compacted fill test with compacted fill adjacent to the cap (Test 4) obtained from string potentiometer and shape array measurements.....139

Figure 8-29 Comparison of depth versus deflection curves for the piles in pile cap 4 from the north inclinometer with shape array 104 and the north and south inclinometers with shape array 106 for the compacted fill test with compacted fill adjacent to the cap (Test 4) 140

Figure 8-30 Deflection versus depth curves for pile cap 4 for each increment of the compacted fill test with compacted fill adjacent to the cap (Test 4), with pile head displacements from the string potentiometers also shown.....141

Figure 8-31 Moment versus depth curve for the north center pile of pile cap 4 (4-N) based on incremental deflection versus depth curves measured from shape array 104 during the compacted fill test with compacted fill adjacent to the cap (Test 4), with point moments measured from strain gauges at various depths also shown (Dashed extension lines are extrapolations) 142

Figure 8-32 Moment versus depth curve for the center pile of pile cap 4 (4-M) based on incremental deflection versus depth curves measured from shape array 106 during the compacted fill test with compacted fill adjacent to the cap (Test 4).....143

Figure 8-33 Moment versus depth comparison for the piles in pile cap 4 based on deflections measured from the north and south inclinometers, shape array 104 and shape array 106 during the compacted fill test with compacted fill adjacent to the cap (Test 4) 144

Figure 8-34 Maximum negative moment (base of cap) versus total pile cap load for piles (a) 4-N, (b) 4-M, and (c) 4-S in cap 4 during the compacted fill test with compacted fill adjacent to the cap (Test 4) 146

Figure 8-35 Maximum positive moment versus total pile cap load for piles (a) 4-N, (b) 4-M, and (c) 4-S in cap 1 during the compacted fill test with compacted fill adjacent to the cap (Test 4) 147

Figure 9-1 Schematic plan view of Test 6 150

Figure 9-2 Plot of continuous pile cap displacement versus applied load for pile cap 4 during the RAP test (Test 6) 152

Figure 9-3 Plot of pile cap displacement versus peak applied load for each increment of the RAP test (Test 6).....152

Figure 9-4 Peak pile cap load versus pile head rotation for cap 4 during the RAP test (Test 6) obtained from string potentiometer and shape array measurements 153

Figure 9-5 Comparison of depth versus deflection curves for the piles in pile cap 4 from the north inclinometer with shape array 104 and the north and south inclinometers for the RAP test (Test 6).....155

Figure 9-6 Deflection versus depth curves for pile cap 4 for each increment of the RAP test (Test 6), with pile head displacements from the string potentiometers also shown 156

Figure 9-7 Moment versus depth curve for the north center pile of pile cap 4 (4-N) based on incremental deflection versus depth curves measured from shape array 104 during the RAP test (Test 6), with point moments measured from strain gauges at various depths also shown....157

Figure 9-8 Moment versus depth curve for the south center pile of pile cap 4 (4-S) based on strain gauge readings at various depths for the RAP test (Test 6)....158

Figure 9-9 Moment versus depth comparison for the piles in pile cap 4 based on deflections measured from the north and south inclinometers and shape array 104 during the RAP test (Test 6)....159

Figure 9-10 Maximum negative moment (base of cap) versus total pile cap load for piles (a) 4-N, (b) 4-M, and (c) 4-S in cap 4 during the RAP test (Test 6)....160

Figure 9-11 Maximum positive moment versus total pile cap load for piles (a) 4-N, (b) 4-M, and (c) 4-S in cap 1 during the RAP test (Test 6)....161

Figure 9-12 Schematic plan view of Test 7....163

Figure 9-13 Plot of continuous pile cap displacement versus applied load for pile cap 4 during the RAP test after excavation (Test 7)....165

Figure 9-14 Plot of pile cap displacement versus peak applied load for each increment of the RAP test after excavation (Test 7)....165

Figure 9-15 Peak pile cap load versus pile head rotation for cap 4 during the RAP test after excavation (Test 7) obtained from string potentiometer and shape array measurements....167

Figure 9-16 Comparison of depth versus deflection curves for the piles in pile cap 4 from the north inclinometer with shape array 104 and the north and south inclinometers for the RAP test after excavation (Test 7)....168

Figure 9-17 Deflection versus depth curves for pile cap 4 for each increment of the RAP test after excavation (Test 7), with pile head displacements from the string potentiometers also shown....169

Figure 9-18 Moment versus depth curve for the north center pile of pile cap 4 (4-N) based on incremental deflection versus depth curves measured from shape array 104 during the RAP test after excavation (Test 7), with point moments measured from strain gauges at various depths also shown....170

Figure 9-19 Moment versus depth curve for the south center pile of pile cap 4 (4-S) based on strain gauge readings at various depths for the RAP test after excavation (Test 7)....171

Figure 9-20 Moment versus depth comparison for the piles in pile cap 4 based on deflections measured from the north and south inclinometers and shape array 104 during the RAP test after excavation (Test 7)....172

Figure 9-21 Maximum negative moment (base of cap) versus total pile cap load for piles (a) 4-N, (b) 4-M, and (c) 4-S in cap 4 during the RAP test after excavation (Test 7).....173

Figure 9-22 Maximum positive moment versus total pile cap load for piles (a) 4-N, (b) 4-M, and (c) 4-S in cap 1 during the RAP test after excavation (Test 7) 174

Figure 10-1 Comparison of peak pile cap load versus pile head displacement curves for pile caps 1 and 2 during virgin clay tests before (Test 1) and after excavation (Test 2). 178

Figure 10-2 Development of passive force for virgin clay around pile cap 1. 179

Figure 10-3 Load versus rotation curves for virgin clay tests before (Test 1) and after excavation (Test 2).....180

Figure 10-4 Selected maximum positive moment versus load plots from virgin clay tests (Tests 1 and 2) illustrating general trends experienced by pile cap 1. 182

Figure 10-5 Selected maximum negative moment versus load plots from virgin clay tests (Test 1 and 2) illustrating general trends experienced by pile cap 1.....182

Figure 10-6 Selected maximum negative moment versus load plots of pile cap 1 from the virgin clay tests (Tests 1 and 2) compared to pile cap 4 from the test with compacted fill under the cap (Test 5) illustrating general trends. 183

Figure 10-7 Selected maximum positive moment versus load plots of pile cap 1 from the virgin clay tests (Tests 1 and 2) compared to pile cap 4 from the test with compacted fill under the cap (Test 5) illustrating general trends. 183

Figure 10-8 Load displacement comparison of virgin clay and compacted fill under the pile cap with clay against the cap face.....184

Figure 10-9 Comparison of load-displacement curves for compacted sand extending 5 ft beyond the cap and native clay without soil against the cap face.....186

Figure 10-10 Comparison of load-displacement curves for pile cap 4 with and without fill adjacent to the pile cap. 187

Figure 10-11 Load versus rotation curves for virgin clay and a layer of compacted fill under the pile cap with clay against the pile cap face 190

Figure 10-12 Load versus rotation comparison for virgin clay and compacted fill with soil against the pile cap 191

Figure 10-13 Load versus rotation comparison of virgin clay and compacted fill without soil against the pile cap face 191

Figure 10-14 Selected load versus maximum negative moment comparisons for virgin clay and compacted fill against the pile cap face 192

Figure 10-15 Selected load versus maximum positive moment comparisons for virgin clay and compacted fill against the pile cap face 193

Figure 10-16 Selected load versus maximum negative moment comparisons for virgin clay and compacted fill without soil against the pile cap face 193

Figure 10-17 Selected load versus maximum positive moment comparisons for virgin clay and compacted fill without soil against the pile cap face 194

Figure 10-18 Selected load versus maximum negative moment comparisons for compacted fill with and without fill compacted against the face of the pile cap 195

Figure 10-19 Selected load versus maximum positive moment comparisons for compacted fill with and without fill compacted against the face of the pile cap 195

Figure 10-20 Load-Displacement comparison of virgin clay and RAP with soil against the pile cap face 197

Figure 10-21 Load-Displacement comparison of virgin clay and RAP without soil against the pile cap face.....198

Figure 10-22 Load-displacement comparison of virgin clay and RAP with soil against the pile cap face, also showing compacted fill against pile cap face.....199

Figure 10-23 Load-displacement comparison of virgin clay and RAP without soil against the pile cap face, also showing compacted fill against pile cap face.....199

Figure 10-24 Load-Displacement comparison of RAP with and without soil against the face of the pile cap, also showing virgin clay without clay against the pile cap face 200

Figure 10-25 Load versus rotation comparison of virgin clay and RAP with soil against the face of the pile cap 201

Figure 10-26 Load versus rotation comparison of virgin clay and RAP without soil against the face of the pile cap 202

Figure 10-27 Selected load versus maximum negative moment comparison for virgin clay and RAPs with soil against the pile cap face 203

Figure 10-28 Selected load versus maximum positive moment comparison for virgin clay and RAPs with soil against the pile cap face 203

Figure 10-29 Selected load versus maximum negative moment comparisons for virgin clay and RAPs after excavation of soil from against the pile cap face.....204

Figure 10-30 Selected load versus maximum positive moment comparisons for virgin clay and RAPs after excavation of soil from against the pile cap face.....204

Figure 10-31 Selected load versus maximum negative moment comparisons for RAPs before and after excavation of soil from the face of the pile cap 205

Figure 10-32 Selected load versus maximum positive moment comparisons for RAPs before and after excavation of soil from the face of the pile cap 206

Figure A-1 Front view of the corbel steel where the actuator would connect to the corbel 217

Figure A-2 The #9 bar main reinforcement for the corbel 218

Figure A-3 The transverse or hoop reinforcement for the corbel 219

Figure A-4 Corbel design calculated values using ACI section 11.9. 220

Figure B-1 PYCAP two-dimensional analysis summary for compacted fill 221

1 INTRODUCTION

The aging infrastructure of the United States Interstate system has come under increasing scrutiny, with many bridge structures being deemed structurally unsound. Many of the bridge structures associated with the interstate system were designed and built many years before seismicity and the associated design parameters were taken into consideration for bridge design. These bridges are in need of retrofits to meet current seismic code specifications. In the past, structural components were added to the foundations to improve lateral resistance, which improves the foundations' performance in the event of an earthquake. Recently, strengthening the soft soil surrounding the piles and pile cap, in lieu of structural retrofits, has been a suggested alternative to increase the lateral resistance of driven pile foundations at reduced cost.

Compacted fill has been widely used as a means of increasing the strength of foundation soils. However, most applications of this technique are designed to increase the axial bearing capacity of the treated soils prior to construction. In these applications, significant increases in both strength and stiffness have been observed. Compacting a competent fill in place of soft soil allows structures and embankments to be constructed over soft soils without slope stability failure and with reduced settlement.

Rammed Aggregate Piers (RAPs) (also known by the proprietary name of geopiers[1]) are a relatively new soil reinforcement technique which involves excavation of native soil and replacement with highly compacted competent aggregate. As with compacted fill, RAPs were designed to increase the vertical bearing strength of a soil upon which a structure is to be founded. Significant increases in bearing strength have been observed in many projects utilizing RAPs. Installation of RAPs prior to construction also increases the bond between the foundation and the soil. The increase in lateral resistance of a pile group foundation due to the installation of RAPs has not been tested previously.

In addition, no testing has been done in the past to quantify the increase in lateral resistance of a pile cap due to the use of compacted fill or RAPs as a retrofit in soft clay. The lateral resistance of deep foundations is primarily developed within 5 to 10 pile diameters of the ground surface. For typical piles with diameters of 1 to 2 ft, this corresponds to a total depth of 10 to 20 ft. Fortunately, this is also the depth range which current RAP systems are designed to treat; however, compacted fill can only be placed as deep as the stability of the surrounding soil will allow if excavation support is not provided. RAPs offer the potential of significantly increasing lateral pile foundation resistance without the need for expensive structural retrofits to bridge abutments. In addition, increased strength gained from the use of either method could also increase the passive resistance acting against bridge abutments and pile caps, which would further increase the lateral resistance of a bridge foundation system.

[1] "Geopier" is a registered trademark of Geopier, Inc. and Rammed Aggregate piers are a trademark technology of Geopier, Inc.

1.1 Project Objectives

The objectives of our research were four-fold:

- Evaluate the increase in lateral pile group resistance due to the installation of compacted fill and RAPs
- Evaluate the increase in lateral passive resistance on the pile cap due to the installation of compacted fill and RAPs
- Compare the cost and effectiveness of soil improvement relative to additional structural foundation elements
- Produce a well-documented case history of field performance for calibration of computer models so that additional parametric studies can be performed

The research for this project was one component of a much larger research project which is funded by the National Cooperative Highway Research Program (NCHRP). The NCHRP has outlined specific tasks that it would like to ultimately accomplish through this investigation. The above list represents four of the specific tasks that were to be accomplished through this research.

This report will focus only on the increased lateral resistance to pile group foundations through treatment of the soft soil surrounding the foundation using compacted fill and Rammed Aggregate Piers; however, these were not the only soil improvement techniques implemented during this phase of research. Pile foundations were also tested after the soft soil surrounding the foundations was treated with mass mixing, jet grouting, and flowable fill. Reports of the results associated with these particular soil treatments can be found in the related thesis work of Herbst (2008), Adsero (2008), Miner (2009), and others.

1.2 Scope of Investigation

Four identical full-scale foundations, spaced 30 ft from one another, were designed, constructed, and tested during this phase of research. Each foundation consisted of nine piles, in a 3 x 3 configuration, driven to a depth of approximately 40 ft below grade. Prior to driving, the piles were also instrumented with strain gauges at predetermined depths. Inclinometer and shape accelerometer array casings, which extended the length of the driven piles, were also placed in selected middle row piles. A 9-ft square reinforced concrete pile cap, which extended from the ground surface to 2.5 ft below grade, was constructed on top of the piles. A reinforced concrete corbel was attached to the concrete pile cap to create a load transfer surface during testing of the foundation systems. A hydraulic actuator was placed between two foundations which were being tested. Steel pipe extensions were attached to each end of the actuator to span the distance between the actuator and foundation. The extensions were then attached to the corbel to enable lateral load transfer from the actuators to the pile caps.

The foundations were first tested under virgin soil conditions. One test was performed with soil directly behind the pile cap; the second test was performed with the soil directly behind the pile cap excavated to the depth of the pile cap. The results of these two tests were used to determine the total and passive forces acting on the foundation when it was loaded laterally under native soil conditions. The shape arrays, strain gauges, and inclinometers were used to determine the deflections and moments in the piles with respect to depth below grade. After these tests were completed, another series of tests was performed on a pile cap with sand compacted below the pile cap to a depth of 3.5 ft below the base of the pile cap and extending 5 ft beyond the pile cap on one side and flush with the pile cap on the other side. During the installation of the piles, the ground heaved and approximately1 ft of compacted fill had to be

removed from under the pile cap to maintain the design thickness of the pile cap. Therefore, in the first test, the compacted fill on one side extended from 5 ft below the ground surface (2.5 ft below the base of the pile cap) to the base of the cap (2.5 ft from the ground surface). Subsequently, another lateral load test was performed on the same foundation with fill compacted directly in front of the pile cap to the ground surface, forming a 5 ft region along the width of the pile cap extending from the ground surface down 5 to 6 ft. A comparison of these two tests demonstrates the passive resistance increase due to installation of the compacted fill. Lastly, another lateral load test was performed by pushing the pile cap in the opposite direction into virgin clay soil which existed beyond the edge of the pile cap. The results from the compacted fill tests were then compared with the results obtained when the foundations were tested in virgin soil conditions to determine the degree of improvement to both lateral pile resistance and passive resistance on the pile caps themselves.

Another series of two lateral load tests was performed by pushing the pile cap into an array of RAPs that were constructed through the virgin clay soil on one side of the pile cap. A final test was performed after excavating to the base of the pile cap along its entire width to remove any contact between the soil and the pile cap. The results from these tests were also compared to each other and the tests performed on the pile caps in virgin soil in order to determine the degree of improvement to both lateral pile resistance and passive resistance on the pile cap.

2 LITERATURE REVIEW

Excavation of weak soil and replacement with compacted fill is a very dependable and simple way to increase the strength of a soft soil site. It has been proven in practice for many years. The use and effects of RAPs, however, have not been as broadly assessed neither in the laboratory nor in practice, and thus they are not as widely used. This chapter will describe the installation procedure and some uses for both methods.

2.1 Excavation and Replacement with Compacted Imported Natural Soil Backfill

Excavation and replacement with compacted soil is the simplest, most reliable, and least expensive technique, provided good quality imported soil is readily available. Well compacted cohesive sandy or gravelly backfill to replace soft clays or loose silts will provide good performance in terms of increased lateral resistance. Laboratory tests to optimize compaction specifications with respect to stiffness and strength and to assess properties for design would be required in practice.

In connection with research studies, field load tests have been performed on two pile groups where the native clay soil was excavated and replaced with compacted granular soil. These studies were primarily undertaken to evaluate group interaction factors under lateral loading. Group interaction refers to the phenomenon that occurs when a group of piles is loaded laterally and the leading row of piles resists a greater portion of the load than do the trailing

rows. Figure 2-1 is a representation of a nine-pile cap showing the stress zones for each of the piles. The leading piles are able to develop their full capacity, but the leading piles interrupt the development of the full capacity in the trailing piles. Brown et al. (1987) conducted lateral load tests on a nine pile group in saturated stiff clay. Later, Brown et al. (1988) excavated the clay, compacted sand around the pile group, and repeated the lateral load test. Rollins et al. (2005)

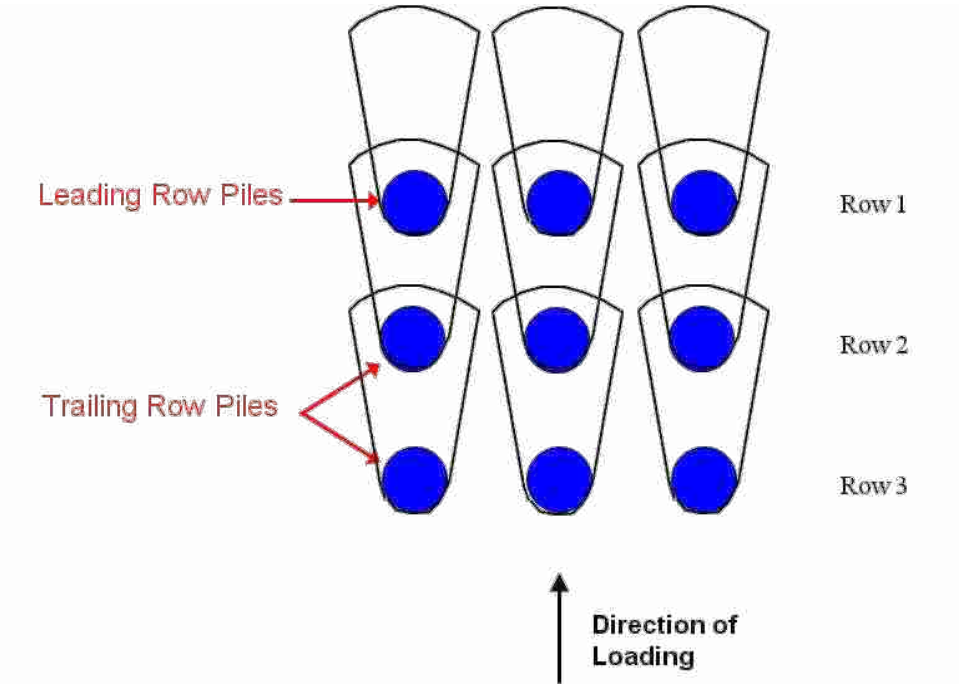

Figure 2-1 Pile group interaction effect

performed cyclic lateral load tests on a 15 pile group in medium consistency clay. Later, Walsh (2005) excavated the clay, replaced it with clean sand and performed additional lateral pile group load tests. Although these tests were not designed to evaluate the effect of excavation and replacement on lateral pile group resistance, the test results can be compared to provide this information.

The pile group tested by Brown et al (1987, 1988) was a nine-pile group consisting of 0.25-m (0.82-ft) diameter steel pipe piles filled with cement grout. The piles were driven in a 3 x 3 arrangement with a 0.75-m (2.5-ft) center-to-center (3 pile diameters or 3D) spacing in both

directions. The original clay profile consisted of stiff, overconsolidated clay with an undrained shear strength of about 57 kPa (1150 psf) at the ground surface which increased to about 150 kPa (3000 psf) at a depth of 5.5 m (18 ft) below the ground. Approximately 9 ft of the clay was excavated and replaced with a relatively uniform clean sand compacted to a dry unit weight (γ_d) of 15.4 kN/m^3 (98 pcf) which is a relative density of about 50 percent. A direct shear test indicated a friction angle of 38.5°, but back-calculated friction angles using LPILE suggest a friction angle of around 50°, which is greater than would normally be used in engineering practice. A plot showing the total load versus deflection curves for the pile group in both clay and sand are presented in Figure 2-2. At deflections less than about 20 mm, the lateral resistance of the pile group in clay was about the same as that in sand. However, at greater deflections, the lateral resistance of the pile group in sand eventually exceeded that for the pile group in clay by over 28 percent despite the fact that the clay was relatively stiff.

The pile group tested by Walsh (2005) and Rollins et al. (2003) consisted of fifteen 12.75-inch diameter steel pipe piles driven closed-ended to a depth of about 40 ft. The piles were driven in a 3 x 5 grouping with a center-to-center spacing of 4.17 ft (3.92D) in the direction of loading and 3.5 ft (3.29D) transverse to loading. The upper 2.5 m (8.2 ft) of clay in the original soil profile had an undrained shear strength of about 900 psf. The pile group reacted against two 4-ft diameter drilled shafts. Prior to the second set of tests, the upper 1 m (3.3 ft) of clay was excavated and replaced with sand. In addition, an extra 1.5 m (4.9 ft) of sand was compacted above the original ground elevation so that the upper 2.5 m (8.2 ft) of the profile consisted of clean sand compacted to 93 percent of the modified Proctor maximum density. The load versus deflection curves for the pile group in clay and sand are compared in Figure 2-3. Because the clay strength was relatively soft, the lateral resistance of the pile group in sand was

considerably higher than that for the pile group in clay. Analyses using the computer program GROUP were very successful in matching the measured response of the pile groups in clay. However, for the pile groups in sand, successful agreement with measured response generally required the use of friction angles which are higher than would normally be used in engineering practice (40° for D_r of 50 percent). These comparative tests indicate that the increase in lateral resistance achieved by using compacted fill is strongly dependent on the undrained shear strength of the clay being replaced.

Two field test studies have evaluated the passive force on a pile cap as a function of soil type and density. Mokwa and Duncan (2001) performed tests on a 1.1 m (3.5 ft) deep and 1.9 m (6.3 ft) wide anchor block. The block was originally poured flush against an excavation into partially saturated stiff clay and a lateral load test was performed. The clay was then excavated and replaced with a compacted sandy gravel backfill and the test was repeated. Rollins et al. (2008) evaluated the passive force provided by various soils against a pile cap that was 1.1 m (3.67 ft) deep and 5.2 m (17 ft) wide. Tests were conducted on dense and loose silty sand and on loose silty sand with a 0.91 to 1.83 m (3 to 6 ft) wide zone of dense compacted gravel immediately adjacent to the pile cap.

The native clay in the tests performed by Mokwa and Duncan (2001) was partially saturated. Triaxial shear tests on the clay at the natural moisture content indicate that the cohesion was 1000 psf and that the friction angle ranged from 32° to 38°. The clay was excavated to the base of the cap and replaced with compacted sandy gravel. The sandy gravel (GW-GM) was compacted to a relative density of approximately 80 percent. Triaxial shear tests indicate that the friction angle could range from a low of 48° to a high of 52°. A comparison

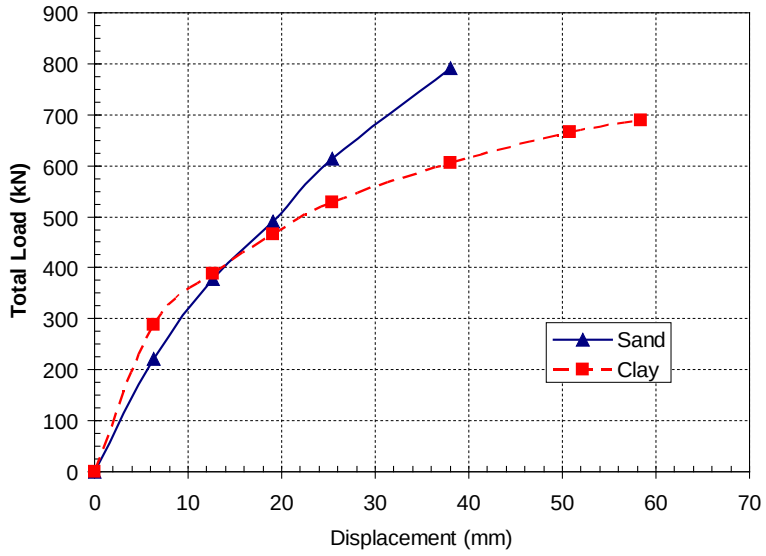

Figure 2-2 Load versus deflection curves for 9 pile group in stiff clay and dense sand based on Brown et al (1987) (1988)

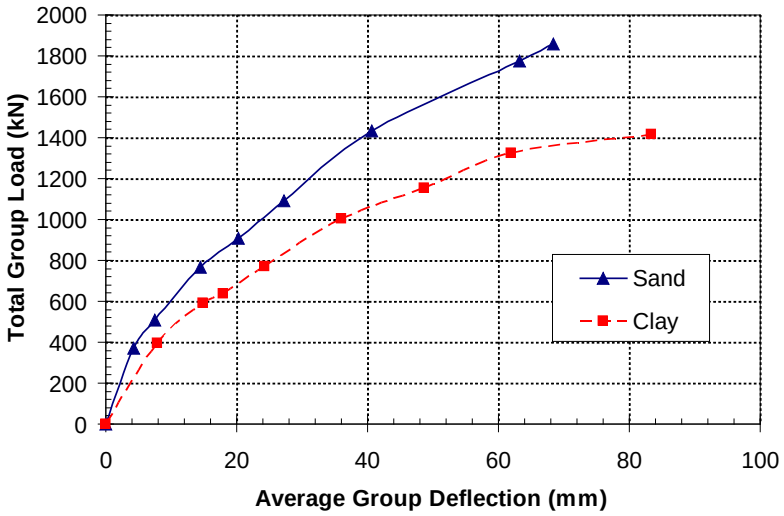

Figure 2-3 Load versus deflection curves for 15 pile group in medium stiff clay and dense sand based on Rollins et al (2005) and Walsh (2005)

between the passive force-deflection curves for the clay and gravel is provided in Figure 2-4. In this case, the lateral resistance provided by the stiff, partially saturated clay was considerably higher than that for the gravel at the shallow depths involved. As a result, the lateral resistance actually decreased substantially when the compacted gravel was used in place of the clay. Duncan and Mokwa (2001) concluded that the log-spiral method provided the best estimate of

the ultimate capacity and that the passive-force deflection relationship could be reasonably estimated using a hyperbolic curve.

Rollins, Kwon, and Gerber (2008) performed lateral load tests on a pile cap supported by twelve 0.324-m (1.06-ft) diameter pipe piles. The piles provided sufficient vertical resistance so that the full wall friction force could develop. Basic passive force-deflection relationships were developed for two tests involving silty sand compacted at 88 percent and 98 percent of the modified Proctor maximum unit weight as shown in Figure 2-5. The increased compactive effort produced a considerable increase in passive resistance. Preliminary analyses indicate that this behavior is predicted quite well using the Mokwa-Duncan approach along with the soil properties measured in the field.

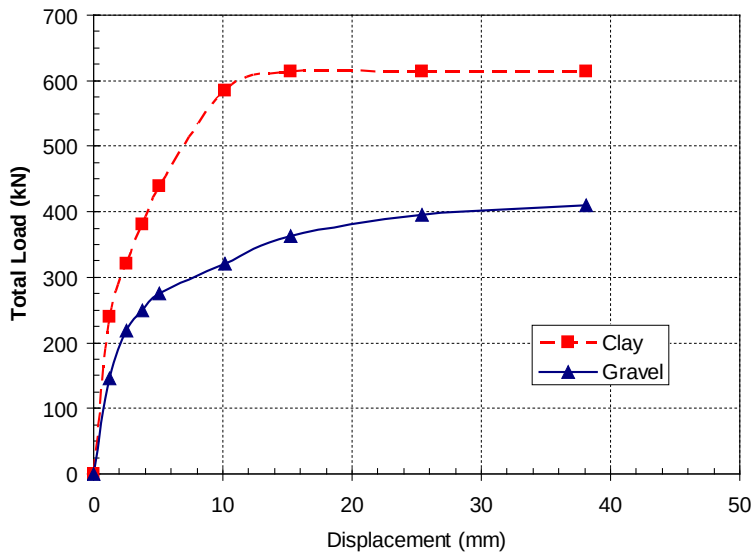

Figure 2-4 Comparison of passive force provided by stiff partially saturated clay and compacted sandy gravel against 1.1m deep x 1.9 m wide cap block (Mokwa and Duncan 2001)

Tests were also performed using the loose silty sand backfill along with a well-compacted zone of sandy gravel adjacent to the pile cap. The compacted zones were 0.9 m (3 ft) and 1.83 m (6 ft) thick. These tests indicate that compacting relatively narrow zones (3 to 6 ft wide) of sandy gravel around a pile cap can significantly increase the passive resistance as

illustrated in Figure 2-6. In this case, replacing a 0.9 m (3 ft) zone of loose silty sand around the pile cap with compacted gravel increased the lateral resistance on the pile cap from an initial value of 70 kips to over 180 kips which is an increase of over 200 percent. Crack patterns from the tests, shown in Figure 2-7, indicate that the compacted gravel zone increases the effective width of the pile cap and reduces the pressure on the loose silty sand behind it thereby increasing passive resistance.

Designers for the Legacy Parkway north of Salt Lake City, Utah have planned to use excavation and replacement techniques to increase the lateral resistance at the abutments of several bridges on the project. The soil at these sites consists of soft clay to very soft clay to a

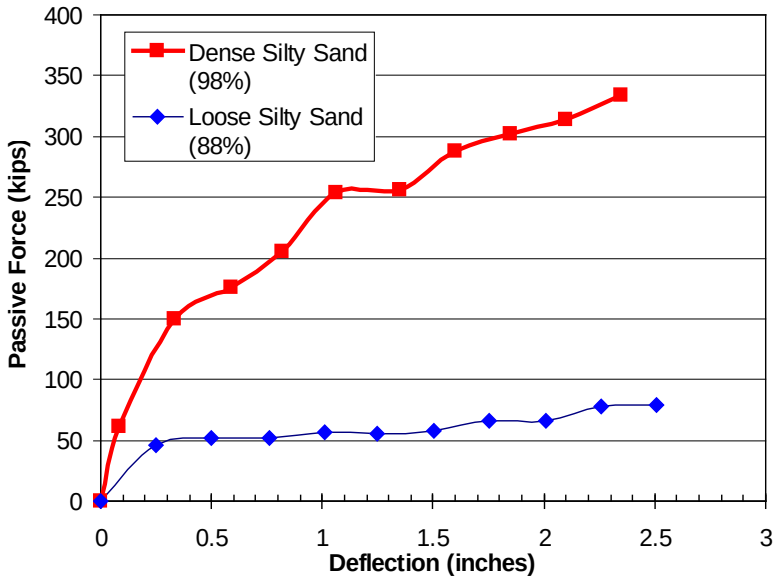

Figure 2-5 Measured passive force versus deflection relationships for two full-scale tests with silty sand compacted to 88 percent and 98 percent of the modified Proctor maximum unit weight (Rollins, Kwon, and Gerber 2008)

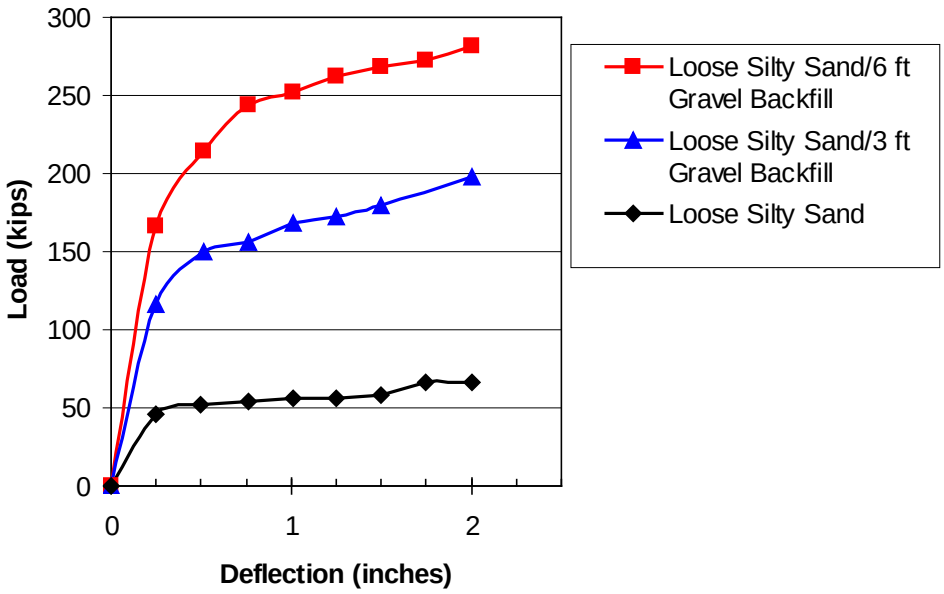

Figure 2-6 Passive force versus deflection curves for loose silty sand against a 17 ft wide by 3.67 ft high pile cap and after excavation and replacement with 3 ft and 6 ft zones of compacted gravel backfill against the cap (Rollins, Kwon, and Gerber 2008)

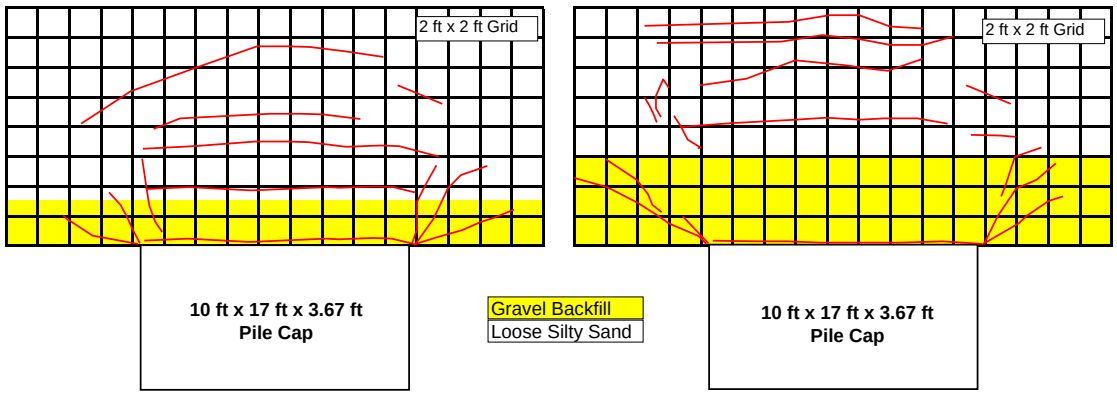

(a) 3 ft sandy gravel zone plus loose silty sand backfill (b) 6 ft sandy gravel zone plus loose silty sand backfill

Figure 2-7 Plan view of crack patterns behind a pile cap after excavation and replacement of loose silty sand with (a) a 3-ft and (b) a 6-ft zone of compacted sandy gravel behind the pile cap (Rollins, Kwon, and Gerber 2008)

depth of about 5 m (16.4 ft) and the seismic demand due to a M7.0 earthquake producing 0.65 g peak acceleration is high. Computer analyses using GROUP indicated that the cost of foundations could be significantly reduced by removing the soft clay to a depth of 3 m (9.84 ft) below the base of the footing in the cross-hatched area around the abutment footings as shown on the plans in Figure 2-8 and replacing the soil with compacted gravel fill (A-1 material). In one

typical case where 24 high-strength (65 ksi) steel pipe piles would have been required at an abutment within the weak native soft clay, the use of compacted fill would reduce the required number of piles to only 12. The foundation capacity would benefit from increased lateral pile resistance as well as increased passive earth pressure on the abutment wall. On the down side, the construction difficulties associated with excavating and replacing the soft clay could substantially reduce the anticipated cost savings. This project was scheduled for construction in 2007.

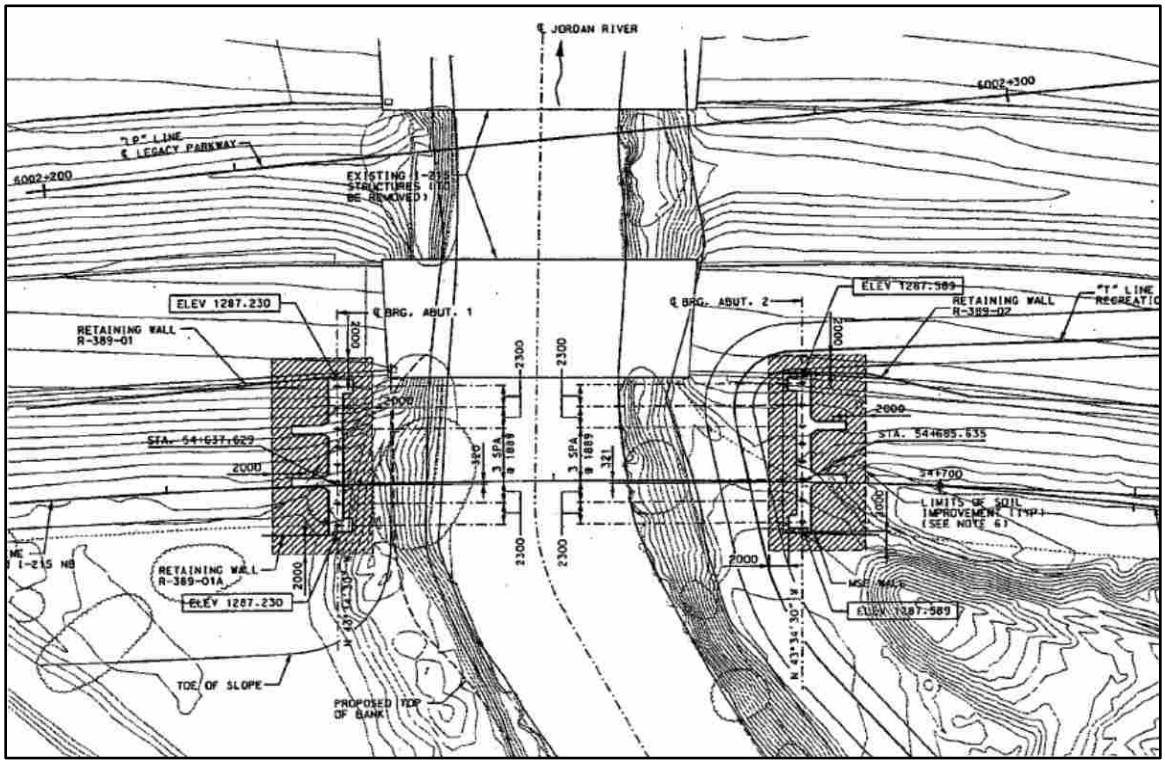

Figure 2-8 Plan view of "improvement areas" around abutments at a bridge site on the Legacy Parkway project north of Salt Lake City, Utah (Higbee 2007)

2.2 Rammed Aggregate Piers

Rammed Aggregate Pier (RAP) systems, developed by Geopier Foundations, are an alternative to stone column treatment or compacted fill for increasing resistance to uplift forces, lateral loads, and to prevent excessive settlement and liquefaction in any soil type. RAPs are

designed to act like shallow footings, reducing the need for deep foundations by increasing the strength of the bearing soil. RAPs are generally installed by drilling a hole 6 to 20 ft deep and then ramming coarse granular soil into the base of the excavation with a telescoping rammer to create an initial consolidated base for the RAP. Well-graded aggregate is then placed into the hole in relatively thin lifts (8 to 12 inches) and compacted to a density commonly beyond 100 percent of the modified Proctor unit weight using the same rammer that was used to create the initial base.

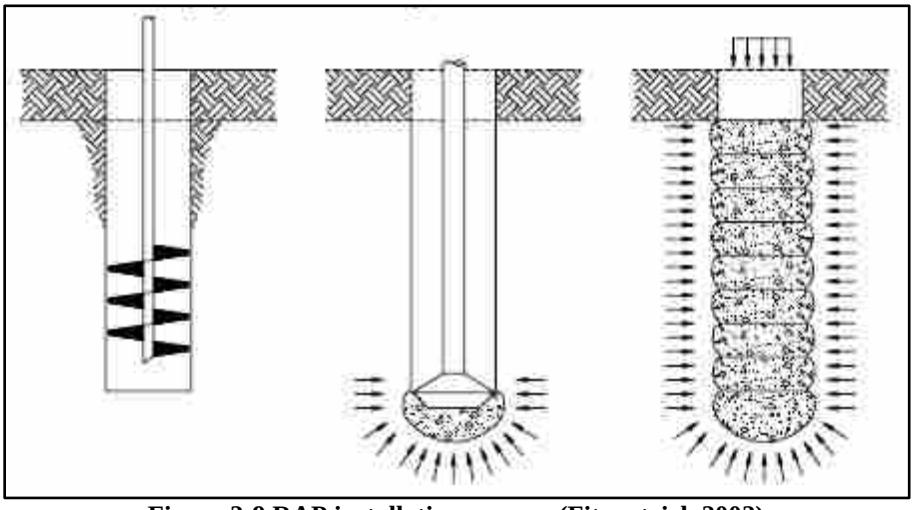

Figure 2-9 RAP installation process (Fitzpatrick 2002)

If uplift resistance is needed, a steel plate is inserted into the hole after the initial compaction and rods are run from the plate up into the new foundation as shown in Figure 2-10.

Once the RAPs have been placed, the foundation is poured directly on top of them. The increased friction angle of the RAPs and the rough interface between the foundation and the RAPs increase the lateral resistance in RAP-reinforced foundations. RAPs are convenient in that only a small excavation needs to be made and, depending on the number of piers needed, can be

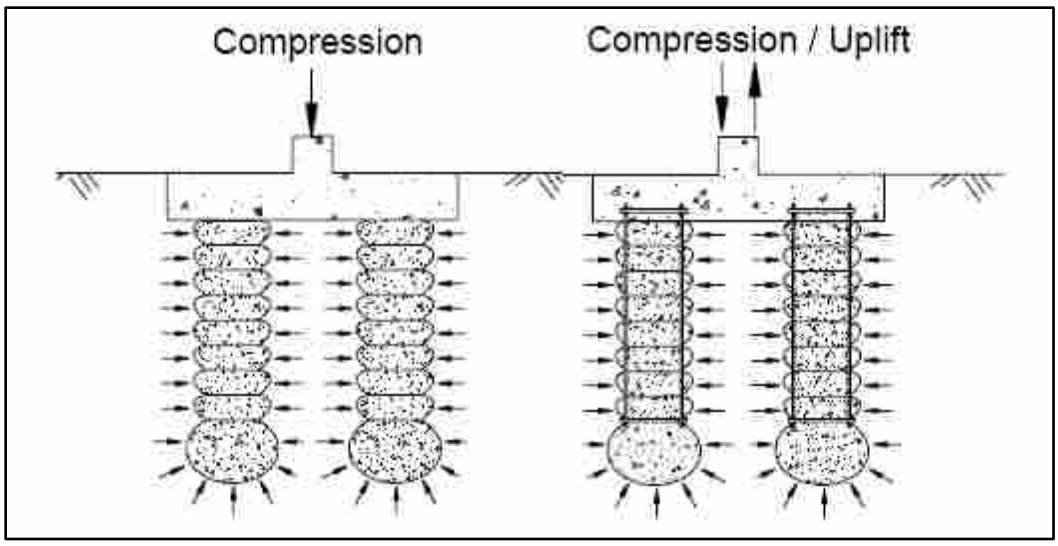

Figure 2-10 Typical RAP installation (Fitzpatrick 2002)

installed in one working day. Another advantage of using RAPs is the high friction angle that can be obtained within the pier itself (exceeding 50° in most cases). One disadvantage is that if the piers are subjected to uplift forces, their lateral strength decreases significantly. RAPs are also not designed to penetrate much more than 20 ft. Because a rammer is required to compact the aggregate in a RAP, one can only be made as deep as a rammer will reach. In shallow foundations, the lateral strength of a RAP system with an area of 6.5 ft x 6.5 ft was found to exceed that of a conventional foundation with an area of 10 ft x 10 ft (Wissman and Fox 2000). These piers are generally used as alternatives to deep foundations rather than in conjunction with them.

One set of tests was performed by Dr. Evert Lawton (1999) of the University of Utah to test the lateral capacity of a RAP system as compared to a deep-foundation system. The test was done in conjunction with a pushover analysis of an existing bridge bent along I-15 in Salt Lake City, Utah as shown in Figure 2-11. A steel frame with a hydraulic actuator to load the bent was erected and supported by two RAP foundation groups.

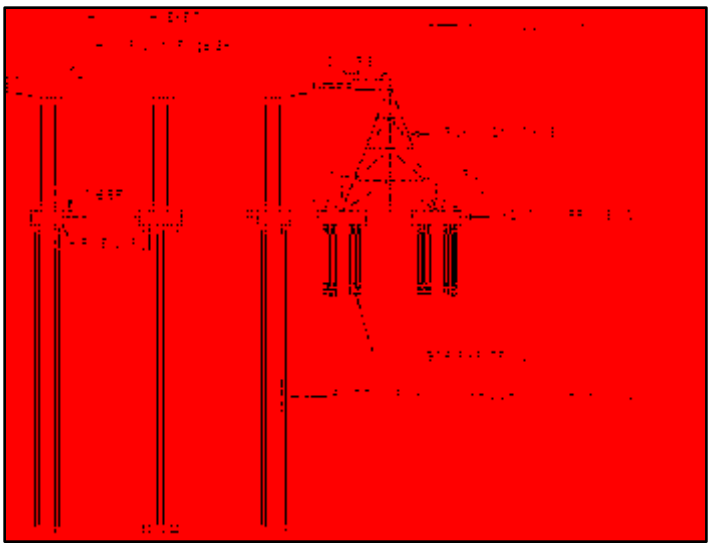

Figure 2-11 I-15 lateral load test schematic (*Figure courtesy of Evert Lawton)*

The only resistance provided against lateral load was the uplift on the foundation from the reaction frame and the interface friction between the foundation and the RAPs with the matrix soil. The RAP foundation was then reacted against the deep foundation of the bridge bent and displacement and stress analyses were made on the system. The test showed that RAPs are resilient and would likely keep their strength even after such events as earthquakes. The RAP foundations demonstrated a greater strength-deflection ratio as compared to the pile foundations for small deflections, but for greater deflections, the pile foundations exceeded that of the RAP foundations. Lawton found that RAPs are relatively ductile and would not lose excessive serviceability in an earthquake event and the permanent deformations from the loadings were small. The rough interface between the RAPs and the foundation substantially increased the shearing resistance along the bottom of the foundation. Lawton and Merry (2000) also found that 21 to 42 percent of the peak lateral resistance was provided by the stiffness of the uplift bars.

RAPs have been used in new construction, but not very extensively in retrofit projects. The list of projects listed by Geopier Foundation Company (2010) shows that RAPs have been used mainly for uplift control, settlement and sensitive soil mitigation, and slope and MSE wall

stabilization and support. RAPs are a relatively inexpensive alternative to deep foundations, but would typically cost more than a vibro-replacement stone column (Rollins and Anderson 2004).

3 GEOTECHNICAL SITE CHARACTERIZATION

The following chapter will describe the soil conditions of the site used for testing. The site was located north of Salt Lake City, Utah at the interchange of Redwood Road and I-215 on a Utah Department of Transportation right-of-way. An aerial view of the site is shown in Figure 3-1. The top 4 ft of the site were littered with huge pieces of asphalt, which necessitated the excavation of the top 4 ft of soil over the entire site. All of the geotechnical field investigation took place before the excavation, and the results in the following chapter will generally refer to the soil conditions below the excavation.

3.1 Field Investigations

Geotechnical site conditions were evaluated using field and laboratory testing. Field testing included one drilled hole with undisturbed sampling, four cone penetration test (CPT) soundings, and shear wave velocity testing. Laboratory testing included unit weight and moisture content determination, Atterberg limits testing, and undrained shear testing. A plan view of the borehole and CPT locations relative to the finished pile caps is shown in Figure 3-2.

3.2 Soil Profile, Classifications, and Shear Strengths

A generalized soil boring log at the test site is provided in Figure 3-3(a). The depth is referenced to the top of the excavation, which was 2.5 ft above the base of the pile cap as shown

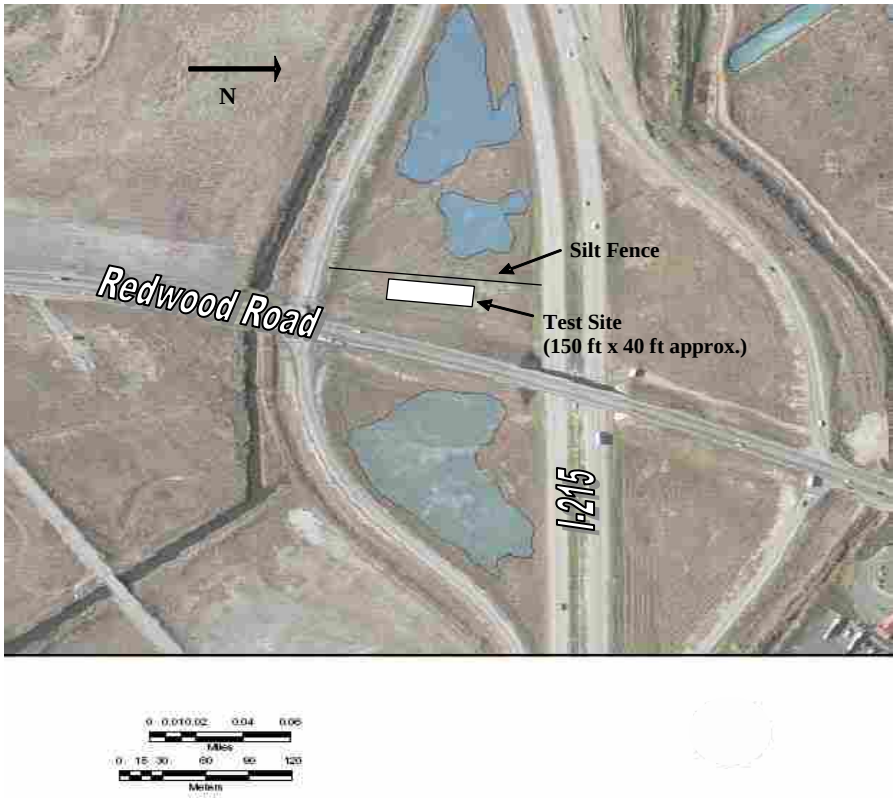

Figure 3-1 Aerial view of the test site and surrounding area

in the figure. The soil profile consists predominantly of cohesive soils; however, some thin sand layers are located throughout the profile. The cohesive soils in the upper 15 ft of the profile typically classify as CL or CH materials with plasticity indices of about 20 as shown in Figure 3-3(a) & (b) and Table 3-1. In contrast, the soil layer from a depth of 15 to 25 ft consists of interbedded silt (ML) and sand (SM) layers as will be highlighted by the subsequent plots of CPT cone tip resistance. The liquid limit, plastic limit and natural moisture content are plotted in Figure 3-3(b) at each depth where Atterberg limit testing was performed. The water table was at a depth of 2.0 ft, which is equivalent to a depth of 6.0 ft below the pre-excavation ground surface. The natural water content is less than the liquid limit near the ground surface suggesting that the soil is overconsolidated. However, the water content is greater than the liquid limit for soil specimens from a depth of 5 to 27 ft suggesting that these materials may be sensitive. Below

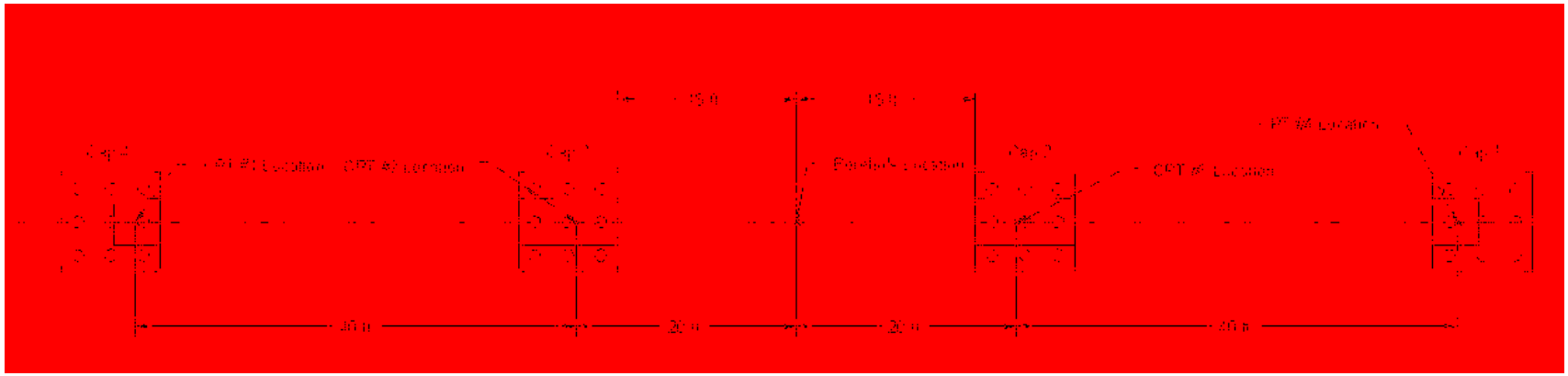

Figure 3-2 Plan view showing location of boring, CPT soundings relative to pile caps

a depth of 30 ft the water content is approximately equal to the liquid limit suggesting that the soils are close to normally consolidated.

The undrained shear strength is plotted as a function of depth in Figure 3-3(c). Undrained shear strength was measured using a miniature vane shear test, or Torvane test, on undisturbed samples immediately after they were obtained in the field. In addition, unconfined compression tests were performed on most of the undisturbed samples. Both the Torvane and unconfined compression tests indicated that the undrained shear strength decreases rapidly from the ground surface to a depth of about 6 ft. However, the undrained shear strength from the unconfined compression tests was typically about 30 percent lower than that from the Torvane tests. After a depth of 6 ft the trend reverses, and the shear strength begins to increase with depth. This profile is typical of a soil profile with a surface crust that has been overconsolidated by desiccation. The unconfined compression tests at a depth of 27 and 48 ft yielded soil strengths substantially lower than those from the Torvane test. These unconfined compression tests appear to have been conducted on soil with sand lenses, and are not likely to be representative of the in-situ soil. The undrained shear strength was also computed from the cone tip resistance using the correlation equation:

$$s_u = \frac{(q_c - \sigma)}{N_k} \qquad (3\text{-}1)$$

where q_c is the cone tip resistance, σ is the total vertical stress, and N_k is a correlation coefficient which typically ranges from 10 to 20 and was taken to be 15 for this study (Briaud and Miran 1992). The undrained shear strength obtained from the above equation is also plotted versus depth in Figure 3-3(c) and the agreement with the strengths obtained from the Torvane and unconfined compression tests is reasonably good. Nevertheless, there is a greater disparity

between the Torvane results and unconfined compression test results with depth, as the penetrometer displaces through the sand lenses. The shear strength in the sand layers has been excluded because the correlation with cone tip resistance is not applicable in these materials. A summary of laboratory test results is provided in Table 3-1.

Table 3-1 Summary of laboratory results

	In-Place		Atterberg Limits					
Depth below Excavated Surface (ft)	Saturated Unit Weight (pcf)	Natural Water Content (%)	Liquid Limit (%)	Plastic Limit (%)	Plastic Index (%)	Unconfined Compressive Strength (psf)	Miniature Vane Shear Strength (Torvane) (psf)	Unified Soil Classification Symbol
1.25	117.6	34.2	39	18	21	1104	-	CL
2.75	117.4	34.4	38	18	20	626	620	CL
5.75	104.6	56	51	21	30	384	320	CH
8.5	112.4	41.5	38	18	20	684	534	CL
11.5	110.8	44.1	38	19	19	741	500	CL
16.5	126.6	24.2	19	18	1	1081	560	ML
26.75	116.9	35	27	14	13	237	780	CL
33.5	124.6	26.1	27	14	13	1306	780	CL
36.75	117.1	34.8	35	17	18	1381	840	CL
41.75	112.0	42.1	46	17	29	1037	520	CL
48	117.2	34.6	33	16	17	297	660	CL

3.3 Cone Penetration and Seismic Cone Testing

Four cone penetration tests (CPT) were performed across the test site. Plots of cone tip resistance, friction ratio, and pore pressure for the centermost test are provided as a function of depth in Figure 3-4. In addition, the interpreted soil profile is also shown. From the ground surface to a depth of about 15 ft the soil profile appears to be relatively consistent with a cone tip resistance of about 6 tsf and a friction ratio of about 1 percent. However, one sand layer is clearly evident between about 6.5 and 7.5 ft. The cone tip resistance, friction ratio, and pore pressure plots clearly show the interbedded silt and sand layering in the soil profile between 15 and 27 ft below the ground surface. Figure 3-5 provides plots of the cone tip resistance, friction

ratio and pore pressure as a function of depth for all four of the CPT soundings. The measured parameters and layering are generally very consistent for all four soundings which indicate that the lateral pile load tests can be compared readily from one foundation to the next.

Penetration of the cone penetrometer through a soft soil causes compression of the soil surrounding the cone. This increases the pore pressures measured by the cone beyond hydrostatic pressure conditions. As the cone penetrometer enters a granular soil, the measured pore pressures typically decrease back to static pressure conditions (Briaud and Miran 1992). This behavior is displayed in Figure 3-4(d). The pore pressures measured through the clay layers are much larger than those measured as the penetrometer enters a sand lens.

Figure 3-6 also provides a plot of the shear wave velocity as a function of depth obtained from the downhole seismic cone testing. The interpreted soil profile and cone tip resistance are also provided in Figure 3-6 for reference. The shear wave velocity in the upper 10 ft of the profile is between 300 and 400 ft/sec. This velocity is relatively low and suggests low shear strength. Between depths of 10 to 20 ft the velocity increases to about 550 ft/sec. This increase in velocity is likely associated with the interbedded sand layers in these depths. Below 20 ft, the velocity drops to a value of around 500 ft/sec and remains relatively constant to a depth of 45 ft, the maximum depth of testing.

For comparison purposes a site with an average shear wave velocity of 600 ft/sec in the upper 100 ft of the profile is classified as a soft clay site (Site E) according to the International Building Code (IBC 2006). The site class definitions, as taken from the IBC, are displayed in Table 3-2. Knowledge of the average shear wave velocity, standard penetration resistance, and undrained shear strength of the soil to a depth of 100 ft is generally necessary to determine a

a) b) c)

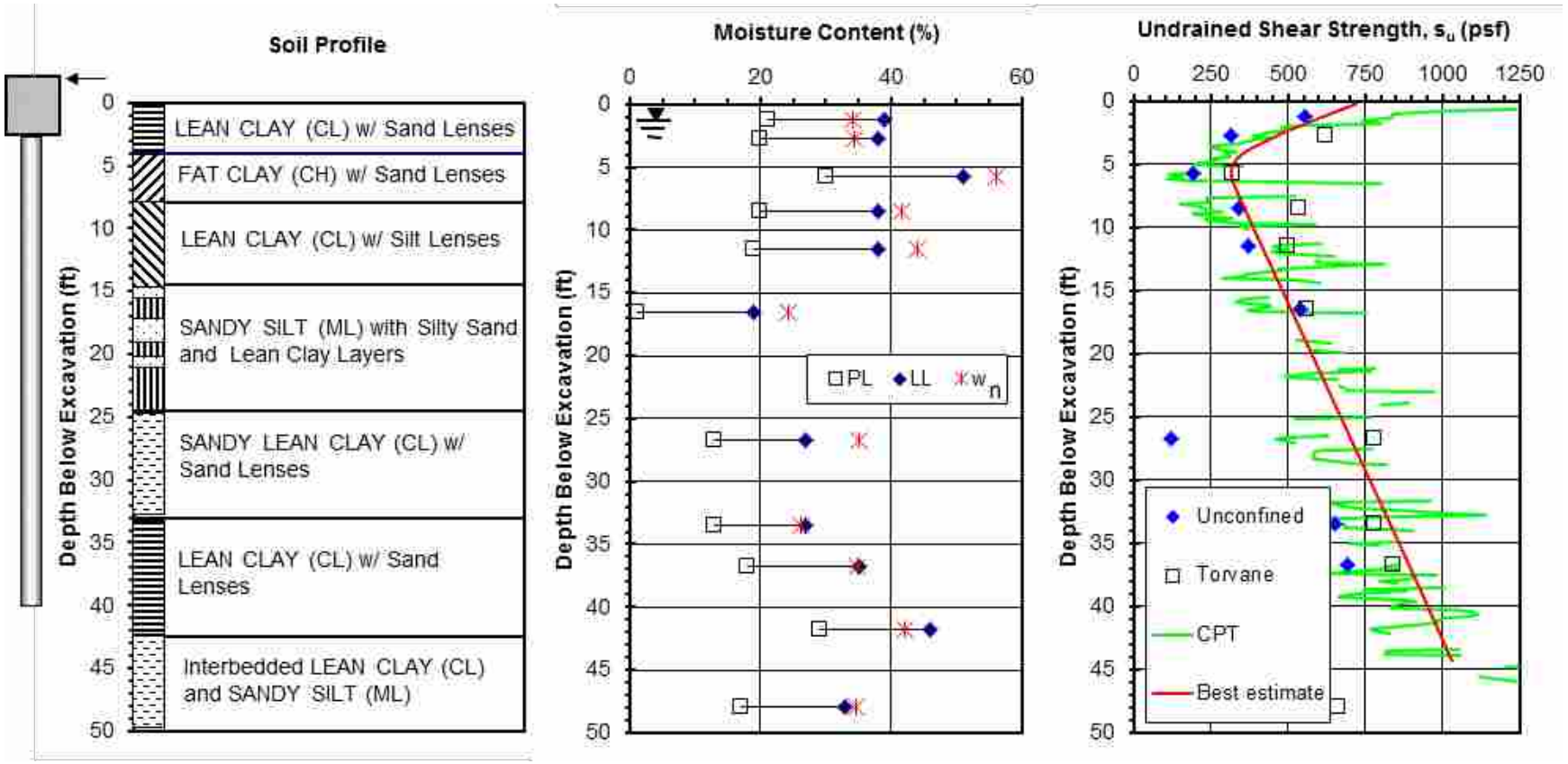

Figure 3-3 Plot of (a) soil profile, (b) Atterberg limits and natural water content versus depth, and (c) undrained shear strength versus depth

specific International Building Code (IBC) seismic site classification. However, this is not necessarily the case if the site is classified as Site Class E. Regardless of the average shear wave velocity, any soil profile with more than 10 ft of soil having the following characteristics is classified as a Site Class E, namely:

1. Plasticity index, PI < 20
2. Moisture content, w ≥ 40%
3. Undrained shear strength, S_u < 500 psf

Table 3-2 Seismic site class definitions from the IBC 2006 code

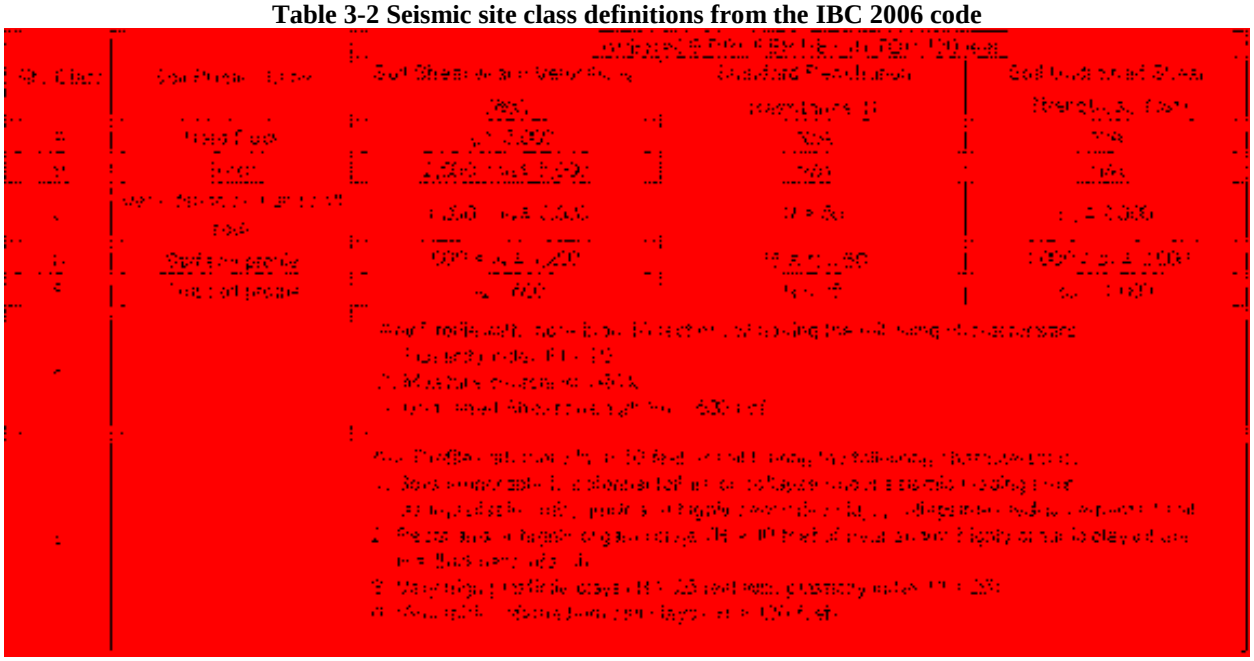

A close look at Table 3-1 or Figure 3-3 shows that the zone from about 4 to 15 ft has an undrained shear strength less than 500 psf and a moisture content greater than 40 percent which both meet the criteria for site class E. The PIs in this layer are 30, 20 and 19 which are either above or right at the boundary of 20 specified in the code, which makes evaluation of the third criterion somewhat more problematic. Considering that the 11-ft layer clearly meets two of the criteria and that the average PI of 23 for the layer would meet the third criteria, the site could

reasonably be considered site class E. In any event, knowledge of the site conditions in the last 50 ft of the profile would likely show that the site would at least classify as site class D.

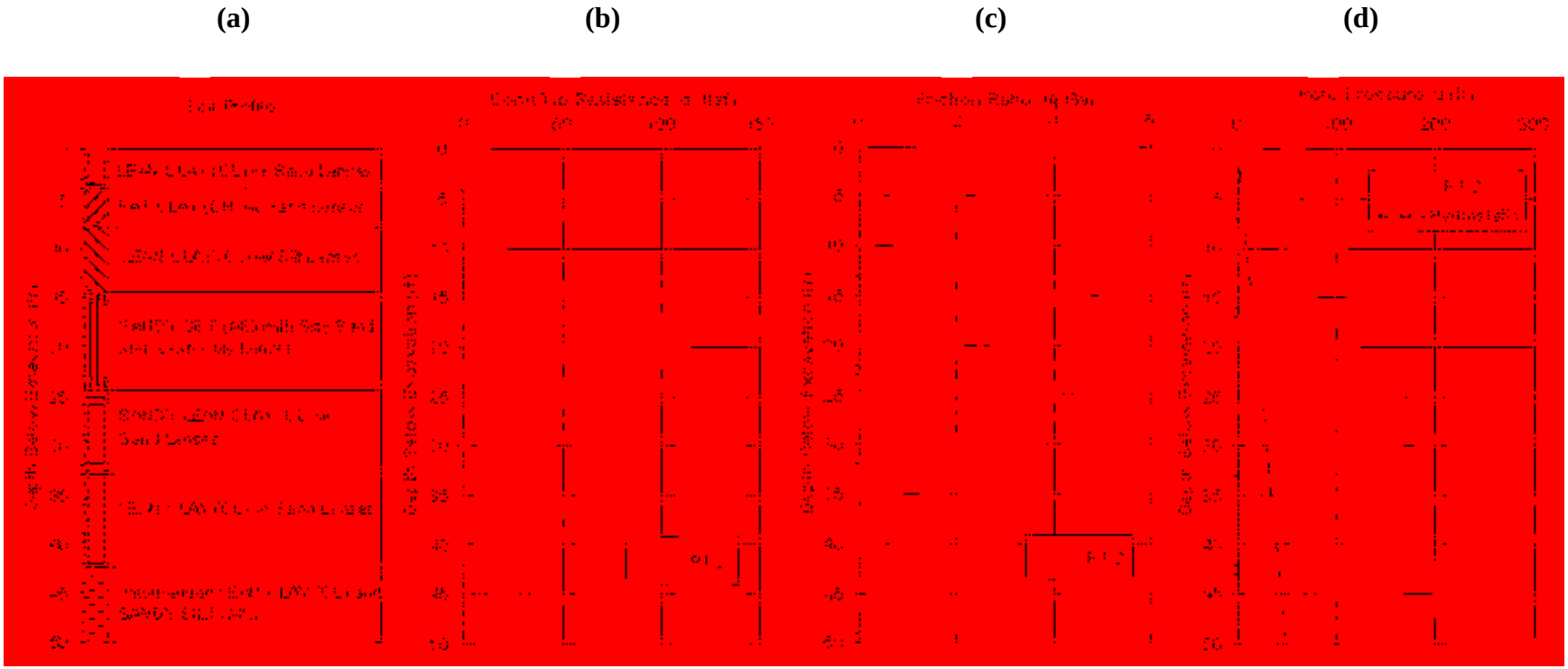

Figure 3-4 Plot of (a) soil profile, (b) cone tip resistance versus depth, (c) friction ratio versus depth, and (d) pore pressure versus depth curves from cone penetration test (CPT) sounding 2 near the center of the site

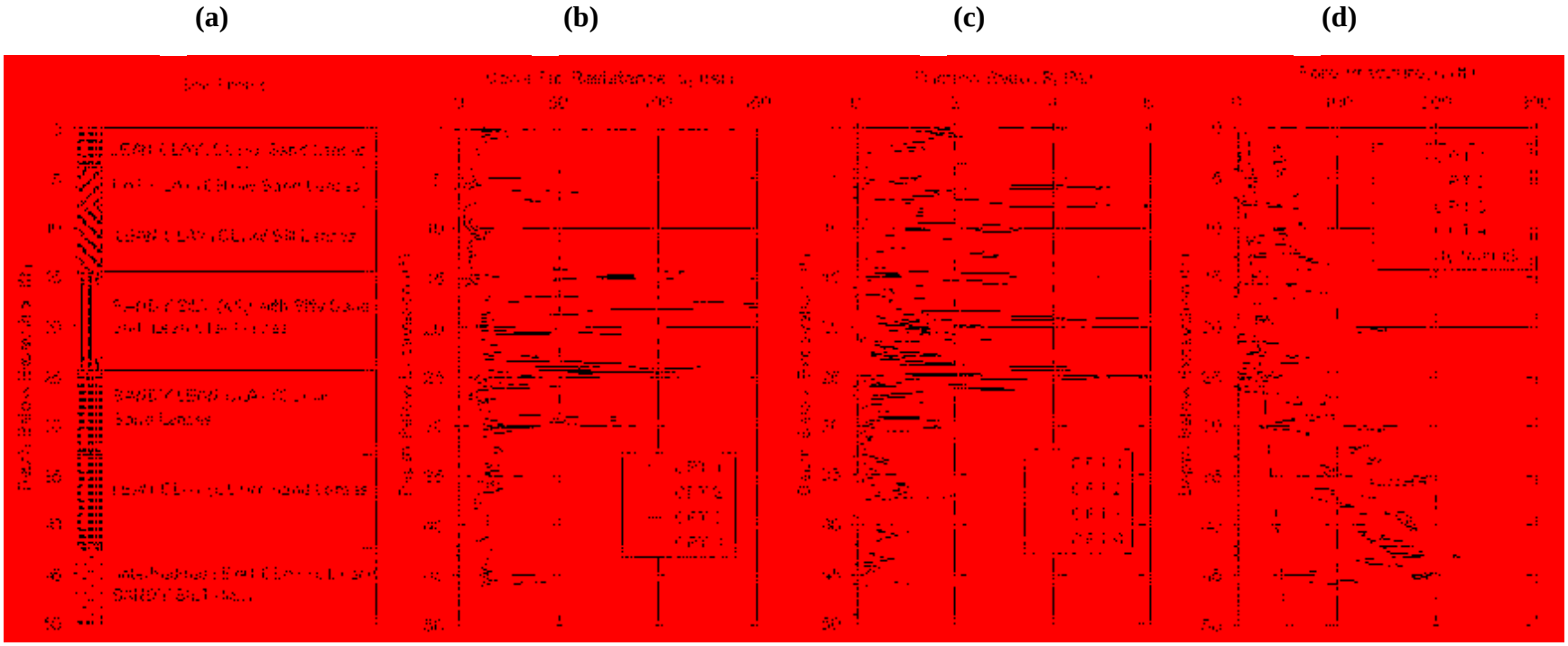

Figure 3-5 Plot (a) soil profile, (b) cone tip resistance versus depth, (c) friction ratio versus depth and, (d) pore pressure versus depth from all four cone penetration test (CPT) soundings

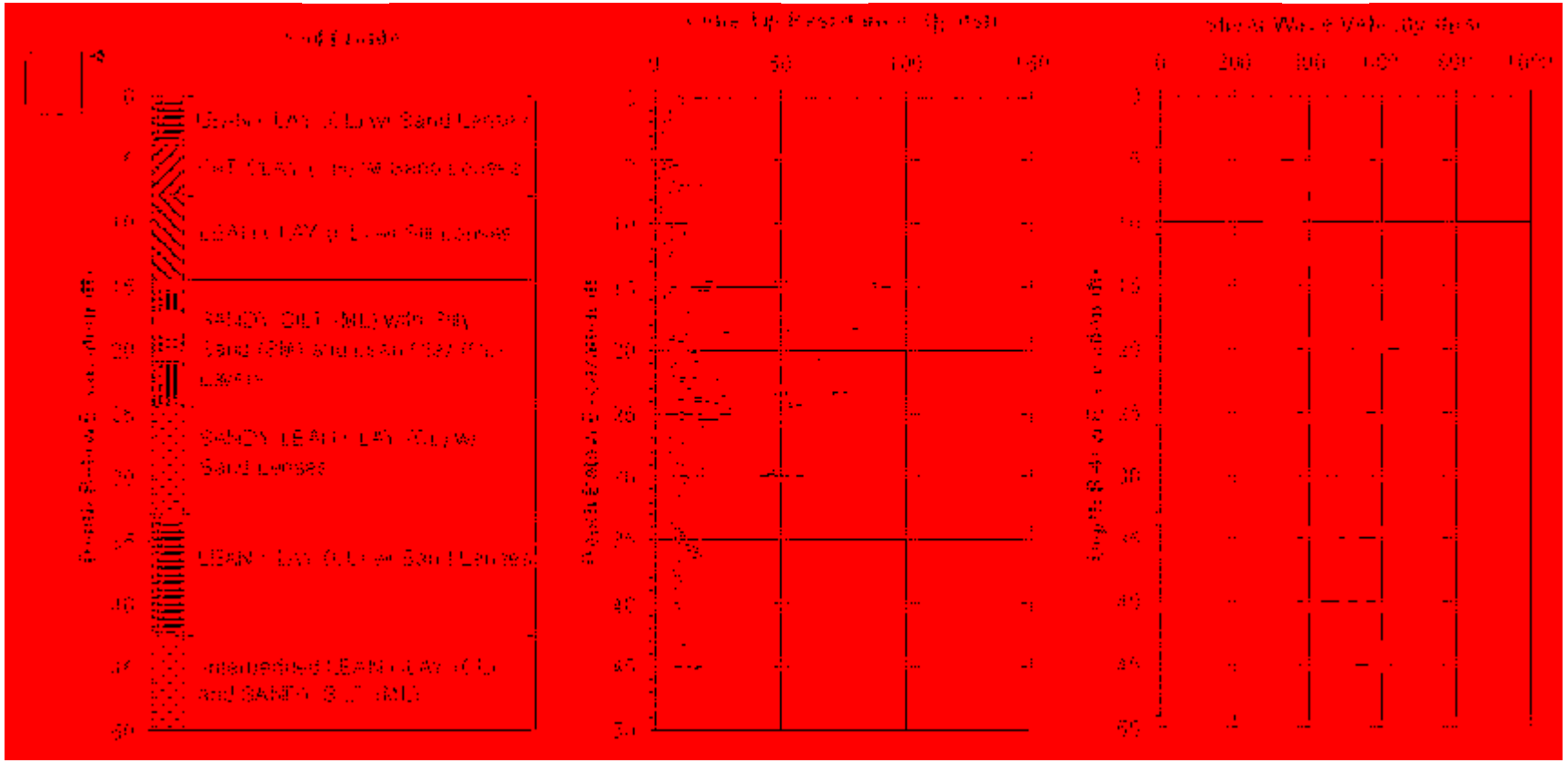

Figure 3-6 Plot of (a) soil profile, (b) cone tip resistance versus depth, and (c) shear wave velocity versus depth from seismic cone testing

4 TEST LAYOUT AND PROCEDURE

The following section will detail the construction process of the foundations, and the properties of the materials used to create the foundations. This section will also explain the basic layout of the actuators and pile caps, along with the instrumentation configuration on each of the foundations.

4.1 Construction, Layout, and Materials

Once the site had been excavated to the proper elevation of 4 ft below the original grade and the locations of the four pile caps were excavated an additional 2.5 ft, the pile groups were driven. An overall plan view of the four pile group locations is shown in Figure 3-2. The plan and profile drawings of pile caps 1 and 2 are presented in Figure 4-1 for the conditions during the first test of the virgin soil. As shown in Figure 4-1, each pile group consisted of nine test piles which were driven in a 3 x 3 orientation with a nominal center-to-center spacing of 3 ft. The test piles were 12.75 inch OD steel pipe piles with a 0.375 inch wall thickness, and they were driven closed-ended with a hydraulic hammer to a depth of approximately 45 ft below the excavated ground surface on June 13-15, 2007. The test piles had a beveled end which allowed a 1.5 inch thick plate to be welded flush with the edge of the pile at the bottom. The steel conformed to ASTM A252 Grade 2 specifications and had a yield strength of 58,700 psi based on the 0.2 percent offset criteria. The moment of inertia of the pile itself was

279 in^4; however, angle irons were welded on opposite sides of two to three test piles within each group, as discussed hereafter, which increased the moment of inertia to 342 in^4.

The center piles of each row were instrumented with strain gauges prior to installation for pile caps 1 and 3 (see Figure 4-2). However, for caps 2 and 4, the center pile of the middle row was not instrumented with strain gauges. The strain gauges were placed at pre-determined depths of 2, 6, 11, and 13.5 ft below the tops of the piles. Strain gauges were placed along the north and south sides of the piles in the direction of loading. The strain gauge depths were determined through computer modeling to be the most critical depths in developing bending moment curves for the laterally loaded piles. Figure 4-3 is a photo of an installed pile group.

The piles were driven so that they would extend 2 ft into the base of the pile cap. In some instances this objective was not precisely accomplished, so the piles were cut off to the correct elevation. A steel reinforcing cage was installed at the top of each test pile to connect the test piles to the pile cap. The reinforcing cage consisted of 6 #8 reinforcing bars which were confined within a #4 bar spiral with a diameter of 8 inches and a pitch of 6 inches. The reinforcing cage extended 2.25 ft above the base of the cap and 8.75 ft below the base. The steel pipe pile was filled with concrete with an average unconfined compressive strength of 5150 psi as determined based on tests of four specimens. A drawing showing the cross-section for the test piles is provided in Figure 4-4. Once the piles were filled, construction of the pile cap was then commenced.

Figure 4-1 shows plan and profile drawings of pile caps 1 and 2. Pile caps 1 and 2 (the two northern-most pile caps) were constructed by excavating 2.5 ft into the virgin clay. The concrete was poured directly against vertical soil faces on the front and back sides of each pile cap. This construction procedure made it possible to evaluate passive force against the front and

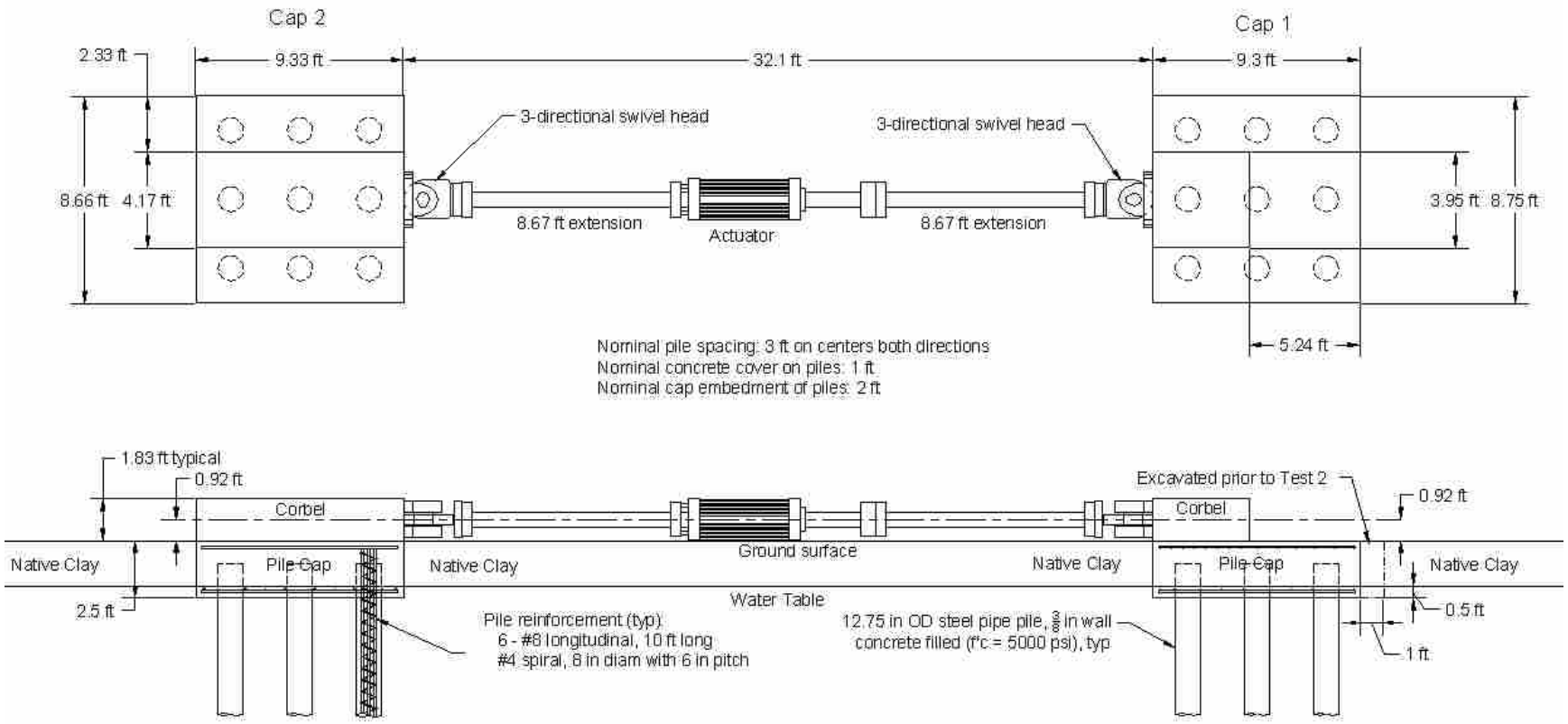

Figure 4-1 Plan and profile drawings of pile caps 1 and 2 during Test 1

back faces of the pile caps. In contrast, plywood forms were used along the sides of all of the caps and were braced laterally against the adjacent soil faces. This construction procedure created a gap between the cap sidewall and the soil so that side friction would be eliminated.

Pile cap 3 was constructed in a similar manner, except that flowable fill was installed under the pile cap to a depth of 7 ft below the top of the finished cap, 9 ft wide, and 13.5 ft in the direction of loading before piles were driven. Flowable fill was also installed on the north side of the cap to the same depth as that installed under the cap and then, after cap installation, up the side at a width of 4.5 ft from the pile cap to the level of the top of the cap. Additional information on the flowable fill application can be found in Miner (2009). Pile cap 4 was constructed in the same way as cap 3, except that compacted fill was installed. The compacted fill was installed to a depth of 6 ft below the top of the pile cap with a width of 9 ft. In the direction of loading, the compacted fill was flush with the south side of the pile cap and extended 5 ft beyond the north side for a total length of approximately 14 ft. Compacted fill was also installed along the north side of the cap to the level of the cap.

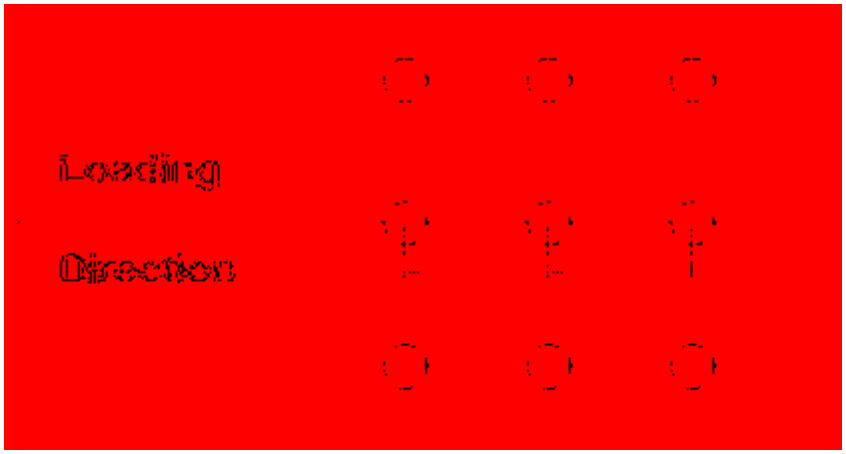

Figure 4-2 Three by three driven pile group, all 3ft OC in both directions (strain gauge instrumented piles circled with dotted line)

Figure 4-3 Driven pile layout prior to cap construction

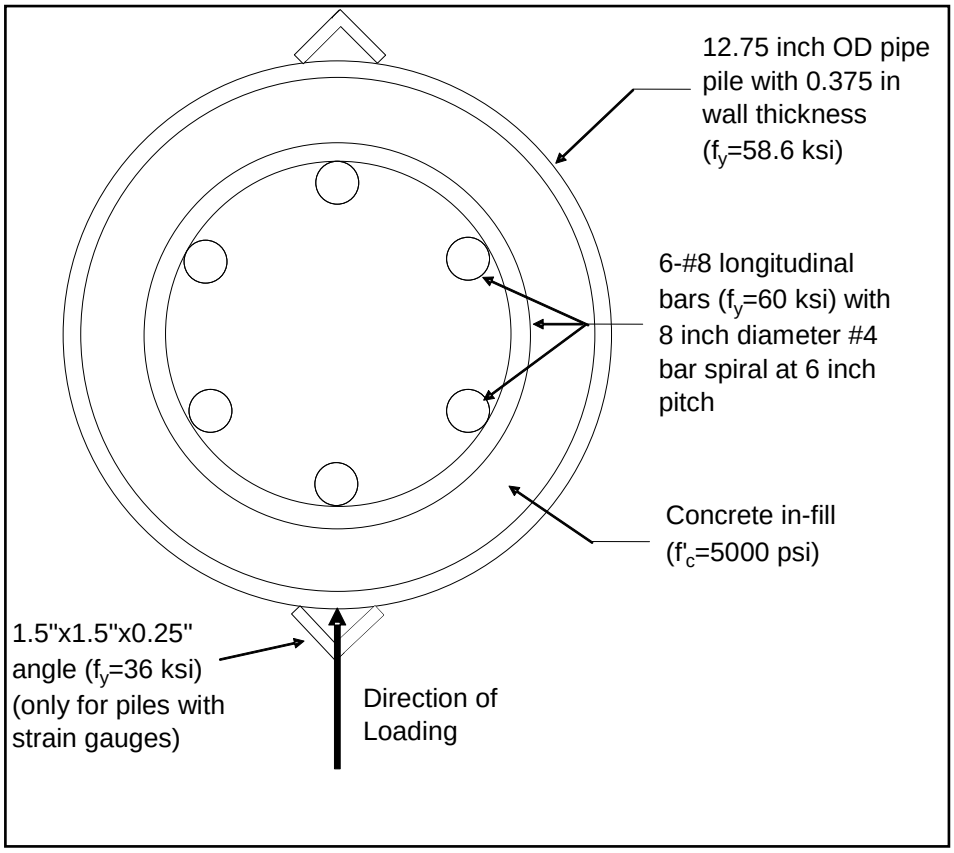

Figure 4-4 Cross-section of piles within the pile groups

Steel reinforcing mats were placed in the top and bottom of each cap with a 3 inch concrete cover. The top reinforcing mat in the pile caps was designed with #7 bars at 10 inch spacing in both directions, with a decrease in spacing to 6 inches in the transverse direction

under the short corbel on caps 1 and 4. The bottom mats were designed with #9 bars at 6.5 inch spacing longitudinally and #7 bars at 10 inch spacing transverse to the load direction. Plan view drawings of the bottom and top reinforcing mats for pile caps 1, 2, 3, and 4 are provided in Figure 4-5 and Figure 4-6, respectively.

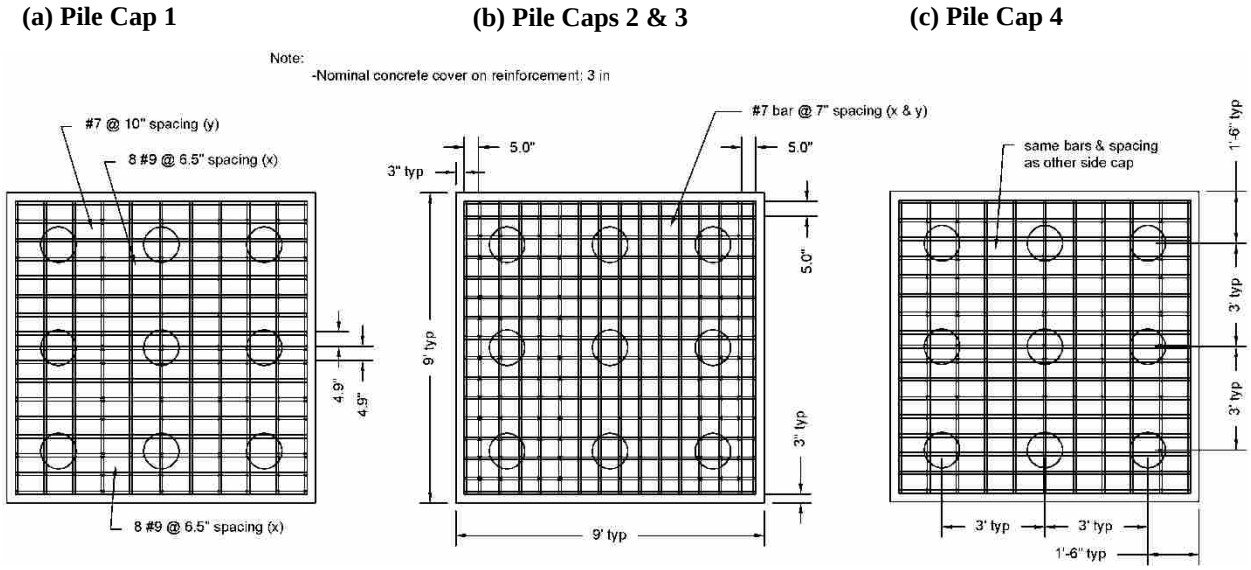

Figure 4-5 Bottom reinforcing mat layout for the test pile groups

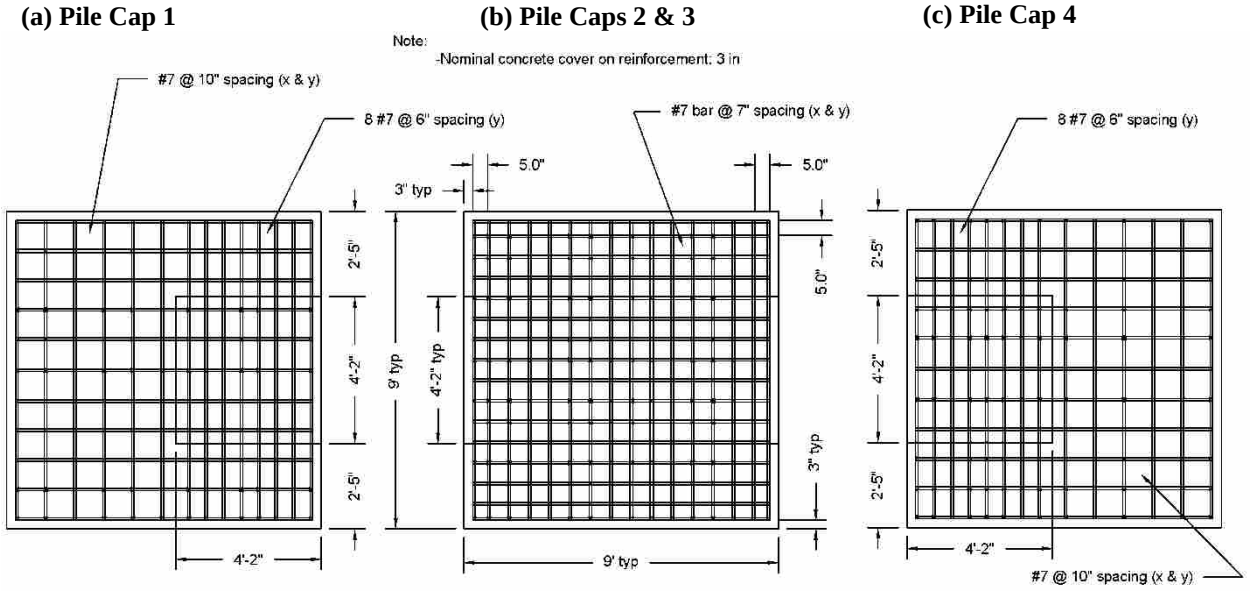

Figure 4-6 Top reinforcing mat layout for the test pile groups

A corbel was constructed on each cap to allow the actuator to apply load above the ground surface without affecting the soil around the pile cap. The corbel extended the full length of the pile cap for cap 2 but was only about half of the pile cap length in cap 1 as shown in Figure 4-1 and similarly for caps 3 and 4 respectively. The corbel was designed in accordance with ACI Standard 318. The corbel was reinforced with #5 bar hoops and #9 bars as main reinforcement as shown in Figure 4-7 and Figure 4-8. Design calculations and steel reinforcement drawings are available and found in the appendix.

4.2 Actuator Layout

Most of the tests performed involved reacting one pile group against another, through applying a lateral load with an MTS actuator with the load centered at a height of 0.92 ft (11 inches) above the top of the pile cap. Each actuator had a capacity of approximately 450 kips in tension and 600 kips in compression. The pile groups were spaced approximately 30 ft apart. This spacing was considered large enough to ensure that the volumes of soil affected by the displacement of each foundation would not interfere with any of the other soil being tested. The actuators were fitted with two 8.67-ft extension pieces each made of 8.5 inch diameter, 69 ksi steel pipe with a wall thickness of 0.75 inches in order to span the distance between the two foundations. Plates were welded to the ends of the extensions to connect the extensions to the actuators and the pile caps. The actuators were attached to each corbel using steel tie-rods which extended through PVC sleeves in the corbel and were bolted to the back face of the corbel. The tie-rods were post-tensioned to minimize displacement of the extensions and actuators during the load tests. A three-dimensional swivel head was located at each end of the actuator to provide a zero moment or “pinned” connection. Each swivel could accommodate ± 5^{o} of vertical pile cap

rotation and ± 15º of horizontal pile cap rotation. Figure 4-9 is a photo of the actuators and extensions positioned between two pile caps.

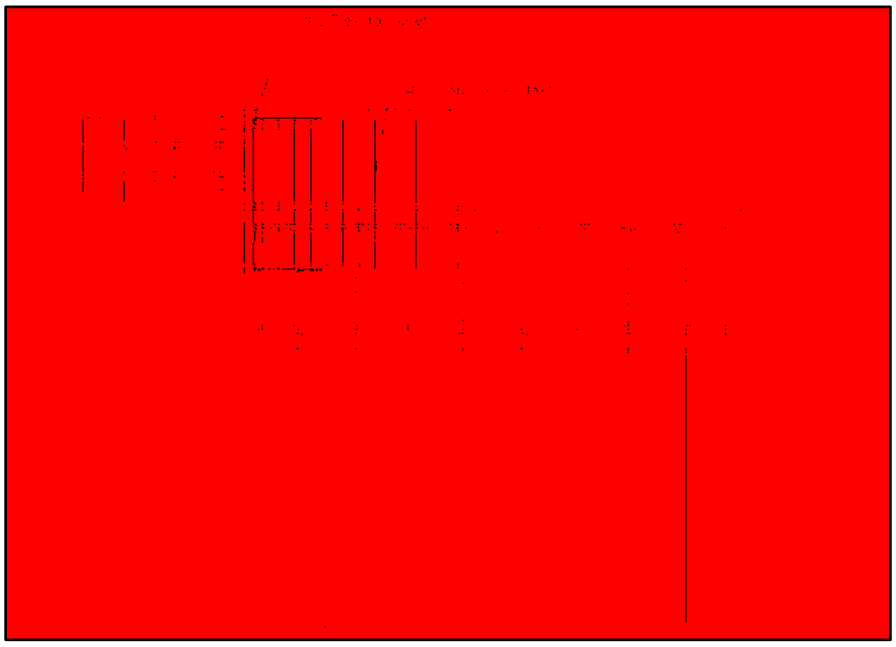

Figure 4-7 Corbel steel layout for caps 1 and 4

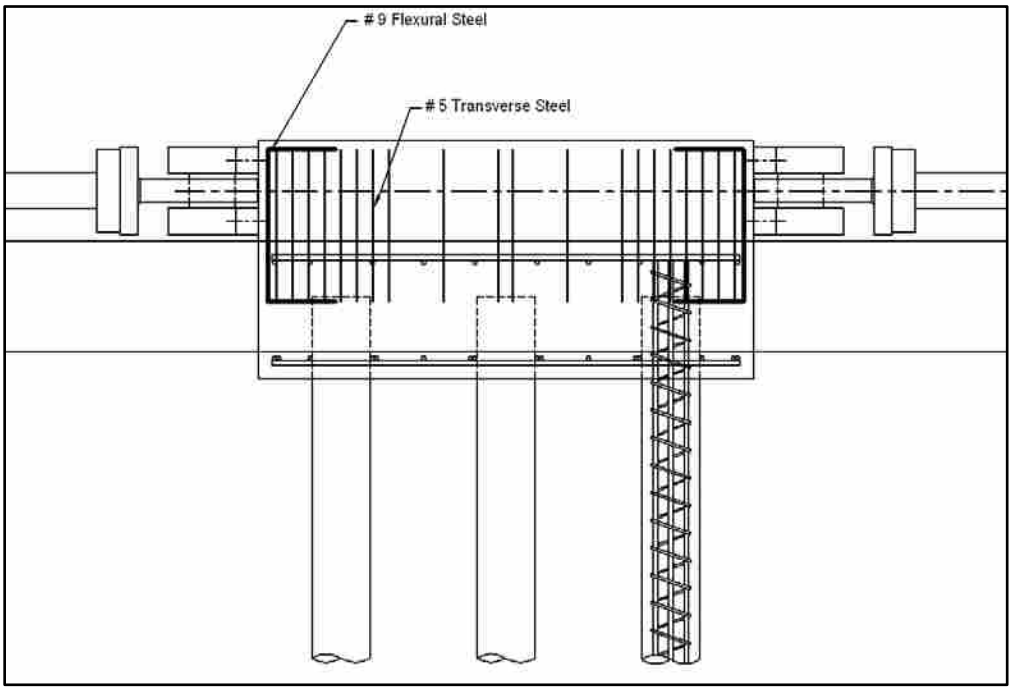

Figure 4-8 Corbel steel layout for caps 2 and 3

Figure 4-9 Photo of actuator setup between caps 1 & 2

4.3 Instrumentation

Six types of instrumentation were used during the tests. Strain gauges, inclinometers, shape arrays, string potentiometers, actuator pressure transducers (for load measurements), and surface grids were the primary methods of instrumentation. As mentioned before, the middle piles were instrumented with strain gauges at depths of 2, 6, 11, and 13.5 ft and the angle iron was used to protect the strain gauges during pile driving. The depths of the strain gauges will vary slightly due to the different driving depth of each individual pile. However, the individual driving depth of each pile was carefully recorded so the actual depths of the strain gauges could be obtained. Some of the strain gauges were damaged in the installation process and therefore some instrumented piles will not have data for all strain gauge depths.

In addition to the strain gauges, the middle piles of the north and south rows of each pile group were instrumented with inclinometer casings. These casings were placed in the center of the piles before they were filled with concrete and extended the entire depth of the pile. After the concrete was poured and cured, the inclinometer casings provided an effective means of obtaining the pile and pile cap deflections during testing. Inclinometer measurements were typically performed before testing and then again once the 1.5-inch nominal displacement increment had been reached. Using a standard inclinometer and corresponding data acquisition unit, the pile deflections were recorded at 2-ft depth intervals.

A 1-inch PVC pipe was also placed next to the inclinometer casings before the concrete pour. These pipes were fitted with a new measuring technology called shape accelerometer arrays (shape arrays) manufactured by Measurand, Inc. In addition to the middle north and south piles, the center piles were also equipped with the shape arrays. Each shape array consisted of a 25-ft long, flexible, waterproof cable which had triaxial micro-electrical-mechanical (mem) type accelerometers embedded at 1-ft intervals. By double integrating the accelerations at each level throughout time, the shape arrays provided real-time displacement versus depth profiles at 1-ft intervals throughout the entire testing period relative to the initial deflected shape. The shape arrays were designed to provide displacements with accuracy similar to that obtained from an inclinometer. To provide accurate measurements from the shape arrays, a tight fit between the 1 inch PVC pipe and the shape array must be maintained. To accomplish this, nylon webbing of various thicknesses was inserted along the length of the shape array to minimize any gaps between the shape array and the PVC pipe.

Lateral pile cap displacement was measured using two string potentiometers (string pots) attached to the pile cap at the elevation of the loading point (0.92 ft above the top of the cap) on

the east and west sides of the actuator attachment point. Lateral pile cap displacement was also measured on the back side of each corbel with two string pots attached 0.167 ft (2 inches) and 1.75 ft (21 inches) above the top of the pile cap directly in line with the load direction. Finally,

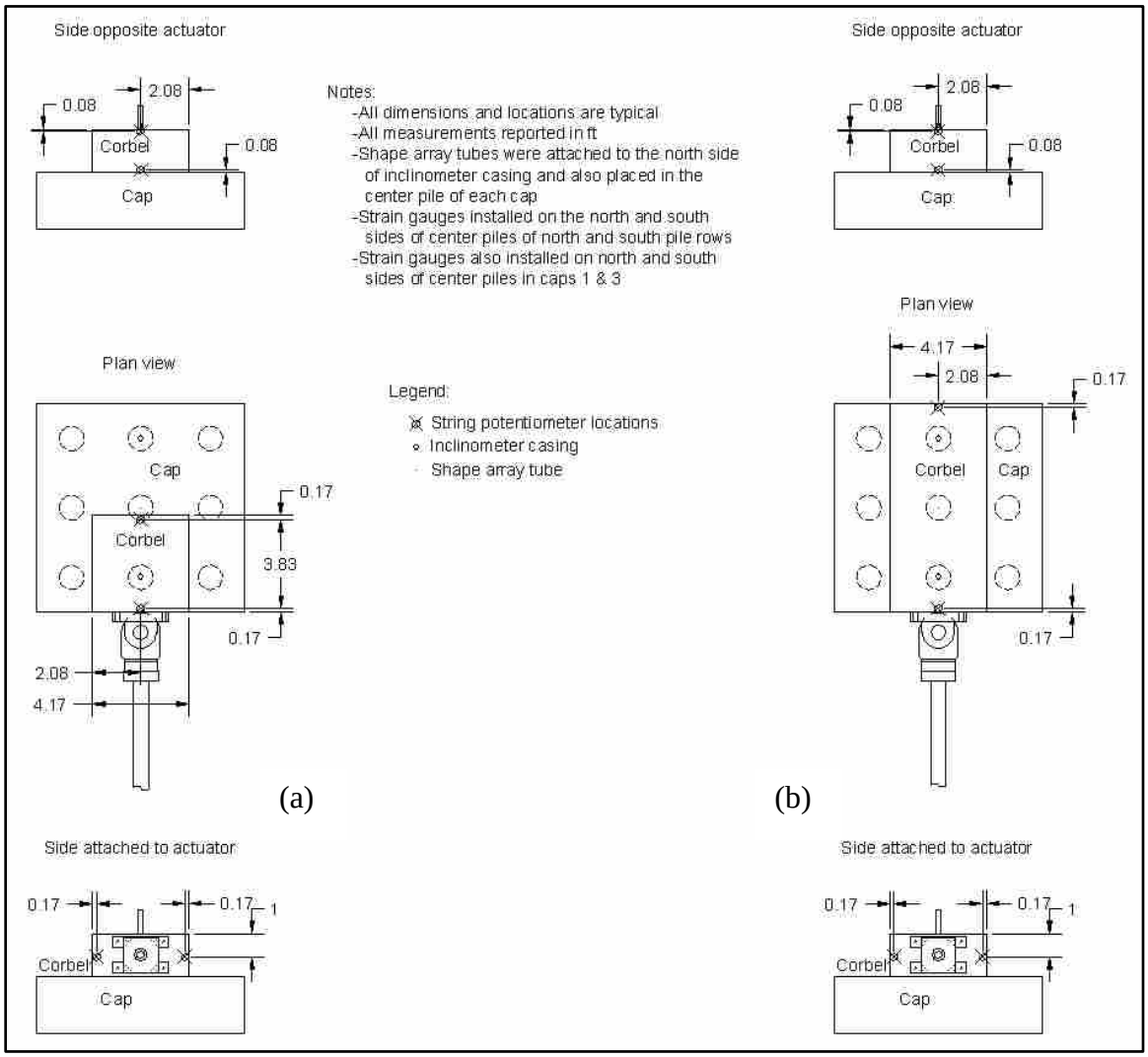

Figure 4-10 Typical instrumentation layout for pile caps with (a) a partial length and (b) a full length corbel

vertical pile cap displacement was measured at two points along the length of each pile cap to evaluate pile head rotation. Each potentiometer was attached to an independent reference beam supported at a distance of about 6 ft from the side of the pile cap. Figure 4-10 shows the

locations of the string pots used in the various tests (with any exceptions being noted in the corresponding test results section(s)).

Applied load was measured directly by the load cell on the actuator which was calibrated in the laboratory prior to testing in the field. Load data were recorded using the actuator control computer and software, with a data sampling rate of 20 scans per second.

4.4 Test Procedure

This section describes the general lateral load test procedure used for this series of tests. Any variations will be individually discussed.

Lateral pile group load testing was conducted from July 16 to August 29, 2007. The piles had been driven about one month prior to the first test. Load was applied to the pile caps using the actuator which was powered by a portable pump with a 60 gallon/minute capacity. The pump unit was powered by a portable diesel generator. At times, the actuators loaded the pile caps for an extended period of time, which caused the circulating hydraulic fluid in the pumps to rapidly rise in temperature. The hydraulic pumps were programmed to disengage when the temperature of the fluid reached about 132° F. In order to keep the temperature of the hydraulic fluid from reaching this critical temperature, water was circulated through the hydraulic pumps to cool the fluid. The lateral load tests were carried out with a displacement-control approach with actuator displacement increments of approximately 0.125, 0.25, 0.50, 0.75, 1.0, and 1.5 inches. However, these increments were used as rough predictions of the displacement of the pile caps. During this process the actuator extended or contracted at a rate of about 1.5 inches/minute. In addition, at each increment, 10 cycles with peak displacement amplitudes of about ±0.05 inches were applied with a frequency of approximately 1 Hz to evaluate the cycle

response of the pile cap. After these small cyclic displacements at each increment, the actuator was pulled back to the initial starting point prior to loading it to the next higher displacement increment. Due to differences in resistance between the adjacent pile groups, the pile caps were not pulled back to their exact starting positions along with the actuators. Typically, the testing procedure was paused at the end of the 1.5 inch (final) test increment cyclic portion and held for 20 to 30 minutes while inclinometer measurements were made before ramping back down to zero displacement. Schematic layouts of each of the tests performed on the virgin soil, the compacted fill, and the RAPs will be shown with the test results in chapters 7, 7.2.5, and 9. The plan and profile views of the layouts for the compacted fill tests and the RAP tests are also included in the following chapter under their respective installation procedures.

5 SOIL IMPROVEMENT INSTALLATION PROCEDURES

The installation of both the compacted fill and the RAPs involved excavation and replacement of the in-situ soil with a more competent material. As indicated previously, these compacted fill and RAP zones were designed to increase the lateral resistance of the pile caps and the tests were used to evaluate the potential soil improvement that could be expected.

5.1 Compacted Fill Installation Procedure

Compacted fill was used to strengthen the soft clay surrounding one full-scale pile cap supported by driven pile foundations. Before installation of pile cap 4, the soft clay was excavated and replaced with compacted sand from a depth of 6 ft below the ground surface to 2.5 ft below the ground surface over an area of 9 ft by 14 ft in 6 inch lifts. Clean concrete sand generally conforming to ASTM C-33 specifications was used as the fill in the compacted fill tests. The modified Proctor dry unit weight of the fill was 111 pcf and it was relatively insensitive to moisture content within the range of 5 to 1 percent (Walsh 2005). Figure 5-2 shows the grain size distribution curve for the sand used at the site. Based on measurements from a nuclear density gauge, the sand was compacted to an average in-place dry density of 104 pcf, which is 93.7 percent of the modified Proctor density ($\gamma_{d,max}$). Compaction was performed using a hydraulic plate compactor attached to the end of a track hoe as shown in Figure 5-1. The initial compaction of soil occurred before the installation of the piles. When the

Figure 5-1 Compaction of fill under future pile cap 4 using a hydraulic plate compactor attached to the arm of a track hoe

piles were installed, the ground heaved and, in order to maintain the correct pile cap thickness, approximately1 ft of fill had to be removed, leaving approximately 2.5 ft under the cap. Due to this heave, the density of the fill under the pile cap may have changed prior to testing. Figure 4-3 is a picture of the piles and the sand compacted around them.

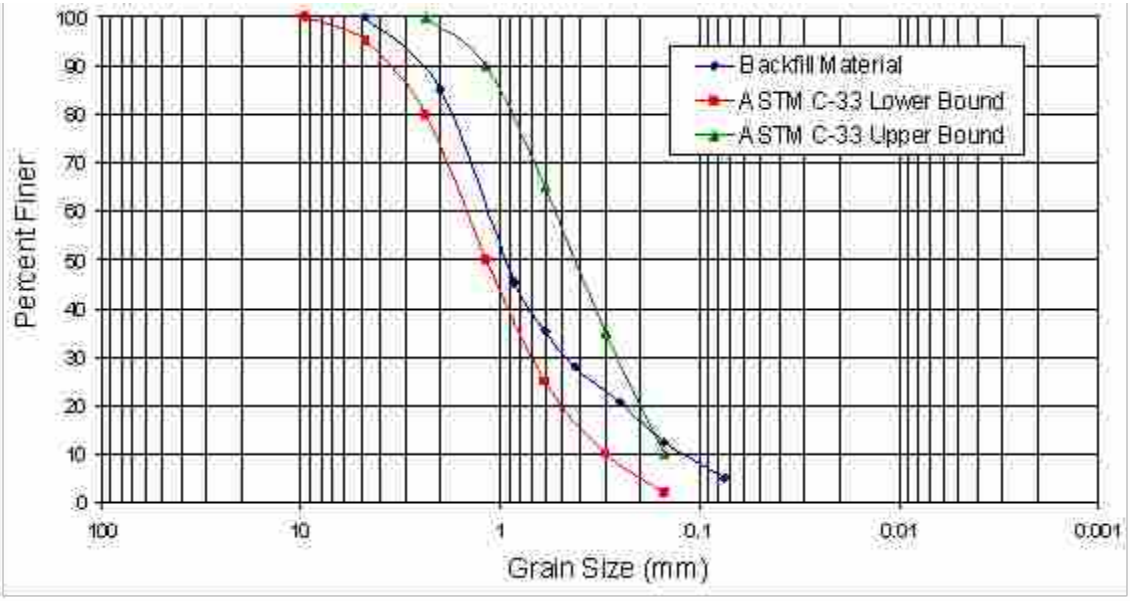

Figure 5-2 Grain size distribution curve including upper and lower limits (Walsh 2005)

After the pile cap was poured and cured, the first test on the pile cap underlain with compacted sand was performed. During the first test performed on the pile cap (Test 3), no soil was placed against the pile cap so that there was no passive resistance against the pile cap. Once this test was completed, sand was compacted from the level of the base of the cap in one 12 inch lift, one 6 inch lift, and three 4 inch lifts using a jumping jack type manual compactor as shown in Figure 5-3. The bottom layer was thicker to provide a base against the soft clay to facilitate compaction of the subsequent layers. The sand was compacted to an average dry unit weight of 110.7 pcf based on nuclear density gauge tests. The results from the nuclear gauge testing are shown in Table 5-1. This density was approximately equal to 100 percent relative compaction based on the modified Proctor maximum unit weight. The new compacted fill covered an area extending1 ft beyond the cap on either side (east to west) of the cap to a distance of 5 ft from the north face. Plan and profile drawings of the layout of the compacted fill zone for the test involving compacted fill extending beyond the pile cap 5 ft with no compacted fill against the face of the pile cap are provided in Figure 5-4. Plan and profile drawings of the layout of the other tests involving compacted fill are provided in Figure 5-5.

Table 5-1 Nuclear density gauge test results for compacted fill in front of cap 4

Depth below top of pile cap (inches)	Lift thickness (inches)	Dry unit weight (lb/ft^3)	Moisture content (%)
18	12	110.8	7.5
12	6	110.2	5.4
8	4	110.0	11.5
4	4	110.3	10.4
0	4	112.1	11.7

The test sequence on this pile cap was designed to evaluate the effect of having a 5 ft zone of compacted sand on one side of the cap and native clay on the other side. By comparing the results from pushing the pile cap into the two different soils, the overall difference in resistance was evaluated.

Figure 5-3 Passive resistance region of compacted sand fill being compacted

5.2 RAP Installation Procedure

RAPs are a shallow alternative to deep foundations. They create a dense gravel column which reinforces the surrounding soil. In addition, they increase the normal stress in the surrounding soil and will also compact the soil if it is cohesionless. When testing was complete on the compacted fill, 30-inch diameter RAPs were installed in a grid pattern south of pile cap 4. Plan and profile drawings are shown in Figure 5-9.

Geopier Northwest did the design, installation, and quality control for the RAPs used in this study. The thirteen RAPs were installed in the order and geometry depicted in Figure 5-6. The RAPs were spaced at 36 inches in the direction of loading and 40 inches in the direction

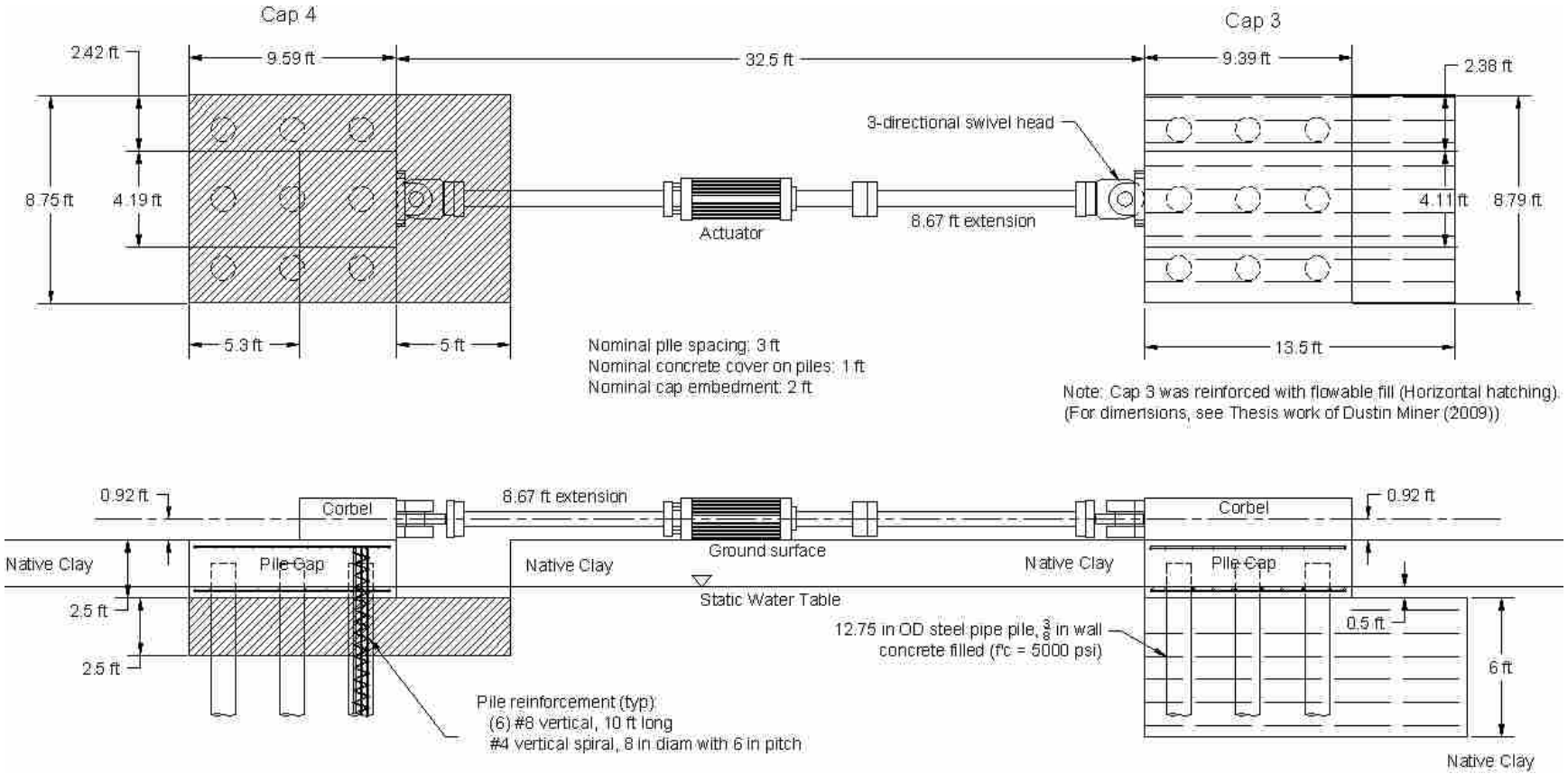

Figure 5-4 Plan and profile of compacted fill treated area for Test 3 (diagonal hatching)

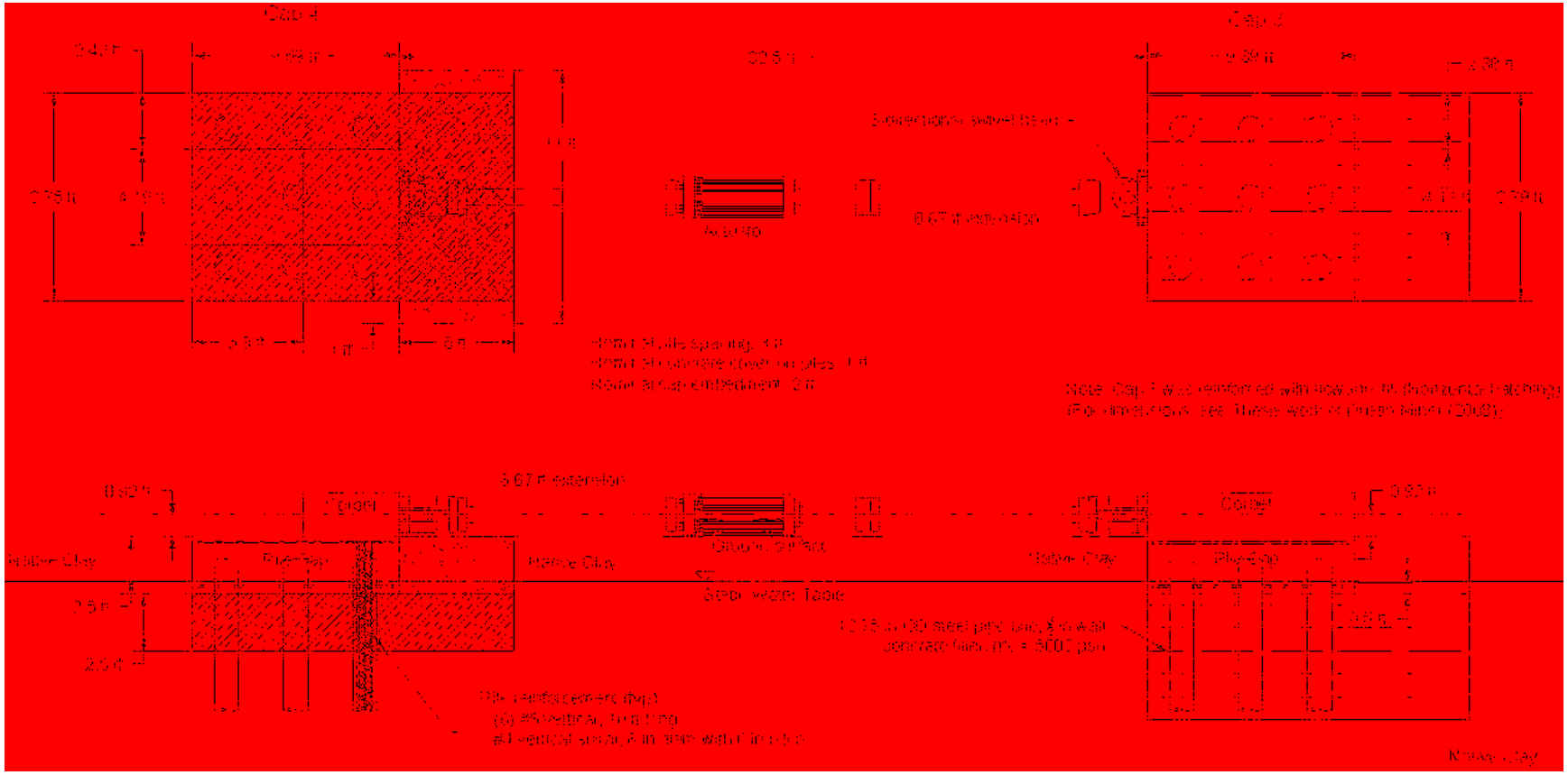

Figure 5-5 Plan and profile of compacted fill treated area for Tests 4 & 5 (diagonal hatching and spotted hatch)

transverse to loading. The 13-pier configuration consisted of 4 piers next to the cap, 5 piers in the middle row, and 4 piers in the row farthest from the cap. Installation of the RAPs was started and completed on 9 August 2007.

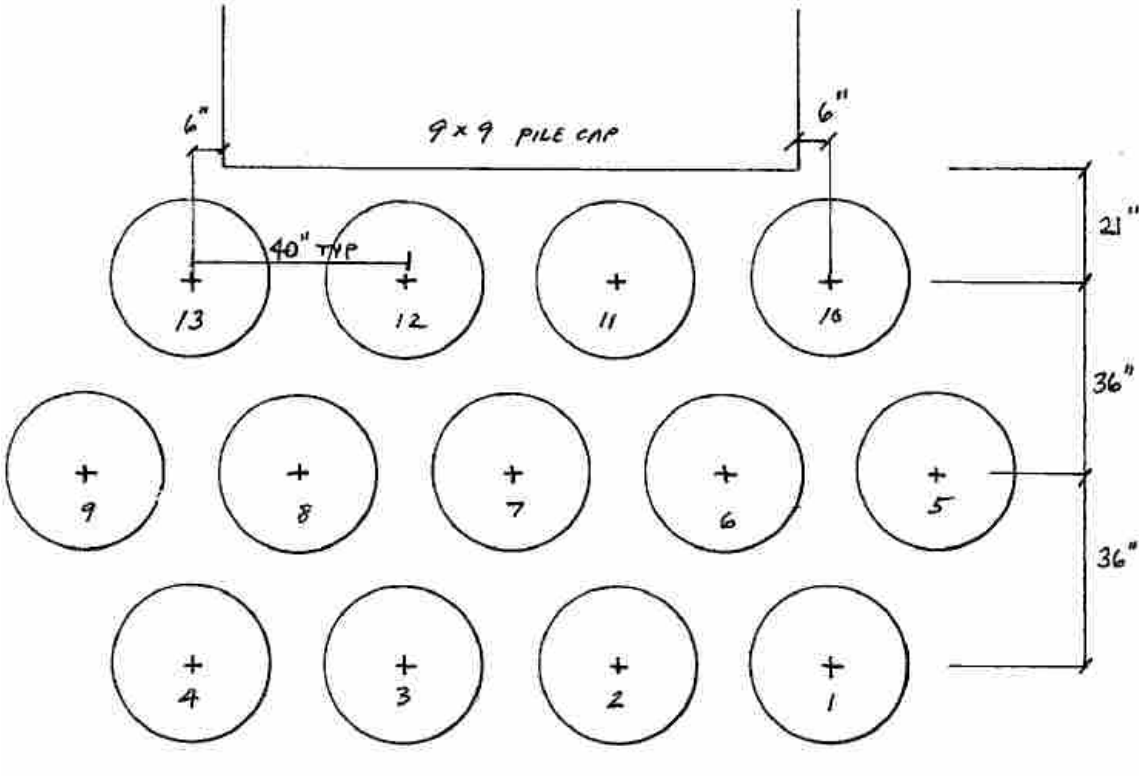

Figure 5-6 RAP installation configuration

Compared to other soil reinforcement methods, the installation process for RAPs is relatively simple (see Figure 2-9). First, a hole needs to be excavated to the desired depth (see Figure 5-7). Then, large aggregate (3 to 6 inch minus material) is compacted into the bottom of the hole to create a firm base upon which to build the rest of the RAP (see Figure 5-8). Once the base is in place, thin layers (approximately1 ft compacted thickness) of smaller aggregate (1 inch minus with <10 percent fines) are compacted using a high-powered, hydraulic rammer on top of the base until the pier reaches the level of the ground surface (see Figure 5-1).

Figure 5-7 Excavation for RAP installation

Figure 5-8 Ramming of base material into bottom of excavated RAP hole

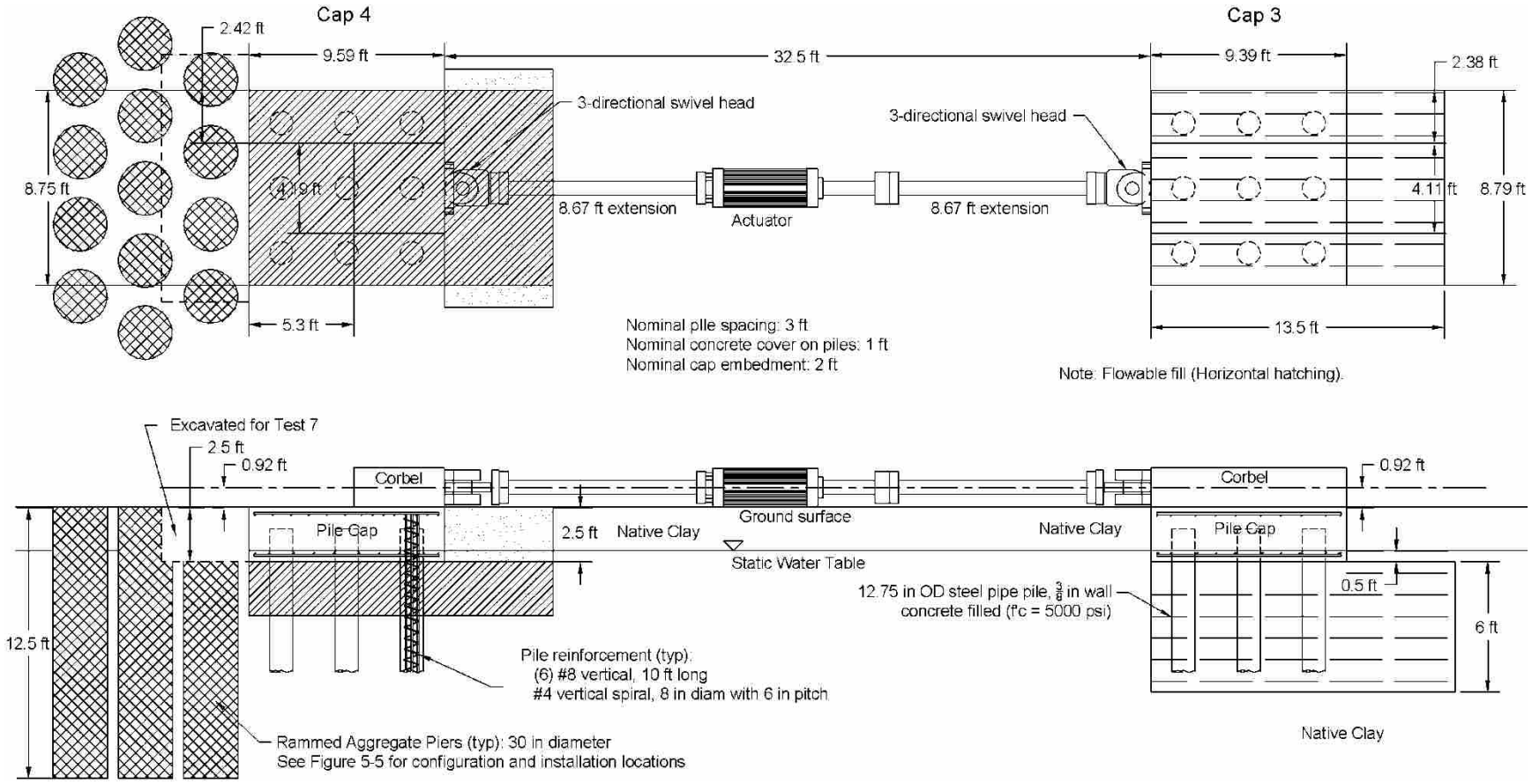

Figure 5-9 Plan and profile for Tests 6 and 7 on RAPs: diamond hatching representing RAPs and dashed line representing soil excavated for Test 7

During the installation process, density measurements were taken to ensure consistent and sufficient compaction of the aggregate. Dynamic cone penetration tests were performed on two of the columns and penetration resistance exceeded 40 blows per 1.75 inches of penetration. This indicates that the RAP is in a very dense state. Figure 5-2 shows the quality control log for the installation of the RAPs used in this test series.

Figure 5-1 Placement of 1 ft lift for compaction of main body of RAP

GEOPIER FOUNDATION COMPANY

GEOPIER
DAILY QUALITY CONTROL FORM

Project Name: BYU Research Installer: Geopier Northwest Project No.:

Date: 8/9/2007 QC: Rob Jackson Page 1 of 1

Footing Location/ Grid	Pier No.	Top of Pier Depth	Drill Depth (ft) Plan	Drill Depth (ft) Actual	Field Test Results No. Lifts	Stiffness BST	Stiffness DCPT	Conditions Encountered [1]	Casing? Y/N
	1	0	12.5	12.5	14				N
	2	0	12.5	13.5	16		40+		N
	3	0	12.5	12.5	14				N
	4	0	12.5	12.5	14				N
	5	0	12.5	12.5	15				N
	6	0	12.5	13	15				N
	7	0	12.5	12.5	13				N
	8	0	12.5	12.5	15		40+		N
	9	0	12.5	13	15				N
	10	0	12.5	12.5	14				N
	11	0	12.5	12.5	14				N
	12	0	12.5	12.5	14				N

Figure 5-2 Quality control table for RAPs

As with the compacted fill, two tests were performed on the RAPs once installation was complete. The first test involved pushing pile cap 4 into the newly installed RAPs with the native clay against the face of the pile cap as shown. The upper portion of the area adjacent to the pile cap was then excavated to the level of the base of the pile cap and the second test was performed without soil against the front face of the pile cap. Figure 1-3 contains photos of the excavation process and the finished excavation. In the finished excavation, the lighter gray portions are clay and the darker material is from the RAPs. Figure 1-13 further illustrates the contrast.

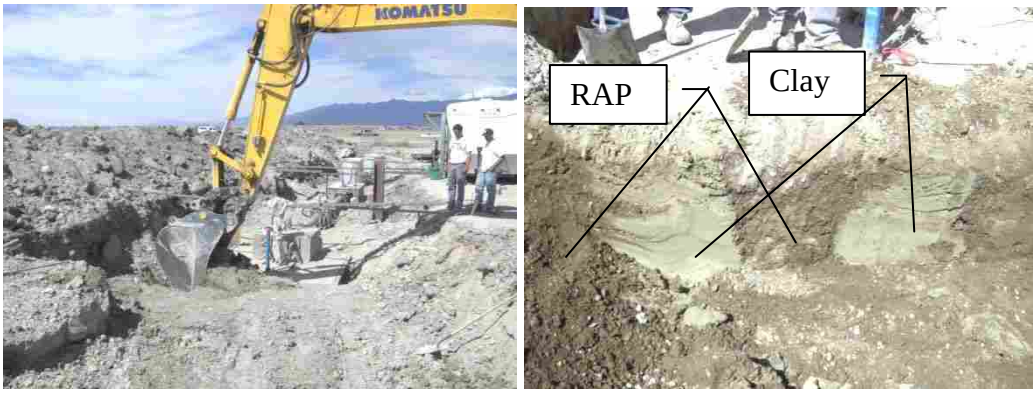

Figure 1-3 Photos of excavating of top layer of RAPs and of the excavation showing the difference between the clay and the material from the RAPs

Figure 1-13 Photo of finished excavation with the RAP columns highlighted

6 TEST RESULTS INTRODUCTION

The following chapter will present the results of the two tests performed in untreated native clay along with the test performed on untreated native clay with the pile cap underlain with compacted fill. The two subsequent chapters will present the results from the tests performed in soil treated with compacted fill and RAPs. The basic approach to each of the tests was to first laterally load the pile groups in either the virgin native clay or in the treated clay. Next, the soil adjacent to the pile cap was excavated away from the face to the base of the cap and the pile cap was once again laterally loaded. This was done to determine the approximate soil resistance acting on the face of the pile cap during load testing. Test 1 was performed on virgin clay and Test 2 was performed in virgin clay following excavation of material along the face of the cap. Test 5 was performed with virgin clay against the face of the pile cap but with the pile cap underlain with compacted fill. Tests 3 and 4 were performed on the compacted fill, while Tests 6 and 7 were performed on the treated soil following installation of the RAPs.

A number of other types of data were also collected during the tests. The following list introduces the results which will be displayed for each of the tests, as well as the instruments which were used to obtain the data from which the results are based.

1. Continuous plot of actuator load versus pile cap displacement
    - Instruments: pressure transducers and string potentiometers (string pots)
2. Plot of peak actuator load versus pile cap displacement per test increment
    - Instruments: pressure transducers and string pots

3. Plot of pile head rotation versus actuator load
    - Instruments: pressure transducers and string pots
4. Plot of displacement versus depth below bottom of pile cap for instrumented piles
    - Instruments: shape arrays and inclinometers
5. Plot of moment versus depth below bottom of pile cap for instrumented piles
    - Instruments: shape arrays, strain gauges, and inclinometers
6. Plot of maximum bending moment versus applied load for instrumented piles
    - Instruments: shape arrays, strain gauges, and pressure transducers

6.1 Baseline Selection and Test Numbering

Each of the pile caps were displaced multiple times and in opposite directions. Thus, each of the displacements and strains measured with the above instrumentation are all measured relative to the original position of the piles and pile caps prior to testing. Therefore, any residual displacement created from previous tests will result in a non-zero value for the initial displacement of the foundation for subsequent tests. Also, deflections were all measured as positive in the direction of loading during a particular test. A good example of this can be seen in the plots of actuator load versus pile cap displacement for the three native clay tests in Chapter 7. For the first test, pile caps 1 and 2 were pulled together during testing. Following the test and after disengaging the actuators, pile caps 1 and 2 remained displaced towards each other approximately 0.3 inches from their original positions. This value is the starting displacement of each of the pile caps in Test 2, and can be seen in Figure 7-24. The starting displacement is plotted as a negative value because the residual displacements left over from Test 1 were a result of pulling the pile caps together and were in the opposite direction of loading for Test 2. Two

different foundation positions were chosen as the baseline for foundation displacement during testing. The first baseline was chosen as the position of the pile cap prior to the beginning of any testing (i.e. before Test 1). This baseline was used to measure displacements for Test 1 and Test 2. The second baseline was chosen as the position of the foundation prior to Test 3. This was the position of the foundation prior to testing the compacted fill. The reference frames and instrumentation were necessarily removed from pile caps 1 and 2 and connected to pile caps 3 and 4 between Tests 2 and 3, making it impossible to continue using the original baseline. Therefore, this new baseline was selected. The new baseline was used for Test 3 through Test 7.

Additionally, the numbered tests in the following chapters relate to those tests which were performed to evaluate the strength improvement from the compacted fill and RAPs. As mentioned previously, the results from testing done on flowable fill, jet grouting, and mass mixing will not be presented in this thesis.

6.2 Bending Moment Curve Construction

When evaluating the lateral resistance of deep foundations, it is important to know the maximum bending moment and the depth in the pile where it occurs. The bending moment, M, was calculated from the shape array and inclinometer deflection data using the equation

$$M = EI\frac{\partial^2 y}{\partial x^2} \tag{6-1}$$

where E is the modulus of elasticity, I is the moment of inertia, and $\partial^2 y/\partial x^2$ is the curvature along the length of the pile. This equation can be approximated numerically using the equation

$$M = \frac{EI(f_{-1} - 2f_0 + f_1)}{h^2} \qquad (6\text{-}2)$$

where f_{-1} is the horizontal displacement one level above the point of consideration, f_0 is the displacement at the point of interest, f_1 is the displacement one level below the point of interest, and h is the distance between equally spaced displacement measurement depths. The moment computed using Equation (6-2) is very sensitive to minor variations or errors in the measured displacement versus depth curves. To reduce the influence of minor variations in the measured displacement data on the computed moment, a multi-order polynomial equation was developed from the measured data to smooth the displacement versus depth curves. Fourth through sixth order polynomial curves were used to develop the smoothed curves depending on the curvature of the plot of the measured data. The polynomial curve which gave the most realistic results was chosen to define the final smoothed curve. The displacements used in Equation (6-2) were then based on smoothed values computed with the polynomial equation. While the difference in the displacement values at any depth were generally very small, this procedure produced moment versus depth curves with more realistic shapes.

As indicated previously, the spacing between the shape array nodes is 12 inches, which corresponds to the interval h. A composite EI of 14.15 x 10^9 lbs-in^2 for the concrete filled pile was used based on the EI of the steel pile and the EI of the concrete used to fill the pile. To calculate the EI of the steel pile, a modulus of elasticity of 29 x 10^6 psi and a moment of inertia of 344 in^4 was used. Similarly for the EI of the concrete, a modulus of elasticity of 4.1 x 10^6 psi based on the 5100 psi unconfined compressive strength and a moment of inertia of 1018 in^4 was used. Additionally, using Equation (6-2) a positive displacement will produce a maximum bending moment directly under the cap which will be negative.

To complement the bending moments obtained from the shape arrays, strain gauges were also used to derive bending moments. As mentioned before, strain gauges were placed at depths of 2, 6, 11, and 13.5 ft below the top of the pile and the top of the piles were driven with approximately 2 ft of stickup. Since piles cannot be driven precisely to a given elevation, these depths vary to some degree. The bending moments from the strain gauges where obtained from the equation

$$M = \frac{EI\varepsilon_{Combined}}{y} \tag{6-3}$$

where *EI* is the composite modulus of elasticity and moment of inertia for the pile which are the same values used in the shape array bending moments equation, $\varepsilon_{Combined}$ is the difference in strain obtained from the strain gauges located opposite each other at the depth of interest, and *y* is the diameter of the pile or 12.75 inches.

The notation chosen to describe the sign convention of the moments was that a positive displacement of the cap would result in a negative moment at the pile-pile cap interface, and a positive moment at depth. The datum of these graphs was changed to be measured as the depth below the bottom of the pile cap. This was done because once the piles enter the pile cap the EI changes and becomes difficult to estimate without a large degree of uncertainty. The negative bending moments measured at the interface of the piles and pile cap will have some degree of error due to the changing EI. This error is minimized to some degree by the fact that the displacements used to derive the bending moments included those that were obtained from within the pile cap. These bending moments were then truncated to the bottom of the pile cap where the EI could be estimated.

Using Equations (6-2) and (6-3) with the procedures described above, moment versus depth graphs were created. The curves were obtained from the shape arrays and inclinometer readings, while point moments were computed at the locations of the strain gauges. The maximum total load associated with each target displacement is also listed in the legend for each figure.

Occasionally, the polynomial-based bending moment calculations produced unrealistic curves after the point of maximum bending moment and at the pile-pile cap interface. The bending moment calculations are based on curvature, and knowledge of the curvature of the pile above and below the point of interest is needed to calculate a realistic value for bending moment in the pile. The shape arrays generally only extended about 18 to 20 ft below the bottom of the pile cap. The maximum positive bending moment in the piles generally occurs between 10 and 15 ft below the bottom of the pile cap for the maximum loads applied during testing. Therefore, the bending moment curves are not always well defined below the point of maximum positive bending moment. The top 4 to 5 ft of the shape array exited the pile and measured the deflections of the pile cap. Deflection inside the pile cap didn't generally follow the parabolic deflection of the pile. At times, this caused a significant change in the slope of the depth versus deflection curve at the pile-pile cap interface, which affected the bending moment calculations for the upper few feet of the pile before it entered the pile cap. The slope of the upper few feet of the bending moment curve would increase dramatically, or at times the slope would change signs. If the bending moment curves exhibited a drastic change or a reversal in slope near the pile-pile cap interface, those curves were truncated back to the point directly before the curvature started changing drastically. The results for both the extrapolated and calculated maximum negative bending moment at the pile-pile cap interface should not be considered as accurate as

the rest of the bending moment curve (unless validated by strain gauge data). The bending moment curves in the following sections are generally truncated at two locations: the pile-pile cap interface and the point at which the bending moment curve comes back to zero below the point of maximum moment.

A few instances of spurious data points were encountered in the processing of field test data. These points were generally omitted from the figures in subsequent sections.

7 VIRGIN CLAY TEST RESULTS

7.1 Virgin Clay – Test 1

The first test was performed on the virgin clay between pile cap 1 and pile cap 2, the northern-most pile caps. This particular test pulled pile caps 1 and 2 together, as can be seen in the schematic layout in Figure 7-1. The objective of this test was to find the lateral resistance for virgin soil conditions for comparison to later soil improvements.

Initial measurements for string potentiometers, shape arrays, inclinometers, actuator pressure transducer, and strain gauges were taken prior to the test. The locations of all the instrumentation for pile caps 1 and 2 were presented in Section 4.3. Strain gauges on pile cap 1 were located on the three middle piles, but only on the north and south piles of pile cap 2. The test followed the standard testing procedure with one exception. Once the maximum displacement was reached (1.5 inches), the actuator proceeded to perform cyclic loading, and then ramped back down to zero displacement and was not held at the maximum displacement point for inclinometer readings. In order to obtain the inclinometer readings for the 1.5 inch test increment, an additional reload ramp was necessary from which the inclinometer measurements were taken. Finally, since this was the first test, the values measured were all zero-set to the initial values of this test just prior to commencement of testing.

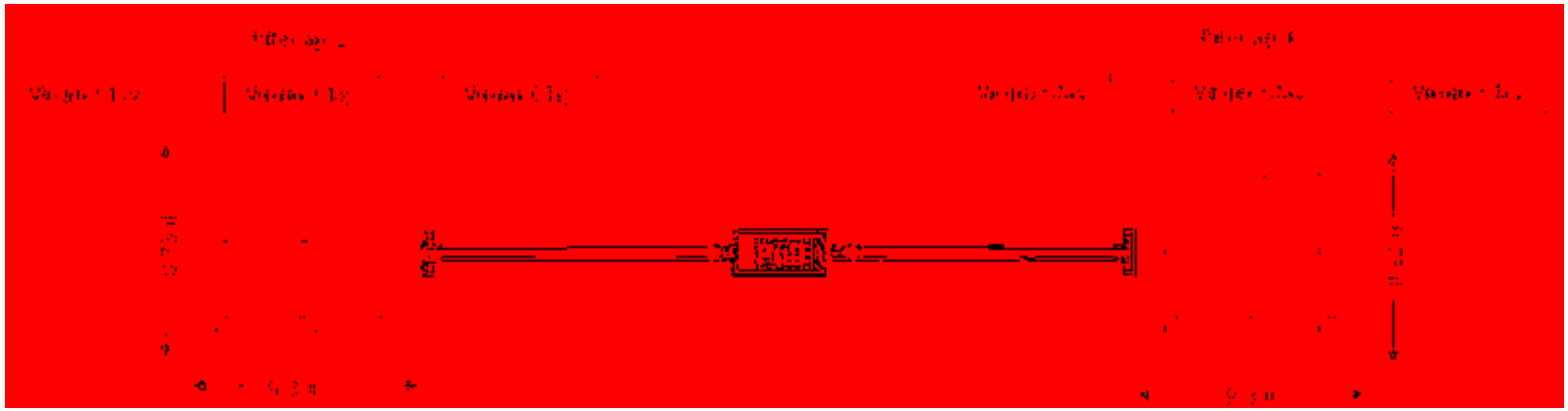

Figure 7-1 Schematic plan view of Test 1

7.1.1 Load versus Pile Cap Displacement

Plots of the continuous pile cap load versus displacement curves for pile cap 1 and pile cap 2 for test 1 are presented in Figure 7-2 and Figure 7-3. These curves were obtained from the actuator pressure transducer and the string potentiometers attached to their corresponding pile cap. These plots illustrate the load path taken during loading, unloading, and reloading for each loading cycle. At the end of each loading cycle it was necessary to apply a tensile force to bring the pile cap back to zero deflection. This residual deformation does not appear to be a result of yielding in the pile based on measured bending moments. The observed residual deformations could have been a result of flow of weak soil into the gap behind the pile during loading or lateral resistance due to side shear on the pile as it moved in the opposite direction. During reloading, the load is typically less than that obtained during virgin loading and considerably more linear. The peak load during reloading is typically about 90 percent of the peak load during the initial loading. After the deflection exceeds the maximum previous deflection for a given cycle, the load increases and the load-deflection curve transitions into what appears to be a virgin loading curve.

The virgin pile cap load versus displacement curves for each pile group have been developed in Figure 7-4 by plotting the peak values and eliminating the unload and reload segments. Although the actuator was set to push the pile caps to target displacement increments of 0.125, 0.25, 0.5, 0.75, 1.0, 1.5 inches, small seating movements in the connection points between the actuator and pile cap at the start of each loading cycle led to somewhat smaller displacements than anticipated. For example, the actual peak displacement increments for pile cap 1 were 0.08, 0.18, 0.38, 0.59, 0.85, and 1.50 inches respectively. Peak displacement increments for pile cap 2 were 0.08, 0.19, 0.39, 0.61, 0.87, and 1.48 inches respectively as

measured by the corresponding string potentiometers. Because selection of the increments were somewhat arbitrary, these small discrepancies are insignificant.

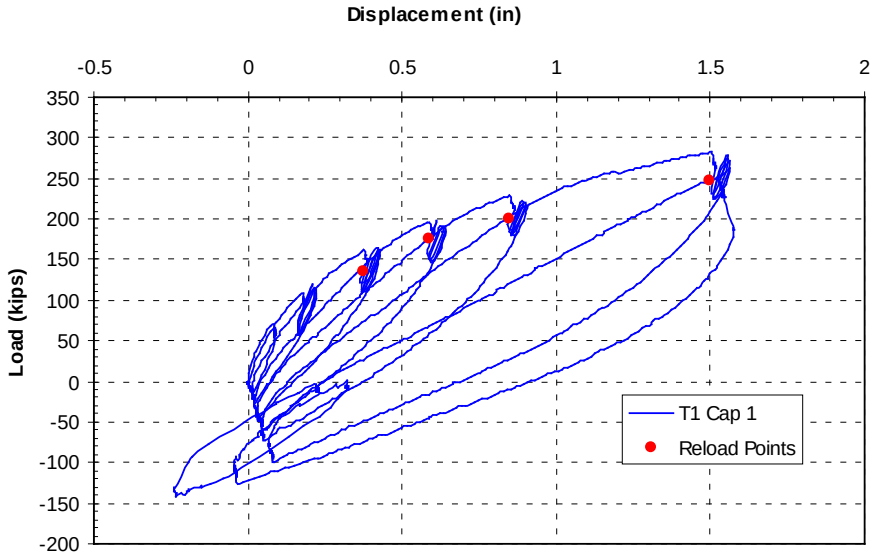

Figure 7-2 Plot of continuous pile cap displacement versus applied load for pile cap 1 during the virgin clay test (Test 1)

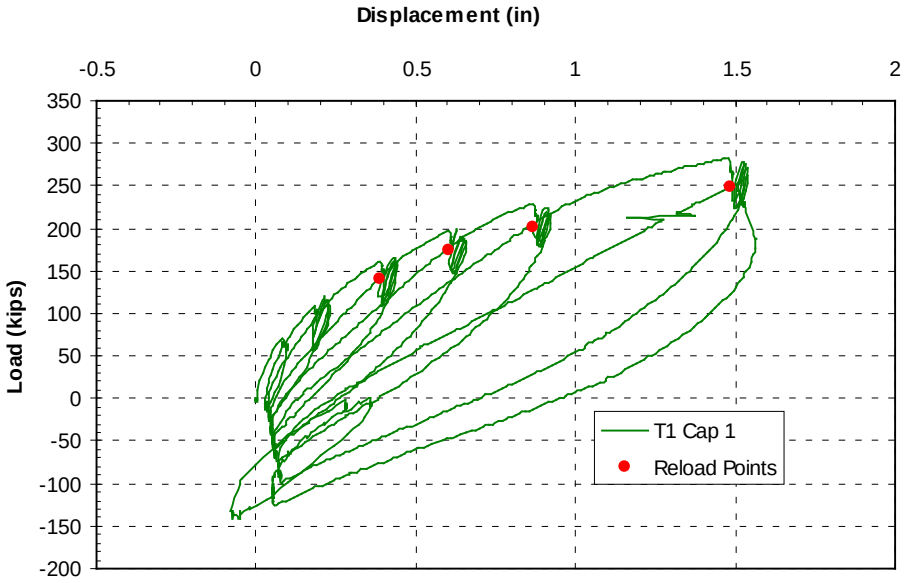

Figure 7-3 Plot of continuous pile cap displacement versus applied load for pile cap 2 during the virgin clay test (Test 1)

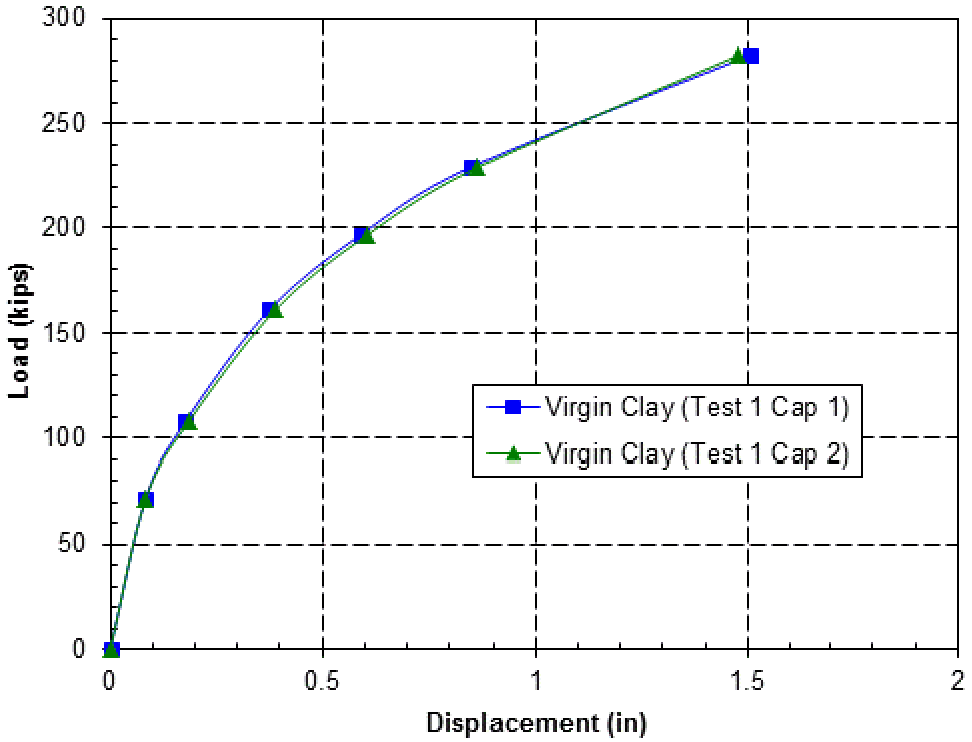

Figure 7-4 Plot of pile cap displacement versus peak applied load for each increment of the virgin clay test (Test 1)

The curves in Figure 7-4 exhibit a typical hyperbolic shape that would be expected for a pile in soft clay. However, because the peak displacement was limited to 1.5 inches to prevent excessive moments in the piles, the slope of the load versus displacement curve never reached a nearly horizontal asymptote. Nevertheless, the last part of the curve is relatively linear suggesting that the lateral resistance is primarily due to the flexural resistance of the piles. The maximum applied load during the last pull was 282.2 kips and resulted in a displacement of 1.50 inches for pile cap 1 and 1.48 inches for pile cap 2. For comparison with other tests a load of 283 kips at 1.5 inch displacement will be used for the virgin soil. For analysis of results from this test, a load of 282 kips will be used for the final push increment. Despite the fact that the two pile groups were 32 ft apart and had minor variations in construction details, the two load-displacement curves shown in Figure 7-4 are nearly identical. These results suggest that the soil properties across the entire site are sufficiently uniform that valid comparisons can be made

between different pile caps with various soil improvement techniques relative to the untreated conditions on pile caps 1 and 2.

7.1.2 Pile Head Rotation versus Load

Pile head rotation versus applied load curves based on the shape array and string potentiometer measurements for pile cap 1 during Test 1 are provided in Figure 7-5. Rotation was measured from the string potentiometers located directly above the corbel of pile cap 1. The distance between the string potentiometers was approximately 45.25 inches. Refer to Figure 4-10 for a review on the position of the string pots on pile cap 1. Rotation was also measured from the shape arrays. The difference in node deflections near the bottom of the pile cap and the top of the pile cap was used to measure rotation from shape array 106 and shape array 104; the distance between these nodes was 24 inches. The rotations measured from the string potentiometers and shape arrays differ by a maximum 0.07° until the final loading increment, at which point, the rate of rotation increases more rapidly. The difference in measurement during the final loading was 0.14° for shape array 106 and 0.17° for shape array 104. The reason for these discrepancies could have been the fact that the string potentiometers were measuring rotation over a much longer distance. It is assumed therefore, that the string potentiometers are more accurate.

Pile head rotation versus load curves based on the string potentiometer and shape array measurements for pile cap 2 during Test 1 are provided in Figure 7-6. Rotation was measured from the string potentiometers located directly above the corbel of pile cap 2. The distance between the string potentiometers was approximately 108.9 inches. Refer to Figure 4-10 for a review on the position of the string pots on pile cap 2. Rotation was also measured from the shape arrays. The difference in node deflections near the bottom of the pile cap and the top of

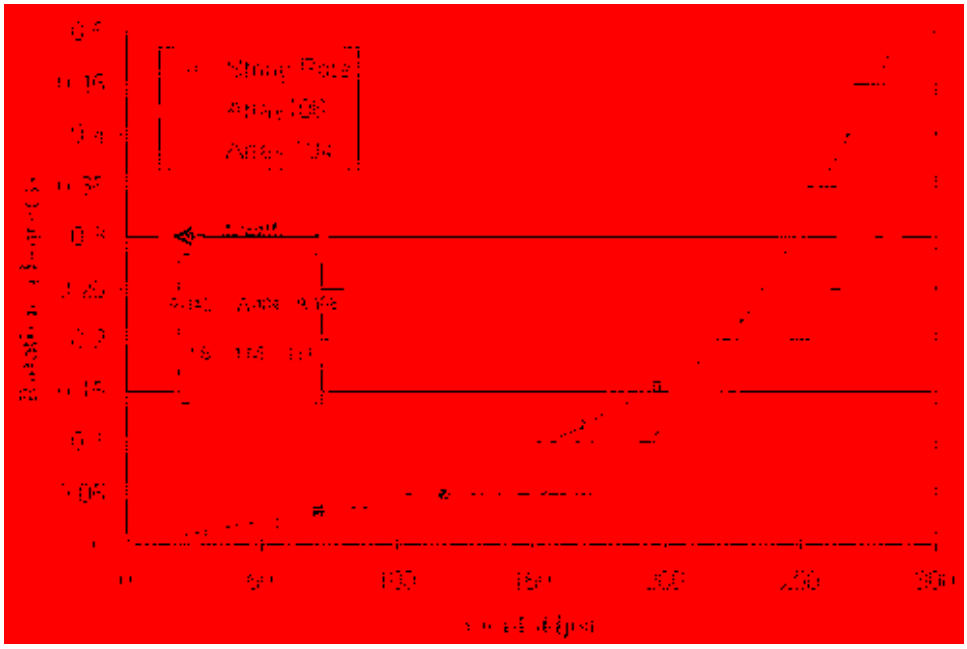

Figure 7-5 Peak pile cap load versus pile head rotation for pile cap 1 during the virgin clay test (Test 1) obtained from string potentiometer and shape array measurements

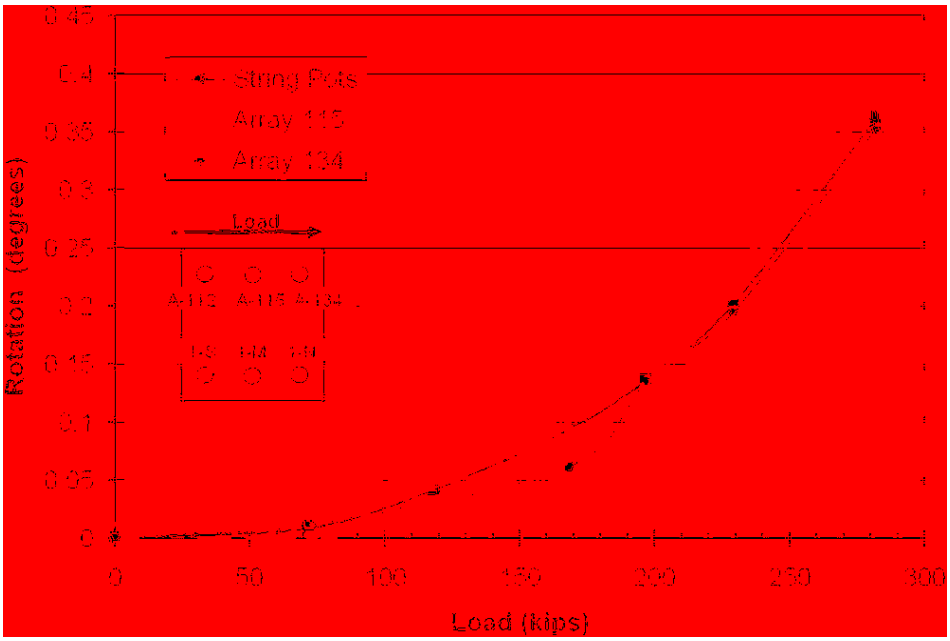

Figure 7-6 Peak pile cap load versus pile head rotation for pile cap 2 during the virgin clay test (Test 1) obtained from string potentiometer and shape array measurements

the corbel was used to measure rotation from shape array 115 and shape array 134; the distance between these nodes was 48 inches. The rotations measured from the string potentiometers and

either shape array differ by a maximum 0.03° throughout the test. This level of agreement suggests that the rotations measured by each of the instruments are relatively accurate.

7.1.3 Pile Deflection versus Depth

The shape arrays and inclinometers were used to record pile deflection versus depth profiles in the piles during the tests. The shape arrays recorded continuously during loading and could therefore be used to provide displacement profiles at any point in the test. In contrast, 15 to 20 minutes were required to make inclinometer measurements on the four instrumented piles at a given displacement increment. Therefore, inclinometer measurements were only made immediately prior to testing and after the final maximum displacement increment to prevent disruption of the testing procedure. To provide an indication of the accuracy of the downhole measurements, displacements from the string potentiometers at the elevation of the applied load are compared to those obtained from the shape arrays at the maximum load for each loading increment. In addition, displacement profiles from the inclinometers were compared to those from the shape arrays during the extended hold portion of the final loading test increment.

Deflection versus depth curves obtained from the shape accelerometer arrays in the piles within pile caps 1 and 2 are provided in Figure 7-7 and Figure 7-8, respectively. The location of the shape arrays relative to the piles in the group and the loading direction are shown by the legends in each figure. The average displacements measured by the string potentiometers at the elevation of the load application for each load increment are also shown in these figures for comparison purposes. Due to a defective shape array, the data collected from the south (A-142) shape array on pile cap 1 were erroneous as indicated by irregular displacement output. As a result, only the center shape array (A-104) and the north shape array (A-106) are used to compare to the string potentiometer and inclinometer data shown subsequently. Similarly, the

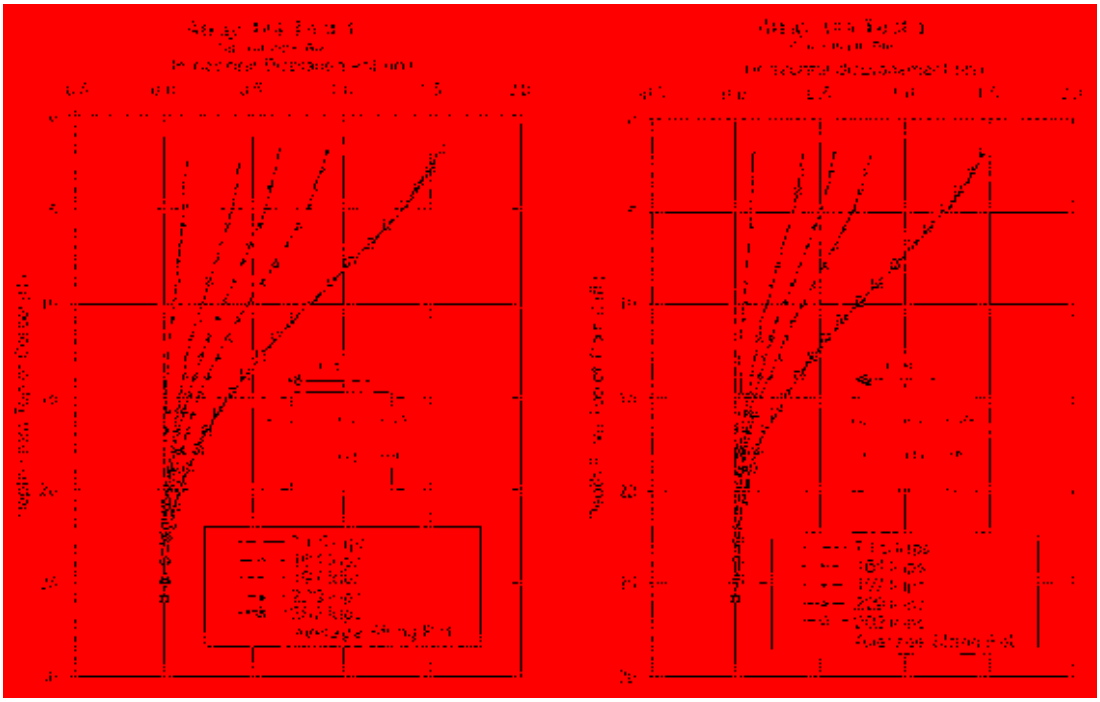

Figure 7-7 Deflection versus depth curves for pile cap 1 for each increment of the virgin clay test (Test 1), with pile head displacements from the string potentiometers also shown

south shape array (A-112) on pile cap 2 also produced irregular displacement data which will not be presented. Nevertheless, the center shape array (A-115) and the north shape array (A-134) provide useful comparisons which are shown in Figure 7-8. Additionally, due to operator error no shape array data were recorded for the target 0.25 inch displacement increment, therefore this data is missing from the plots in Figure 7-7 and Figure 7-8.

To make an accurate comparison between the shape arrays and the string potentiometers in Figure 7-7**,** the shape array data for pile cap 1 had to be extrapolated to the same depth as the string potentiometers since the shape arrays terminated at the base of the corbel. To do this, a linear trend line was created using the measured displacements at depths of 1.83 and 2.83 ft below the top of the corbel and extrapolating 0.92 ft upward to the elevation of the load point. At these depths it can be assumed that the shape array would behave linearly as that portion of the shape array was enclosed in the concrete pile cap. Using this approach, the pile head

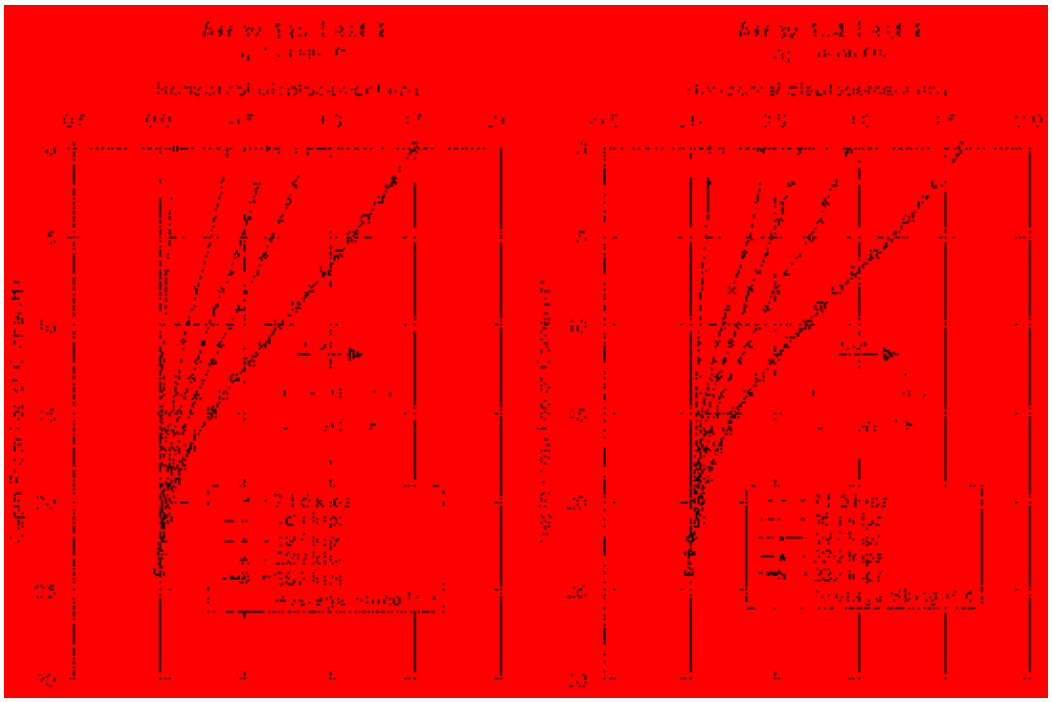

Figure 7-8 Deflection versus depth curves for pile cap 2 for each increment of the virgin clay test (Test 1), with pile head displacements from the string potentiometers also shown

displacement obtained from shape array 106 varied less than 0.05 inches from that measured by the string potentiometer, while the difference in pile head displacement from shape array 104 and the string potentiometer varied from 0.1 inches at 282 kips to 0.01 inches at 71.5 kips. Thus, shape array 106 tends to give more accurate results than shape array 104 when compared to the string potentiometers on pile cap 1. The displacements from the shape arrays on pile cap 2 showed even greater agreement with those from the string potentiometers as seen in Figure 7-8. For example, in the worst case, pile head displacements from shape array 115 in the center pile were less than 0.04 inches different from those from the string potentiometers. Shape array 134 in the north pile also provided close agreement with slightly higher displacements than the string potentiometers and a difference of only 0.04 inches or less.

Figure 7-9 provides comparisons between the displacement versus depth curves obtained from the shape arrays and the two inclinometer pipes in pile cap 1 at the maximum pile head

displacement of 1.5 inches. When looking at the inclinometer and shape array comparison for pile cap 1, the slopes of the center shape array 104 and the inclinometers are nearly identical from the top of the corbel until about 17 ft below the top of corbel; however, the displacements at the same depths during that same interval vary from 0.17 to 0.14 inches. On the other hand, displacements from shape array 106 and the north inclinometer vary by less than 0.05 inches with the greatest discrepancy at a depth of 15 ft below the base of the pile cap. The full reason for the differences in displacements between the center shape array 104 and the inclinometers is to a degree unknown. One reason for the discrepancies could be the fact that the shape arrays were only 24 ft long whereas the inclinometers ran the entire length of the piles. If there was any displacement in the pile deeper than the shape arrays could measure, the shape arrays could not account for it since they were set up to reference displacement with respect to the deepest node. As seen in Figure 7-9, the inclinometers often indicate a negative displacement at depths below the shape arrays, which could account for some of the discrepancies between the shape arrays and the inclinometers.

Another reason for discrepancies between the shape arrays and the inclinometer could be due to the difficulty of getting a tight fit between the shape array and the pipe. If the fit is not tight, the shape array could move within the PVC pipe housing the shape array and yield displacements which were different, usually less, than those in the pile. One other consideration for the discrepancies could be the fact that shape array 104 and the inclinometers are measuring different piles in the pile cap. This could account for some small discrepancies, but not to the full degree that is shown by shape array 104 in this test. Figure 7-10 shows the inclinometer and shape array comparisons for pile cap 2. Shape array 115 shows a slope variance with the inclinometers, which could be due to the fact that it is the middle pile being compared to the

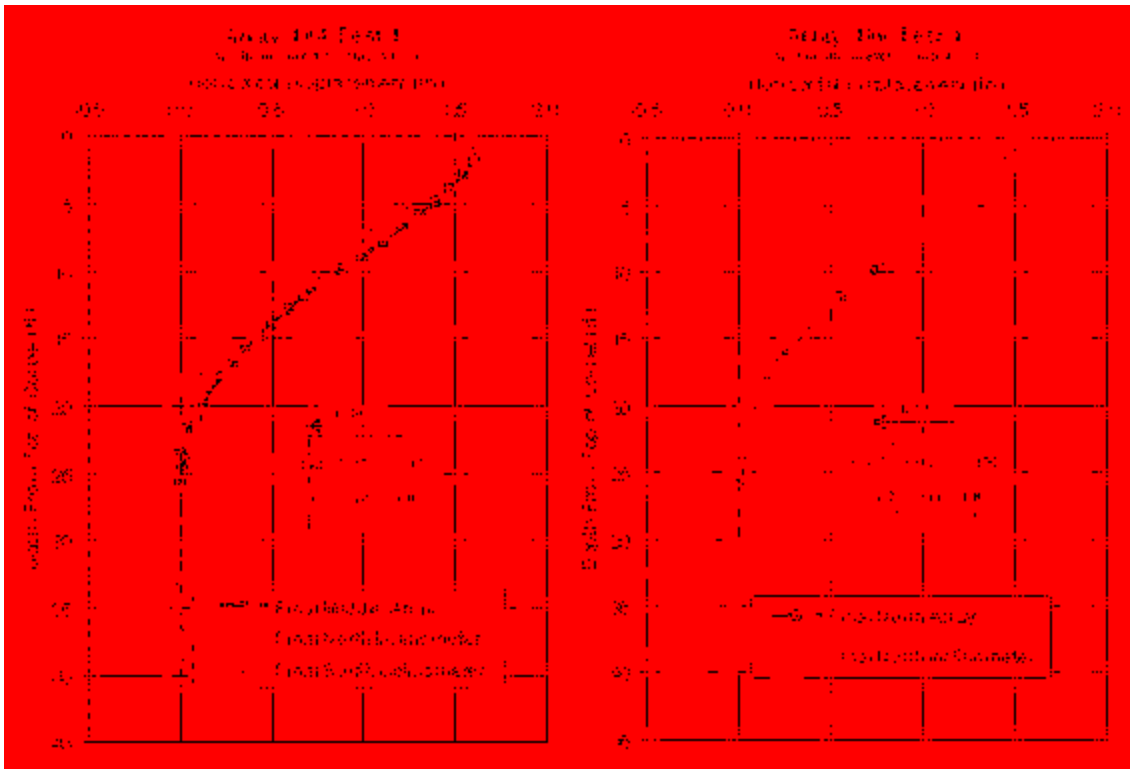

Figure 7-9 Comparison of depth versus deflection curves for the piles in pile cap 1 from the north and south inclinometers, and shape array 104 and shape array 106 in the virgin clay test (Test 1)

north and south piles. Shape array 134 in the north pile shows almost a perfect match with the north inclinometer, only varying by 0.04 inches at its greatest discrepancy.

Overall, the two inclinometer profiles for each pile cap are very similar. The displacement profiles from the shape arrays are also quite consistent with the profiles from the inclinometers. An overview of the results provides increased confidence in the accuracy of the profiles. An overview of the results shows that the piles start to experience bending at about 23 ft below the top of the corbel. The most significant bending tends to occur between 21 and 16 ft below the top of corbel, which is an indication of the location of the maximum bending moments.

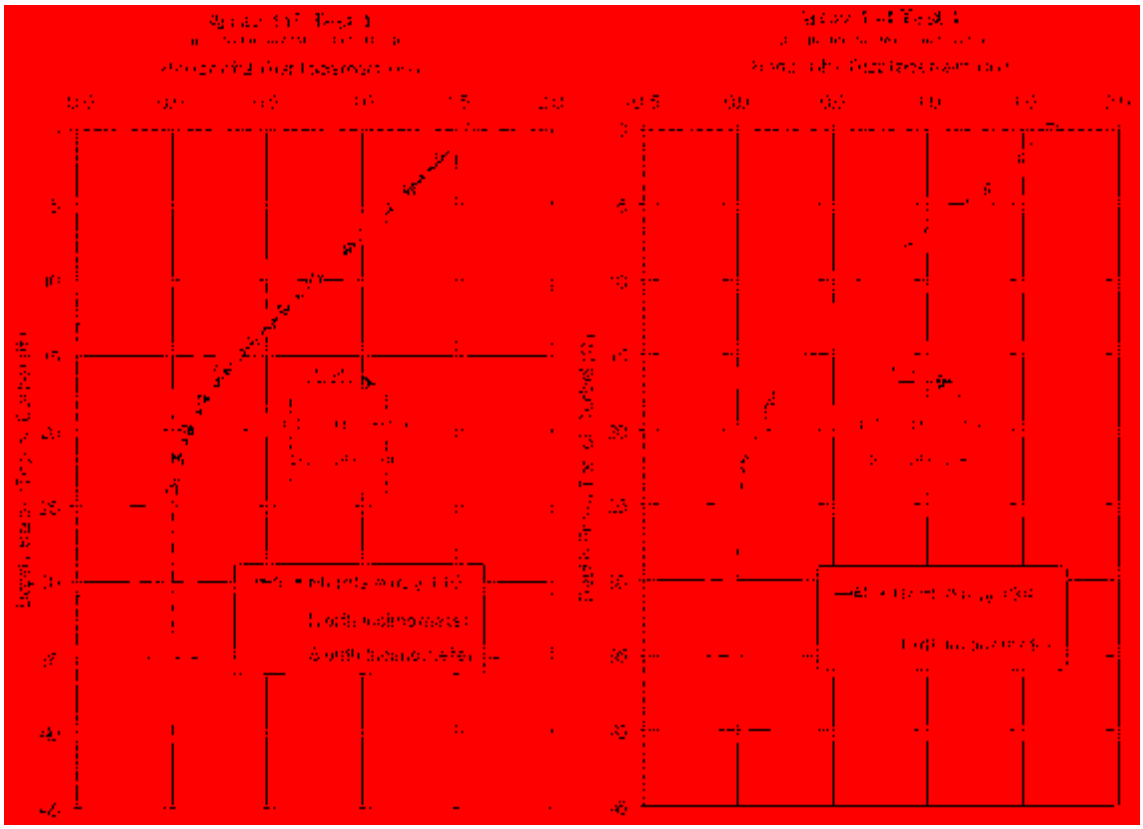

Figure 7-10 Comparison of depth versus deflection curves for the piles in pile cap 2 from the north and south inclinometers, and shape array 115 and shape array 134 in the virgin clay test (Test 1)

7.1.4 Pile Bending Moment versus Depth

Using Equations (6-2) and (6-3) with the procedures described above, moment versus depth graphs were obtained. The curves were obtained from the shape arrays and inclinometer readings while the individual points represent moments computed at the locations of the strain gauges. The maximum total load associated with each target displacement is also listed in the legend for each figure.

Figure 7-11 shows the moment versus depth curves for the middle center pile of pile cap 1. Shape array 104 and the strain gauges measured the maximum positive bending moment between the depths of 9 and 11 ft below the bottom of the pile cap. The maximum positive moment created by the 282 kip load was between 69 and 72 kip-ft. The strain gauges for the middle pile tend to compliment the shape array by varying as little as 1 kip-ft and at most 7 kip-ft

from the moments calculated for the shape arrays. The negative moments measured by the strain gauges in Figure 7-11 tend to be higher than the trend derived from the shape array data. However, if the shape array were to continue on its trend into the pile cap there would still only be about a 10 kip-ft difference or less for all the loads except the 282 kip load. At the 282 kip load the moment from the strain gauge at the bottom of the pile cap measured -79 kip-ft, while the trend of the shape array would be around -59 kip-ft, thus leaving a wide range of possible values for the actual magnitude of the negative moment.

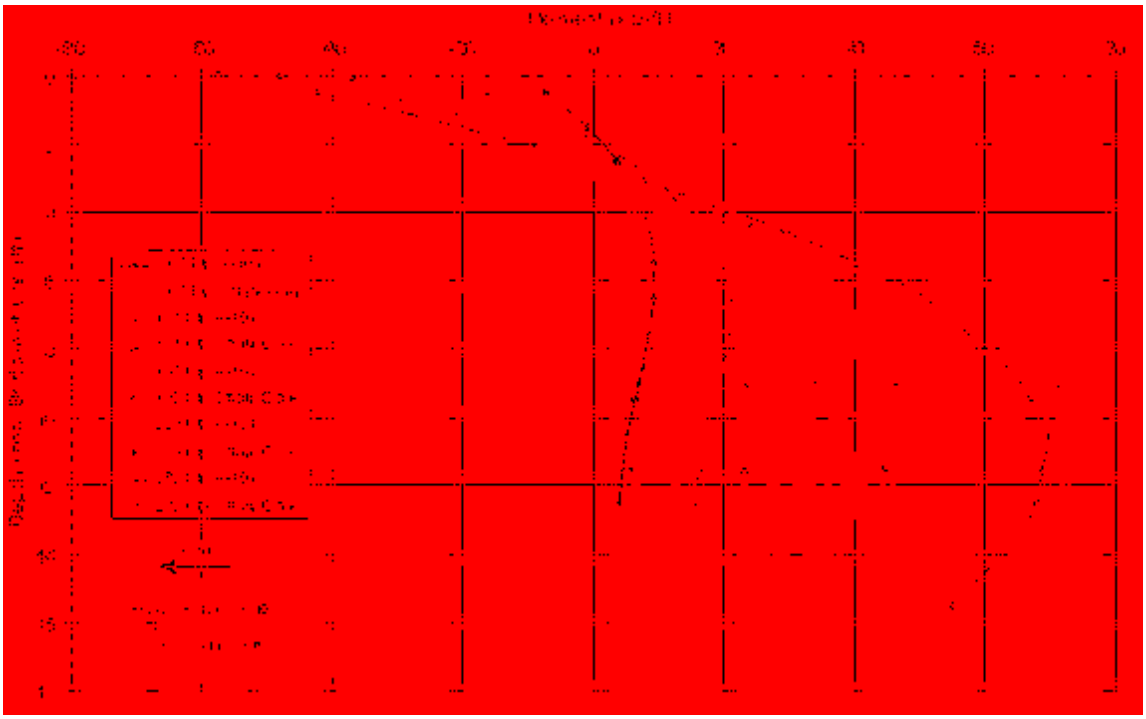

Figure 7-11 Moment versus depth curve for the middle center pile of pile cap 1 (1-M) based on incremental deflection versus depth curves measured from shape array 104 during the virgin clay test (Test 1), with point moments measured from strain gauges at various depths also shown

Bending moments for the north pile were also derived and shown in Figure 7-12. The only strain gauges on this pile that remained operational for the test were at about the bottom of the pile cap and 4 ft below. The shape array shows the maximum positive bending moment occurring between 11 and 13 ft below the bottom of the pile cap. At the 282 kip load the greatest

moment the pile experienced was 73 kip-ft, which is almost identical to the values measured in the middle pile at the same load. The maximum negative moments derived from shape array 106 tend to be higher than the strain gauges if their trend continued to the bottom of the pile cap. At the 282 kip load the moment from the strain gauge at the bottom of the pile cap measured -69 kip-ft, while the trend of the shape array would be around -80 kip-ft.

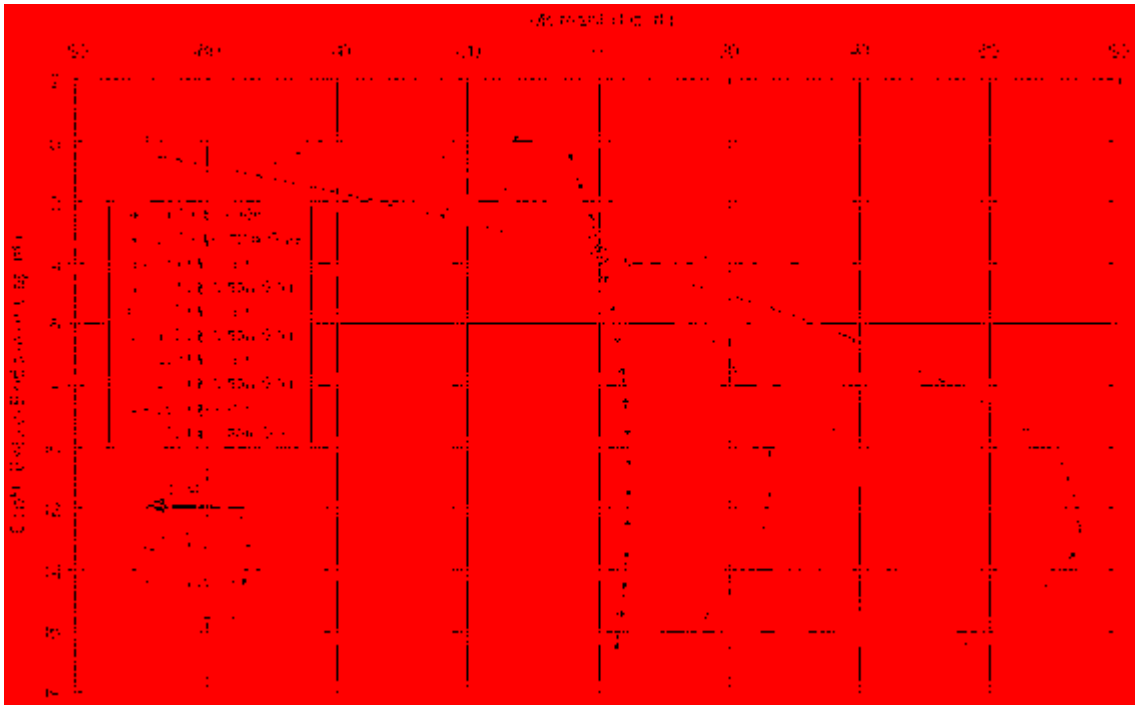

Figure 7-12 Moment versus depth curve for the north center pile of pile cap 1 (1-N) based on incremental deflection versus depth curves measured from shape array 106 during the virgin clay test (Test 1), with point moments measured from strain gauges at various depths also shown

The only significant discrepancy with the data from the north pile is the bending moments at 4 ft below the pile cap. The array data tends to converge to zero moment at that depth, but the strain gauges still show a significant amount of positive moment. In comparing the bending moments of the middle and north piles of pile cap 1, both have similar maximum positive moments, but the north pile's moments seem to be about 1.5 ft deeper. The maximum negative moments for the strain gauges at the bottom of the pile cap varied up to 10 kip-ft at the

maximum load. The arrays vary from -59 kip-ft from the middle pile to -80 kip-ft from the north pile at maximum load. The discrepancies between the arrays are mostly due to the different recorded displacements, but due to similar slopes, the bending moments still demonstrate similar trends.

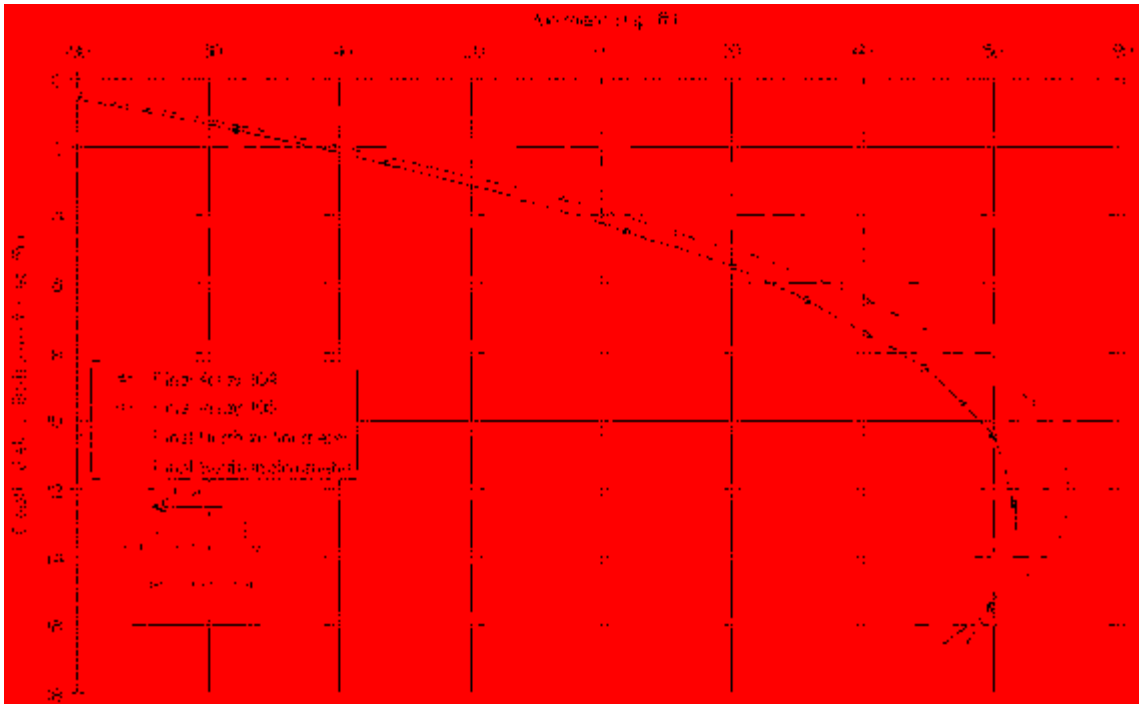

Figure 7-13 Moment versus depth comparison for the piles in pile cap 2 based on deflections measured from the north and south inclinometers, shape array 104 and shape array 106 during the virgin clay test (Test 1)

With the arrays being a fairly new technology, it is important to compare the moments derived from them to the moments derived from the inclinometer data using the same numerical method. The deflections from Figure 7-9 were used to produce Figure 7-13. When looking at the maximum positive moment the inclinometers show significant agreement to each other with only 2 kip-ft difference whereas the arrays differ by about 10 kip-ft. The maximum negative moments show the opposite trend. The negative moments from the arrays only vary by 2 kip-ft, while the negative moments from the inclinometers vary by 16 kip-ft. The instruments together only varied by 10 kip-ft at 16 ft below the pile cap, but increasing deviation occurs as

measurements are taken approaching the pile cap. This leads to some evidence that the method used to derive the bending moments is more accurate at greater depths. Just as bending moments versus depth graphs were obtained for pile cap 1, the same analysis was done for pile cap 2. The results are found in Figure 7-14 through Figure 7-16. As mentioned previously, there were no data for the south pile. The middle pile of pile cap 2 had no strain gauges so there is no comparison in Figure 7-14. Maximum positive bending moments in the middle pile appear to occur between 13 and 14 ft below the bottom of the pile cap, with the greatest moment being 71 kip-ft. The maximum negative moments directly under the pile cap range from -1 to -33 kip-ft.

The location of maximum positive moments for the north pile of pile cap 2 in Figure 7-15 occur a little higher than the middle pile ranging between 10.5 and 11.5 ft below the bottom of the pile cap. The greatest moment in the north pile at the 282 kip load was 69 kip-ft which is comparable to the middle pile. The maximum negative moments for the north pile are a little greater than the middle pile ranging from -5 to -40 kip-ft; nevertheless, they are still considerably lower than what was measured on pile cap 1. When looking at the maximum positive moment, the inclinometers and the north array show significant agreement with about a 4 kip-ft difference whereas the middle array shows about the same magnitude of bending moment, differing in the depth of the moment by about 3 ft. This gives evidence that the discrepancies in measured displacements, although small, have a great impact on the derived bending moments using the numerical method.

The maximum negative moments in Figure 7-16 continue to show a degree of similarity between the north array and the inclinometer. Their results span a range of about 20 kip-ft, but

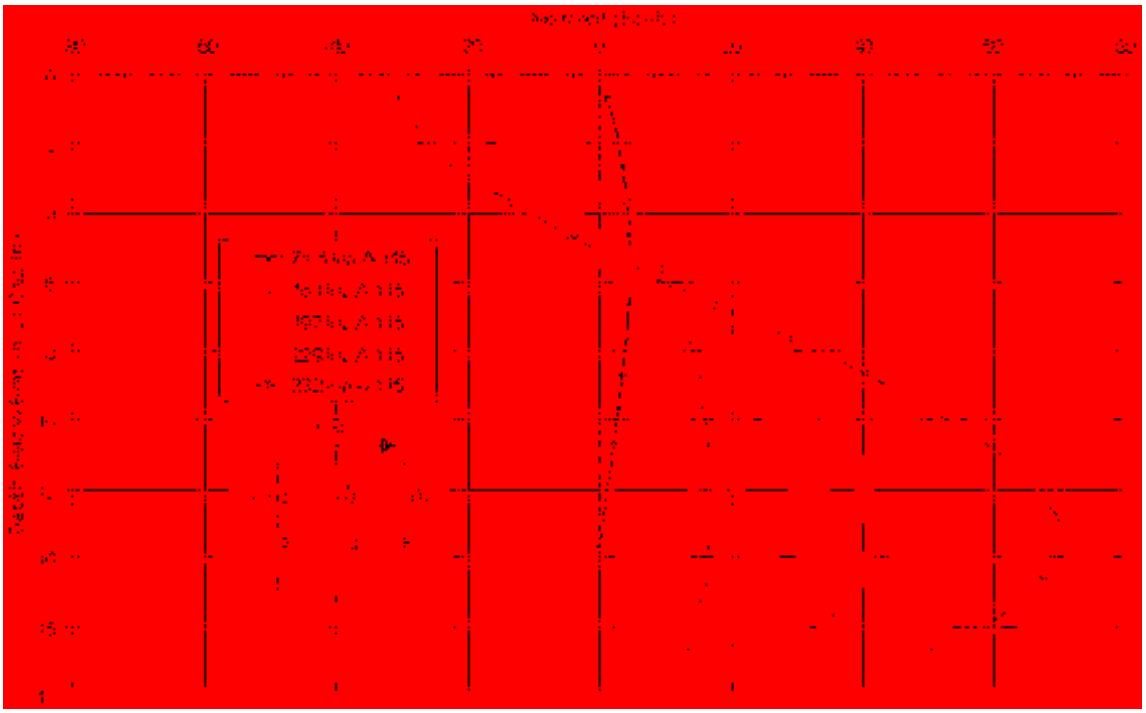

Figure 7-14 Moment versus depth curve for the middle center pile of pile cap 1 (1-M) based on incremental deflection versus depth curves measured from shape array 104 during the virgin clay test (Test 1)

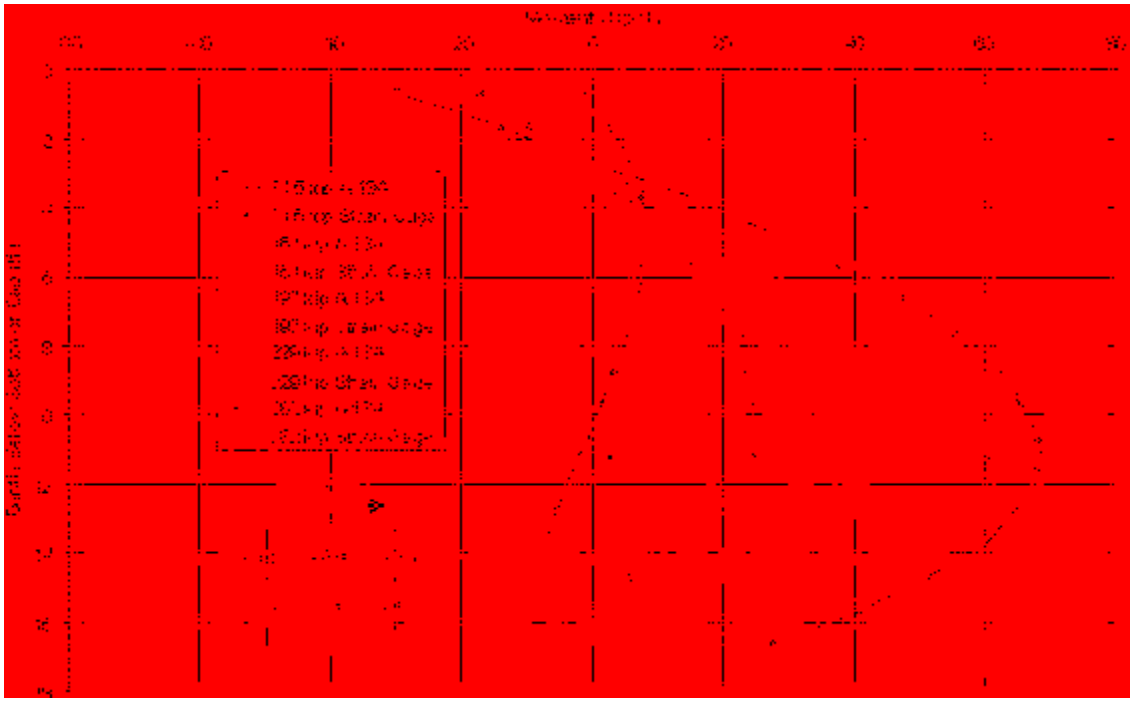

Figure 7-15 Moment versus depth curve for the north center pile of pile cap 2 (2-N) based on incremental deflection versus depth curves measured from shape array 134 during the virgin clay test (Test 1) with point moments measured from strain gauges at various depths also shown

are still 10 to 12 kip-ft lower than what was measured on pile cap 1. Not much can be discerned from the trend of the middle array's negative bending moments as it had to be truncated due to inconsistencies of the numerical method at depths just below the pile cap.

In final review of Test 1, the behavior of both pile caps in the weak virgin clay was consistent. Both pile caps displaced close to 1.5 inches at a load of 282 kips. The depth-versus-displacement comparisons were consistent with the arrays closely matching the string potentiometers and inclinometers with the exception of the middle array of pile cap 1. The results of the bending moments also demonstrate fairly consistent comparisons with the exception of the middle array in pile cap 2. Since the measured behavior on both pile caps was relatively the same, the following can be stated with regards to the bending moments: the negative bending moment is always greatest at the base of the pile cap, while the depth to the maximum positive moment increases from 9 ft to 12 ft below the pile cap as the pile head

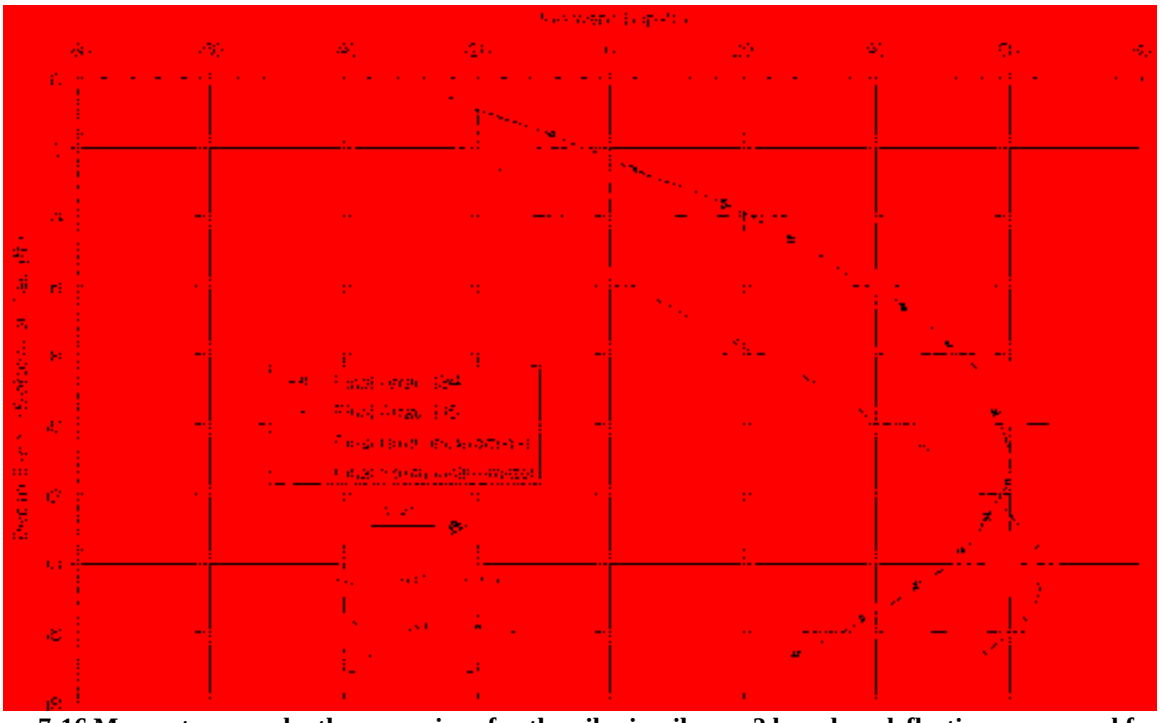

Figure 7-16 Moment versus depth comparison for the piles in pile cap 2 based on deflections measured from the north and south inclinometers, shape array 104 and shape array 134 during the virgin clay test (Test 1)

deflection increases from 0.5 to 1.5 inches. Both the maximum negative and positive moments increase as the pile cap displacement increases. The front piles, closest to the load, experience a maximum bending moment at depths of 10.5 to 11.5 ft below the bottom of the pile cap, the middle piles 9.5 to 12.5 ft, and the back piles 11 to 13 ft. The difference between the array and strain gauge measurements of the maximum positive moments was less than 10 kip-ft. The magnitude of the maximum negative moments was much more variable, which indicates that the moment near the cap may be influenced by the rotation of the pile cap as well as the lateral load applied to the cap. The leading pile tends to show a greater magnitude moment than the other piles, indicating that the leading pile is either taking more of the load, as would occur due to group effects or the leading pile is bending more due to pile cap rotation.

7.1.5 Moment versus Load Results

Figure 7-17 and Figure 7-18 provide plots of the maximum positive and negative bending moments versus applied pile cap load, respectively for cap 1 during Test 1. Similarly, Figure 7-19 and Figure 7-20 provide plots of the maximum positive and negative bending moments versus applied pile cap load, respectively for cap 2 during Test 1. Moment data come from both shape array and strain gauge data when available. The maximum moments from the strain gauges may not be the absolute maximum moments in the pile, but they represent the maximum moments recorded by the strain gauges on their respective piles. Initially, the curves are relatively linear; however, the bending moment tends to increase more rapidly with load at the higher load levels as the soil is loaded past its shear capacity. The curves from the strain gauges provide relatively consistent moment versus load curves with little evidence of group interaction effects for the displacement levels involved. The moments actually appear to indicate that the

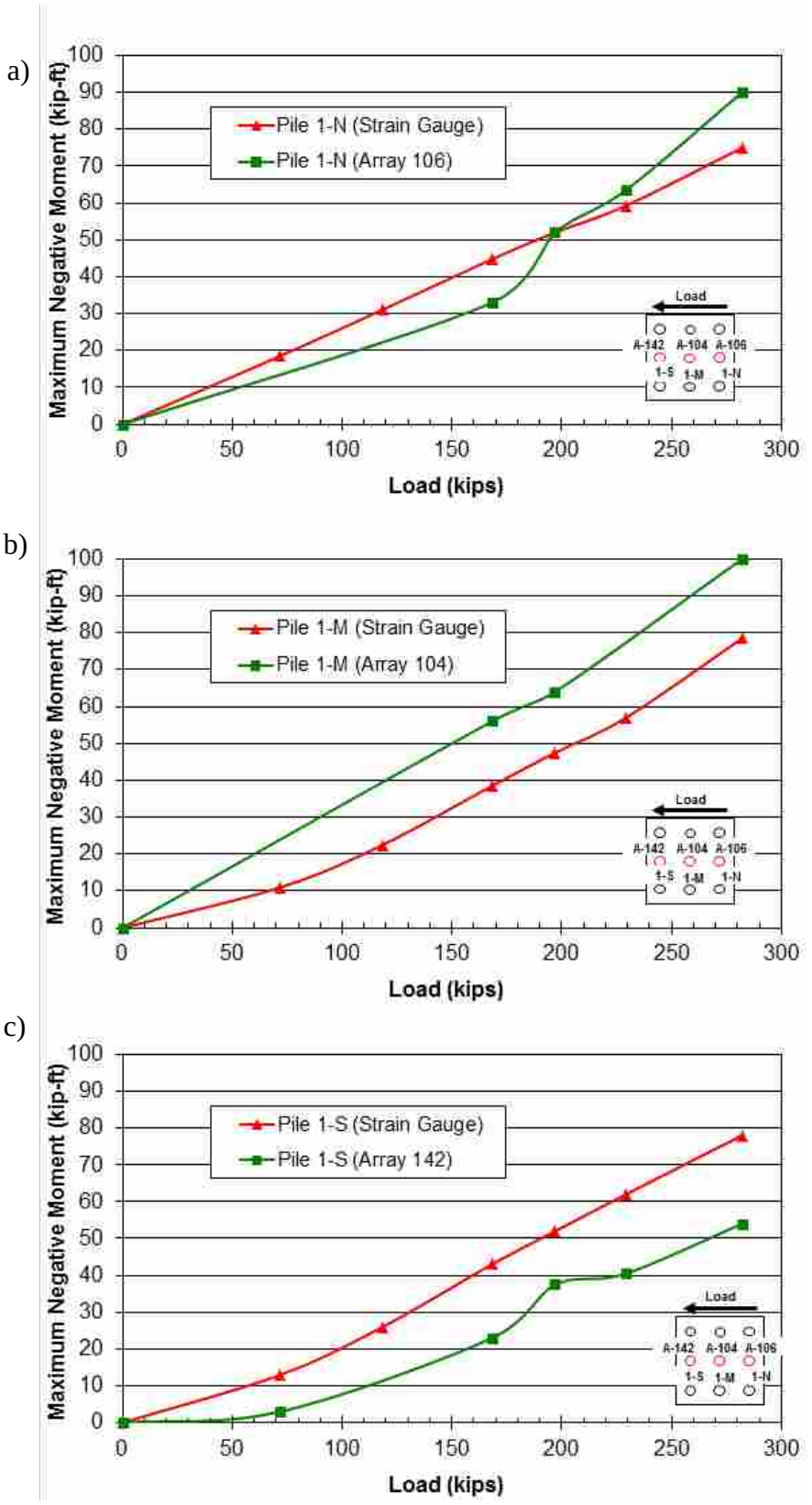

Figure 7-17 Maximum negative moment (base of cap) versus total pile cap load for piles (a) 1-N, (b) 1-M, and (c) 1-S in cap 1 during the virgin clay test (Test 1)

a)

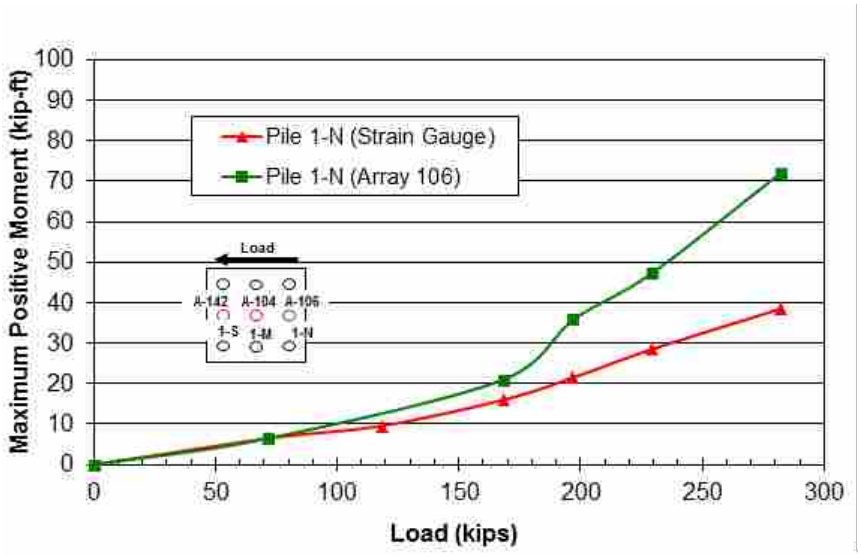

b)

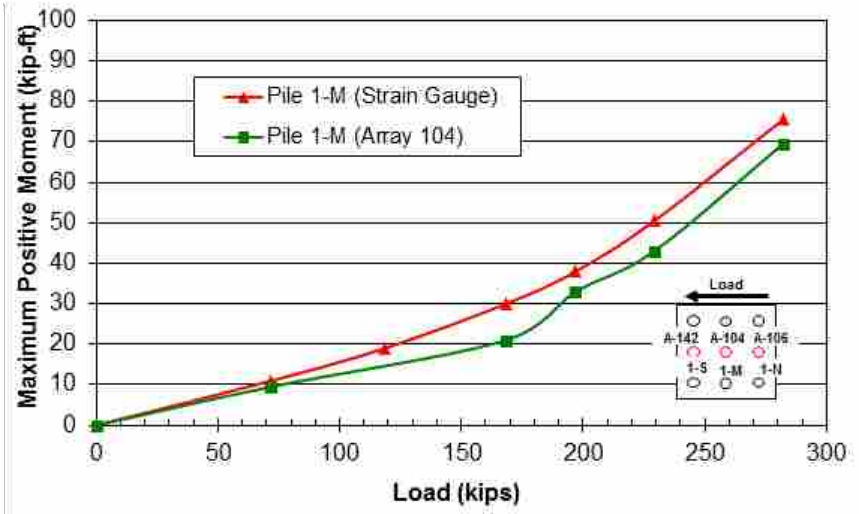

c)

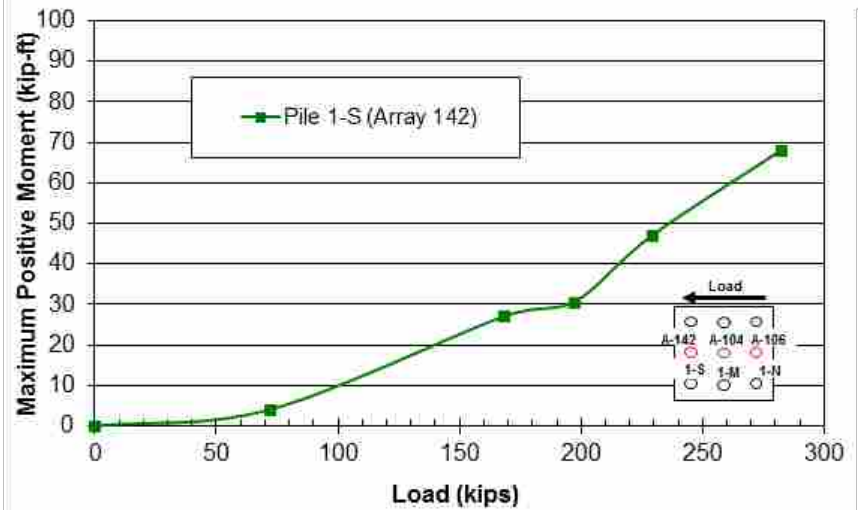

Figure 7-18 Maximum positive moment versus total pile cap load for piles (a) 1-N, (b) 1-M, and (c) 1-S in cap 1 during the virgin clay test (Test 1)

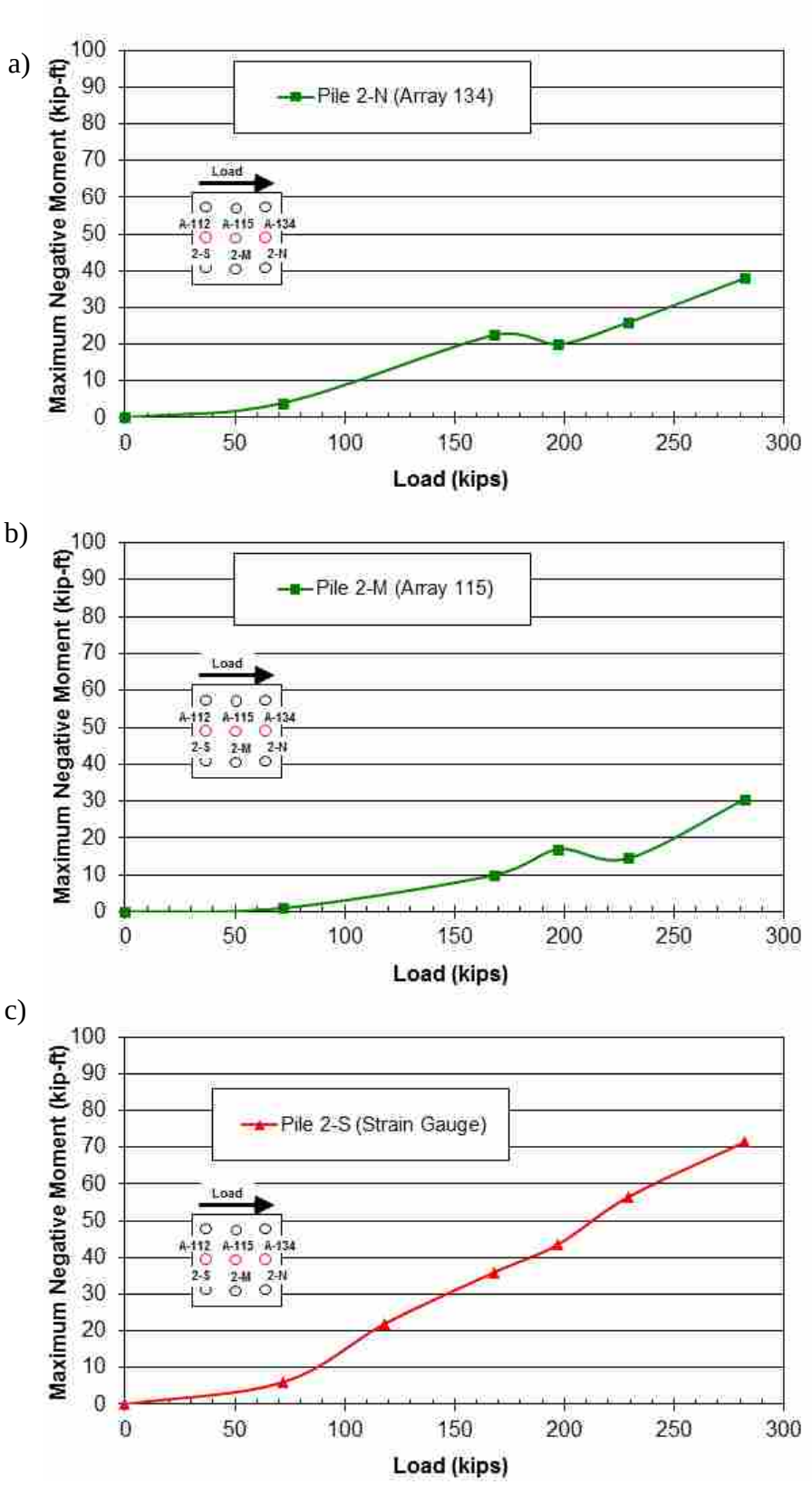

Figure 7-19 Maximum negative moment versus total pile cap load for piles (a) 2-N, (b) 2-M, and (c) 2-S in cap 2 during the virgin clay test (Test 1)

a)

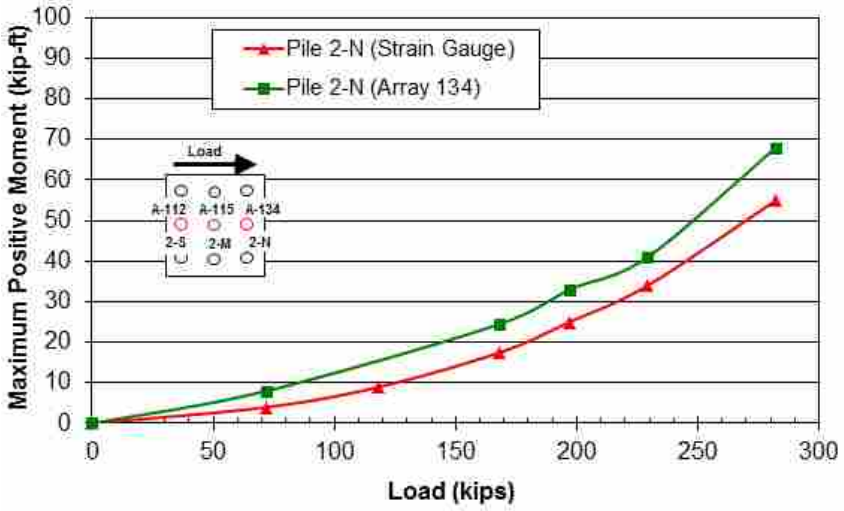

b)

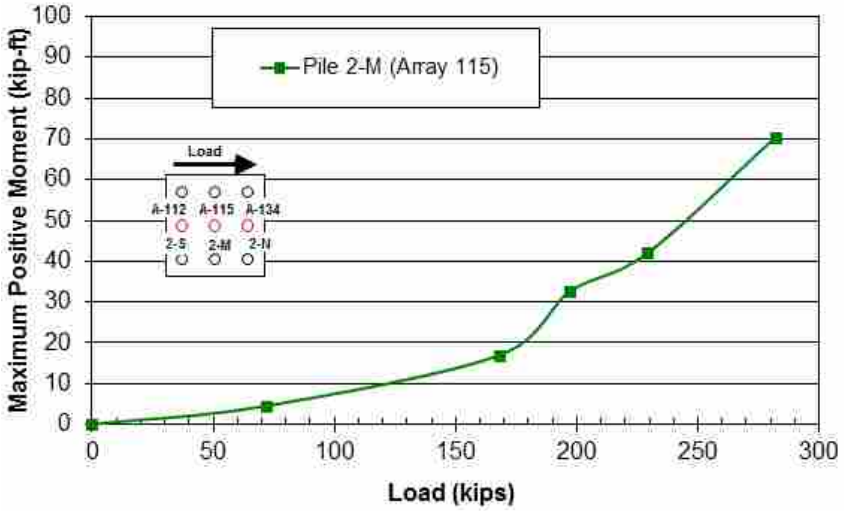

c)

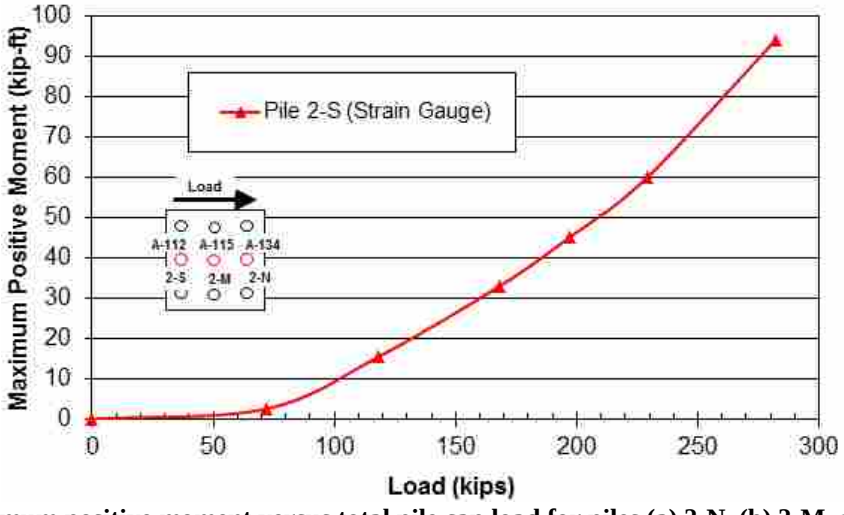

Figure 7-20 Maximum positive moment versus total pile cap load for piles (a) 2-N, (b) 2-M, and (c) 2-S in cap 2 during the virgin clay test (Test 1)

opposite of group effects is occurring; the leading piles seem to have the lowest moments. The agreement between the curves computed by the strain gauges and shape arrays varies.

7.2 Virgin Clay without Passive Resistance – Test 2

In addition to the lateral pull into the virgin soil, a similar test was performed where the passive resistance was removed from the soil directly behind the pile cap. The purpose of this test was to determine how much of the soil's strength in Test 1, the virgin soil test, was due to the passive resistance of the soil behind the pile cap versus the resistance attributed to the piles. To accomplish this, a 1-ft wide excavation of the virgin soil along the north face of pile cap 1 to the depth of the pile cap was made as shown in Figure 7-21. The datum for the displacement of Test 2 was the initial measurements taken prior to Test 1. Since this test took place after the pile caps had been pulled together in the first test of the virgin clay, there was still some residual displacement in the direction of the original displacement once the load was released. Thus, Test 2 started with a negative initial displacement of about 0.3 inches. All instrumentation was in place and identical to that of Test 1. The test followed the standard testing procedure with one exception: due to the residual gap and initial offset resulting from Test 1, the 0.125 inch test increment for Test 2 was omitted.

7.2.1 Load versus Pile Cap Displacement

The lateral load versus displacement plots show the complete load path, including incremental cycles for the test. Figure 7-22 and Figure 7-23 were obtained from the actuator pressure transducer and the string potentiometers attached to their corresponding pile caps. The

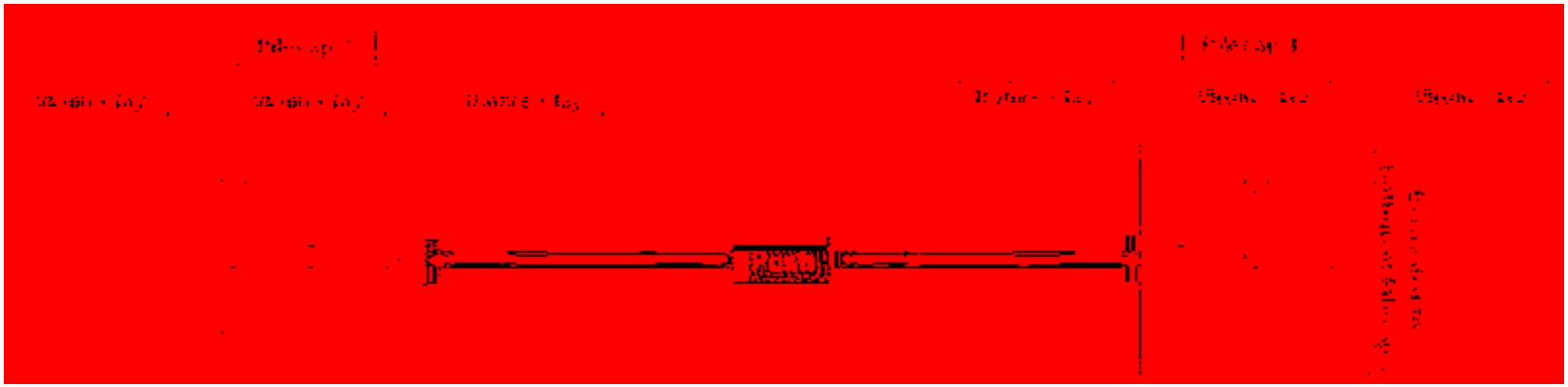

Figure 7-21 Schematic plan view of Test 2

actuator pushed the pile caps to target the prescribed increments of 0.25, 0.5, 0.75, 1.0, and 1.5 inches. Displacement for the tests was referenced to actuator extension length as opposed to being referenced to the displacement of either of the pile caps, which introduced some differences, because pile cap 1 was weaker than pile cap 2. The actual displacements for pile cap 1 with the residual offset of -0.27 inches were -0.01, 0.26, 0.48, 0.75, and 1.28, inches respectively. Pile cap 2 displacements with the residual offset of -0.32 inches were -0.12, 0.06, 0.19, 0.34, and 0.63 inches respectively as measured by the corresponding string potentiometers. These displacements are consistent with expectations, as pile cap 1 had no passive resistance directly behind it, it should have moved more than pile cap 2. A plot of pile cap displacement versus peak applied load for each test increment is displayed in Figure 7-24. For comparison with other tests, an interpolated maximum load at 1.5 inch displacement of 229 kips will be used.

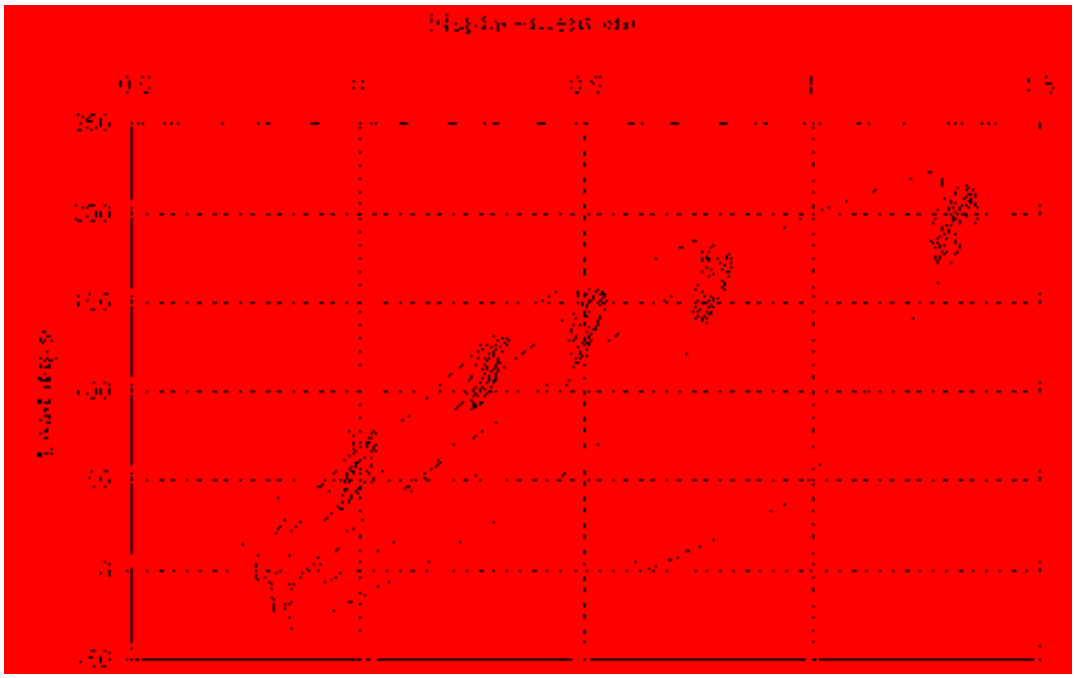

Figure 7-22 Plot of continuous pile cap displacement versus applied load for pile cap 1 during Test 2

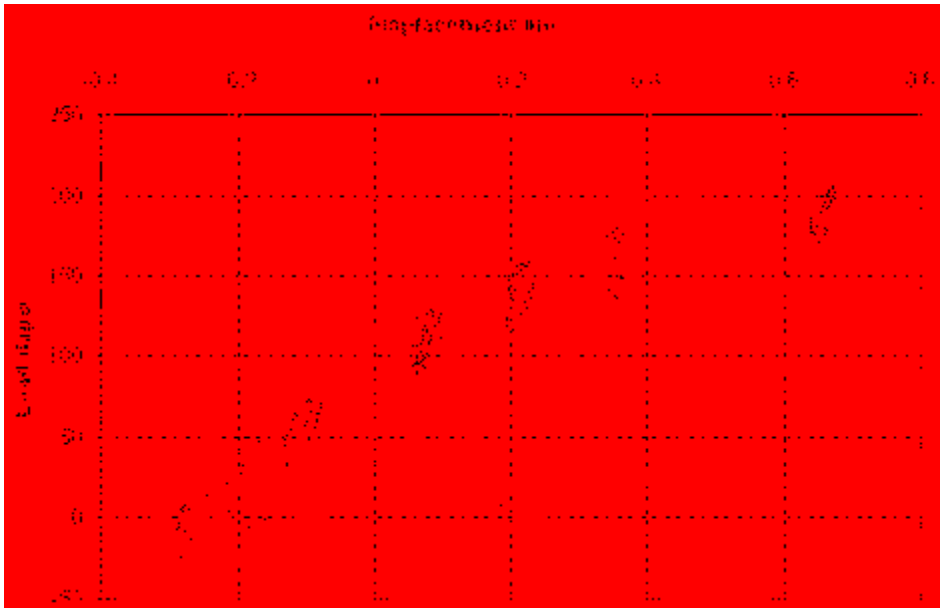

Figure 7-23 Plot of continuous pile cap displacement versus applied load for pile cap 2 during Test 2

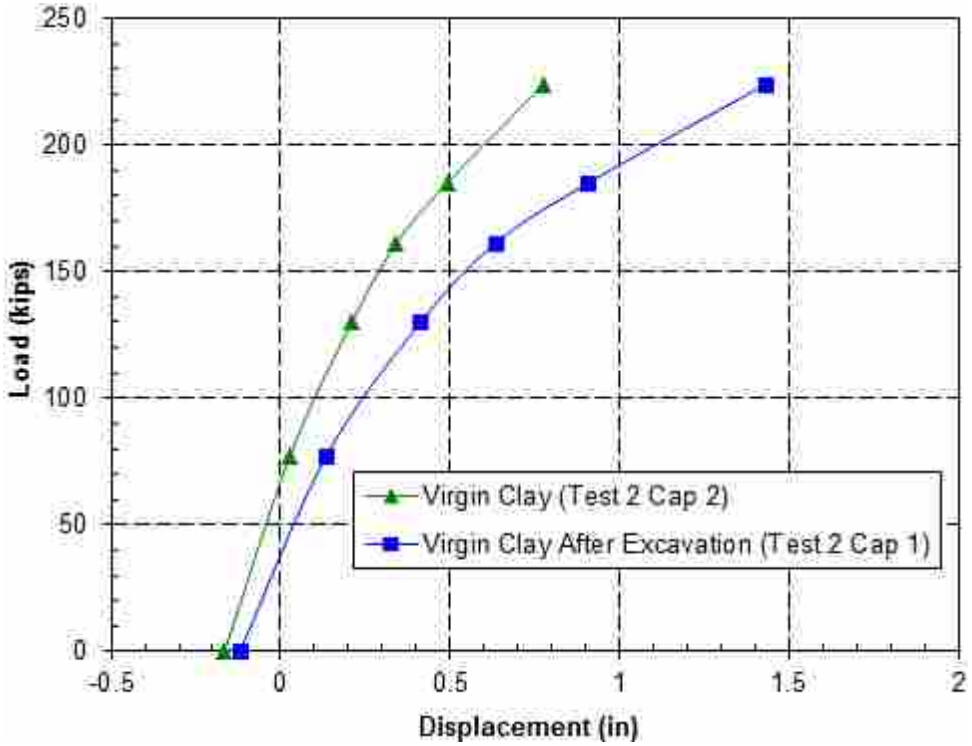

Figure 7-24 Plot of pile cap displacement versus peak applied load for each increment of the virgin clay test after excavation (Test 2)

7.2.2 Load versus Pile Head Rotation

Pile head load versus rotation curves obtained from string potentiometer and shape array measurements for pile caps 1 and 2 during Test 2 are provided in Figure 7-25 and Figure 7-26, respectively. Because of the initial negative offset, the pile caps had a slight negative rotation at the start of the test. As load increased, the rotation shifted to a positive value. Rotation of pile cap 1, where passive force was absent, exceeds that of pile cap 2 at higher load levels as would be expected. The total rotation measured on pile cap 1 was about 0.3°. This value is significantly greater than the rotations observed on either of the caps during Test 1, which measured about 0.17° at the same load. This occurrence also was expected as pile cap 1 during Test 2 had the passive resistance directly behind the cap removed.

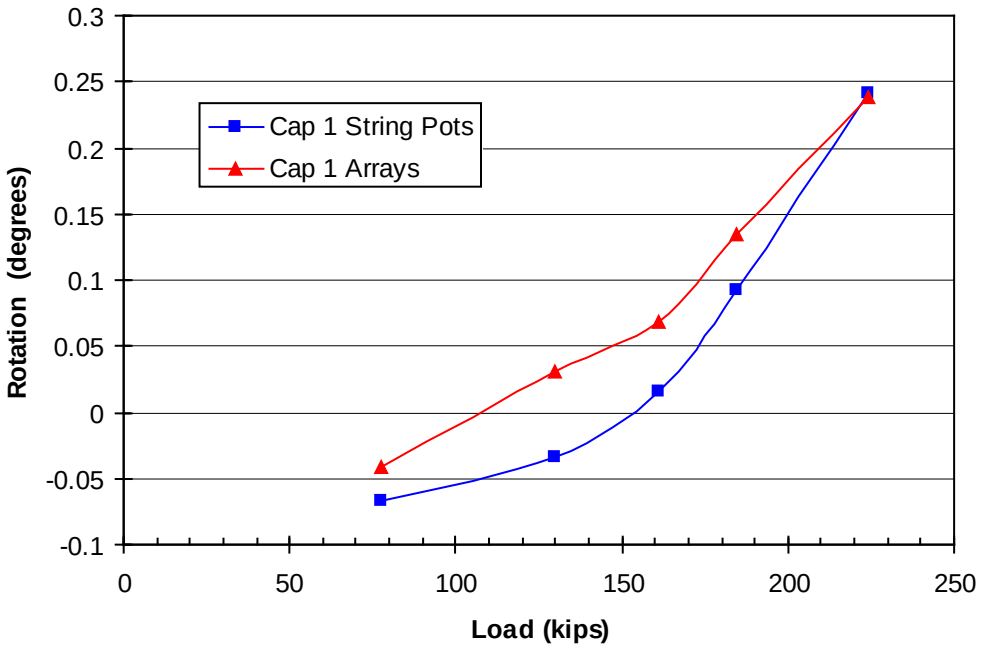

Figure 7-25 Peak pile cap load versus pile head rotation for cap 1 during the virgin clay test after excavation (Test 2) obtained from string potentiometer and shape array measurements

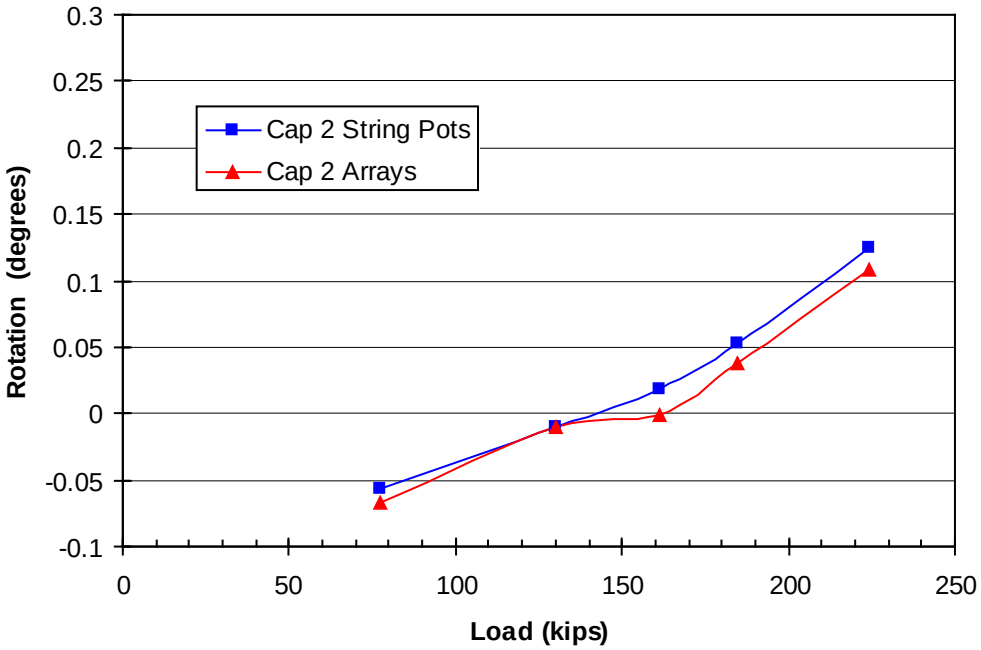

Figure 7-26 Peak pile cap load versus pile head rotation for pile cap 2 during the virgin clay test after excavation (Test 2) obtained from string potentiometer and shape array measurements

7.2.3 Pile Deflection versus Depth

Since pile cap 1 had the passive force on the pile cap removed, the remaining subsections in this section will focus on the results from pile cap 1. It is sufficient to note that the load-displacement curves for pile cap 2 plot consistently with those seen in Test 1, and therefore, had it displaced the same increments, similar results would be apparent. Figure 7-27 shows the pile deflection versus depth profiles of the arrays and inclinometer readings on pile cap 1 at the maximum displacement during Test 2. There is good agreement in the north pile even though there is a slight discrepancy starting at about 6 ft below the top of the corbel. Measurements from the center pile exhibited a little more variance with the greatest discrepancy being about 0.1 inches. These discrepancies are also seen in the string potentiometer comparison with the

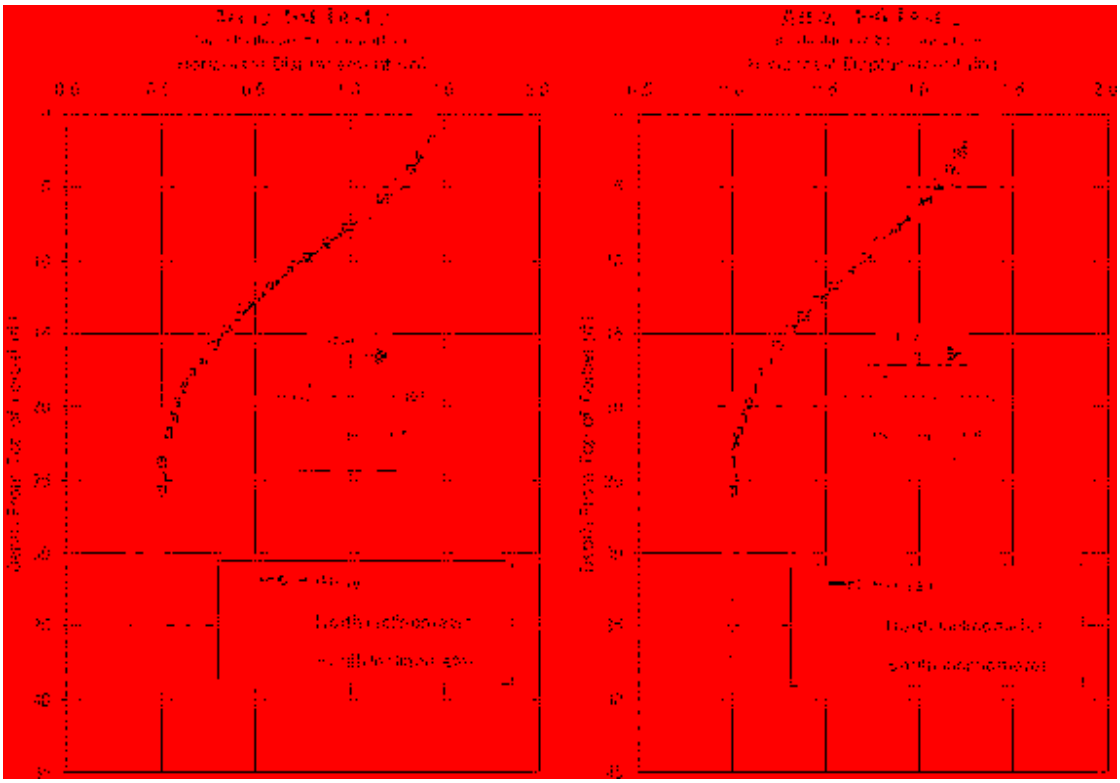

Figure 7-27 Comparison of depth versus deflection curves for the piles in pile cap 1 from the north and south inclinometers, and shape array 104 and shape array 106 in the virgin clay test after excavation (Test 2)

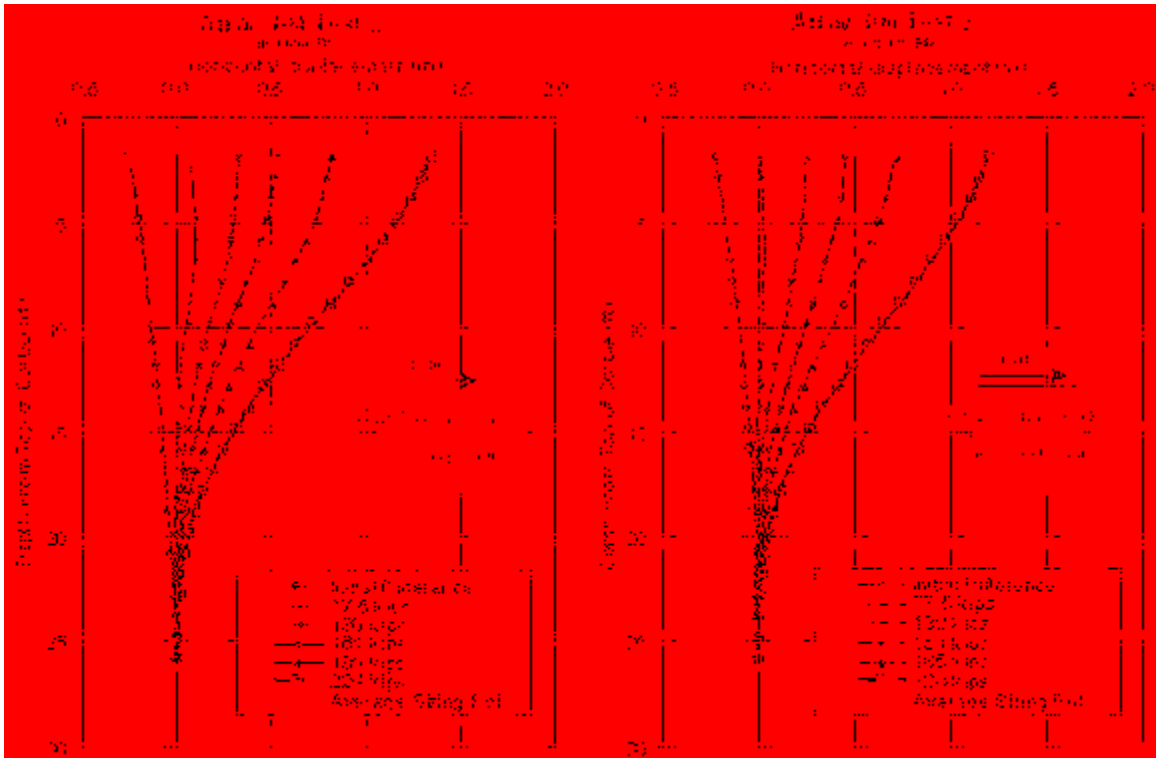

Figure 7-28 Deflection versus depth curves for pile cap 1 for each increment of the virgin clay test after excavation (Test 2), with pile head displacements from the string potentiometers also shown

shape arrays found in Figure 7-28. In spite of the minor discrepancies, the general trend and slope of the depth versus displacement profiles are consistent and provide an accurate representation of the deflections the piles experienced.

7.2.4 Pile Bending Moment versus Depth

Bending moments were estimated from the depth versus displacement profiles from the center and north piles on cap 1 using the methods described in Section 6.2. Figure 7-29 and Figure 7-30 provide bending moment versus depth curves for the piles in pile cap 1 at the five target displacement levels during Test 2. The curves were obtained from the shape arrays while the individual points represent moments computed from the strain gauges. The datum of the

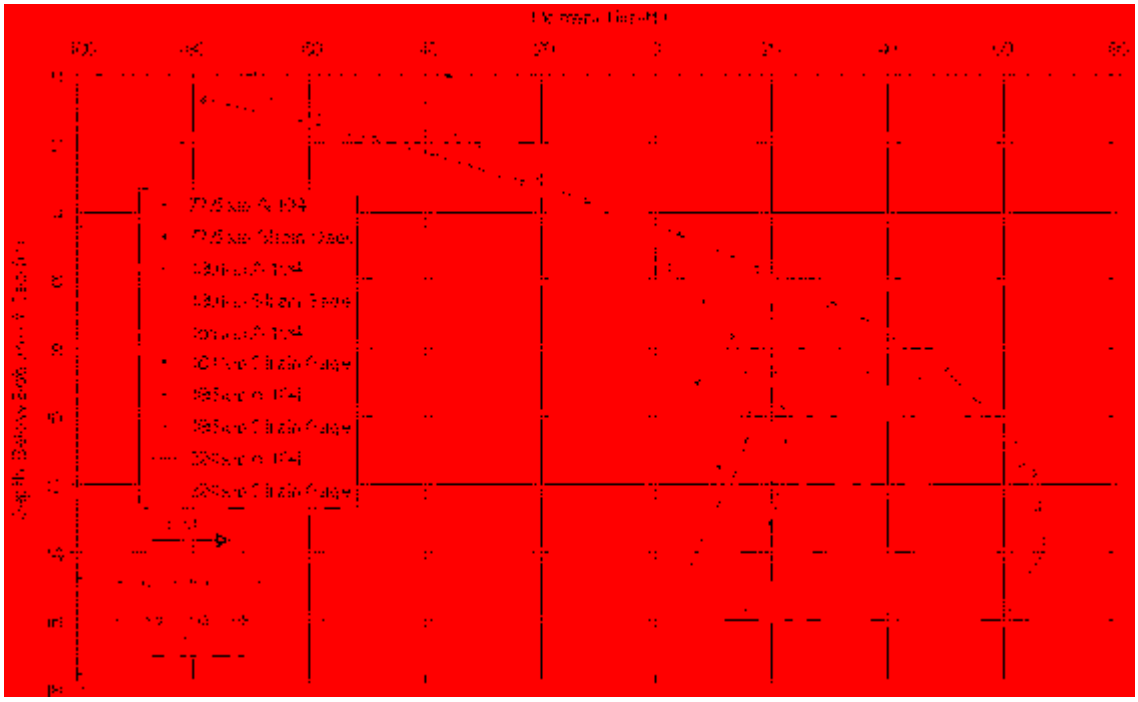

Figure 7-29 Moment versus depth curve for the middle center pile of pile cap 1 (1-M) based on incremental deflection versus depth curves measured from shape array 104 during the virgin clay test after excavation (Test 2), with point moments measured from strain gauges at various depths also shown

figures has been moved from the top of the corbel to the bottom of the pile cap. The maximum load at each target displacement is also listed in each figure's corresponding legend.

The maximum positive bending moments from the center pile array in Figure 7-29 tend to occur from about 11.5 ft to 13.5 ft below the bottom of the pile cap. The positive moments measured from the strain gauges are within 7 kip-ft or less of the moments from the array, with the only exception being the 185 kip load or 1 inch test increment. The positive moments from the north pile in Figure 7-30 seem to be a little more consistent as the depths of the maximum moments occur at about 13.5 ft below the bottom of the pile cap. The moments from the strain gauges are within 7 kip-ft or less of array moments at all test increments. Also, with the exception of the 77.5 kip load or 0.25 inch test increment, the positive moments from the arrays are within 2 kip-ft or less when comparing the two instrumented piles at corresponding loads.

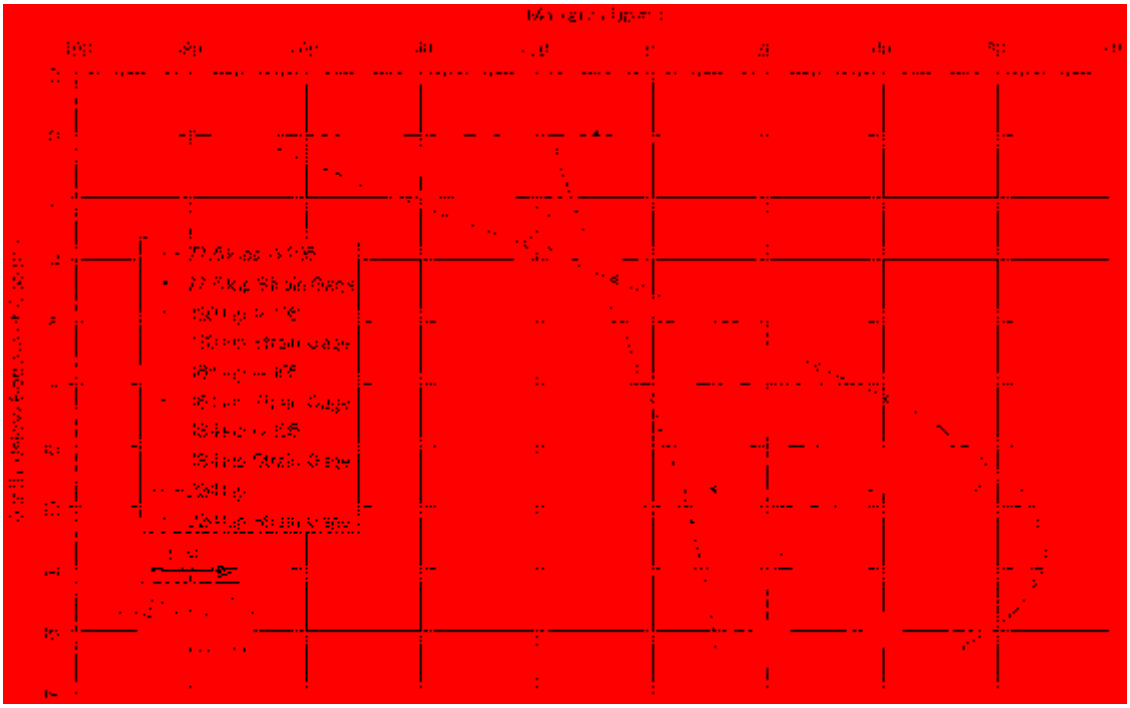

Figure 7-30 Moment versus depth curve for the north center pile of pile cap 1 (1-N) based on incremental deflection versus depth curves measured from shape array 106 during the virgin clay test after excavation (Test 2), with point moments measured from strain gauges at various depths also shown

The trends for the negative moments from the array in the center pile are in close agreement with the moments from the strain gauges. If the array trends were to continue to the

base of the pile cap only the 0.25 inch (77.5 kips) and 0.75 inch (161 kips) test increments would vary by more than 5 kip-ft. On the other hand, the array trends for the negative moments from the north pile are more inconsistent when compared to the strain gauges. Most test increments are off by 8 kip-ft if the array trends were to continue to the bottom of the pile cap. The 1.5 inch or 224 kip load is the only one that appears to be in agreement. In addition, the magnitude of the maximum negative moment at each test increment is about 13 kip-ft higher on the center pile than on the north pile.

A comparison of the moments derived from the arrays and inclinometers at the maximum displacement is shown in Figure 7-31. There is great agreement with the inclinometers; however the array trends vary to a degree. The inclinometers and the center array place the maximum positive bending moment at a depth of about 11.5 ft, but the north array places it lower at 12.5 ft. When looking at the magnitude of the maximum positive moment, the inclinometer measures about 58 kip-ft, the north array 66.5 kip-ft, and the center array 69 kip-ft. The north array and the inclinometers are in fair agreement at the maximum negative moment measuring around -60 kip-ft, while the center array measures a higher value at about -95 kip-ft. The discrepancy in the center array's negative moments is due to the fact that it recorded greater displacements at depths closer to the pile cap than the inclinometers as shown in Figure 7-27. Overall, when comparing these results to those of Test 1, the location of the maximum positive moment in the center pile was about 1 ft lower without the passive force behind the pile cap, but the magnitude stayed relatively the same. On the north pile, the location of the maximum positive moment stayed within 1 ft or closer, but decreased about 5 kip-ft on average without the passive

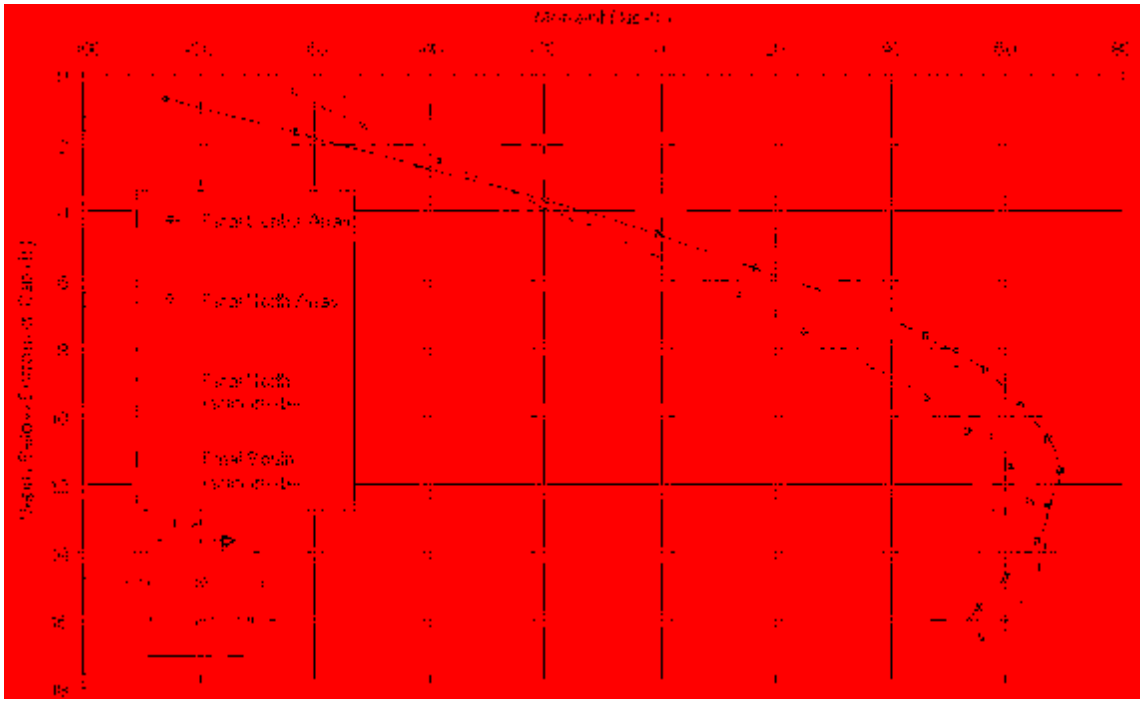

Figure 7-31 Moment versus depth comparison for the piles in pile cap 1 based on deflections measured from the north and south inclinometers, shape array 104 and shape array 106 during the virgin clay test after excavation (Test 2)

resistance. The maximum negative moments on the center pile remained at the bottom of the pile cap, but increased 15 kip-ft on average from Test 1, although it is believed that the negative moments determined from the center pile array were already low compared to the corresponding strain gauges on that test. Therefore, the 15 kip-ft average increase in moment may not be realistic. The maximum negative moments on the north pile also remained at the bottom of the pile cap, but decreased about 13 kip-ft on average without the passive force.

In summary, without the passive force behind the pile cap, the magnitudes of the positive bending moments decreased slightly, while the negative moments decreased on average 13 kip-ft. The location of the positive moments appeared to have dropped about 1 ft, while the location of the maximum negative moments remained at the bottom of the pile cap.

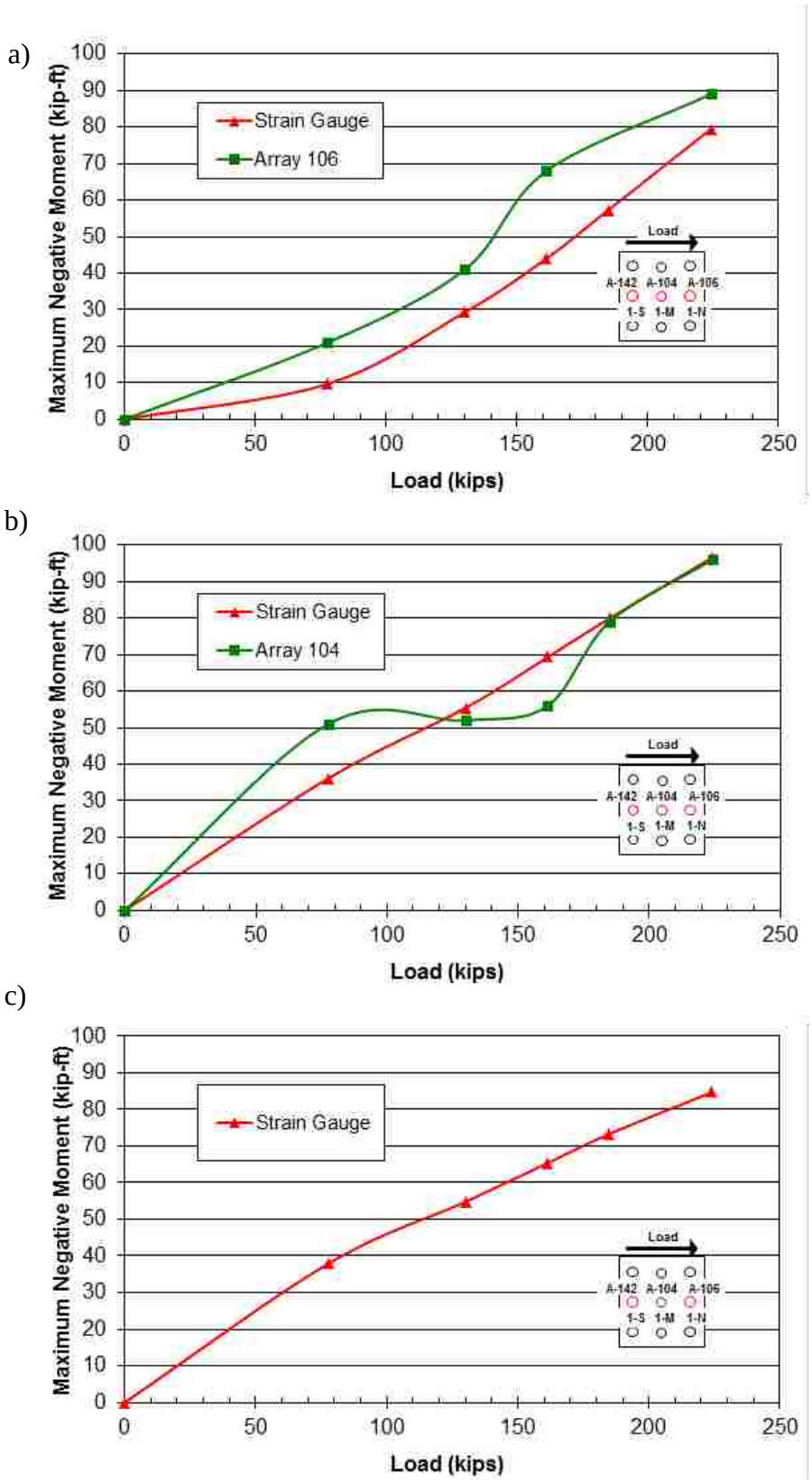

Figure 7-32 Maximum negative moment (base of cap) versus total pile cap load for piles (a) 1-N, (b) 1-M, and (c) 1-S in cap 1 during the virgin clay test after excavation (Test 2)

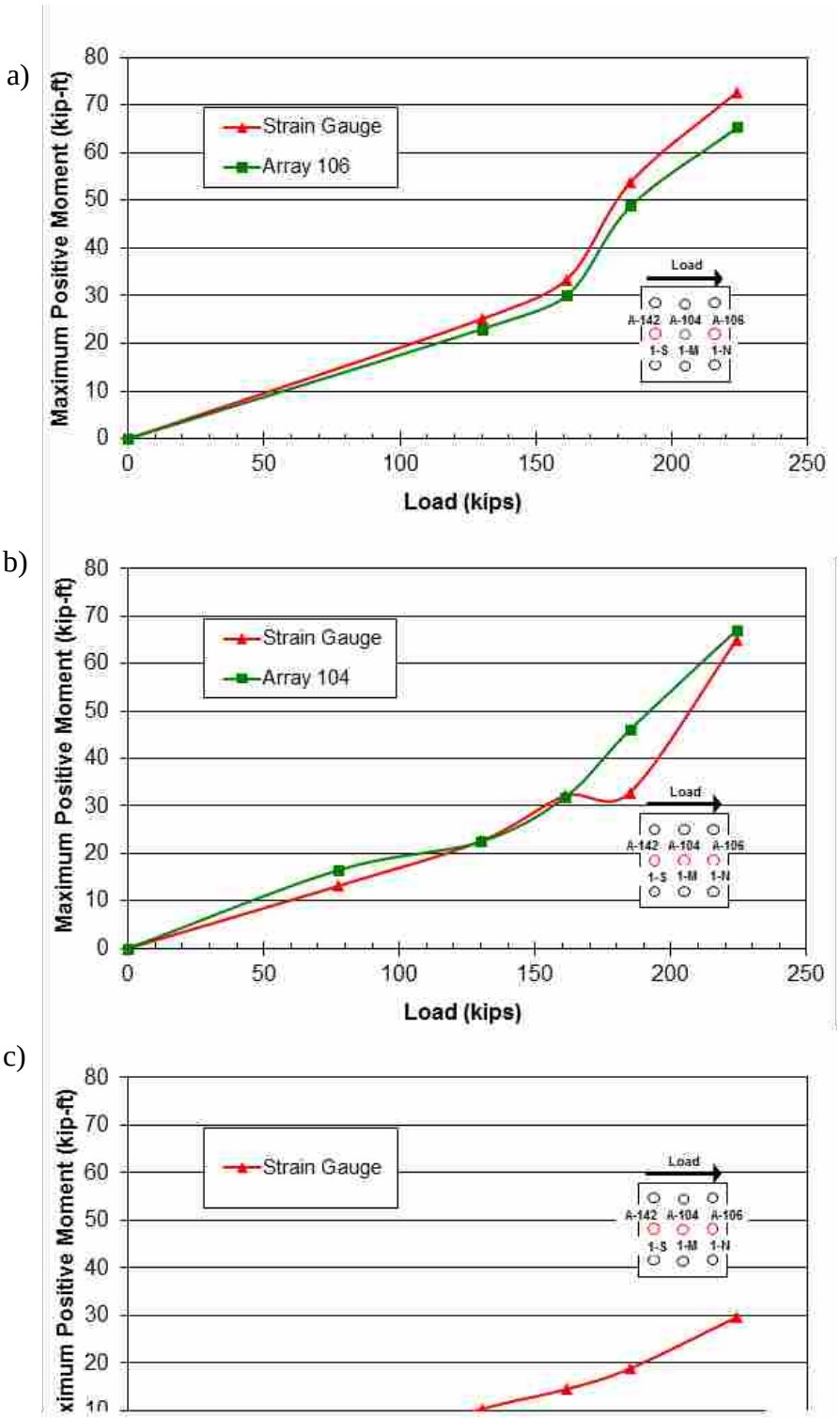

Figure 7-33 Maximum positive moment versus total pile cap load for piles (a) 1-N, (b) 1-M, and (c) 1-S in cap 1 during the virgin clay test after excavation (Test 2)

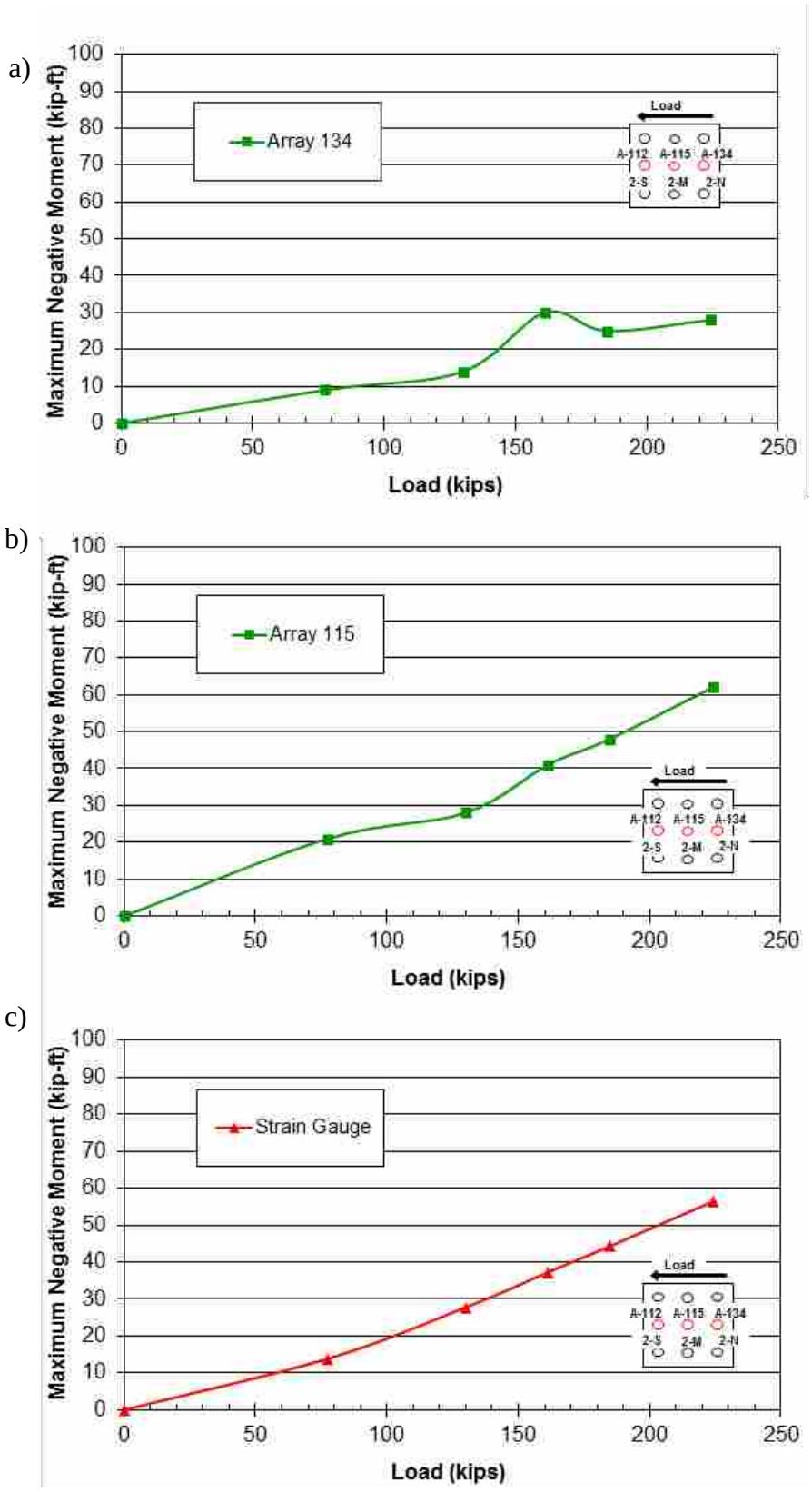

Figure 7-34 Maximum negative moment versus total pile cap load for piles (a) 2-N, (b) 2-M, and (c) 2-S in cap 2 during the virgin clay test (Test 2)

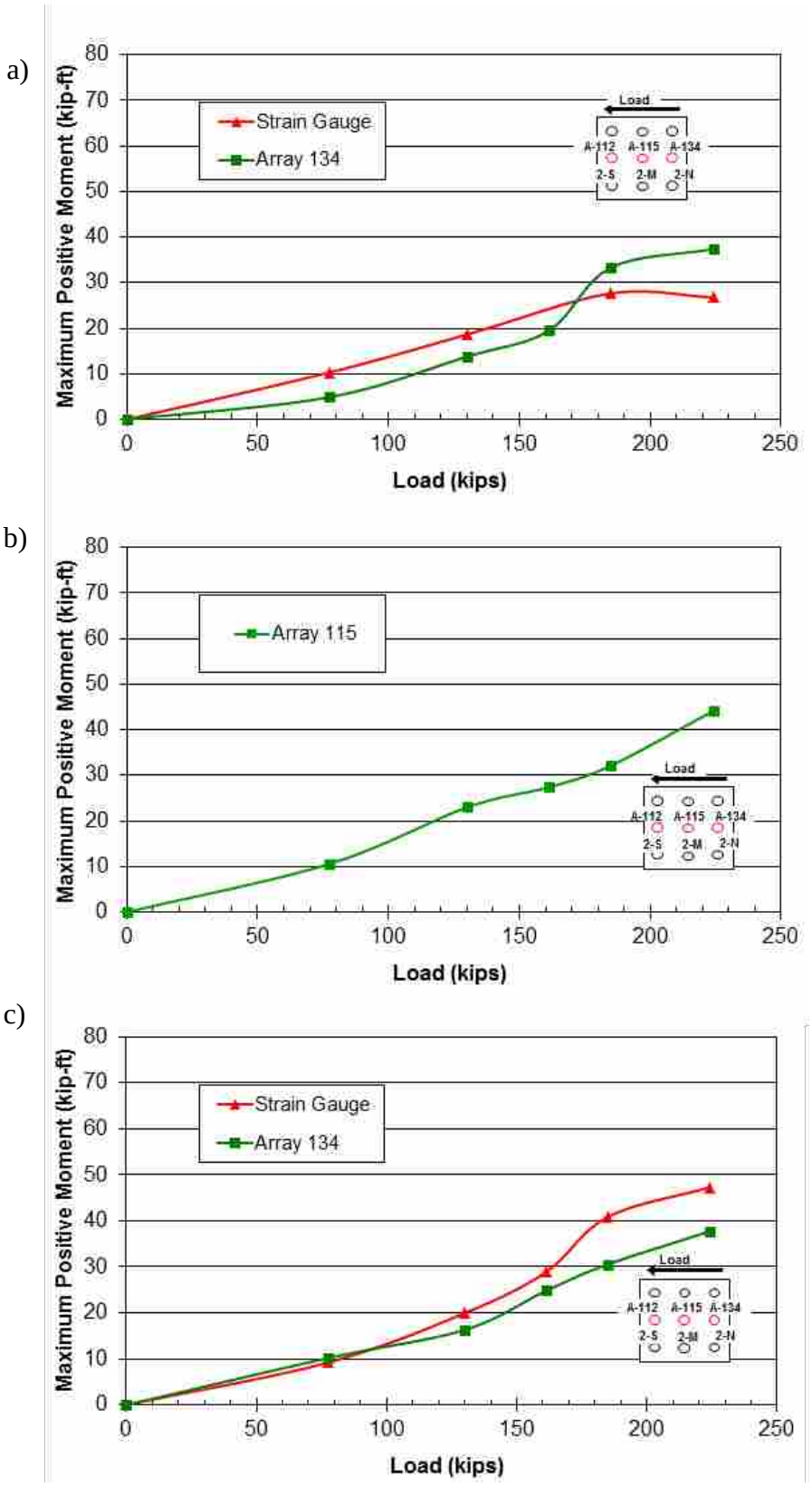

Figure 7-35 Maximum positive moment versus total pile cap load for piles (a) 2-N, (b) 2-M, and (c) 2-S in cap 2 during the virgin clay test (Test 2)

7.2.5 Moment versus Load Results

Figure 7-32 and Figure 7-33 provide plots of the maximum positive and negative bending moments versus applied pile cap load respectively for cap 1 during Test 2. Similarly, Figure 7-34 and Figure 7-35 provide plots of the maximum positive and negative bending moments versus applied pile cap load, respectively for cap 2 during Test 2. Moment data come from both shape array and strain gauge data when available. Initially, the curves are relatively linear; however, the bending moment tends to increase more rapidly with load at the higher load levels as the soil is loaded beyond its shear strength. The curves from the strain gauges provide relatively consistent moment versus load curves with little evidence of group interaction effects for the displacement levels involved. The moments from the leading row do not appear to plot higher than the moments from the trailing rows. The agreement between the curves computed by the strain gauges and shape arrays is generally reasonable. The results appear to be somewhat more consistent for the positive moments than for the negative moments.

8 COMPACTED FILL TEST RESULTS

The tests involving compacted fill were Tests 3, 4, and 5 in a series of 16 tests. As explained earlier in the Section 5.1, three tests performed on a pile cap underlain with compacted fill: one without passive resistance against the face of the pile cap, one with fill compacted to the top of the pile cap, and one with virgin clay against the face of the pile cap. The reason for doing the three tests was to determine how much lateral passive resistance is gained by compacting fill next to a pre-existing pile cap or bridge abutment as compared to having virgin clay against the cap. For plan and profile views of the compacted fill setup, please refer to Figure 5-5. The results from pushing a pile cap into a virgin clay face (Test 5) will be presented first followed by pushing a pile cap with no passive resistance against the face of the pile cap (Test 3). The third test discussed in this chapter involved pushing a pile cap into a compacted fill face (Test 4).

8.1 Virgin Clay Underlain with Compacted Fill – Test 5

Another test was performed in addition to the two purely virgin clay tests in order to set a point of reference for the compacted fill and RAP tests. This test involved pushing the farthest south pile cap, which was underlain with a layer of compacted fill, into a virgin clay face as shown in Figure 8-1. The main purposes of this test were to find out how much increase in lateral capacity can be obtained simply from compacting fill underneath a pile cap before construction and to set a baseline for the testing being done on the compacted fill and RAPs.

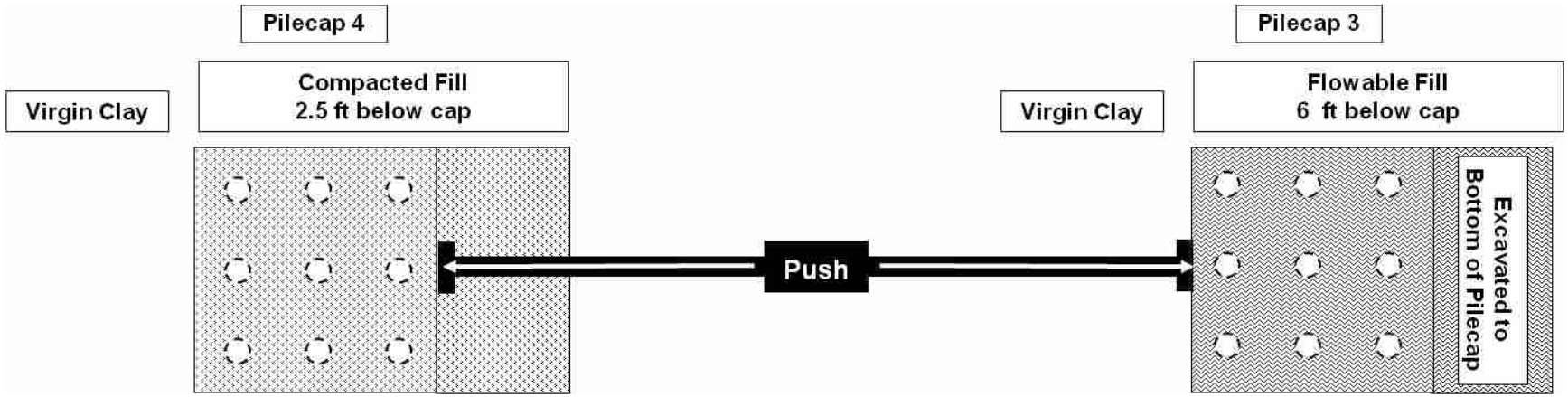

Figure 8-1 Schematic plan view of Test 5 (See Figure 5-5 for dimensions)

The datum for the displacement of Test 5 was the initial measurements taken prior to Test 3 (which will be explained later in the chapter). Since this test took place after the pile caps had been pulled together in Tests 3 and 4 (the compacted fill tests), there was some residual displacement in the direction of the original displacement once the load was released. Thus, Test 5, started with a negative initial displacement of about 0.3 inches. As depicted in Figure 8-1, a pile cap reinforced with flowable fill was also tested with this push. The results and analysis of the flowable fill testing will be addressed in a separate thesis.

All instrumentation of string potentiometers, shape arrays, inclinometers, actuator pressure transducer, and strain gauges were in place in Tests 3 through 5 and initial measurements were taken prior to each test. Several strain gauges were damaged during pile driving and the locations of all the instrumentation for pile cap 4 are shown in Figure 4-10. Strain gauges were located on the north and south piles of pile cap 4. The test followed the standard testing procedure.

8.1.1 Load versus Pile Cap Displacement

The lateral load versus displacement graph shows the complete load path, including incremental cycles for the test. Figure 8-2 was obtained from the actuator pressure transducer and the string potentiometers attached to the pile cap. The actuator pushed the pile caps to the prescribed target increments of 0.125, 0.25, 0.5, 0.75, 1.0, and 1.5 inches based on the actuator extension. The actual displacements for pile cap 4 with the residual offset of -0.28 inches were -0.17, -0.02, 0.17, 0.40, 0.73, and 1.20 inches respectively as measured by the corresponding string potentiometers. A plot of pile cap displacement versus peak applied load for each test increment is displayed in Figure 8-3. It shows that the residual displacement in the opposite direction from Tests 3 and 4 was so large that 96 kips of force was required to push the pile cap

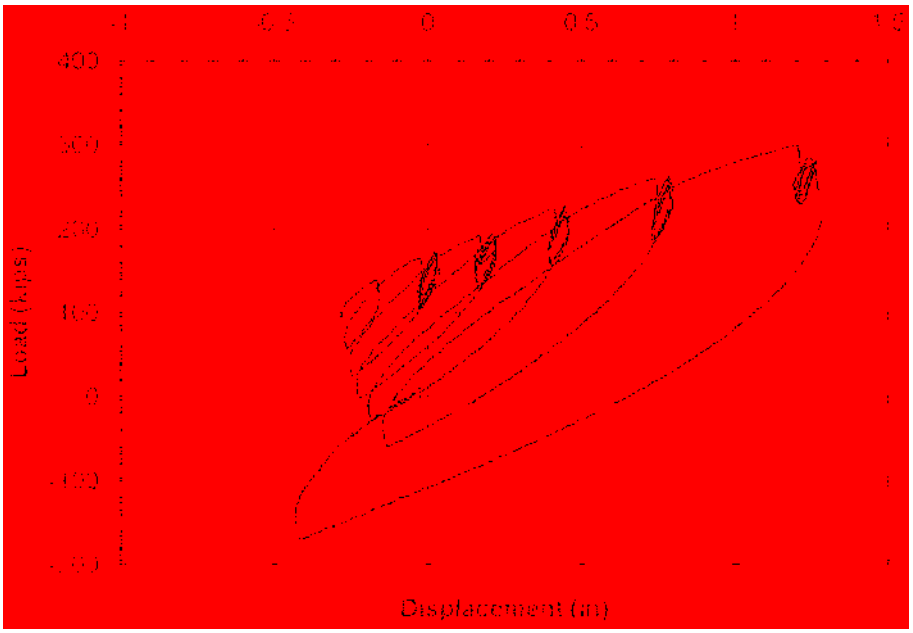

Figure 8-2 Plot of continuous pile cap displacement versus applied load for pile cap 4 during testing of compacted fill under the cap (Test 5)

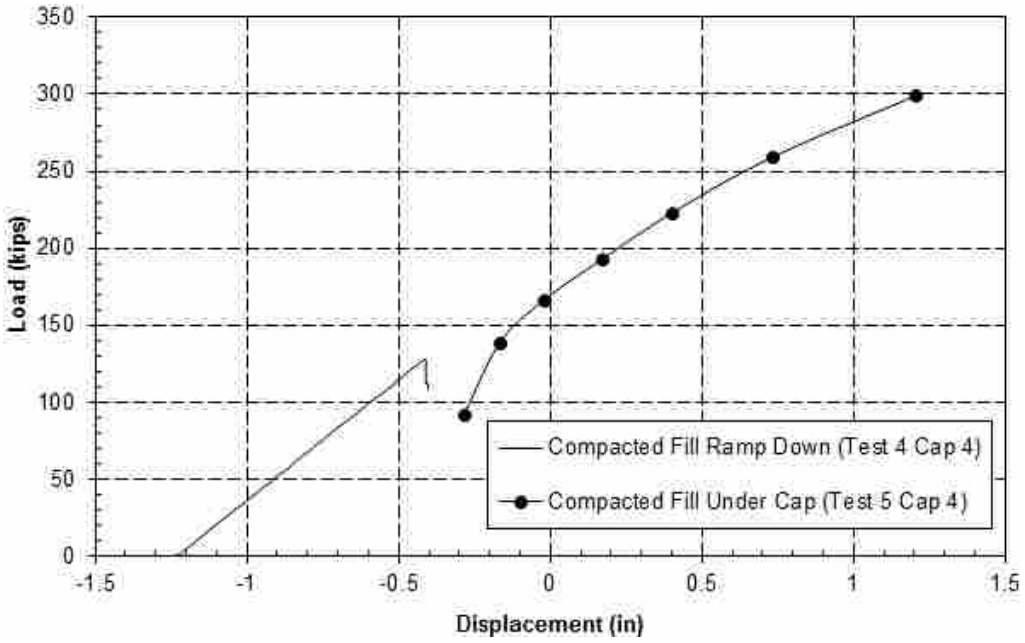

Figure 8-3 Plot of pile cap displacement versus peak applied load for each increment of testing of compacted fill under the cap (Test 5) with the final displacement data from the compacted fill test (Test 4)

back to -0.28 inches of displacement. Because the displacement and load started at such large values, the final ramp down to zero displacement from Test 4 from the point of zero load to the end of the test is included in Figure 8-3. The figure shows that the soil had been reloaded prior

to the beginning of this test. For comparison with other tests, an interpolated maximum load of 307 kips will be used at a displacement of 1.5 inches.

8.1.2 Load versus Pile Head Rotation

Load versus pile head rotation curves obtained from string potentiometer and shape array measurements for pile cap 4 during Test 5 are provided in Figure 8-4. Rotation was measured from the string potentiometers located directly above the corbel of pile cap 4. The distance between the string potentiometers was approximately 46 inches. Refer to Figure 4-10 for a

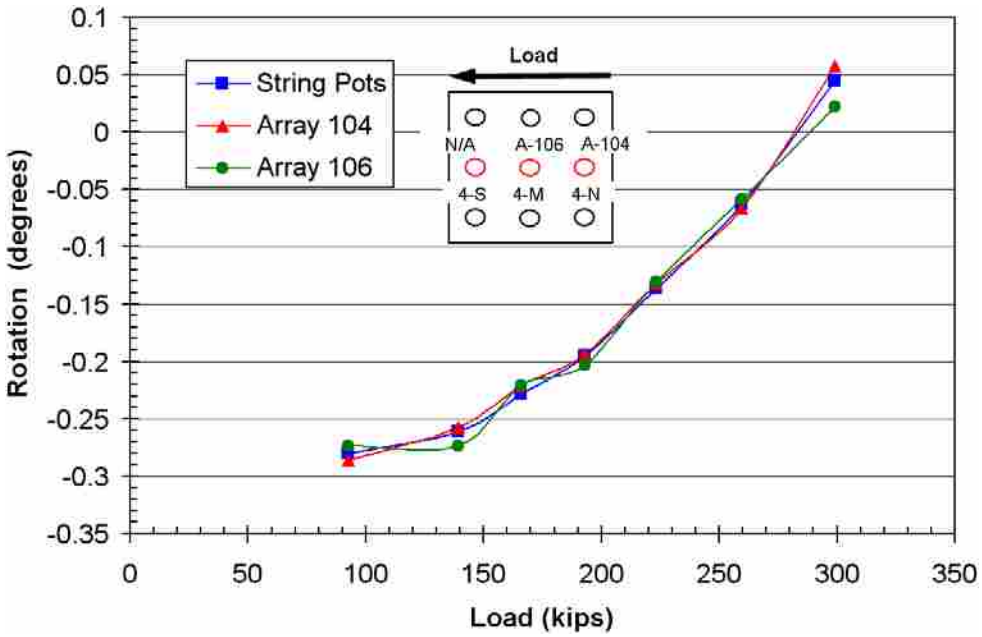

Figure 8-4 Peak pile cap load versus pile head rotation for cap 4 during testing of compacted fill under the cap (Test 5) obtained from string potentiometer and shape array measurements

review on the position of the string pots on pile cap 4. Rotation was also measured from the shape arrays. The difference in node deflections near the bottom of the pile cap and the top of the corbel was used to measure rotation from shape array 104 and shape array 106. The distance between these nodes was 48 inches and 24 inches, respectively. Because of the initial negative offset, the pile caps had a slight negative rotation at the start of the test. As load increased, the

rotation shifted to a positive value. The total rotation as measured by the string pots on pile cap 4 was about 0.045°. The shape arrays show two different rotations: 0.058° from array 104 and 0.022° from array 106. Initial offset of the shape arrays, likely due to seating problems or slippage of the shape array in the PVC pipe, required a -0.22° shift in the measured angles from each of the shape arrays.

8.1.3 Pile Deflection versus Depth

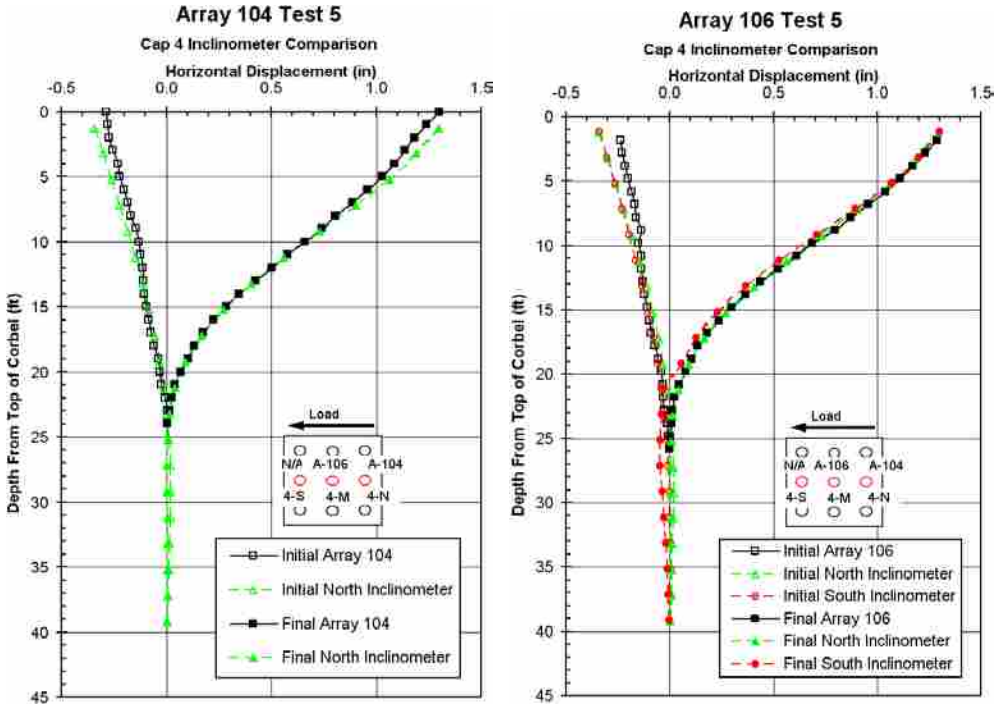

Figure 8-5 Comparison of depth versus deflection curves for the piles in pile cap 4 from the north inclinometer with shape array 104 and the north and south inclinometers with shape array 106 for testing of compacted fill under the cap (Test 5)

Figure 8-5 shows the pile deflection versus depth profiles of the arrays and inclinometer readings on pile cap 4 at their initial positions and at the maximum displacement during Test 5. There is good agreement in the north pile even though there is a slight discrepancy starting at about 9 ft below the top of the corbel. Because there was no inclinometer in the center pile, a

comparison for both the north and south inclinometers is included in Figure 8-5. The center array (array 106) is consistent with the north inclinometer over its entire length and with both inclinometers within the upper 8 ft of measurements. Neither of the arrays' displacement readings matches up very well with the initial inclinometer readings. In order to correct for movement below the end of the shape array, 0.0065 inches were added to the displacements of array 104 in both the inclinometer comparisons. Because there was no inclinometer in the center pile, nothing was added to the displacement readings for array 106. By adjusting the shape array this way, the shape array displacements match better with the inclinometer readings taken at similar depths. The inclinometers show that there was deflection in the piles at depths greater

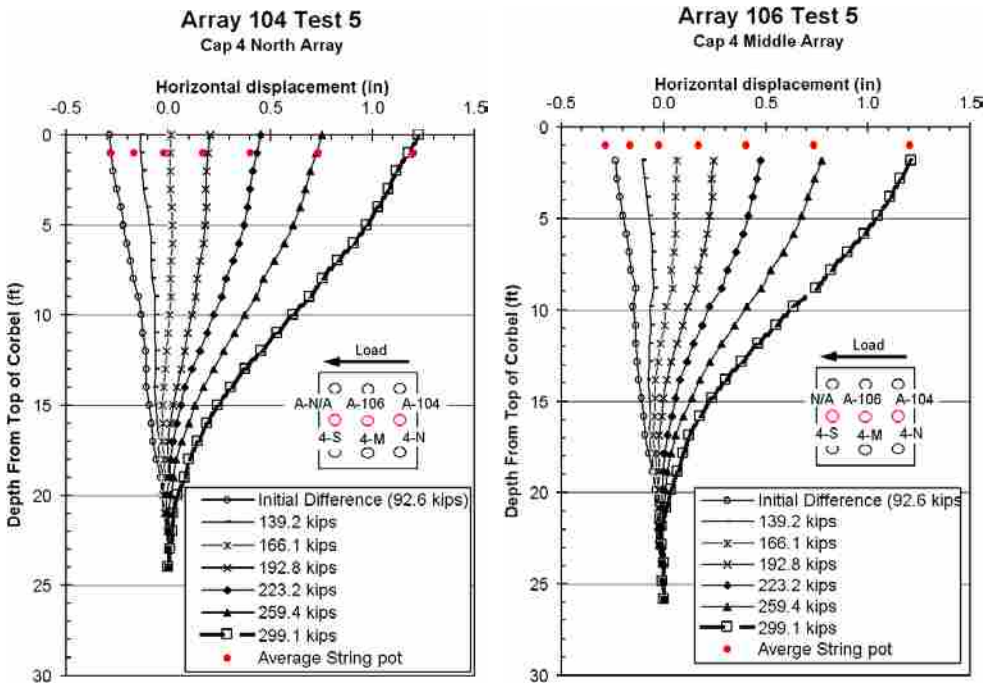

Figure 8-6 Deflection versus depth curves for pile cap 4 for each increment of testing of compacted fill under the cap (Test 5), with pile head displacements from the string potentiometers also shown

than 30 ft. The discrepancy in array 104 is also shown in the string potentiometer comparison with the shape arrays found in Figure 8-6. The difference between the array readings and the string potentiometer readings appears to be due to movement in the pile below the end of the

shape arrays. In spite of the minor discrepancies, the general trend and slope of the depth versus displacement profiles are consistent and provide a reasonably accurate representation of the deflections that the piles experienced.

8.1.4 Pile Bending Moment versus Depth

Bending moments were estimated from the depth versus displacement profiles from the center and north piles on pile cap 4 using the methods described in Section 6.2. Figure 8-7 and Figure 8-8 provide bending moment versus depth curves for the piles in pile cap 4 at the six target displacement levels during Test 5. The curves were obtained from the shape arrays while the individual points represent moments computed from the strain gauges. The datum for these figures has been moved from the top of the corbel to the bottom of the pile cap. The maximum load at each target displacement is also listed in each figure's legend.

The maximum positive bending moments from the north pile array in Figure 8-7 appear to occur from about 12 ft to 14 ft below the bottom of the pile cap. The positive moments measured from the strain gauges are within 24 kip-ft or less of the moments from the array at these depths. Not much can be discerned from the trend of the north array's negative bending moments as it had to be truncated due to inconsistencies of the numerical method at depths just below the pile cap. In order to get an idea of what the array might have measured as a negative moment near the pile cap, a straight line was drawn to extend the observed trend to the base of the cap. These lines show up as dashed lines in Figure 8-7. The regression, in this case, does not show a very consistent correlation between shape arrays and strain gauges.

The maximum positive moments from the center pile in Figure 8-8 occur at depths from about 10.5 ft to 13.5 ft below the bottom of the pile cap. No strain gauges were installed on the center pile of pile cap 4; therefore none are shown in Figure 8-8. Strain gauges were

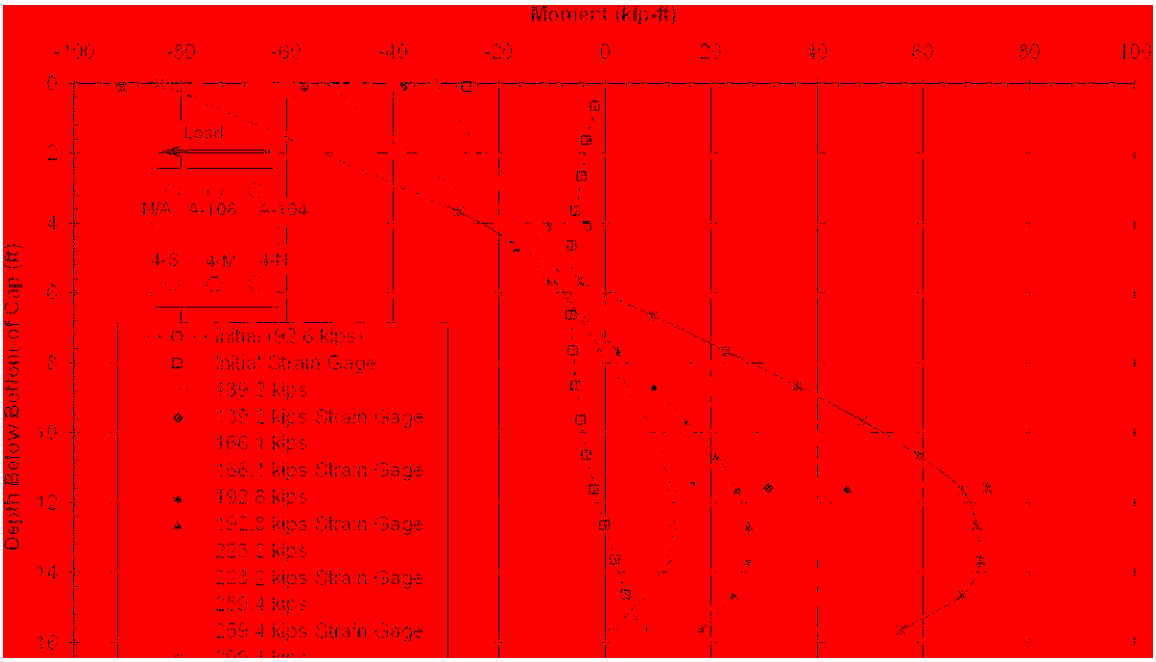

Figure 8-7 Moment versus depth curve for the north center pile of pile cap 4 (4-N) based on incremental deflection versus depth curves measured from shape array 104 during testing of compacted fill under the cap (Test 5), with point moments measured from strain gauges at various depths also shown

installed on the south pile (4-S) and Figure 8-9 shows lower moments than were recorded in either of the other two piles. It appears that the 166.1 kips load, or 0.25 inch test increment, array measurements are not correct for array 106; they do not follow the trends of any of the other instrumentation. With the exception of that test increment, the positive moments from the arrays are within 6.5 kip-ft or less when comparing the arrays in the two instrumented piles at corresponding loads. The trends for the negative moments of the arrays are very inconsistent when compared to the strain gauges. Most test increments are off by over 20 kip-ft if the array trends were to continue to the bottom of the pile cap. In addition, the magnitude of the array readings were taken at the beginning of inclinometer readings, therefore, it was able to maximum negative moment in the north pile at each test increment is about 70 to 80 percent of the maximum negative moment in the center pile. The moments shown in Figure 8-9 are generally

smaller than the corresponding moments in the other two piles, indicating possible group interaction effects in the pile cap.

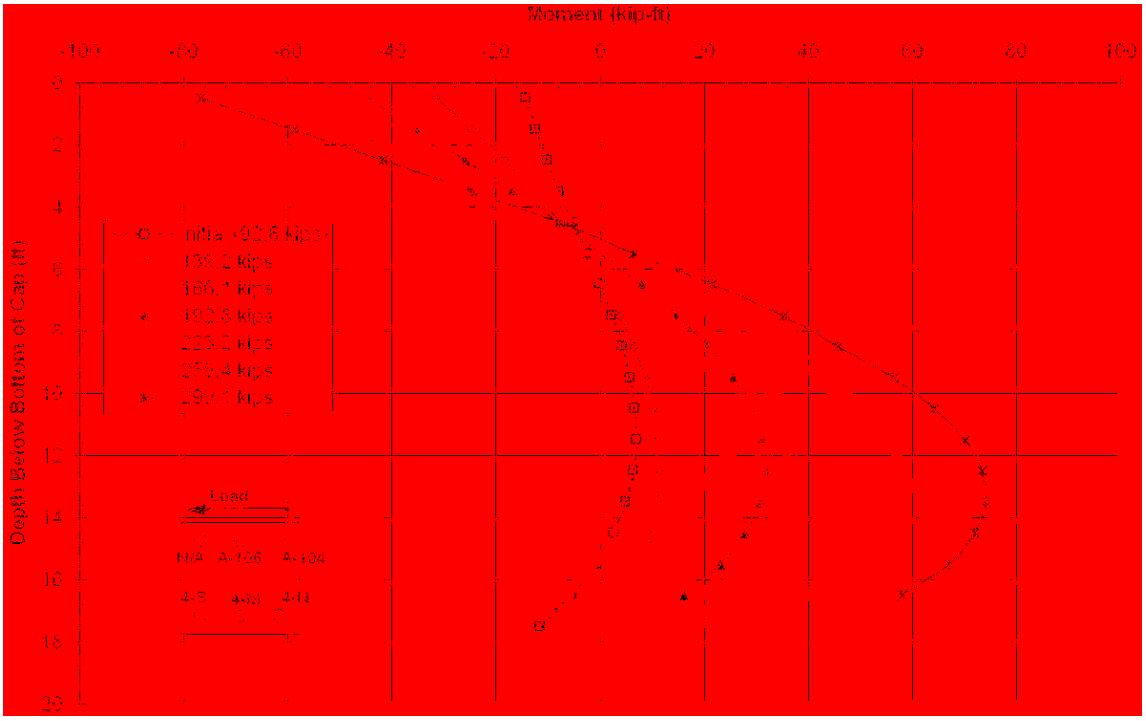

Figure 8-8 Moment versus depth curve for the center pile of pile cap 4 (4-M) based on incremental deflection versus depth curves measured from shape array 106 during testing of compacted fill under the cap (Test 5)

A comparison of the moments derived from the arrays and inclinometers at the initial position and the maximum displacement is shown in Figure 8-10. There is not a particularly good agreement with the inclinometers; however the arrays and inclinometers do show similar trends. The inclinometers place the maximum positive bending moment at about 12 ft, but the arrays place it lower at 13.5 ft. When looking at the magnitude of the maximum positive moment, the north inclinometer measures about 53.5 kip-ft, the south inclinometer 58.6 kip-ft, the north array 67.6 kip-ft, and the center array 74.1 kip-ft. The maximum negative moment as measured by the inclinometers and the shape arrays ranges from about 65 kip-ft from the north array to about 90 kip-ft from the middle array, with the inclinometers falling between those values at around 85 and 80 kip-ft for the north and south inclinometers respectively. One

possible reason for the discrepancy in the negative moments is due to the fact that the further south in the cap the measurement is taken, the greater the bending moment and the lower the pull-out force. Of course, this does not explain the difference between the north array and the north inclinometer. This issue may be addressed by scrutinizing the data sampling methods and time frames used. While the shape array can take 20 readings per second for each of its nodes, the inclinometer requires 15 to 20 minutes to obtain readings for the whole length. The shape

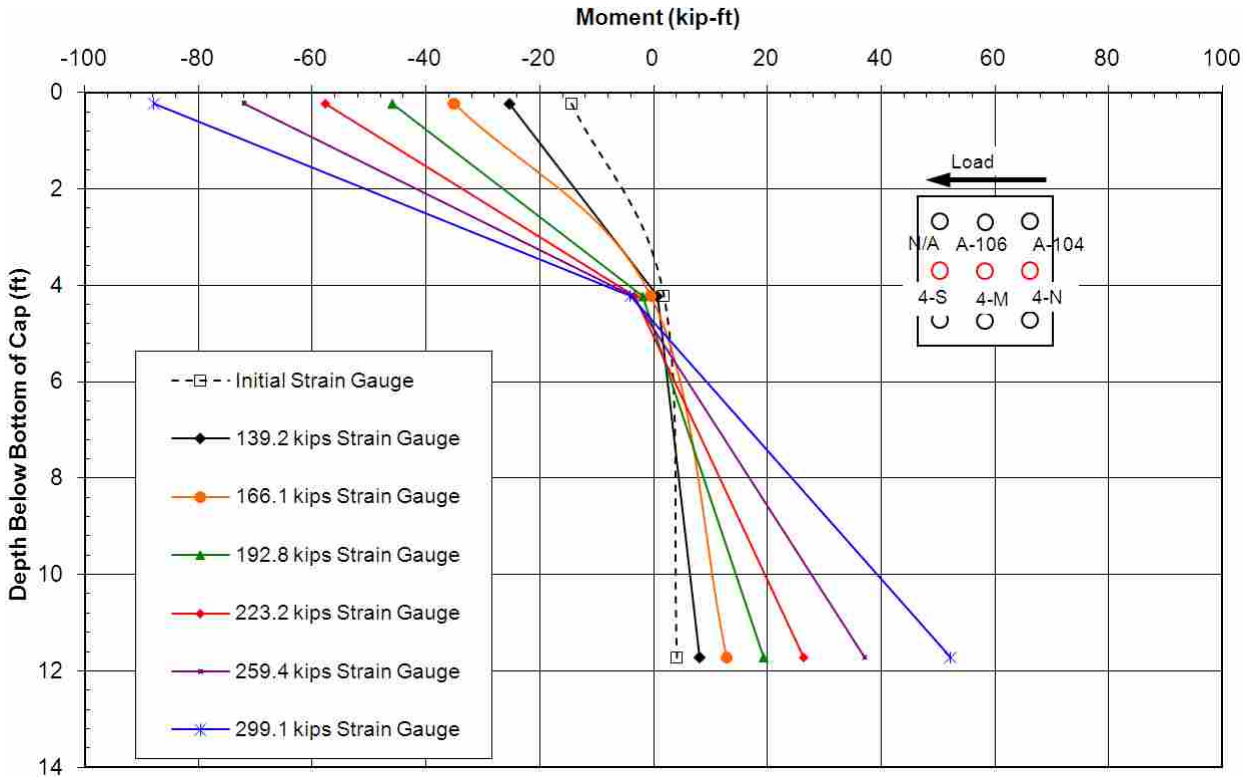

Figure 8-9 Moment versus depth curve for the south pile of pile cap 4 (4-S) based on incremental deflection versus depth curves measured from strain gauges during testing of compacted fill under the cap (Test 5)

capture a better picture of what stresses were in the pile in real time. As the inclinometer readings were taken, the piles had time to relax and the soil along with it, so the inclinometers should report slightly lower moments than do the shape arrays.

Overall, when comparing these results to those of Test 1, the location of the maximum positive moment in the center pile occurred at about the same depth with the compacted fill

under the pile cap, but the magnitude increased by about 10 kip-ft. The location of the maximum positive moment in the north pile occurred about 1 ft deeper with the compacted fill under the pile cap and the magnitude decreased by about 4 kip-ft. The maximum negative moments on all piles should generally occur at the bottom of the pile cap when loaded during testing.

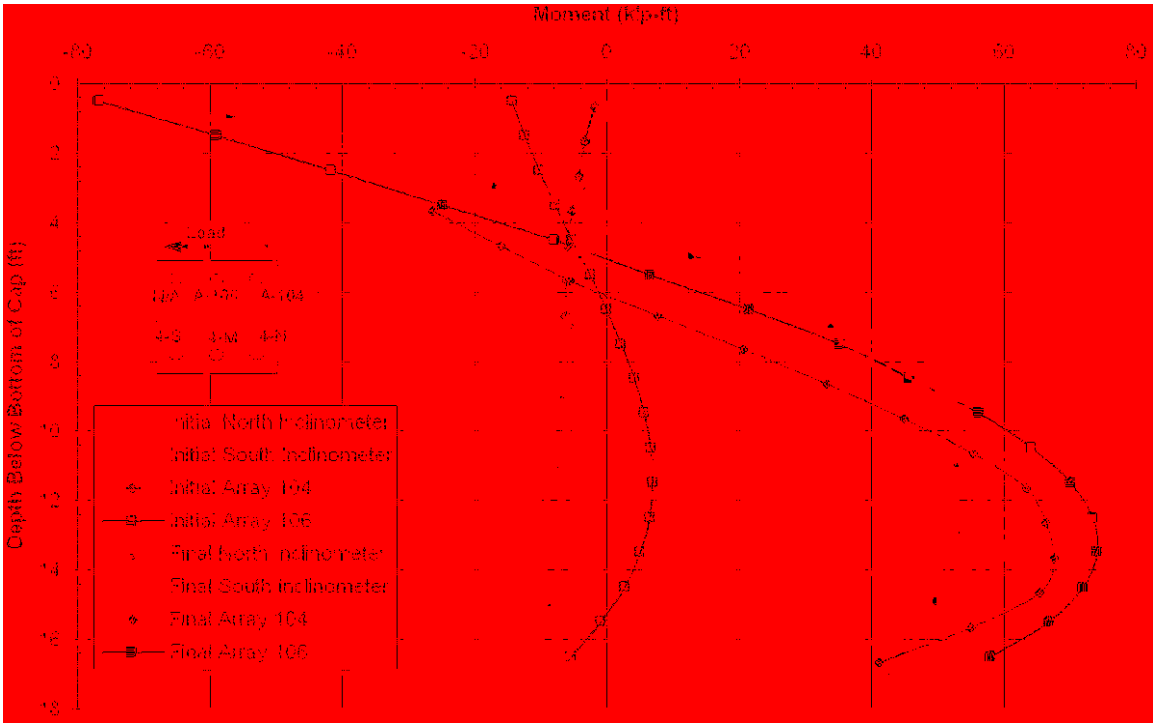

Figure 8-10 Moment versus depth comparison for the piles in pile cap 4 based on deflections measured from the north and south inclinometers, shape array 104 and shape array 106 during testing of compacted fill under the cap (Test 5)

8.1.5 Moment versus Load Results

Figure 8-11 and Figure 8-12 provide plots of the maximum negative and positive bending moments versus applied pile cap load respectively for cap 4 during Test 5. Moment data come from both shape array and strain gauge data when available. The curves are relatively linear as the load increases and the soil resistance is mobilized from the base of the pile cap downward. The curves from the strain gauges provide relatively consistent moment versus load curves but do not show the same indications of group interaction effects that we observed in the shape

arrays and inclinometers. The agreement between the curves computed by the strain gauges and shape arrays is reasonable for the negative moments, but not for the positive moments.

8.2 Compacted Fill Without Passive Resistance – Test 3

In Test 3, pile caps 3 and 4 were pulled together to test the compacted fill without passive resistance. Neither of the pile caps involved in this test had been moved previously. As shown in Figure 5-4 and Figure 8-13, an area of 5 ft by 9 ft of fill was compacted just north of pile cap 4 from a depth of 3.5 ft below the cap to the base of the pile cap prior to driving the piles. The true depth of compacted fill under the pile cap is not known due to swelling of the clay during pile installation. Based on the amount of soil that was excavated prior to pouring the cap, approximately 2.5 ft of compacted fill remained under the level of the bottom of the pile cap during testing. The fill was compacted to a dry unit weight of about 110 pcf as measured by a nuclear density gauge. The results of this test will be compared to the results from Test 2 to determine the effectiveness of compacting fill under and in the area adjacent to a pile cap for increasing lateral resistance.

All instrumentation of string potentiometers, shape arrays, inclinometers, actuator pressure transducer, and strain gauges were in place and initial measurements taken prior to the test. The locations of all the instrumentation for pile cap 4 are as shown in Section 4.3. Strain gauges on pile cap 4 were located on the north and south piles of pile cap 4 (piles 4-N and 4-S). The second deepest set of strain gauges on pile 4-N (the ones installed 11 ft below the top of pile 4-N) were damaged in pile driving, therefore no strain gauge data is available for that depth. The test followed the standard procedure. The data recorded for the 0.25 inch increment from the shape arrays was corrupted, so there is no data for that increment from any of the shape arrays.

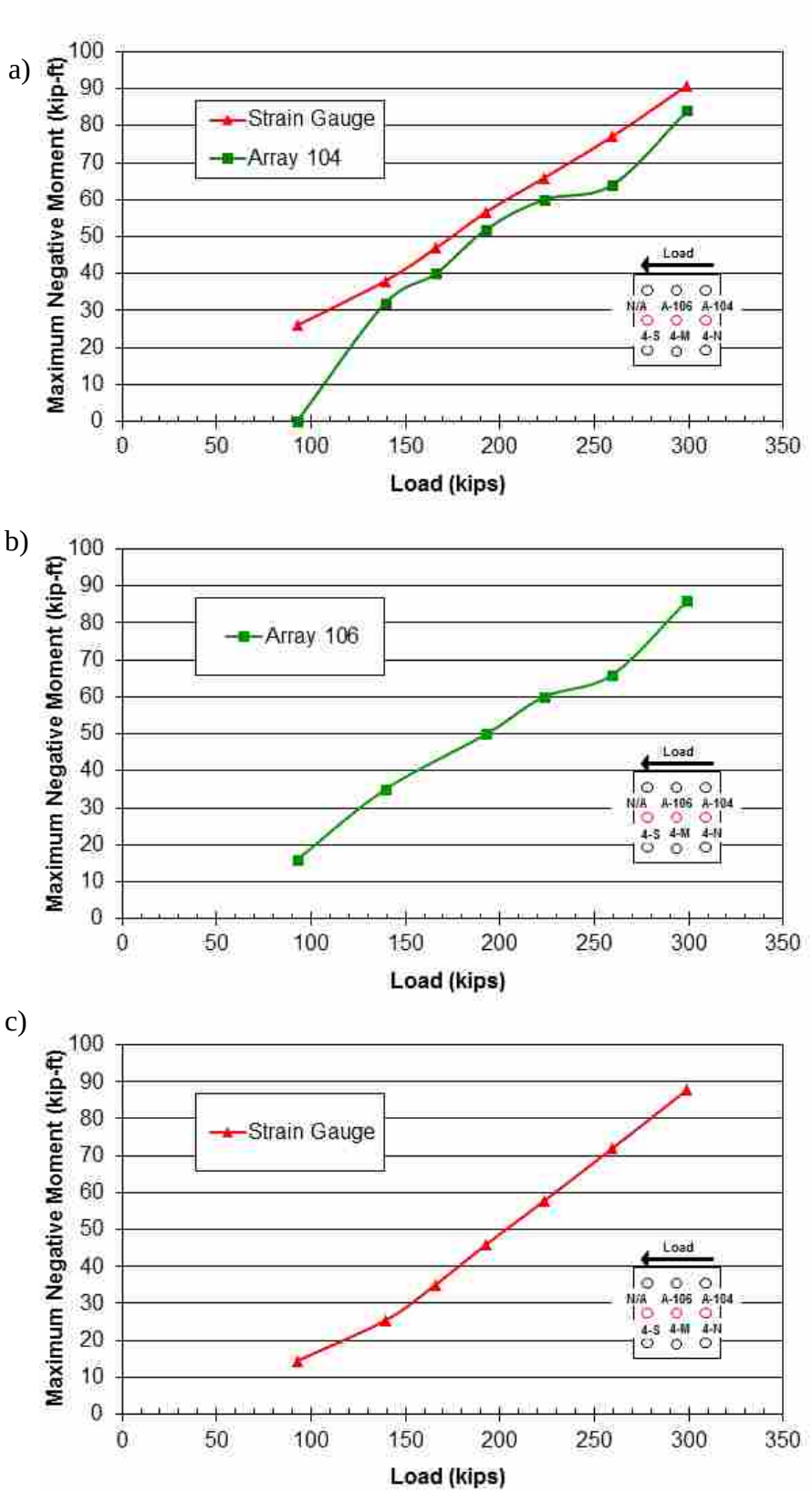

Figure 8-11 Maximum negative moment (base of cap) versus total pile cap load for piles (a) 4-N, (b) 4-M, and (c) 4-S in cap 4 during testing of compacted fill under the cap (Test 5)

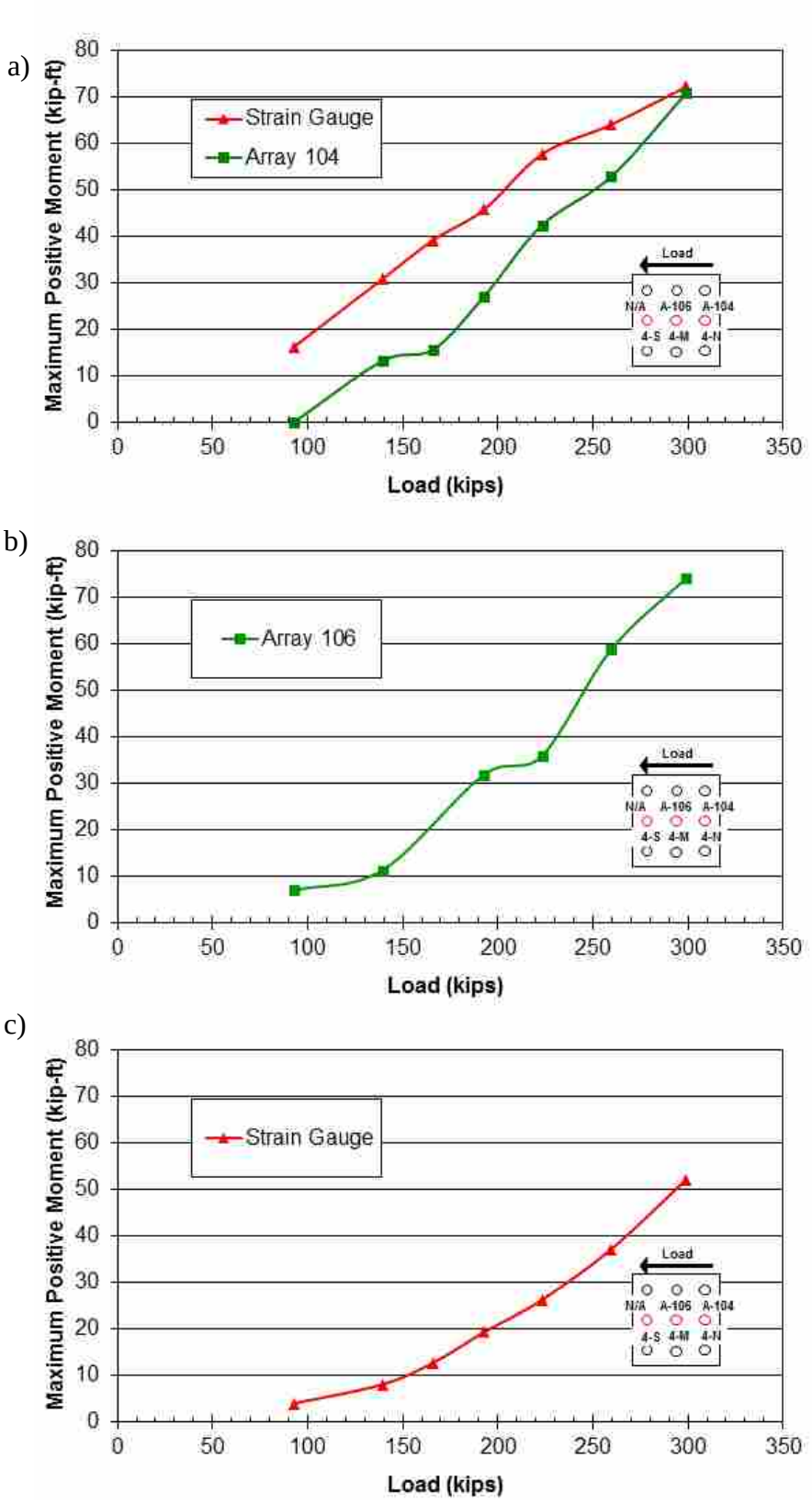

Figure 8-12 Maximum positive moment versus total pile cap load for piles (a) 4-N, (b) 4-M, and (c) 4-S in cap 4 during testing of compacted fill under the cap (Test 5)

Since this was the first test on the two southernmost pile caps, the values measured were all zero-set to the initial values of this test just prior to the commencement of testing

8.2.1 Load versus Pile Cap Displacement

The lateral load versus displacement graph shows the complete load path, including incremental cycles for the test. Figure 8-14 was obtained from the actuator pressure transducer and the string potentiometers attached to the pile cap. The actuator pushed the pile caps to target the prescribed increments of 0.125, 0.25, 0.5, 0.75, 1.0, 1.5 inches, referenced to actuator extension length, which introduced some differences in prescribed versus actual displacements for each of the pile caps involved in the test. The actual displacements for pile cap 4 were 0.08, 0.20, 0.46, 0.74, 0.98, and 1.53 inches respectively as measured by the corresponding string potentiometers. A plot of pile cap displacement versus peak applied load for each test increment is displayed in Figure 8-15. The curve in Figure 8-15 exhibits a typical hyperbolic shape that would be expected for a pile in soft clay. However, because the peak displacement was limited to 1.5 inches to prevent excessive moments in the piles, the slope of the load versus displacement curve never reached a horizontal asymptote. Nevertheless, the last part of the curve is relatively linear suggesting that the lateral resistance is primarily due to the flexural resistance of the piles. The maximum applied load during the last pull was 269.6 kips and resulted in a displacement of 1.53 inches for pile cap 4. For comparison purposes this load of 269 kips at 1.5 inch displacement will be used as the load capacity for the compacted fill with no passive resistance test.

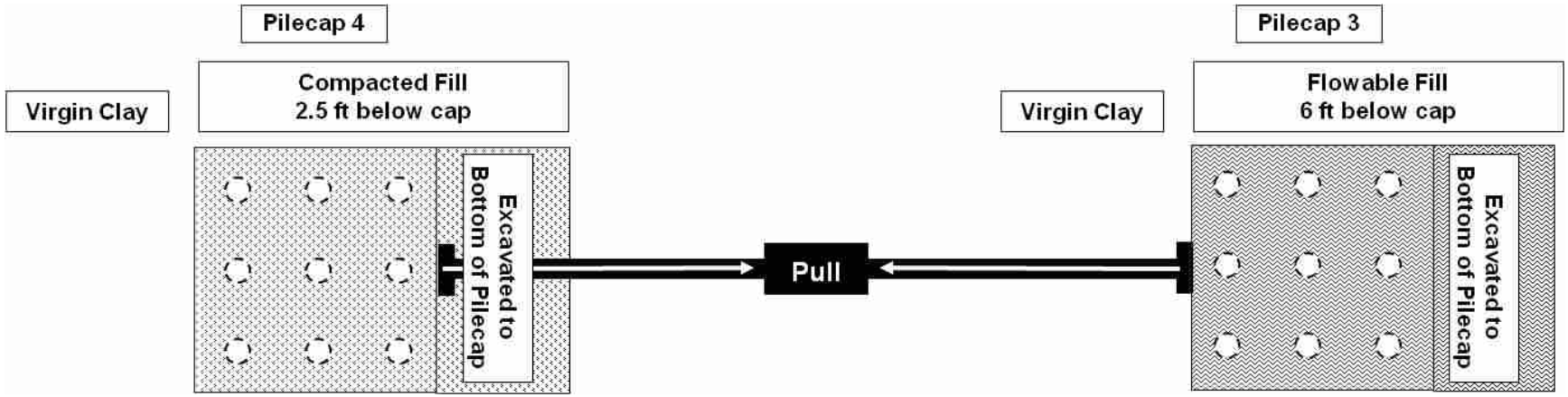

Figure 8-13 Schematic plan view of Test 3 (See Figure 5-4 for dimensions)

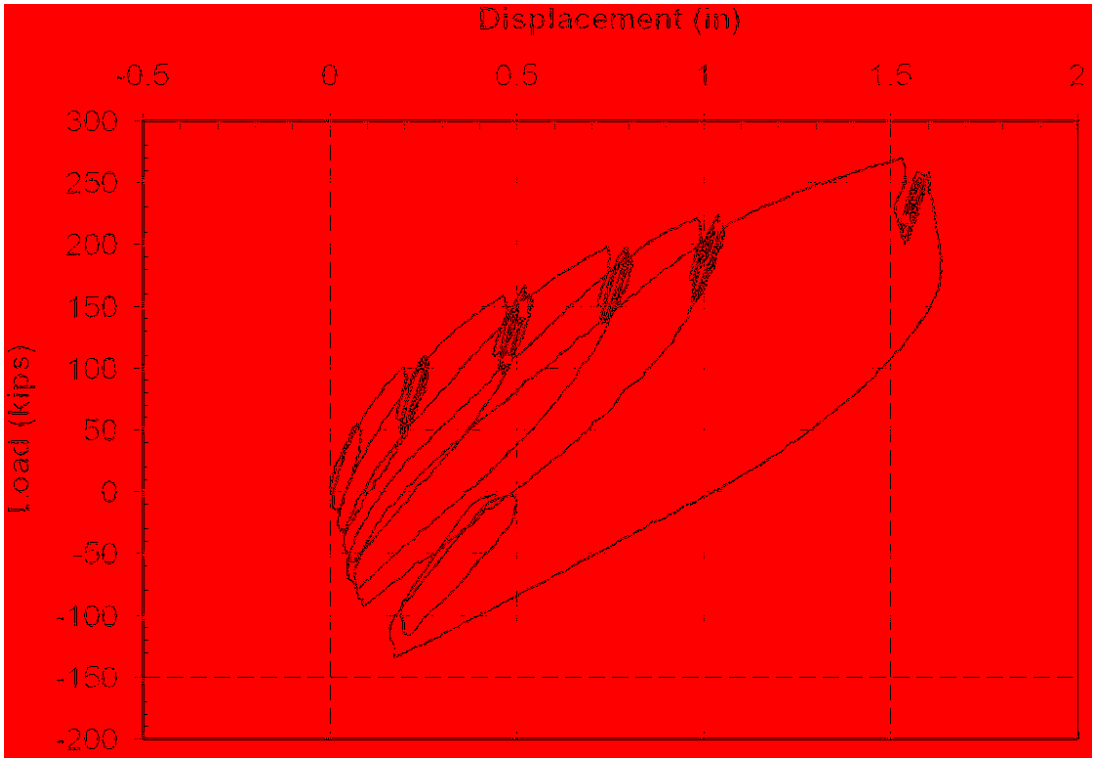

Figure 8-14 Plot of continuous pile cap displacement versus applied load for pile cap 4 during the compacted fill test with no soil adjacent to the cap (Test 3)

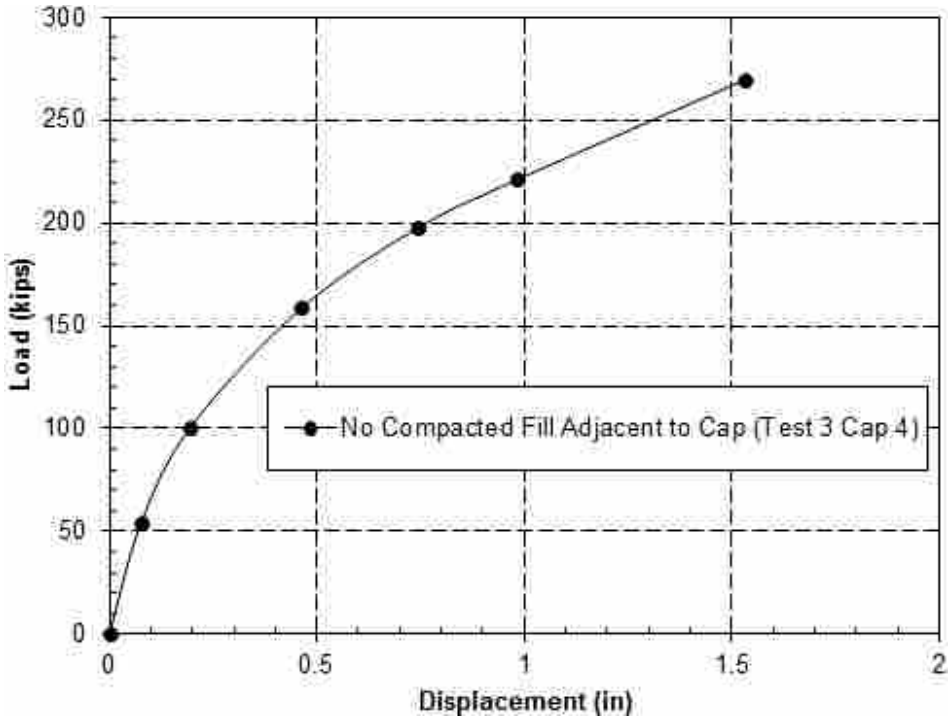

Figure 8-15 Plot of pile cap displacement versus peak applied load for each increment of the compacted fill test with no soil adjacent to the cap (Test 3)

8.2.2 Load versus Pile Head Rotation

Load versus pile head rotation curves obtained from string potentiometer and shape array measurements for pile cap 4 during Test 3 are provided in Figure 8-16. Rotation was measured from the string potentiometers located directly above the corbel of pile cap 4. The distance between the string potentiometers was approximately 46 inches. Refer to Figure 4-10 for a

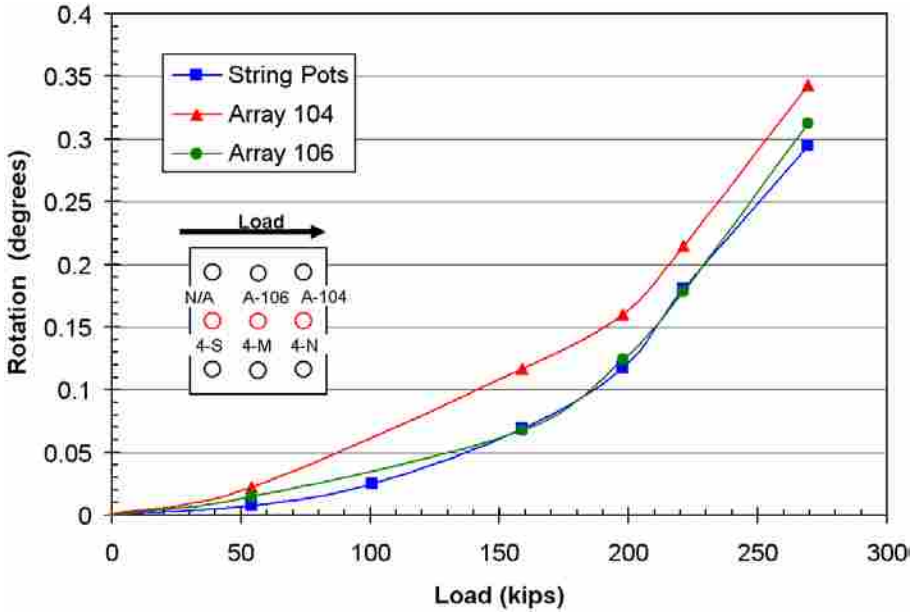

Figure 8-16 Peak pile cap load versus pile head rotation for cap 4 during the compacted fill test with no soil adjacent to the cap (Test 3) obtained from string potentiometer and shape array measurements

review on the position of the string pots on pile cap 4. Rotation was also measured from the shape arrays. The difference in node deflections near the bottom of the pile cap and the top of the corbel was used to measure rotation from shape array 104 and shape array 106; the distance between these nodes was 48 inches and 24 inches, respectively. As can be seen in the figure, the rotations from array 106 match the rotations derived from the string pots much more closely than did array 104. The total rotation as measured by the string pots on pile cap 4 was about 0.295°. The shape arrays show two different rotations: 0.343° from array 104 and 0.312° from array 106.

8.2.3 Pile Deflection versus Depth

Figure 8-17 shows the pile deflection versus depth profiles of the arrays and inclinometer readings on pile cap 4 at the maximum displacement during Test 3 (the initial position is not shown because it is zero along the entire length). There is good agreement between both shape arrays and inclinometers. Because there was no inclinometer in the center pile, a comparison for both the north and south inclinometers with array 106 is included in Figure 8-17. In order to correct for movement below the end of the shape array, 0.012 inches were subtracted from the displacements of array 104 in the inclinometer comparison. Because there was no inclinometer in the center pile, nothing was added to the displacement readings for array 106. By adjusting the shape arrays this way, their displacements match better with the inclinometer readings taken at similar depths. The inclinometers show that there was deflection in the piles at depths greater than 30 ft. At the depth of the base of shape array 104 (24 ft below the top of corbel), the inclinometer reads -0.012 inches of displacement. At the level of the base of array 106 (25.8 ft below the top of corbel) the north inclinometer reads -0.032 inches of displacement and the south inclinometer reads -0.003 inches of horizontal displacement. The difference between the array displacements and string potentiometer readings in Figure 8-18 appears to be due to movement of the pile below the lowest node of the shape arrays. In spite of the minor discrepancies, the general trend and slope of the depth versus displacement profiles are consistent and provide a fairly accurate representation of the deflections the piles experienced.

8.2.1 Pile Bending Moment versus Depth

Bending moments were estimated from the depth versus displacement profiles from the center and north piles on pile cap 4 using the methods described in Section 6.2. Figure 8-19 and

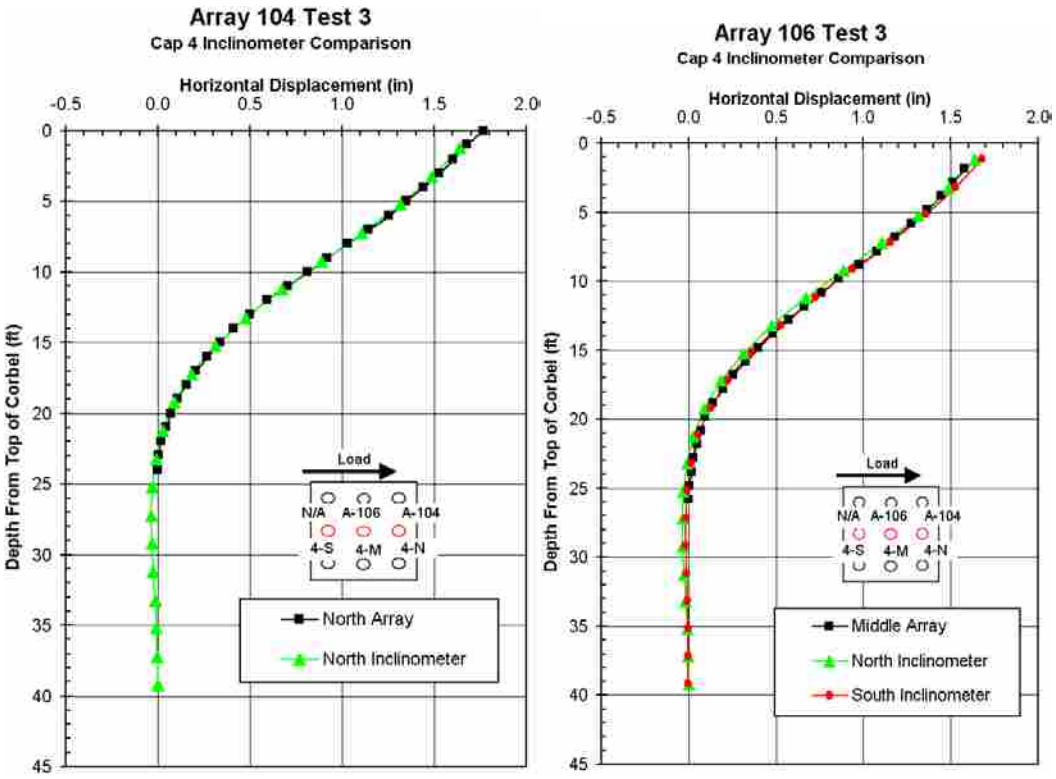

Figure 8-17 Comparison of depth versus deflection curves for the piles in pile cap 4 from the north inclinometer with shape array 104 and the north and south inclinometers with shape array 106 for the compacted fill test with no soil adjacent to the cap (Test 3)

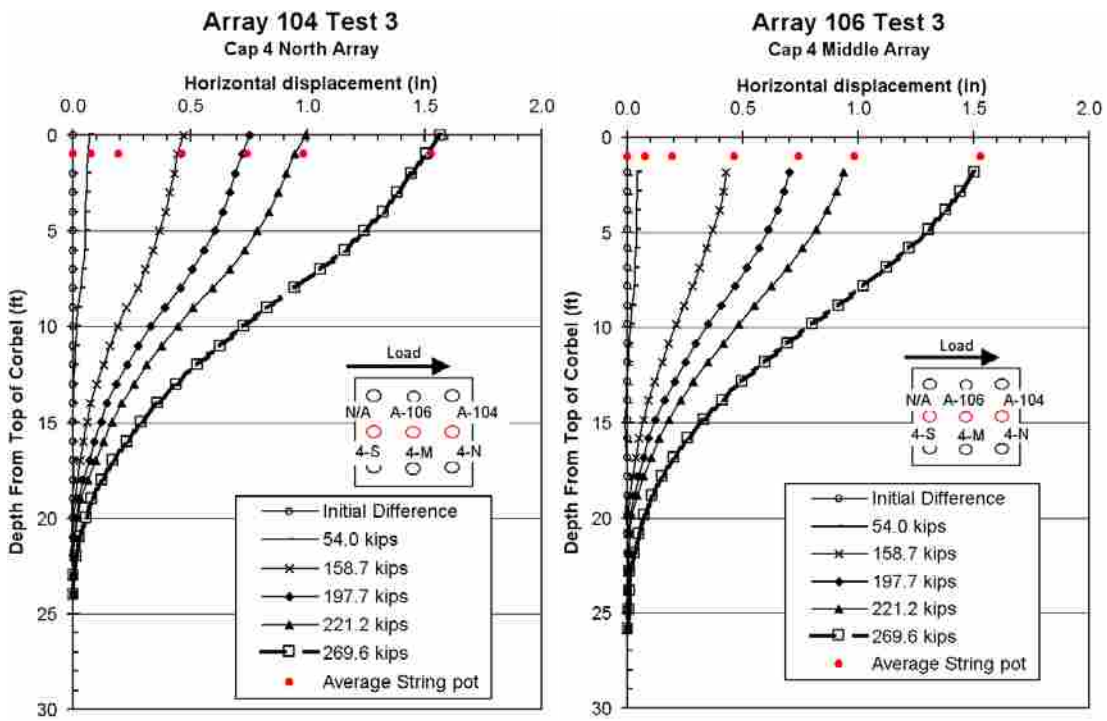

Figure 8-18 Deflection versus depth curves for pile cap 4 for each increment of the compacted fill test with no soil adjacent to the cap (Test 3), with pile head displacements from the string potentiometers also shown

Figure 8-20 provide bending moment versus depth curves for the piles in pile cap 4 at the six target displacement levels during Test 3. The curves were obtained from the shape arrays while the individual points represent moments computed from the strain gauges. The datum for these figures is the bottom of the pile cap. The maximum load at each target displacement is also listed in each figure's legend.

The maximum positive bending moments from the north pile array in Figure 8-19 tend to occur from about 11 ft to 12 ft below the bottom of the pile cap. The positive moments measured from the strain gauges are within 10 kip-ft or less of the moments from the array. Not much can be discerned from the trend of the north array's negative bending moments as it had to be truncated due to inconsistencies of the numerical method at depths just below the pile cap. Judging from the trend up to the truncation point, it appears that the shape array readings would match up with the strain gauge readings if a more rigorous or complete numerical method was employed. The numerical method, in this case, does show a good correlation between shape array and strain gauges at depth.

The maximum positive moments from the center pile in Figure 8-20 occur at depths from about 10.5 ft to 12.5 ft below the bottom of the pile cap. No strain gauges were installed on the center pile of pile cap 4; therefore none are shown in Figure 8-20. The positive moments from the arrays are within 16 kip-ft or less when comparing the arrays in the two instrumented piles at corresponding loads.

The moment trends of the shape arrays demonstrate good consistency when compared to the strain gauges. The shape array curves fall within 10 kip-ft of the lower strain gauges shown (the gauges installed at 6 and 13.5 ft below the top of the piles).

A comparison of the moments derived from the arrays and inclinometers at the maximum displacement is shown in Figure 8-21. There is not great agreement with the inclinometers;

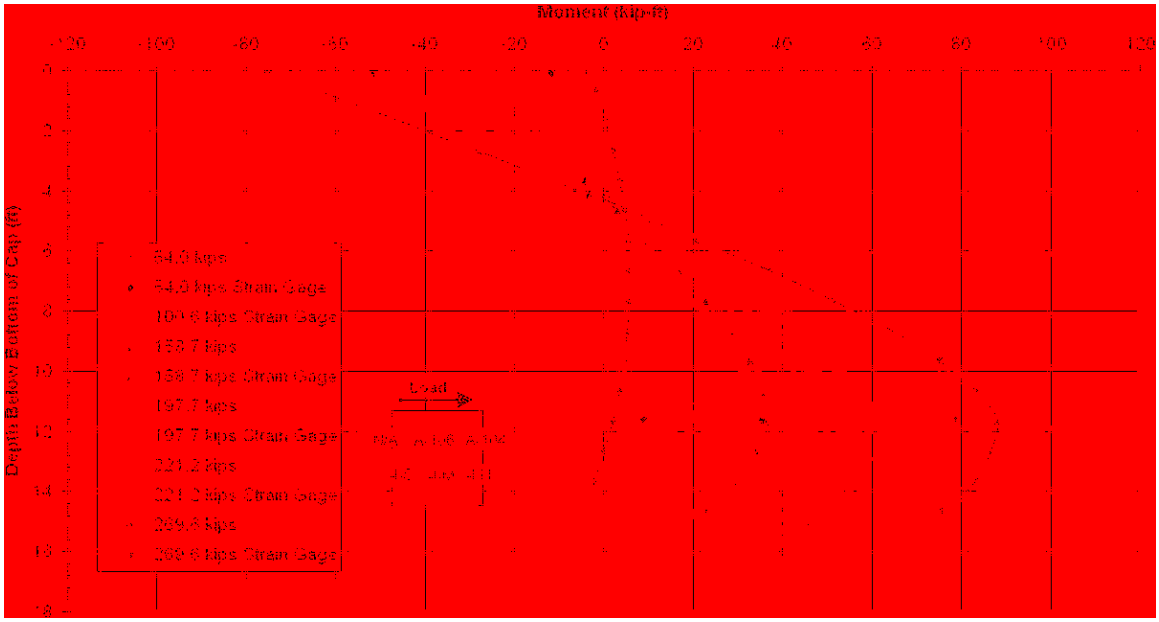

Figure 8-19 Moment versus depth curve for the north center pile of pile cap 4 (4-N) based on incremental deflection versus depth curves measured from shape array 104 during the compacted fill test with no soil adjacent to the cap (Test 3), with point moments measured from strain gauges at various depths also shown (Dashed lines are extrapolations)

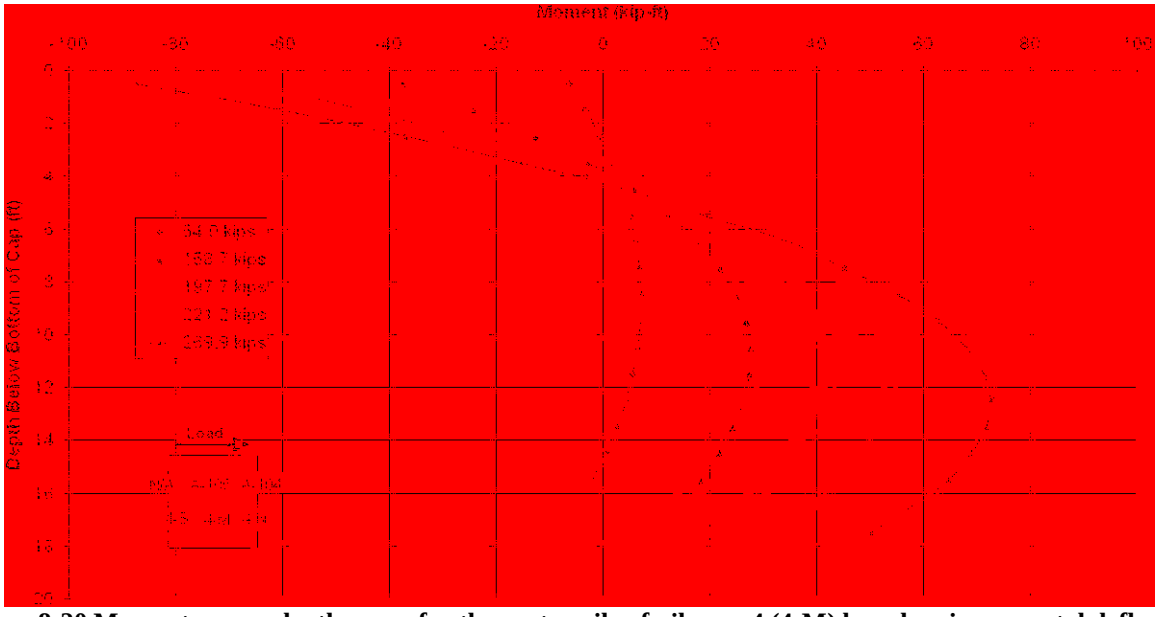

Figure 8-20 Moment versus depth curve for the center pile of pile cap 4 (4-M) based on incremental deflection versus depth curves measured from shape array 106 during the compacted fill test with no soil adjacent to the cap (Test 3)

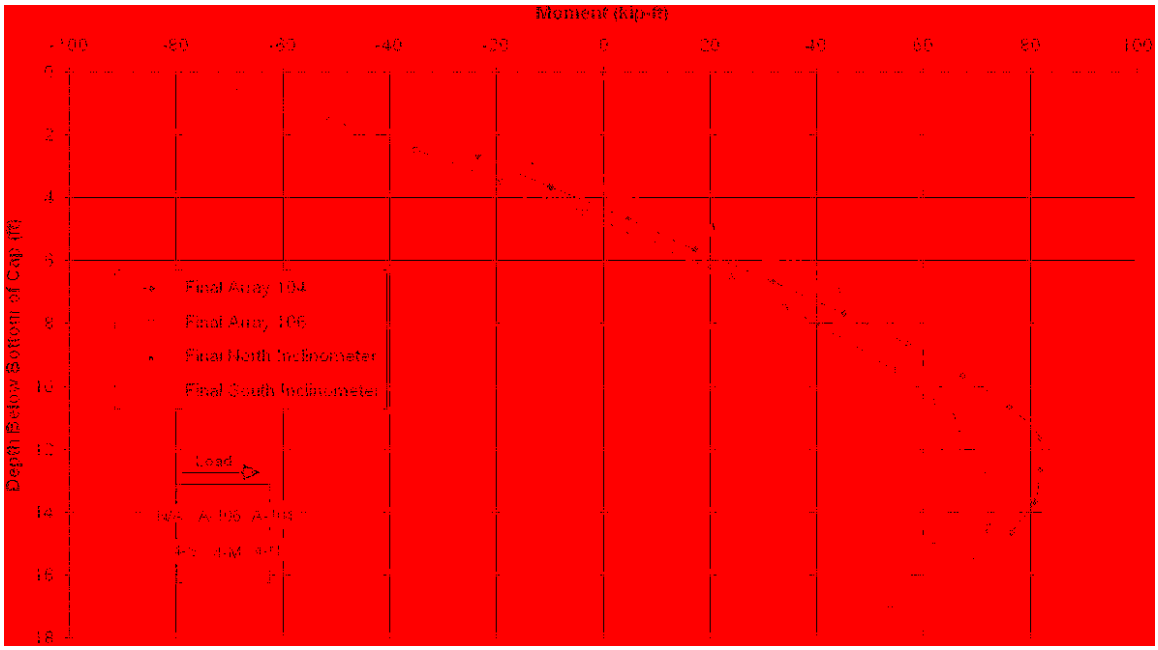

Figure 8-21 Moment versus depth comparison for the piles in pile cap 4 based on deflections measured from the north and south inclinometers, shape array 104 and shape array 106 during the compacted fill test with no soil adjacent to the cap (Test 3)

however the arrays and inclinometers do show similar trends. The inclinometers and array 106 place the maximum positive bending moment at about 14 ft, but array 104 places it higher at around 11.7 ft. When looking at the magnitude of the maximum positive moment, the north inclinometer measured about 67 kip-ft, the south inclinometer 65 kip-ft, the north array 81.9 kip-ft, and the center array 72.7 kip-ft. The maximum negative moment as measured by the inclinometers and the shape arrays ranges from about 60 kip-ft from the north array to about 76 kip-ft from the middle array, with the inclinometers falling between those values at around 62 and 63 kip-ft for the north and south inclinometers respectively. Some of the discrepancy between the shape arrays and inclinometers can be understood by scrutinizing the differences between the two in the way data is collected as well as the relative time frame needed to collect data. The shape array readings were taken at the beginning of inclinometer readings, therefore, it was able to capture a better picture of what stresses were in the pile in real time. As the inclinometer readings were taken, the piles had time to relax and the soil along with it, so the

inclinometers should report slightly lower moments than do the shape arrays. The trends shown in the inclinometer comparison (in Figure 8-21) demonstrate what would be expected showing a higher positive moment the further north the readings are taken. Because the loading occurred toward the north, the northern piles (the leading row) should experience higher loading due to group effects, and hence, they also should experience a higher moment due to pile head fixity

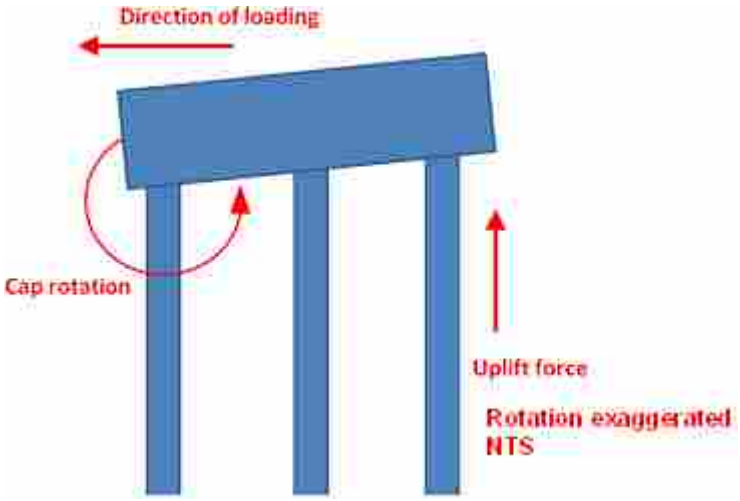

Figure 8-22 Pile cap rotation and resulting loading mechanisms

when compared to piles further to the south. The rotation of the pile cap also contributes to the increased moment in the leading piles. Because the leading piles provide greater resistance, a fulcrum of sorts forms roughly at the location of the leading piles. This fulcrum causes the rotation of the pile cap to center around the leading piles, causing greater moments in the leading piles because they are subjected to higher bending forces. The piles further to the south (the trailing piles) experience higher pullout forces (or less compression) than those to the north (the leading piles). If the leading piles were to plunge, the loads would distribute differently and the fulcrum point would likely tend to shift toward the center row of piles. Figure 8-22 illustrates the mechanism involved with developing increased moment in the leading piles and pullout forces (or at least less compression) in the trailing piles.

Overall, when comparing these results to those of Test 5, the location of the maximum positive moment in the center pile occurred at roughly the same depth without passive resistance as with pushing against a virgin soil face, but the magnitude decreased by about 2 kip-ft. The location of the maximum positive moment didn't really change between Tests 5 and 3 and the magnitude increased by about 10 kip-ft when the passive resistance on the face of the pile cap was removed. The maximum negative moments on all piles should generally occur at the bottom of the pile cap when loaded during testing.

8.2.2 Moment versus Load Results

Figure 8-23 and Figure 8-24 provide plots of the maximum negative and positive bending moments versus applied pile cap load respectively for cap 4 during Test 3. Moment data come from both shape array and strain gauge data when available. The curves become more linear as the load increases and the soil resistance is mobilized from the base of the pile cap downward. The curves from the strain gauges in Figure 8-24 provide relatively consistent moment versus load curves for the different piles whereas Figure 8-23 shows evidence of group interaction effects. Group interaction effects are characterized by a larger portion of the load being carried by leading piles as compared to trailing rows of piles. When comparing strain gauges on pile 4-N to those on 4-S, the negative moments demonstrate group interaction effects, but at the depth of the positive moments, those effects are not evident. Therefore, agreement between the curves computed by the strain gauges and shape arrays is better for the positive moments than for the negative moments. The negative moment array plot for pile 4-M seems to plot high compared to the other piles plotted in Figure 8-23.

a)

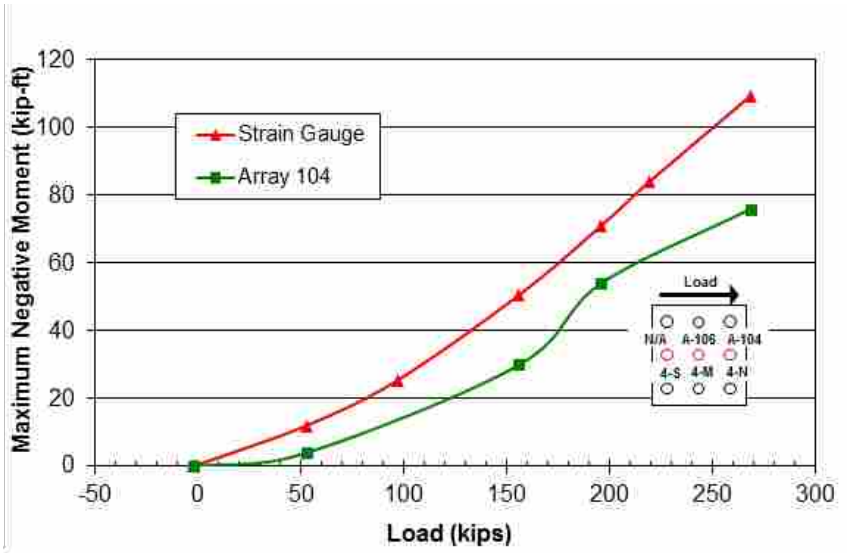

b)

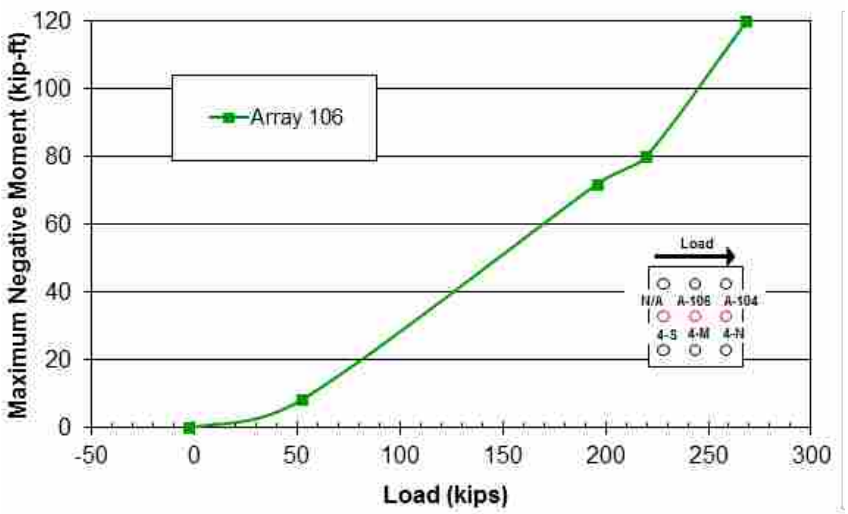

c)

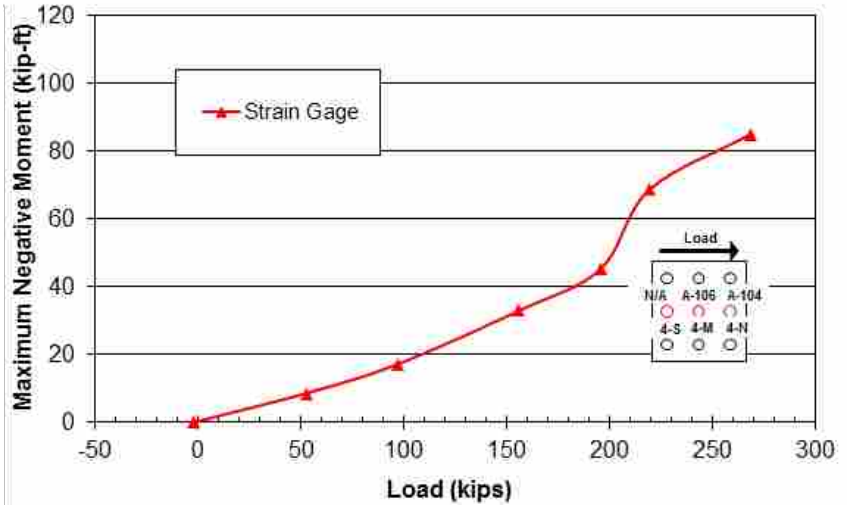

Figure 8-23 Maximum negative moment (base of cap) versus total pile cap load for piles (a) 4-N, (b) 4-M, and (c) 4-S in cap 4 during the compacted fill test with no soil adjacent to the cap (Test 3)

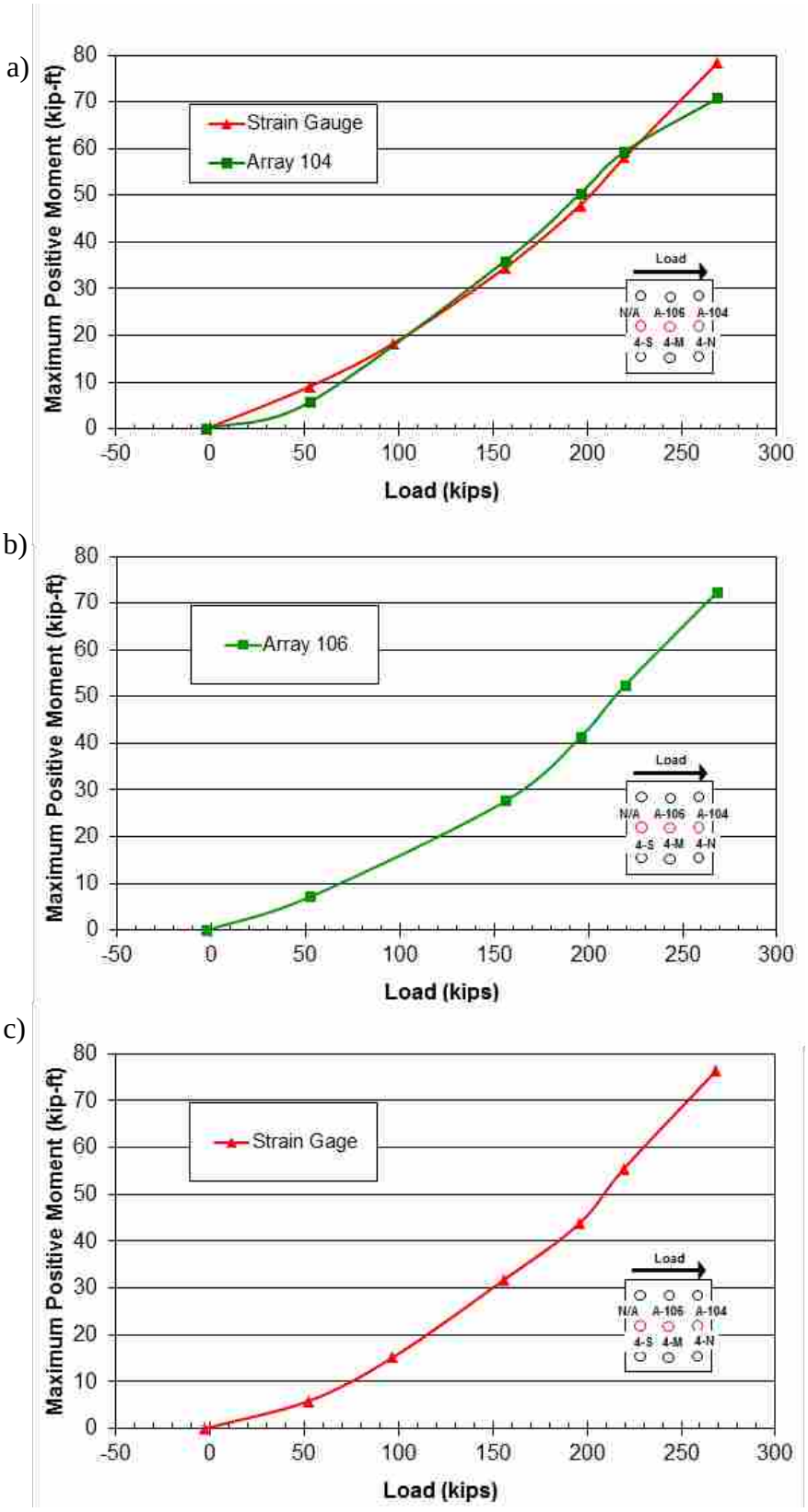

Figure 8-24 Maximum positive moment versus total pile cap load for piles (a) 4-N, (b) 4-M, and (c) 4-S in cap 4 during the compacted fill test with no soil adjacent to the cap (Test 3)

8.3 Compacted Fill – Test 4

In Test 4, pile caps 3 and 4 were pulled together to test the compacted fill with passive resistance on the face of the pile cap. Both of the pile caps involved in this test had been moved previously in Test 3. Following testing without passive resistance, an area of 5 ft by 11 ft of fill was compacted just north of pile cap 4 in five lifts from the base of the cap to the ground surface (at the top of the pile cap). The fill was compacted to an average dry unit weight of about 111 pcf as measured by a nuclear density gauge. The results of this test will be compared to the results from Tests 3 and 5 to determine the effectiveness of compacting fill adjacent to a pile cap for increasing lateral resistance. Since this test took place after the pile caps had been pulled together in Test 3 (the compacted fill without passive resistance test), there was some residual displacement in the direction of the original displacement once the load was released. Thus, Test 4, started with a positive initial displacement of about 0.4 inches.

All instrumentation of string potentiometers, shape arrays, inclinometers, actuator pressure transducer, and strain gauges were in place and initial measurements taken prior to the test. The locations of all the instrumentation for pile cap 4 are as shown in Section 4.3. Strain gauges on pile cap 4 were located on the north and south piles of pile cap 4 (piles 4-N and 4-S). The second deepest set of strain gauges on pile 4-N (the ones installed 11 ft below the top of pile 4-N) were damaged in pile driving, therefore no strain gauge data is available for that depth. The test followed the standard procedure. All values measured were zero-set to the initial values of Test 3 just prior to the commencement of testing.

8.3.1 Load versus Pile Cap Displacement

The lateral load versus displacement graph shows the complete load path, including incremental cycles for the test. Figure 8-26 was obtained from the actuator pressure transducer and the string potentiometers attached to the pile cap. The actuator pushed the pile caps to target the prescribed increments of 0.125, 0.25, 0.5, 0.75, 1.0, 1.5 inches, being referenced to actuator extension length as opposed to referencing either of the pile caps' displacement. The actual displacements for pile cap 4 with the residual offset of 0.39 inches were 0.47, 0.60, 0.85, 1.12, 1.36, and 1.80 inches respectively as measured by the corresponding string potentiometers. A plot of pile cap displacement versus peak applied load for each test increment is displayed in Figure 8-27. The curve in Figure 8-27 somewhat exhibits a typical hyperbolic shape that would be expected for a pile in soft clay. However, because the peak displacement was limited to 1.5 inches to prevent excessive moments in the piles, the slope of the load versus displacement curve never reached a horizontal asymptote. The maximum applied load during the last pull was 330.1 kips and resulted in a displacement of 1.80 inches for pile cap 4. For comparison purposes a load of 297 kips at 1.5 inch displacement will be used as the load capacity for the compacted fill with passive resistance test.

8.3.2 Load versus Pile Head Rotation

Load versus pile head rotation curves obtained from string potentiometer and shape array measurements for pile cap 4 during Test 4 are provided in Figure 8-28. In order to match the array data up with the data from the string potentiometers, 0.14° were added to the rotations from array 104 and 0.17° to those from array 106. Rotation was measured from the string potentiometers located directly above the corbel of pile cap 4. The distance between the string

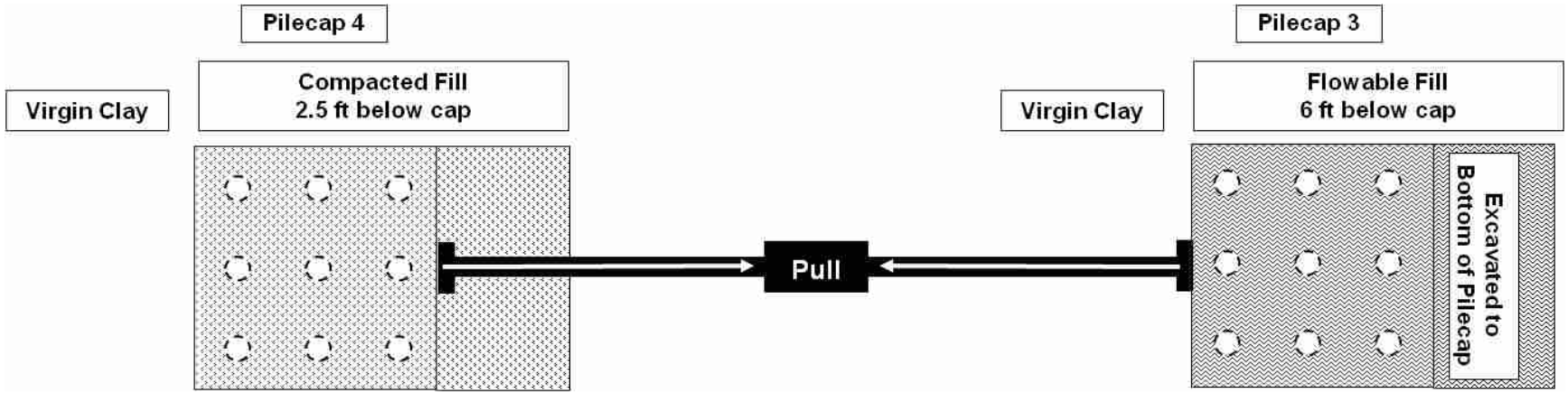

Figure 8-25 Schematic plan view of Test 4 (See Figure 5-2 for dimensions)

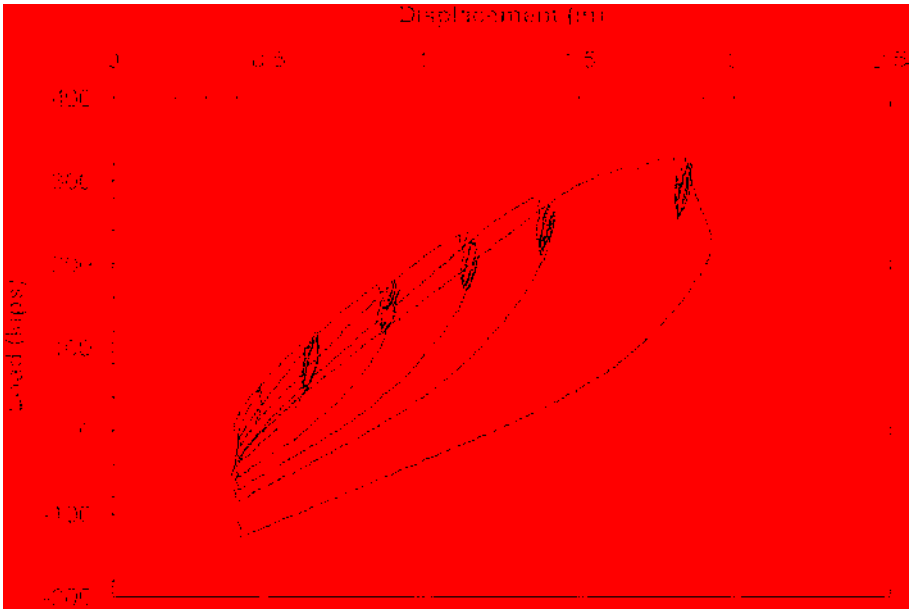

Figure 8-26 Plot of continuous pile cap displacement versus applied load for pile cap 4 during the compacted fill test with compacted fill adjacent to the cap (Test 4)

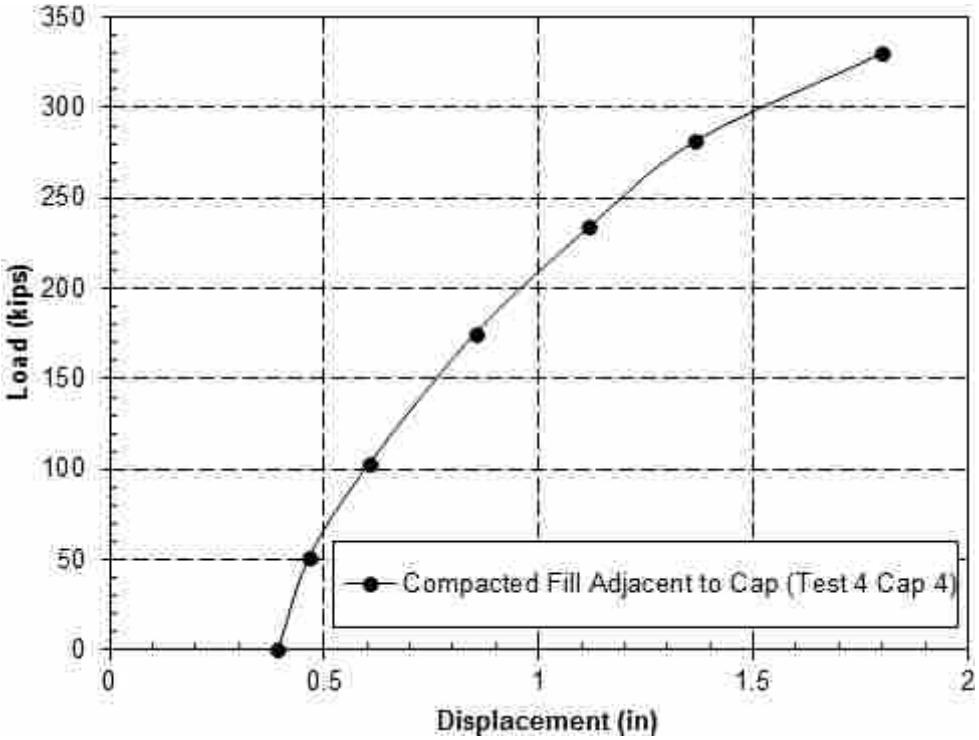

Figure 8-27 Plot of pile cap displacement versus peak applied load for each increment of the compacted fill test with compacted fill adjacent to the cap (Test 4)

potentiometers was approximately 46 inches. Refer to Figure 4-10 for a review on the position of the string pots on pile cap 4. Rotation was also measured from the shape arrays. The difference in node deflections near the bottom of the pile cap and the top of the corbel was used

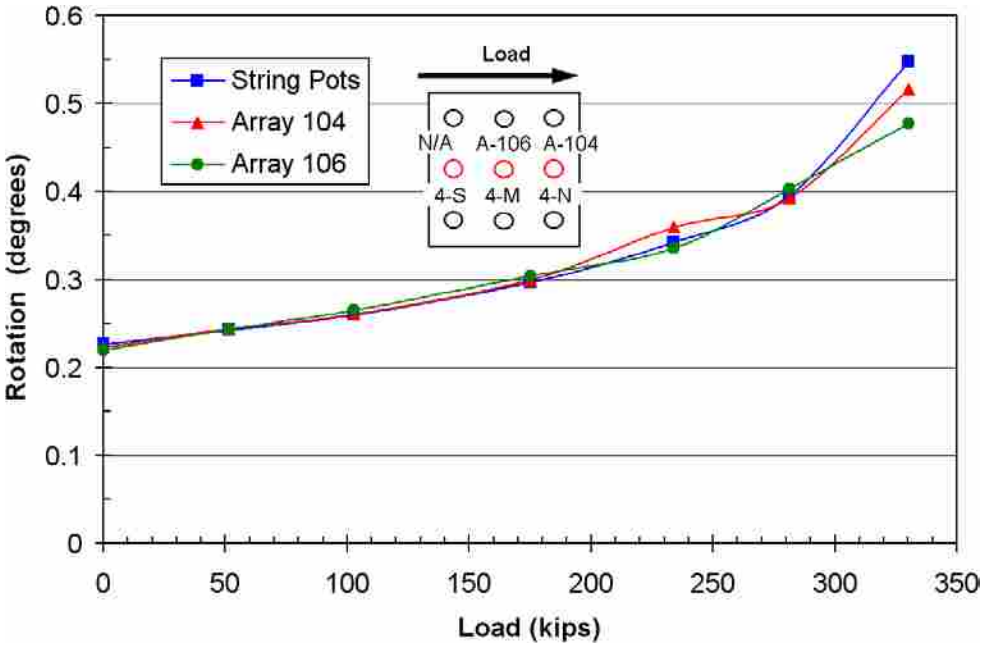

Figure 8-28 Peak pile cap load versus pile head rotation for cap 4 during the compacted fill test with compacted fill adjacent to the cap (Test 4) obtained from string potentiometer and shape array measurements

to measure rotation from shape array 104 and shape array 106; the distance between these nodes was 48 inches and 24 inches, respectively. As can be seen in the figure, the rotations from array 104 match the rotations derived from the string pots much more closely than did array106. The total rotation as measured by the string pots on pile cap 4 was 0.548°. The shape arrays show two different final rotations (even with the adjustments): 0.517° from array 104 and 0.477° from array 106.

8.3.3 Pile Deflection versus Depth

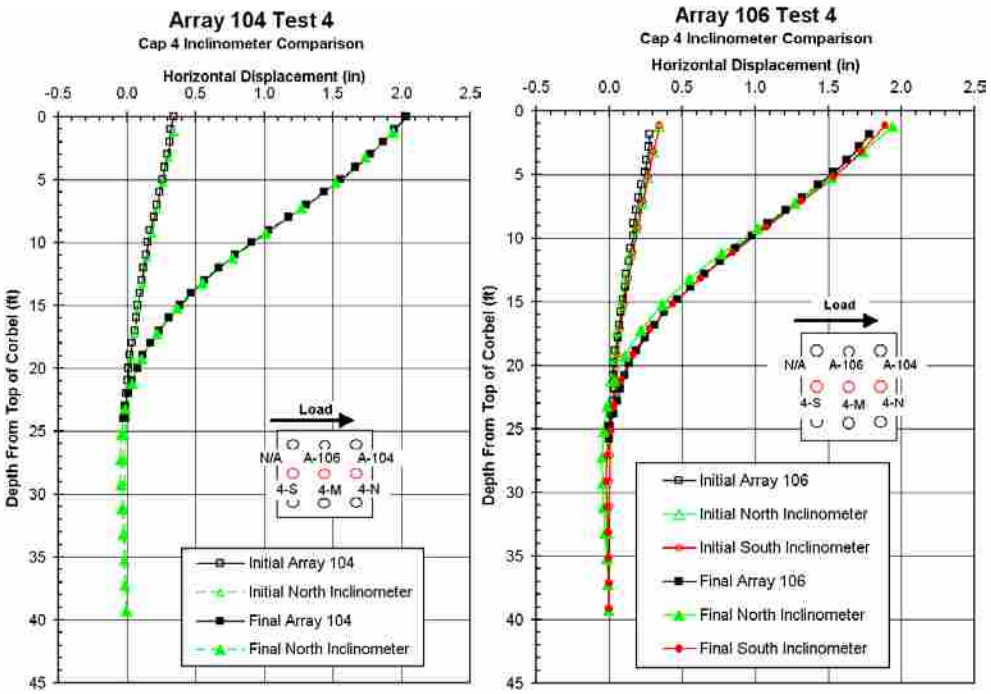

Figure 8-29 Comparison of depth versus deflection curves for the piles in pile cap 4 from the north inclinometer with shape array 104 and the north and south inclinometers with shape array 106 for the compacted fill test with compacted fill adjacent to the cap (Test 4)

Figure 8-29 shows the pile deflection versus depth profiles of the arrays and inclinometer readings on pile cap 4 before testing commenced and at the maximum displacement during Test 4. There is almost perfect agreement with array 104 to the north inclinometer. Because there was no inclinometer in the center pile, a comparison for both the north and south inclinometers with array 106 is included in Figure 8-29. The trend from array 106 follows the trend of the south inclinometer up to about 11 ft below the top of corbel where it starts to deviate. In order to correct for movement below the end of the shape array, 0.006 inches were subtracted from the initial displacements and 0.021inches from the final displacements of array 104 in the inclinometer comparison. Because there was no inclinometer in the center pile, nothing was added to the displacement readings for array 106. By adjusting the shape array in this way, its displacements match more closely with the inclinometer readings taken at similar depths. The

inclinometers show that there was deflection in the piles at depths greater than 30 ft. At the depth of the base of shape array 104 (24 ft below the top of corbel), the inclinometer reads -0.021 inches of displacement at 1.5 inches of pile cap displacement. At the level of the base of array 106 (25.8 ft below the top of corbel) the north inclinometer reads -0.040 inches of displacement and the south inclinometer reads 0.004 inches of horizontal displacement.

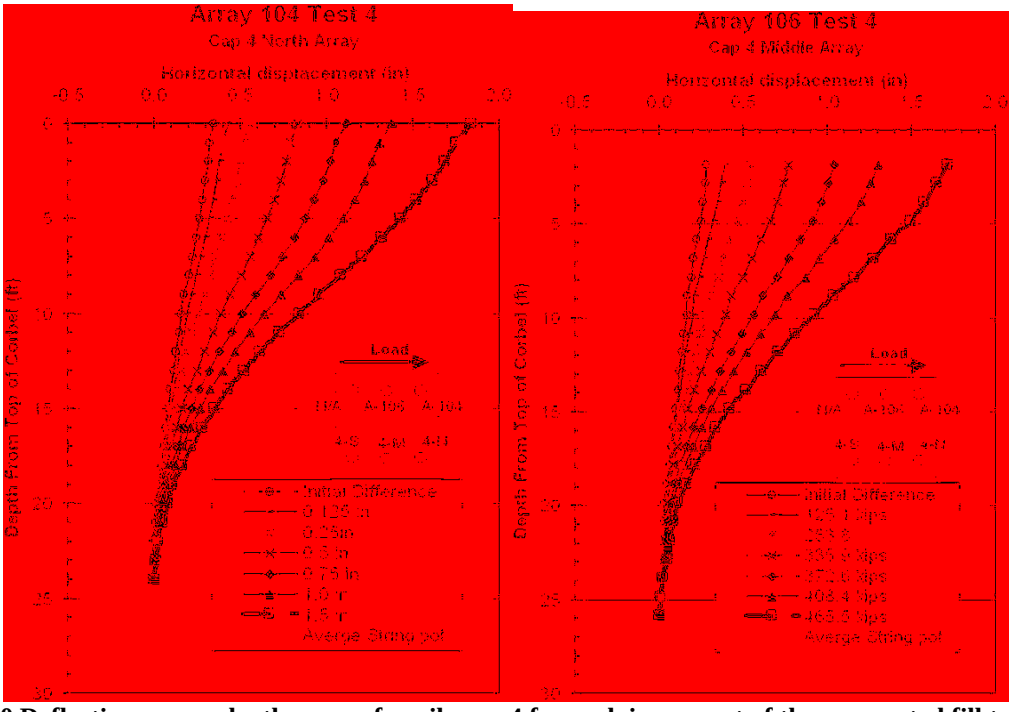

Figure 8-30 Deflection versus depth curves for pile cap 4 for each increment of the compacted fill test with compacted fill adjacent to the cap (Test 4), with pile head displacements from the string potentiometers also shown

Figure 8-30 shows pile deflection versus depth for each of the loading increments in Test 4 along with the corresponding string potentiometer readings. The difference between the array displacements and string potentiometer readings in Figure 8-30 appears to be due to movement of the pile below the lowest node of the shape arrays. In spite of the minor discrepancies, the general trend and slope of the depth versus displacement profiles are consistent and provide a fairly accurate representation of the deflections the piles experienced.

8.3.4 Pile Bending Moment versus Depth

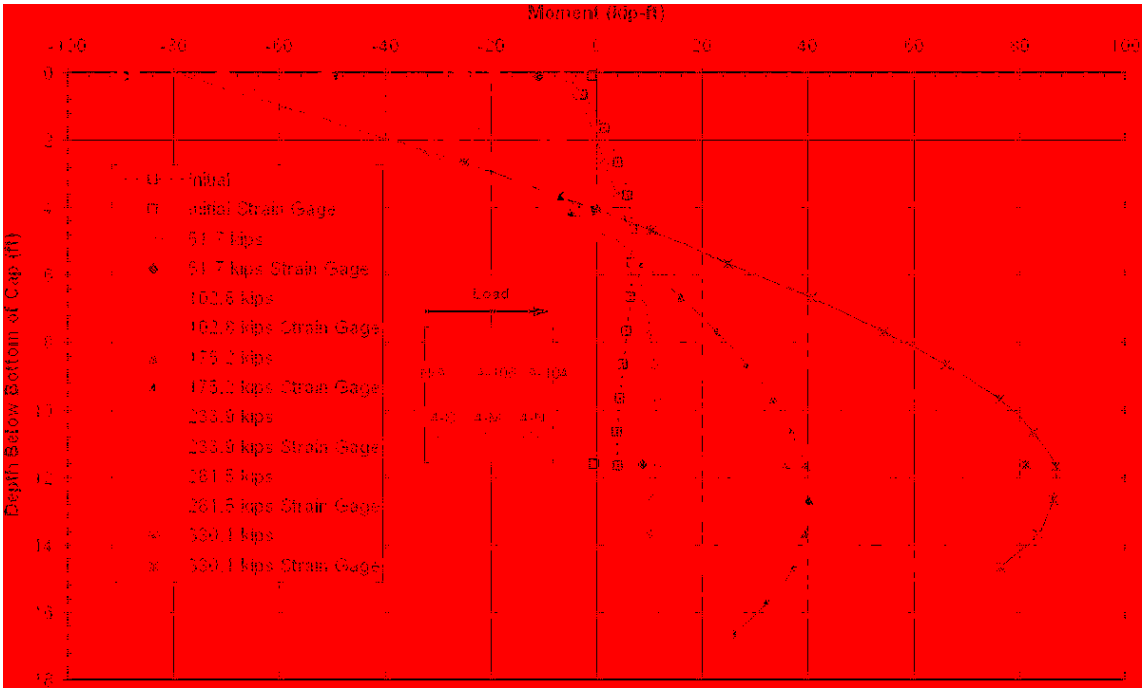

Figure 8-31 Moment versus depth curve for the north center pile of pile cap 4 (4-N) based on incremental deflection versus depth curves measured from shape array 104 during the compacted fill test with compacted fill adjacent to the cap (Test 4), with point moments measured from strain gauges at various depths also shown (Dashed extension lines are extrapolations)

Bending moments were estimated from the depth versus displacement profiles from the center and north piles on pile cap 4 using the methods described in Section 6.2. Figure 8-31 and Figure 8-32 provide bending moment versus depth curves for the piles in pile cap 4 at the six target displacement levels during Test 4. The curves were obtained from the shape arrays while the individual points represent moments computed from the strain gauges. The datum for these figures is the bottom of the pile cap. The maximum load at each target displacement is also listed in each figure's legend.

The maximum positive bending moments from the north pile array in Figure 8-31 tend to occur from about 10.5 ft to 12.7 ft (most of which occurring around 11.5 ft) below the bottom of the pile cap. The positive moments measured from the strain gauges are within 9 kip-ft or less of

the moments from the array. Not much can be discerned from the trend of the north array's negative bending moments as it had to be truncated due to inconsistencies of the numerical method at depths just below the pile cap. Judging from the trend up to the truncation point, it appears that the shape array would match up with the strain gauge readings if a more rigorous or complete numerical method was employed. The numerical method, in this case, does show a good correlation between shape array and strain gauges.

The maximum positive moments from the center pile in Figure 8-32 occur at depths from about 9.5 ft to 12.5 ft below the bottom of the pile cap. No strain gauges were installed on the center pile of pile cap 4; therefore none are shown in Figure 8-32. The positive moments from the arrays are within 10.5 kip-ft or less when comparing the arrays in the two instrumented piles at corresponding loads.

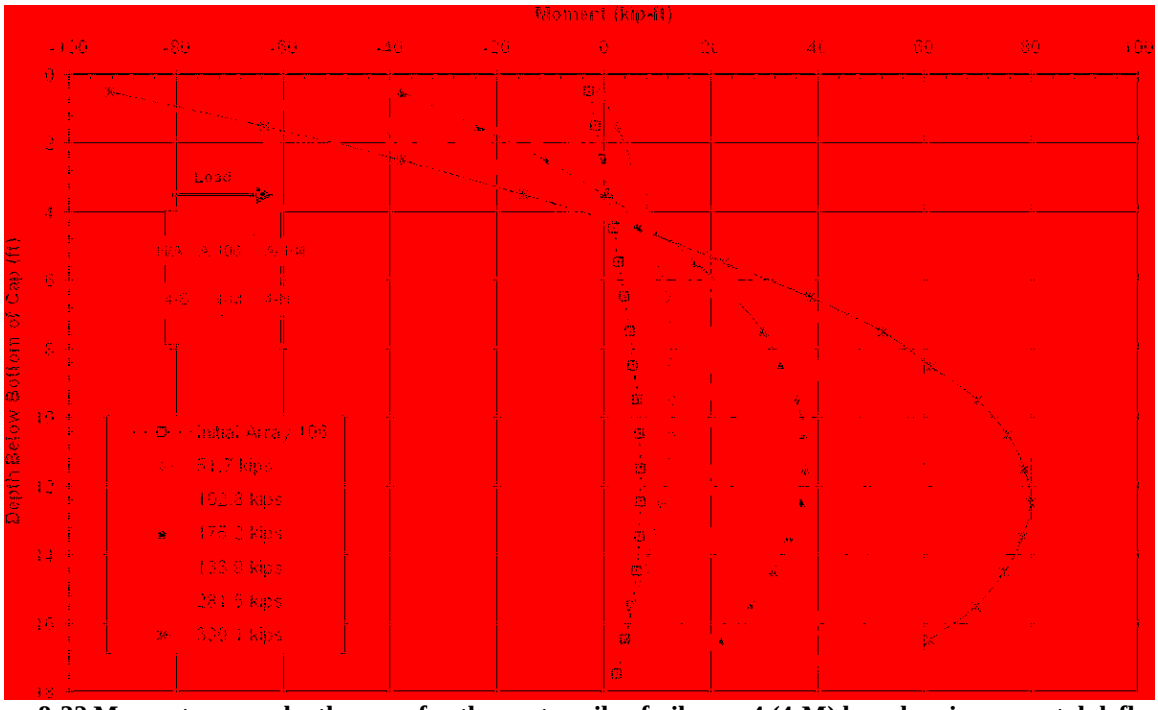

Figure 8-32 Moment versus depth curve for the center pile of pile cap 4 (4-M) based on incremental deflection versus depth curves measured from shape array 106 during the compacted fill test with compacted fill adjacent to the cap (Test 4)

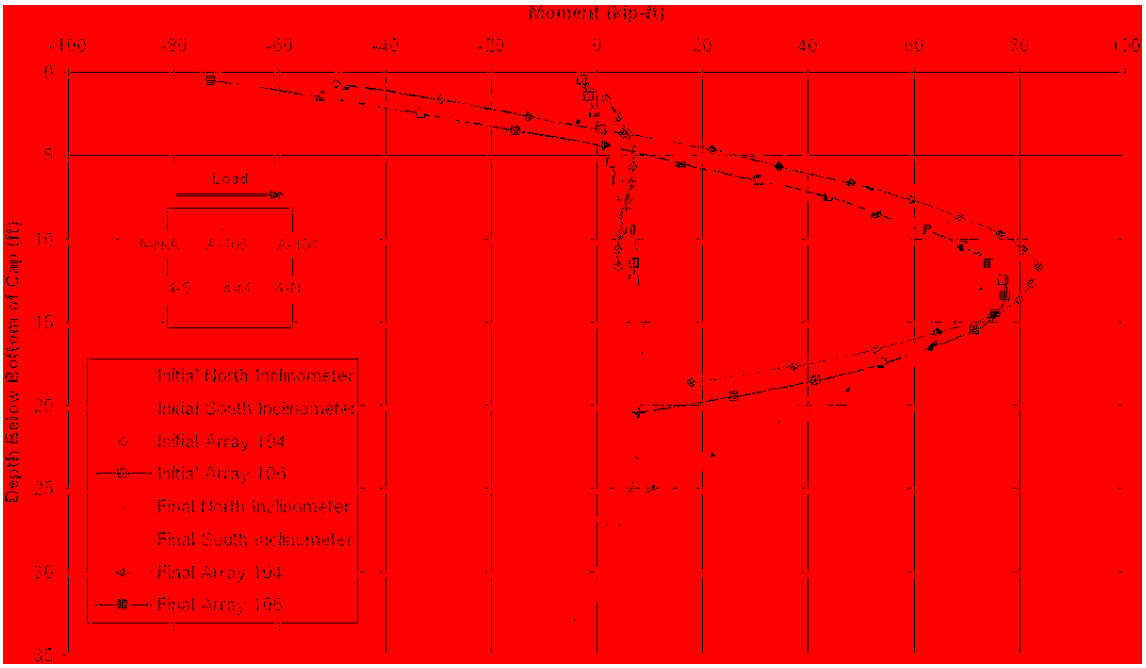

Figure 8-33 Moment versus depth comparison for the piles in pile cap 4 based on deflections measured from the north and south inclinometers, shape array 104 and shape array 106 during the compacted fill test with compacted fill adjacent to the cap (Test 4)

The moment trends of the shape arrays demonstrate good consistency when compared to the strain gauges. The shape array curves fall within 9 kip-ft of the lower strain gauges (the gauges installed at 6 and 13.5 ft below the top of the piles).

A comparison of the moments derived from the arrays and inclinometers at the maximum displacement is shown in Figure 8-33. There is reasonable agreement between the inclinometers and the arrays and inclinometers show similar trends. The north inclinometer and array 104 place the maximum positive bending moment at about 12 ft, but the south inclinometer and array 106 place it lower at around 13 ft. When looking at the magnitude of the maximum positive moment, the north inclinometer measures about 72.6 kip-ft, the south inclinometer 69.5 kip-ft, the north array 83.5 kip-ft, and the center array 77.4 kip-ft. The maximum negative moment as measured by the inclinometers and the shape arrays ranges from about 65 kip-ft from the north array to about 90 kip-ft from the south inclinometer, with the north inclinometer and middle

array falling between those values at around 75 and 85 kip-ft, respectively. The trends shown in both the array and inclinometer comparisons demonstrate what would be expected for a group interaction in showing a higher positive moment the farther north the readings are taken. Because the loading occurred toward the north, the northern piles should undergo a higher moment when compared to piles further to the south due to group interaction effects. The piles farther to the south would feel higher pullout forces than those to the north as illustrated in Figure 8-22. Some of the discrepancy between the shape arrays and inclinometers can be understood by scrutinizing the means of data collection and the amount of time it takes for each of the different methods. The shape array readings were taken at the beginning of inclinometer readings, therefore, it was able to capture a better picture of what stresses were in the pile in real time. As the inclinometer readings were taken, the piles had time to relax and the soil along with it, so the inclinometers should report slightly lower moments than do the shape arrays.

Comparisons of the three compacted fill tests (Tests 3-5) will be given in Chapter 0 along with a cost comparison of using a compacted fill retrofit versus a structural retrofit in Section 10.4.

8.3.5 Moment versus Load Results

Figure 8-34 and Figure 8-35 provide plots of the maximum negative and positive bending moments versus applied pile cap load respectively for cap 4 during Test 4. Moment data come from both shape array and strain gauge data when available. The curves are relatively linear as the load increases and the soil resistance is mobilized from the base of the pile cap downward. The curves from the strain gauges in Figure 8-35 provide relatively consistent moment versus load curves for the different piles whereas Figure 8-34 shows some evidence of group interaction

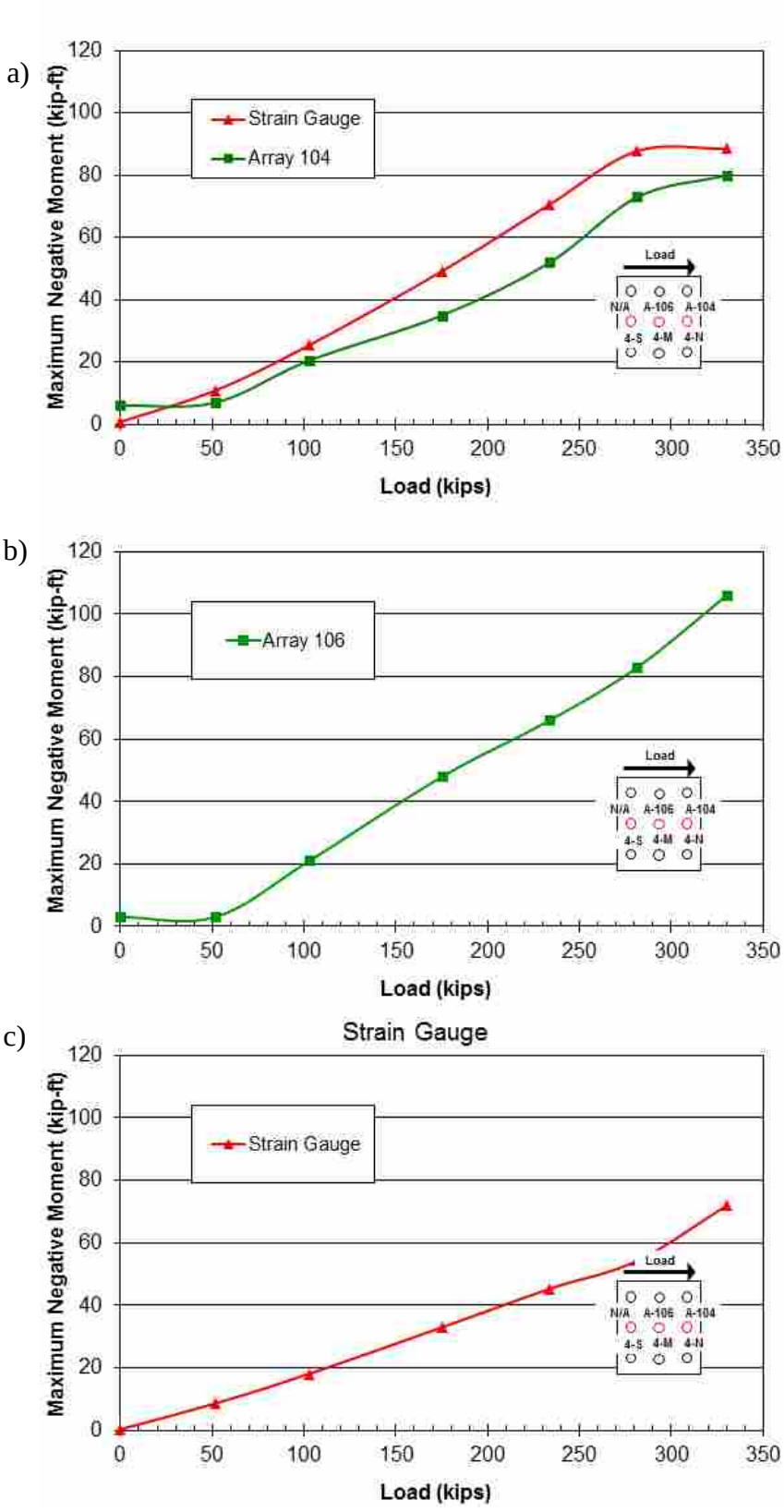

Figure 8-34 Maximum negative moment (base of cap) versus total pile cap load for piles (a) 4-N, (b) 4-M, and (c) 4-S in cap 4 during the compacted fill test with compacted fill adjacent to the cap (Test 4)

a)

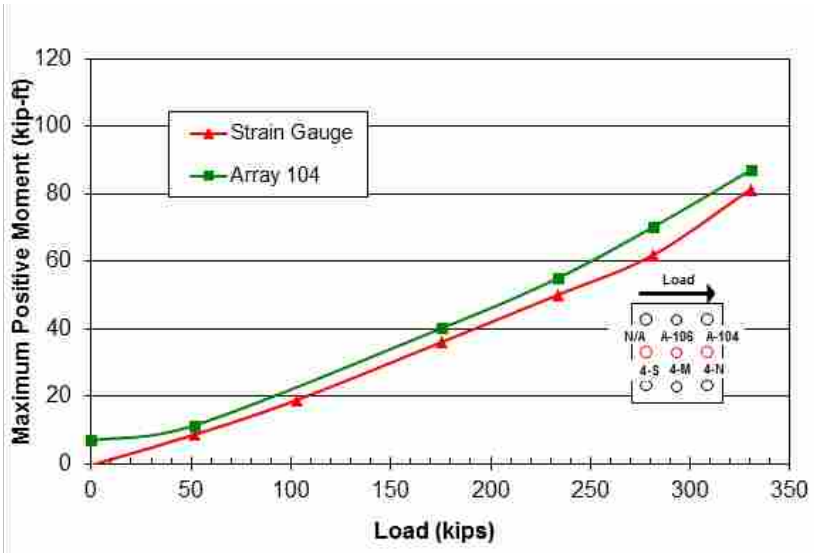

b)

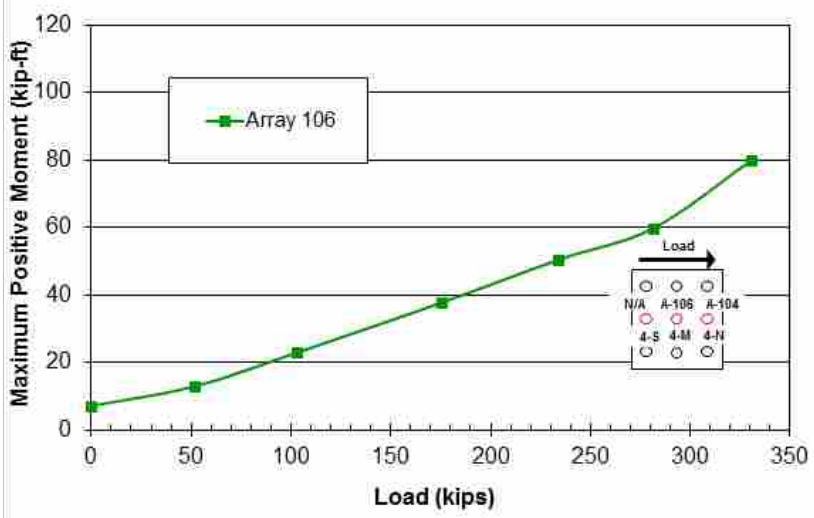

c)

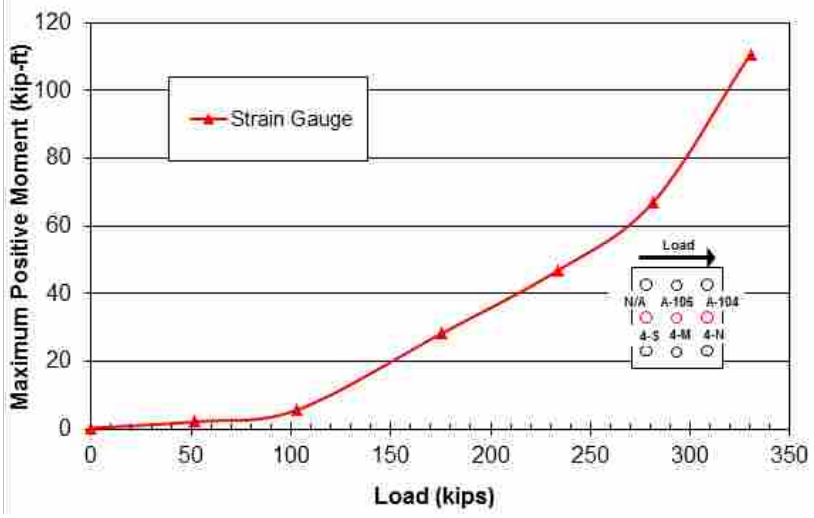

Figure 8-35 Maximum positive moment versus total pile cap load for piles (a) 4-N, (b) 4-M, and (c) 4-S in cap 1 during the compacted fill test with compacted fill adjacent to the cap (Test 4)

effects. Figure 8-34 with Figure 8-35 shows that the maximum positive and negative moments are very close to the same magnitudes. Because the soil had been reloaded multiple times at the time of this test, it was not able to provide support for the pile, thus the positive moment further down in the ground was able to develop to a much greater magnitude than was expected. The agreement between the curves computed by the strain gauges and the shape arrays is reasonable. The negative moment array plot for pile 4-M seems to plot high compared to the other piles plotted in Figure 8-34.

9 RAP TEST RESULTS

The tests involving the lateral push of pile caps retrofit using Rammed Aggregate Piers (RAPs) were Tests 6 and 7 in a series of 16 tests. As explained in Section 5.2, two tests were performed on the RAPs: one without passive resistance on the pile cap and one with RAPs against the face of the pile cap. The two tests were performed to quantify the lateral passive resistance gain associated with installing RAPs adjacent to a pre-existing pile cap or bridge abutment in clay. For plan and profile views of the RAP setup, refer to Figure 5-9.

9.1 RAPs – Test 6

In Test 6, pile caps 3 and 4 were pushed apart to test the RAPs with passive resistance on the face of the pile cap. Both of the pile caps involved in this test had been moved previously in Tests 3 through 5. Following the last test on compacted fill, RAPs were installed on the south side of pile cap 4. The results of this test will be compared to the results from Tests 5 and 7 to determine the effectiveness of installing RAPs adjacent to a pile cap in order to increase lateral resistance in clay. Since this test took place after the pile caps had been pulled together in Tests 3 and 4 (the compacted fill tests) and then pushed out in Test 5, there was some residual displacement to the north once the load was released. Thus, Test 6, started with a negative initial displacement of about 0.2 inches.

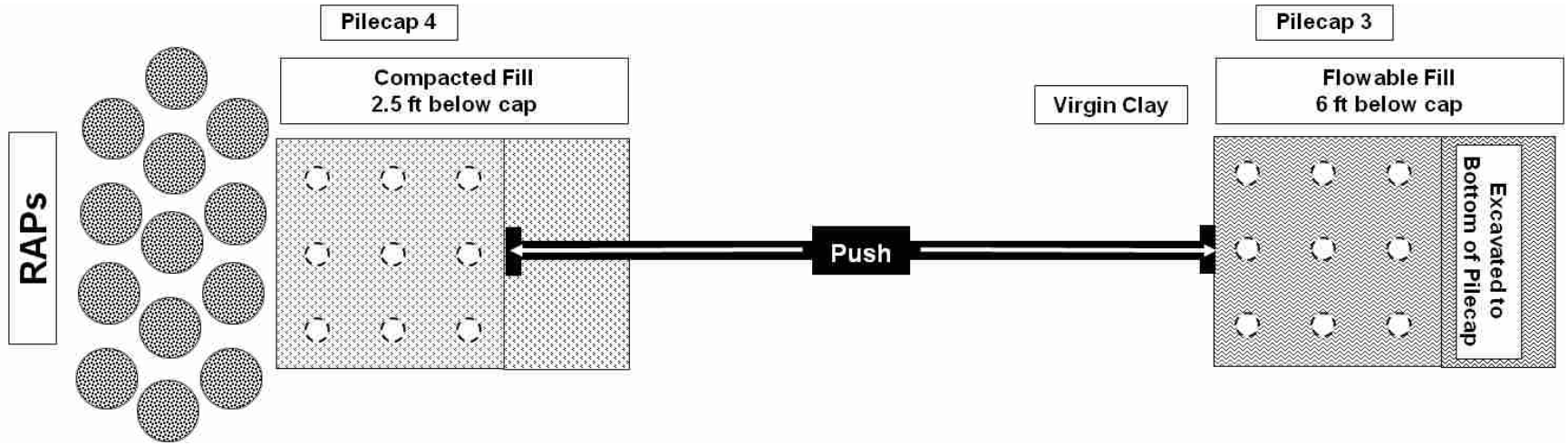

Figure 9-1 Schematic plan view of Test 6

All instrumentation of string potentiometers, shape arrays, inclinometers, actuator pressure transducer, and strain gauges were in place and initial measurements taken prior to the test. All instrumentation except the shape arrays remained connected and in place during the installation of the RAPs. The shape array that was to be used in the south pile (array 115) was damaged sometime during testing and the data collected from it was nonsensical, therefore the only array data recorded was array 104 (placed in pile 4-N). The locations of all the instrumentation for pile cap 4 are as shown in Section 4.3. Strain gauges on pile cap 4 were located on the north and south piles of pile cap 4 (piles 4-N and 4-S). The second deepest set of strain gauges on pile 4-N (the ones installed 11 ft below the top of pile 4-N) were damaged in pile driving, therefore no strain gauge data is available for that depth. The test followed the standard procedure. All values measured were zero-set to the initial values of test 3 just prior to the commencement of testing. Figure 9-1 shows a schematic plan view of Test 6, see Figure 5-6 and Figure 5-9 for dimensions.

9.1.1 Load versus Pile Cap Displacement

The lateral load versus displacement graphs show the complete load path, including incremental cycles for the test. Figure 9-2 was obtained from the actuator pressure transducer and the string potentiometers attached to the pile cap. Because the cap had been loaded previously, it had approximately 0.19 inches of residual displacement from previous testing. The actuator pushed the pile caps to target the prescribed increments of 0.125, 0.25, 0.5, 0.75, 1.0, 1.5 inches, being referenced to actuator extension length. The actual displacements for pile cap 4 with the residual offset of -0.19 inches were -0.12, 0.02, 0.30, 0.60, 0.91, and 1.26 inches respectively as measured by the corresponding string potentiometers. A plot of pile cap displacement versus peak applied load for each test increment is displayed in Figure 9-3. The

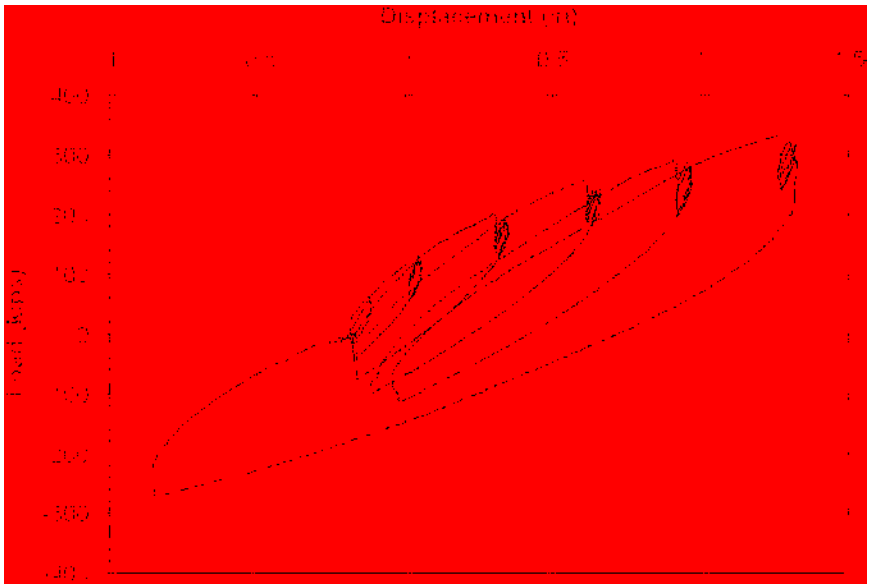

Figure 9-2 Plot of continuous pile cap displacement versus applied load for pile cap 4 during the RAP test (Test 6)

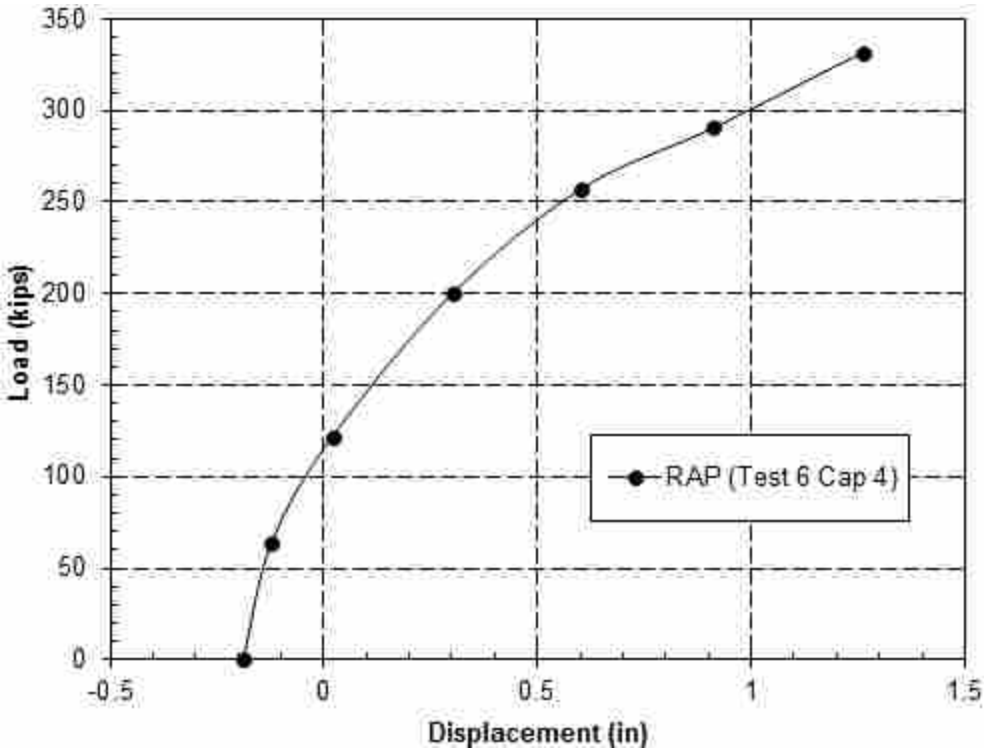

Figure 9-3 Plot of pile cap displacement versus peak applied load for each increment of the RAP test (Test 6)

curve in Figure 9-3 exhibits a typical hyperbolic shape that would be expected for a pile in soft clay. However, because the peak displacement was limited to 1.5 inches to prevent excessive moments in the piles, the slope of the load versus displacement curve never reached a horizontal

asymptote. The maximum applied load during the last push was 331.8 kips and resulted in a displacement of 1.26 inches for pile cap 4. For comparison purposes a load of 335 kips at 1.5 inch displacement will be used as the load capacity for the RAP with passive resistance test.

9.1.2 Load versus Pile Head Rotation

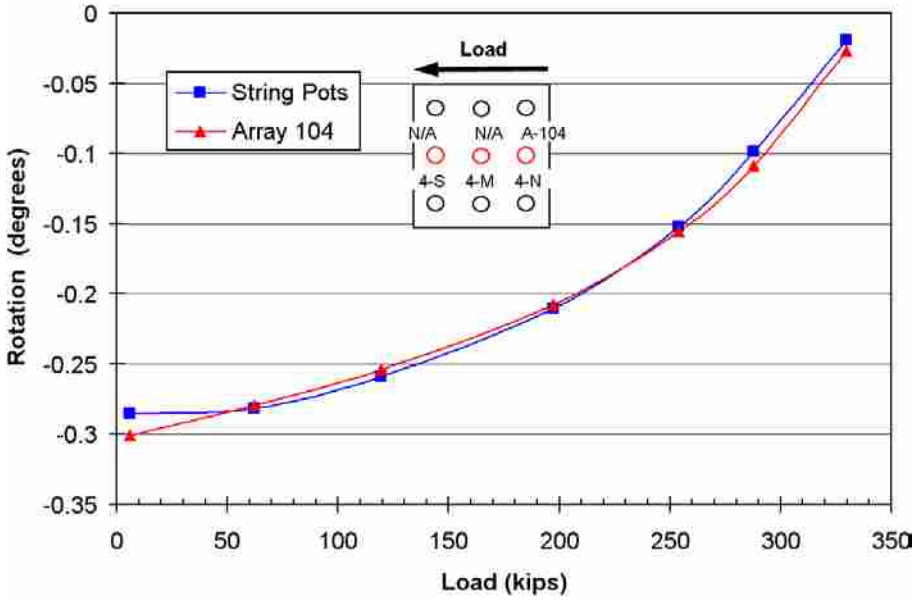

Figure 9-4 Peak pile cap load versus pile head rotation for cap 4 during the RAP test (Test 6) obtained from string potentiometer and shape array measurements

Load versus pile head rotation curves obtained from string potentiometer and shape array measurements for pile cap 4 during Test 6 are provided in Figure 9-4. In order to match the array data up with the data from the string potentiometers, 0.21° were added to the rotations from array 104. Rotation was measured from the string potentiometers located directly above the corbel of pile cap 4. The distance between the string potentiometers was approximately 46 inches. Refer to Figure 4-10 for a review on the position of the string pots on pile cap 4. Rotation was also measured from the shape arrays. The difference in node deflections near the bottom of the pile cap and the top of the corbel was used to measure rotation from shape array

104; the distance between these nodes was 48 inches. As can be seen in the figure, the rotations from array 104 match the rotations derived from the string pots closely except at the beginning of testing. The total rotation as measured by the string pots on pile cap 4 was -0.019°. The shape array shows a slightly different final rotation (even with the adjustments): -0.027°. This shows that even after pushing the cap to the extent of testing, the cap was still rotated toward the north.

9.1.3 Pile Deflection versus Depth

Figure 9-5 shows the pile deflection versus depth profiles of array 104 and the inclinometer readings on pile cap 4 before testing commenced and at the maximum displacement during Test 6. There is almost perfect agreement between array 104 and the north inclinometer except toward the bottom of the array. Because there was no other arrays in the pile cap, a comparison for both the north and south inclinometers is included in Figure 9-5. The plot of the inclinometers indicates that the south inclinometer is more curved than the north inclinometer closer to the pile cap. Greater curvature in the pile indicates a higher moment in the pile, which confirms the observations from previous tests that the extreme pile in the direction of loading will experience a higher moment than the trailing piles. In order to correct for movement below the end of the shape array, 0.014 inches were added to the initial displacements and 0.018inches to the final displacements of array 104 in the inclinometer comparison. By adjusting the shape array in this way, its displacements match more closely with the inclinometer readings taken at similar depths. The inclinometers show that there was deflection in the piles at depths greater than 30 ft. At the depth of the base of shape array 104 (24 ft below the top of corbel), the inclinometer curve reads -0.018 inches of displacement at 1.5 inches of pile cap displacement.

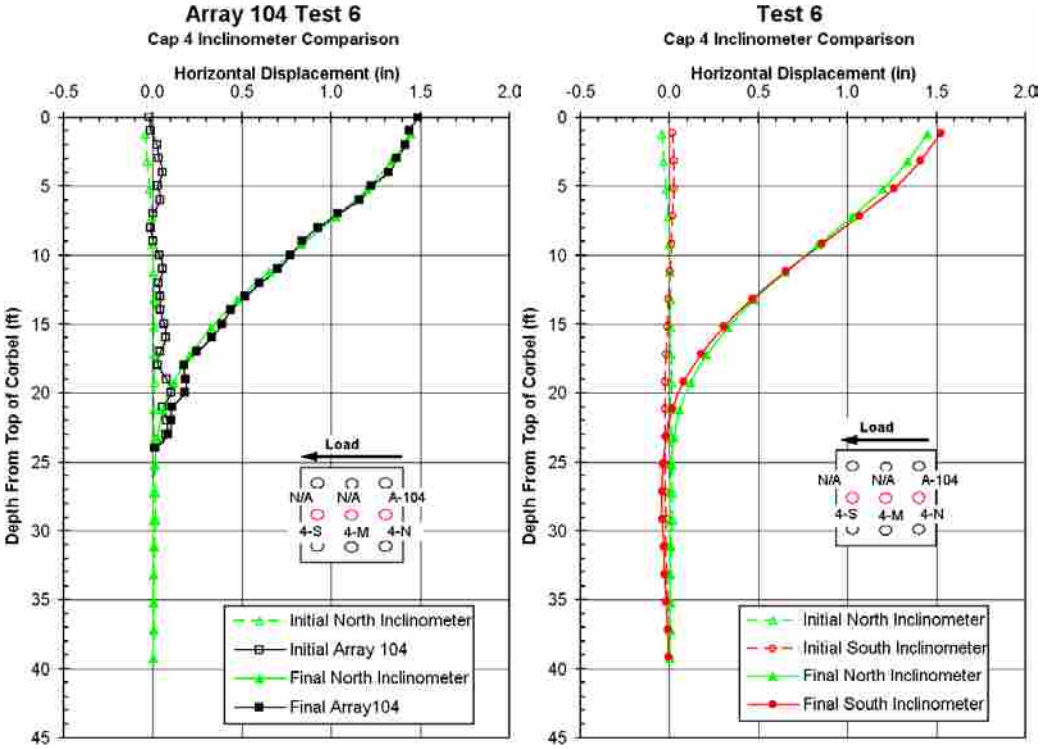

Figure 9-5 Comparison of depth versus deflection curves for the piles in pile cap 4 from the north inclinometer with shape array 104 and the north and south inclinometers for the RAP test (Test 6)

Figure 9-6 shows pile deflection versus depth for each of the loading increments as measured by array 104 in Test 6 along with the corresponding string potentiometer readings. The difference between the array displacements and string potentiometer readings in Figure 9-6 appears to be, at least in part, due to movement of the pile below the lowest node of the shape arrays. In spite of the minor discrepancies, the general trend and slope of the depth versus displacement profiles are fairly consistent and provide a reasonable representation of the deflections the piles experienced.

9.1.4 Pile Bending Moment versus Depth

Bending moments were estimated from the depth versus displacement profiles from the center and north piles on pile cap 4 using the methods described in Section 6.2. Figure 9-7 and

Figure 9-8 provide bending moment versus depth curves for the north and south piles in pile cap 4 at the six target displacement levels during Test 6. The curves in Figure 9-7 were obtained

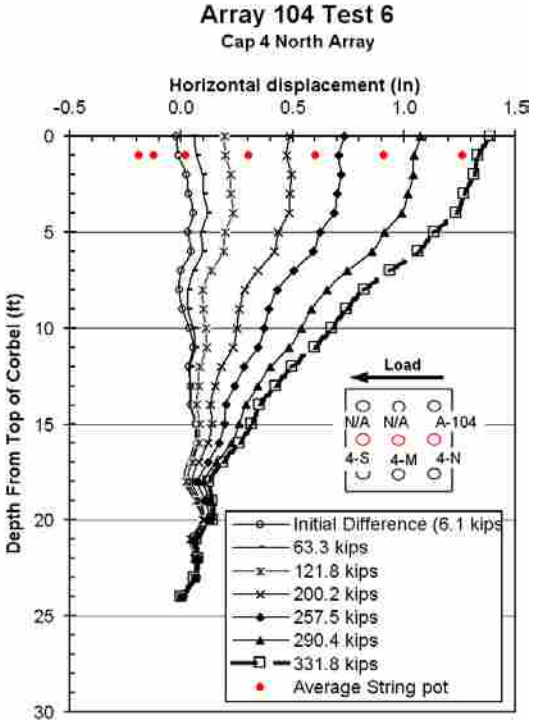

Figure 9-6 Deflection versus depth curves for pile cap 4 for each increment of the RAP test (Test 6), with pile head displacements from the string potentiometers also shown

from the shape arrays while the individual points in Figure 9-7 and the curves in Figure 9-8 represent moments computed from strain gauges. The datum for these figures is the bottom of the pile cap. The maximum load at each target displacement is also listed in each figure's legend.

The maximum positive bending moments from the north pile array in Figure 9-7 tend to occur from about 7.5 ft to 10.7 ft below the bottom of the pile cap. The positive moments measured from the strain gauges do not match very well with the array moments. Judging from the trend up to the truncation point of the curves and extending a line up to the pile cap, it appears that the shape array would match up with the strain gauge readings if a more rigorous or complete numerical method were employed. The numerical method, in this case, does show a

good correlation between shape array and strain gauges for the negative moments at the top of the pile.

The maximum positive moments recorded by the strain gauges in the south pile (Figure 9-8) all occur at the 11 ft strain gauge (which is 9.2 ft below the base of the pile cap). The maximum positive moments from the array are much lower than the moments calculated from the strain gauges on the south pile, but exceed the moments calculated from the strain gauges on the north pile.

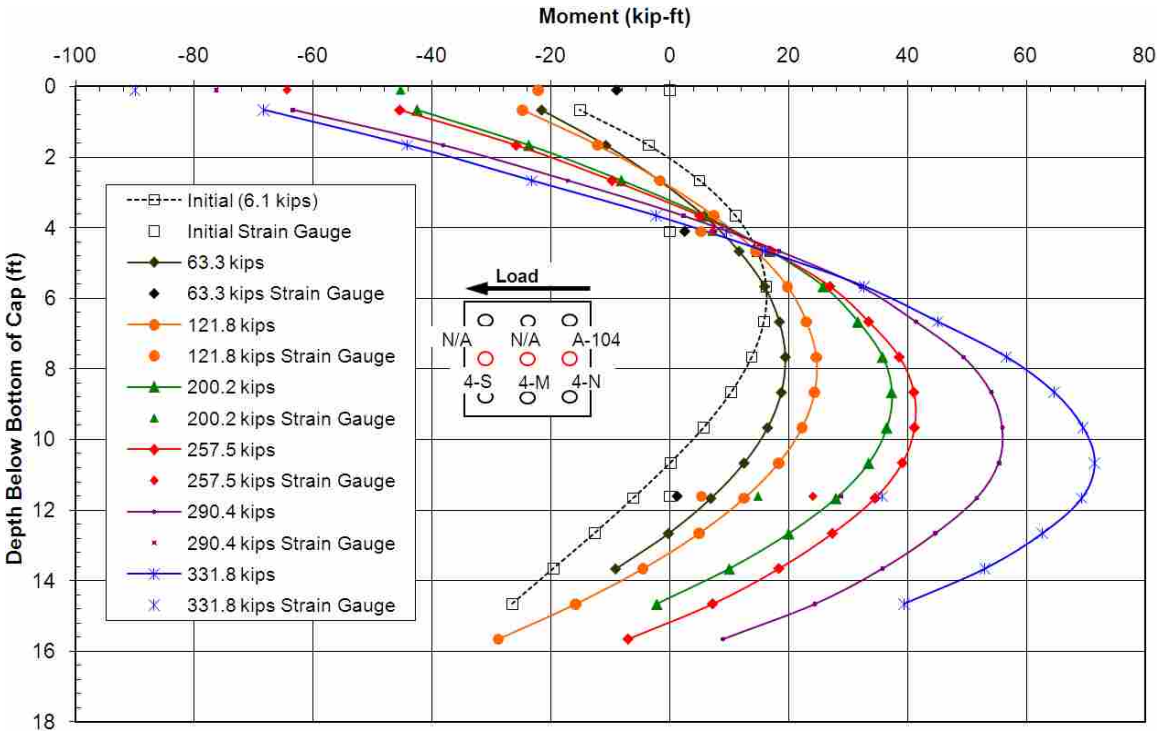

Figure 9-7 Moment versus depth curve for the north center pile of pile cap 4 (4-N) based on incremental deflection versus depth curves measured from shape array 104 during the RAP test (Test 6), with point moments measured from strain gauges at various depths also shown

The moment trends of the shape arrays do not demonstrate good consistency when compared to the strain gauges. The shape array curves do, however, show good correlation with the strain gauge moments for the negative moments toward the top of the north pile and at 4.2 ft below the bottom of the pile cap.

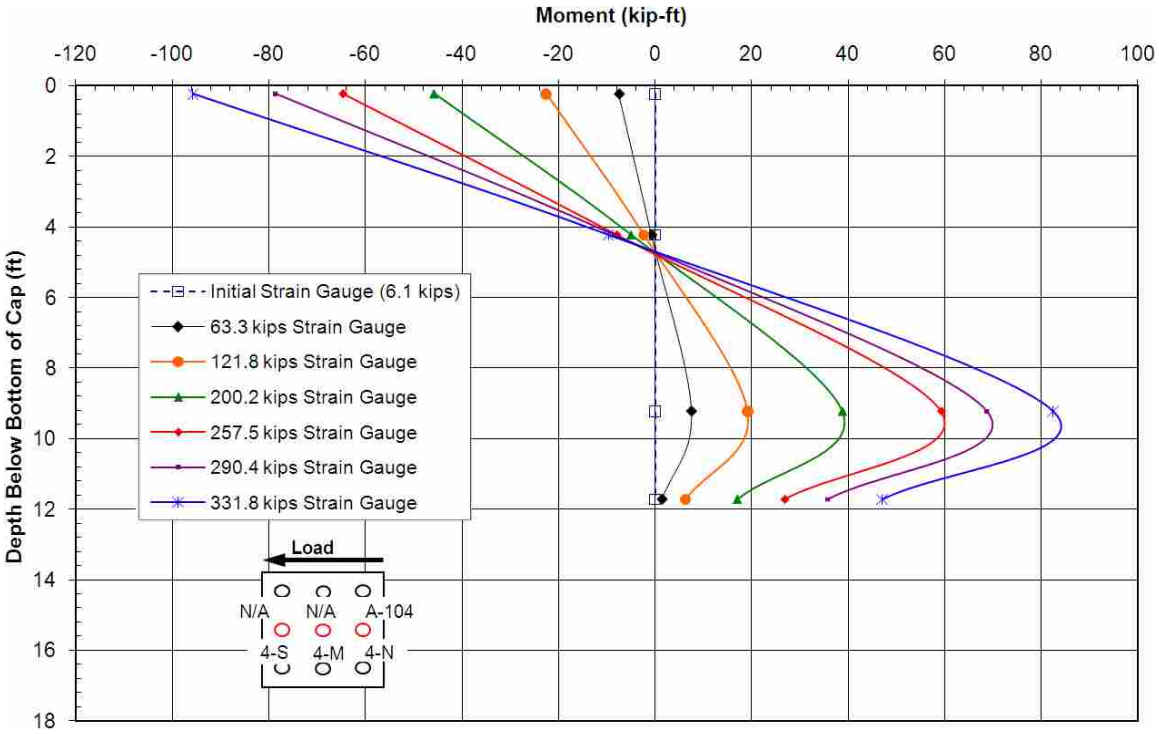

Figure 9-8 Moment versus depth curve for the south center pile of pile cap 4 (4-S) based on strain gauge readings at various depths for the RAP test (Test 6)

A comparison of the moments derived from array 104 and the inclinometers at the initial position and the maximum displacement is shown in Figure 9-9. There is reasonable agreement between the inclinometers and the array for the maximum displacement curves. The inclinometers place the maximum positive bending moment at about 12.8 ft, but array 104 places it higher at around 10.6 ft. When looking at the magnitude of the maximum positive moment, the north inclinometer measures about 58.2 kip-ft, the south inclinometer 64.9 kip-ft, and the north array 64.9 kip-ft. The maximum negative moment as measuring by the inclinometers and the shape array ranges from about 80 kip-ft from the north array to about 94 kip-ft from the south inclinometer, with the north inclinometer falling between those values at around 86 kip-ft. The trends shown in the inclinometer comparison demonstrate what would be expected in showing a higher positive moment the further south the readings are taken. Because the loading occurred toward the south, the southern piles should undergo a higher moment when compared to piles

farther to the north (See Figure 8-22). Some of the discrepancy between the shape arrays and inclinometers can be understood by scrutinizing the means of data collection and the amount of

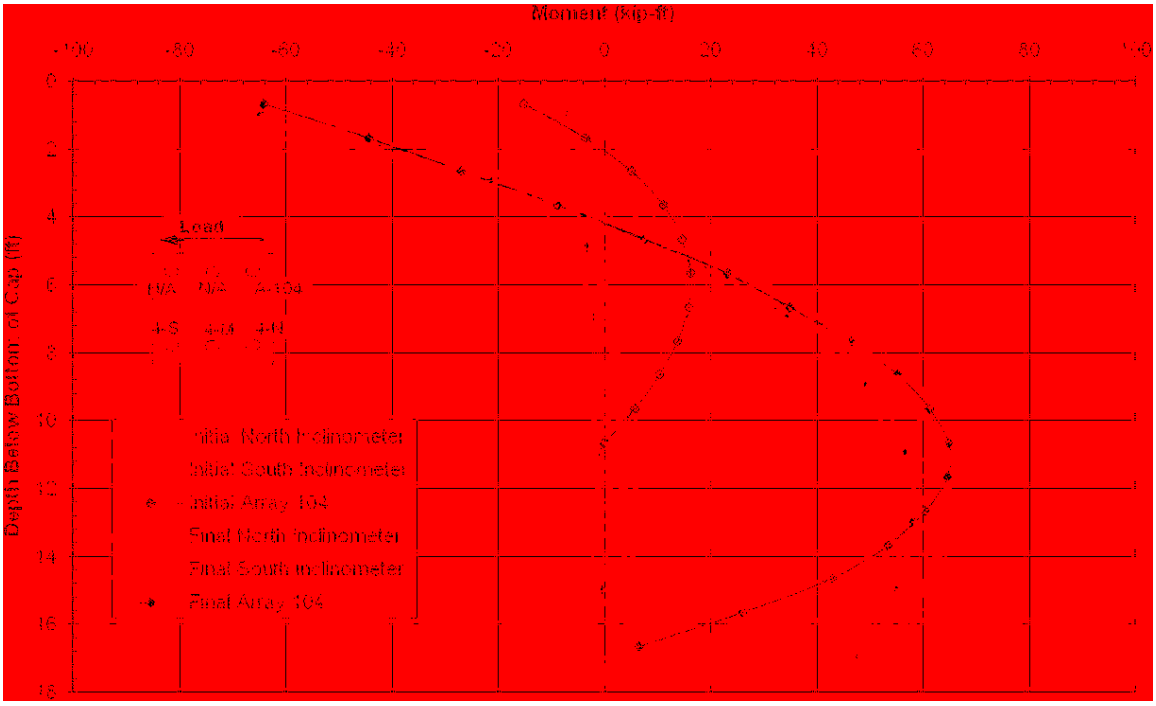

Figure 9-9 Moment versus depth comparison for the piles in pile cap 4 based on deflections measured from the north and south inclinometers and shape array 104 during the RAP test (Test 6)

time it takes for each of the different methods. The shape array readings were taken at the beginning of inclinometer readings, therefore, it was able to capture a better picture of what stresses were in the pile in real time. As the inclinometer readings were taken, the piles had time

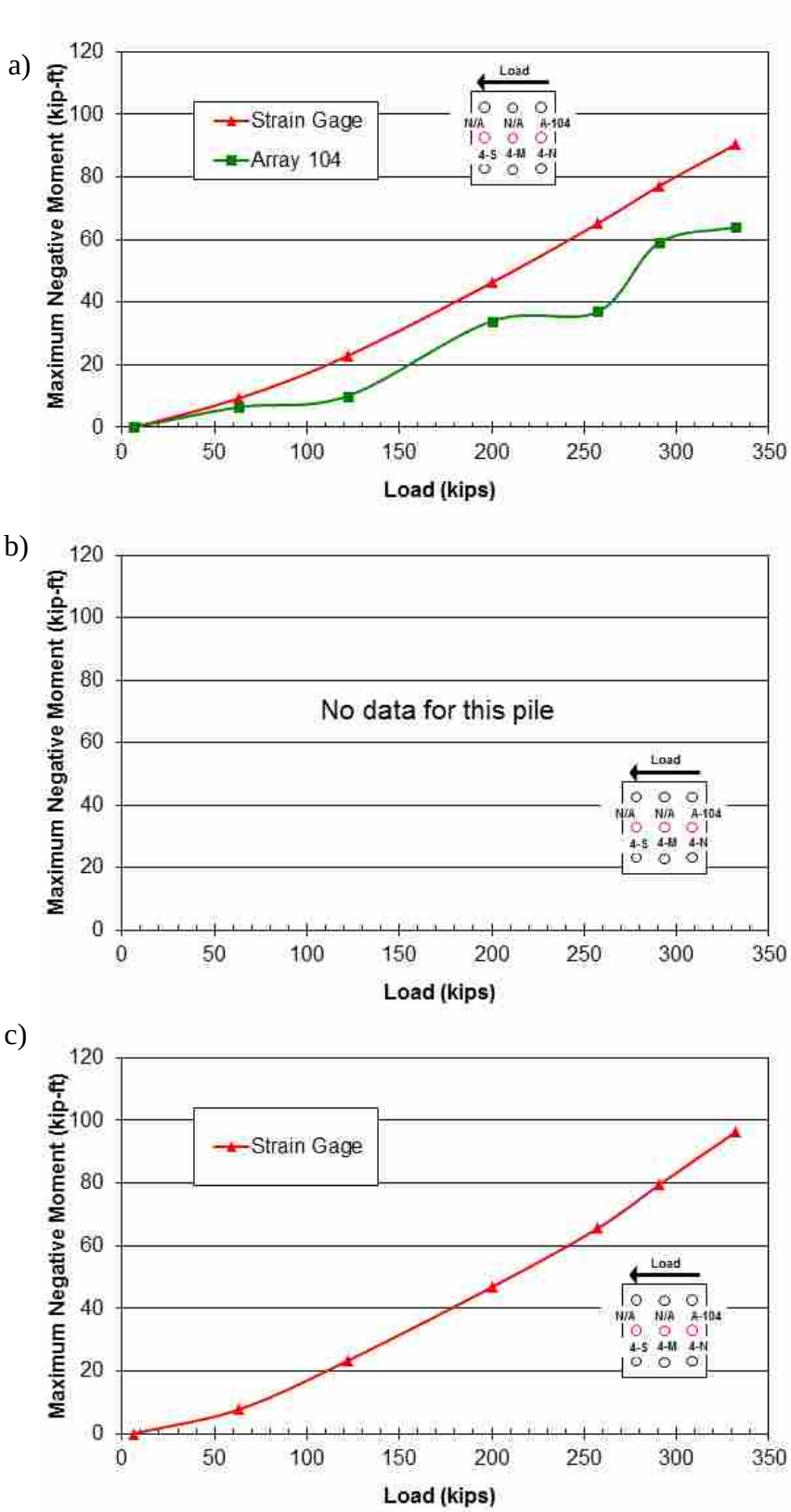

Figure 9-10 Maximum negative moment (base of cap) versus total pile cap load for piles (a) 4-N, (b) 4-M, and (c) 4-S in cap 4 during the RAP test (Test 6)

a)

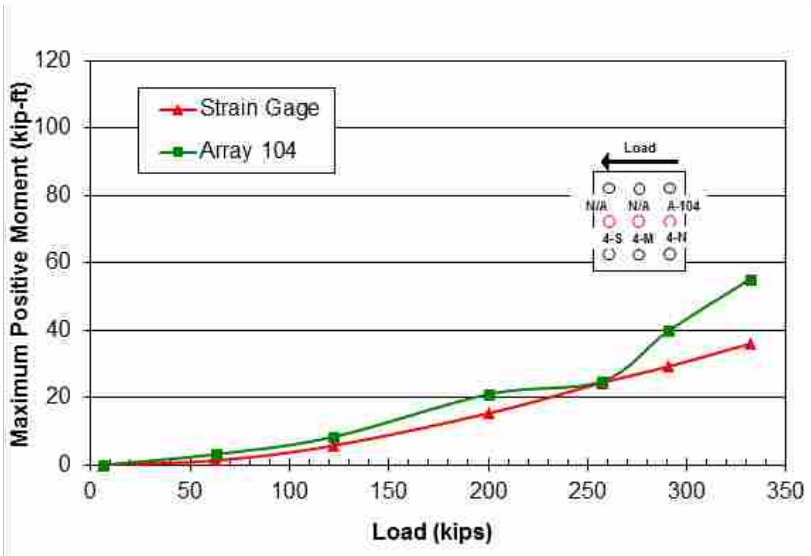

b)

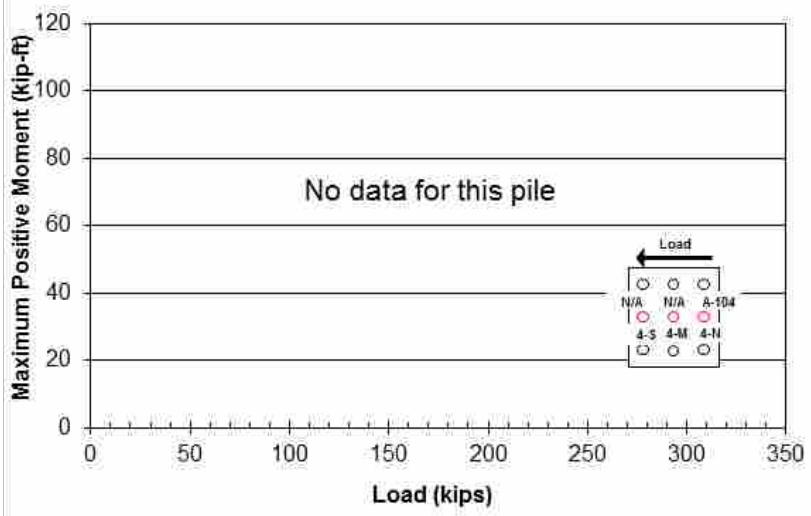

c)

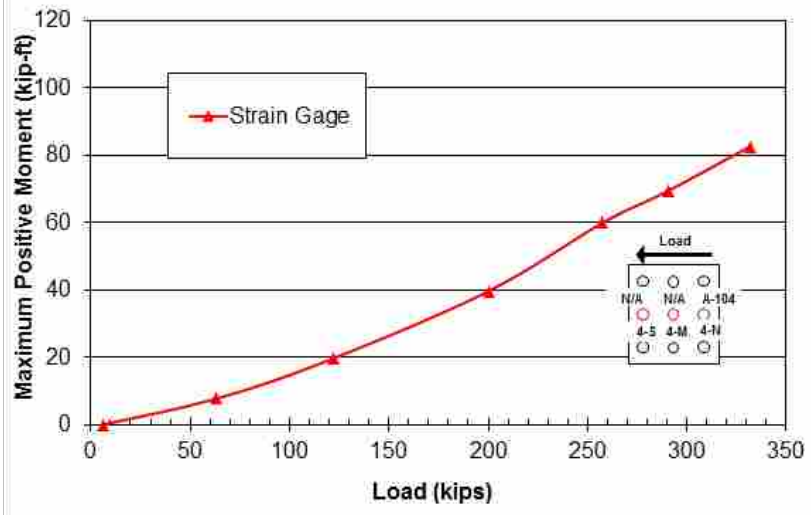

Figure 9-11 Maximum positive moment versus total pile cap load for piles (a) 4-N, (b) 4-M, and (c) 4-S in cap 1 during the RAP test (Test 6)

to relax and the soil along with it, so the inclinometers should report slightly lower moments than do the shape arrays.

9.1.5 Moment versus Load Results

Figure 9-10 and Figure 9-11 provide plots of the maximum negative and positive bending moments versus applied pile cap load respectively for cap 4 during Test 6. Moment data come from both shape array and strain gauge data when available. The curves are relatively linear showing that the soil has been loaded beyond its shear capacity. The curves from the strain gauges provide relatively consistent moment versus load curves with evidence of group interaction effects, especially in the positive moments. The agreement between the curves computed by the strain gauges and shape arrays is somewhat reasonable for the positive moments, but not as much for the negative moments. The negative moments calculated from the array data plot lower than those computed from the strain gauges. Comparisons of the test results from Test 6 and the other tests will be given in Chapter 0 along with a cost comparison of using a RAP retrofit versus a structural retrofit

9.2 RAPs without Passive Resistance – Test 7

In Test 7, pile caps 3 and 4 were pushed apart to test the RAPs without passive resistance on the face of the pile cap. Both of the pile caps involved in this test had been moved previously in Tests 3 through 6. Following the last test, a trench was dug to the depth of the base of the pile cap through the RAPs to remove any passive resistance on the pile cap. The results of this test will be compared to the results from Tests 5 and 6 to determine the amount of passive resistance increase derived from installing Rammed Aggregate Piers as a retrofit for bridge abutments.

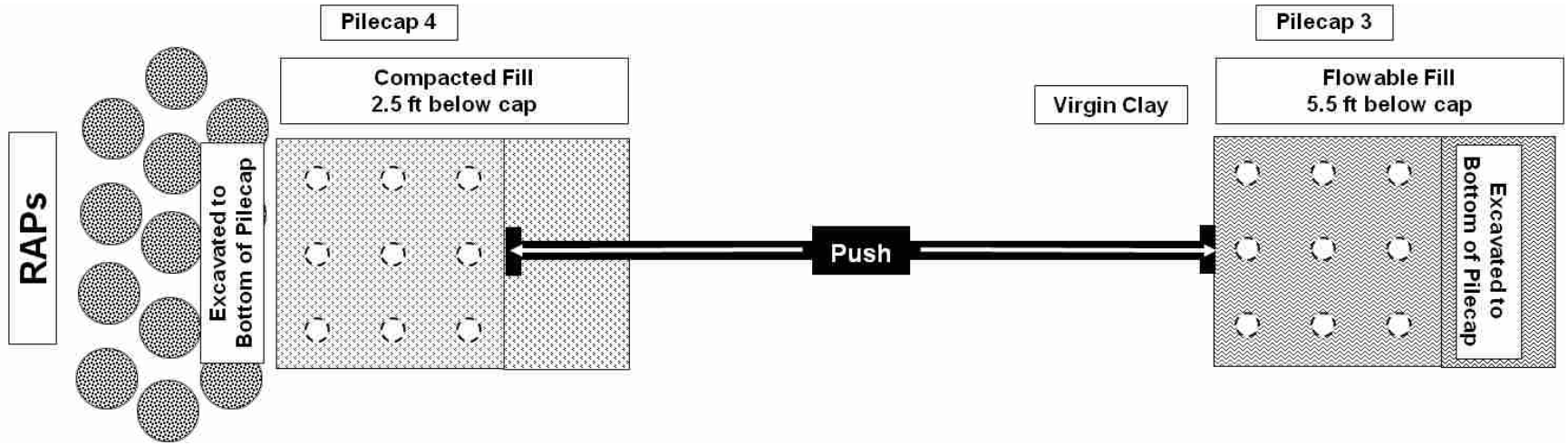

Figure 9-12 Schematic plan view of Test 7

Since this test took place after the pile caps had been pulled together in Tests 3 and 4 (the compacted fill tests) and then pushed out in Tests 5 and 6, there was some residual displacement to the north once the load was released. Thus, Test 7, started with a negative initial displacement of about 0.15 inches.

All instrumentation of string potentiometers, shape arrays, inclinometers, actuator pressure transducer, and strain gauges were in place and initial measurements taken prior to the test. All instrumentation remained connected and in place during the excavation of the top 2.5 ft of the RAPs. The shape array that was to be used in the south pile (array 115) was damaged sometime during testing and the data collected from it was nonsensical, therefore the only array data recorded was array 104 (placed in pile 4-N). The locations of all the instrumentation for pile cap 4 are as shown in Section 4.3. Strain gauges on pile cap 4 were located on the north and south piles of pile cap 4 (piles 4-N and 4-S). The second deepest set of strain gauges on pile 4-N (the ones installed 11 ft below the top of pile 4-N) were damaged in pile driving, therefore no strain gauge data is available for that depth. The test followed the standard procedure. All values measured were zero-set to the initial values of Test 3 just prior to the commencement of testing. Figure 9-12 shows a schematic plan view of Test 7, see Figure 5-6 and Figure 5-9 for dimensions.

9.2.1 Load versus Pile Cap Displacement

The lateral load versus displacement graph shows the complete load path, including incremental cycles for the test. Figure 9-13 was obtained from the actuator pressure transducer and the string potentiometers attached to the pile cap. The actuator pushed the pile caps to target the prescribed increments of 0.125, 0.25, 0.5, 0.75, 1.0, 1.5 inches, being referenced to actuator

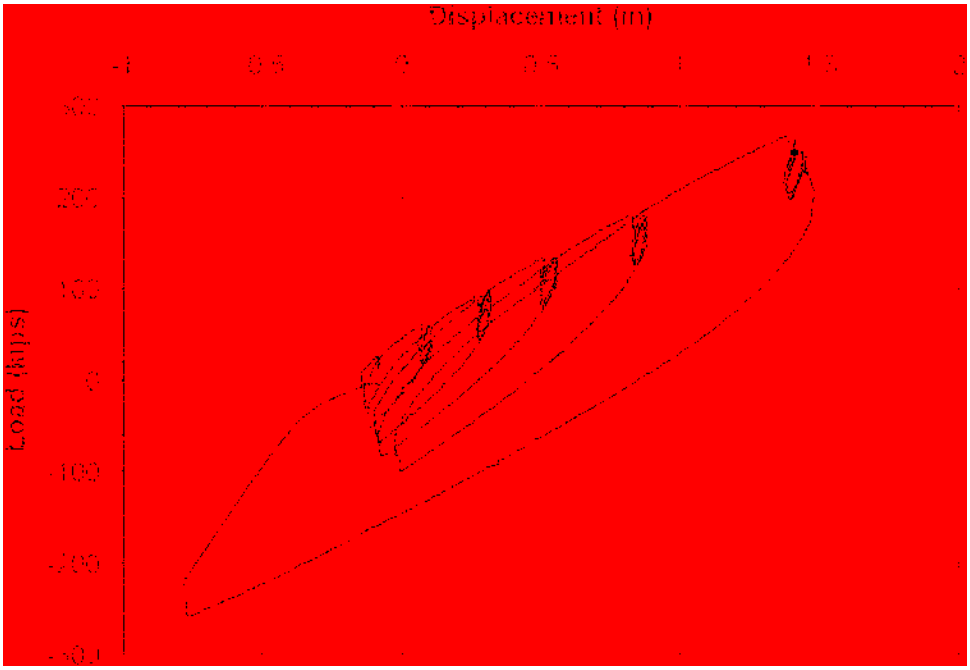

Figure 9-13 Plot of continuous pile cap displacement versus applied load for pile cap 4 during the RAP test after excavation (Test 7)

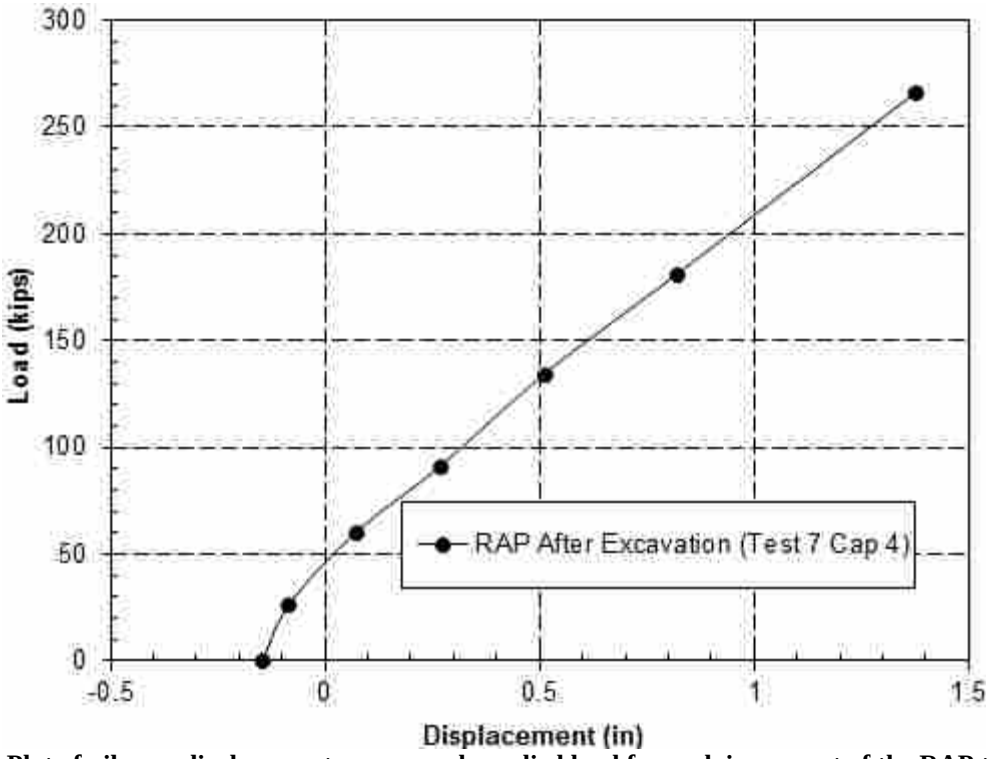

Figure 9-14 Plot of pile cap displacement versus peak applied load for each increment of the RAP test after excavation (Test 7)

extension length. The actual displacements for pile cap 4 with the residual offset of -0.15 inches were -0.08, 0.07, 0.27, 0.51, 0.82, and 1.37 inches respectively as measured by the corresponding string potentiometers. A plot of pile cap displacement versus peak applied load for each test increment is displayed in Figure 9-14. The curve in Figure 9-14 does not exhibit a typical hyperbolic shape that would be expected for a pile in soft clay, most of the plot is relatively linear. The linear nature of the load-displacement curve indicates that the lateral resistance was provided by the flexibility of the piles more than the soil along the pile. The maximum applied load during the last push was 265.9 kips and resulted in a displacement of 1.37 inches for pile cap 4. For comparison purposes a load of 285 kips at 1.5 inch displacement will be used as the load capacity for the RAP without passive resistance test.

9.2.2 Load versus Pile Head Rotation

Load versus pile head rotation curves obtained from string potentiometer and shape array measurements for pile cap 4 during Test 7 are provided in Figure 9-15. In order to match the array data up with the data from the string potentiometers, 0.215° were subtracted from the rotations derived from array 104. Rotation was measured from the string potentiometers located directly above the corbel of pile cap 4. The distance between the string potentiometers was approximately 46 inches. Refer to Figure 4-10 for a review on the position of the string pots on pile cap 4. Rotation was also measured from the shape array. The difference in node deflections near the bottom of the pile cap and the top of the corbel was used to measure rotation from shape array 104; the distance between these nodes was 48 inches. As can be seen in the figure, the rotations from array 104 did not match very closely to the rotations derived from the string pots except at the beginning of testing, but the trends of the two rotation curves are similar. The total rotation as measured by the string pots on pile cap 4 is -0.069°. The shape array shows a quite

different final rotation (even with the adjustments): -0.009°. This shows that even after pushing the cap to the extent of testing, the cap was still rotated toward the north.

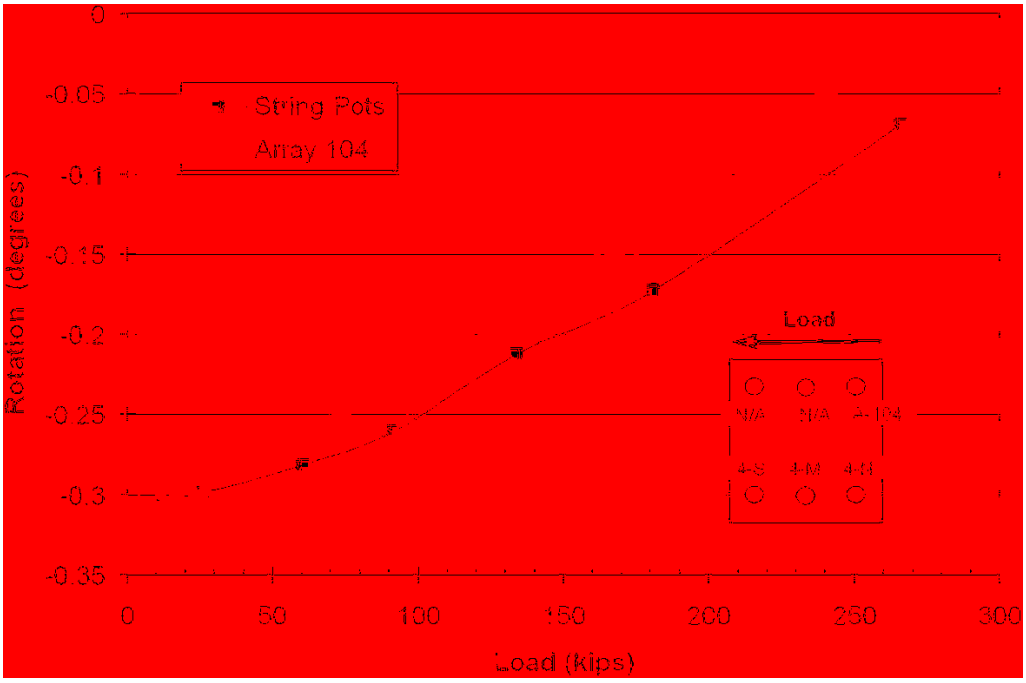

Figure 9-15 Peak pile cap load versus pile head rotation for cap 4 during the RAP test after excavation (Test 7) obtained from string potentiometer and shape array measurements

9.2.3 Pile Deflection versus Depth

Figure 9-16 shows the pile deflection versus depth profiles of array 104 and the inclinometer readings on pile cap 4 before testing commenced and at the maximum displacement during Test 7. There is good agreement with array 104 to the north inclinometer except toward the bottom 10 ft of the array. Because there were no other arrays in the pile cap, a comparison for both the north and south inclinometers is included in Figure 9-16. The plot of the south inclinometer seems to indicate greater curvature than the north inclinometer. This confirms the observations of earlier tests that the extreme pile in the direction of loading should experience a higher bending moment than the trailing piles. In order to correct for movement below the end of the shape array, 0.014 inches were added to the initial displacements and 0.030 inches to the

final displacements of array 104 in the inclinometer comparison. By adjusting the shape array in this way, its displacements match more closely with the inclinometer readings taken at similar depths. The inclinometers show that there was deflection in the piles at depths greater than 30 ft. At the depth of the base of shape array 104 (24 ft below the top of corbel), the inclinometer reads -0.030 inches of displacement at 1.5 inches of pile cap displacement.

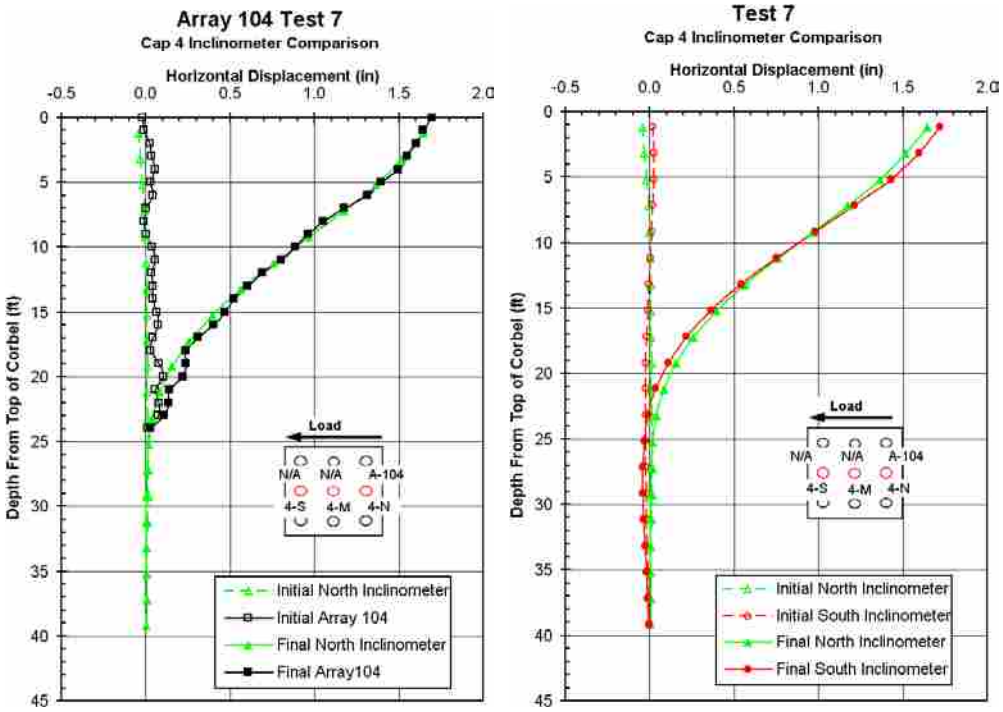

Figure 9-16 Comparison of depth versus deflection curves for the piles in pile cap 4 from the north inclinometer with shape array 104 and the north and south inclinometers for the RAP test after excavation (Test 7)

Figure 9-17 shows pile deflection versus depth for each of the loading increments as measured by array 104 in Test 7 along with the corresponding string potentiometer readings. The difference between the array displacements and string potentiometer readings in Figure 9-17 appears to be, at least in part, due to movement of the pile below the lowest node of the shape arrays. In spite of the minor discrepancies, the general trend and slope of the depth versus displacement profiles are fairly consistent and provide a reasonable representation of the

deflections the piles experienced. The bends in the curve toward the bottom of the shape array do not seem realistic, however.

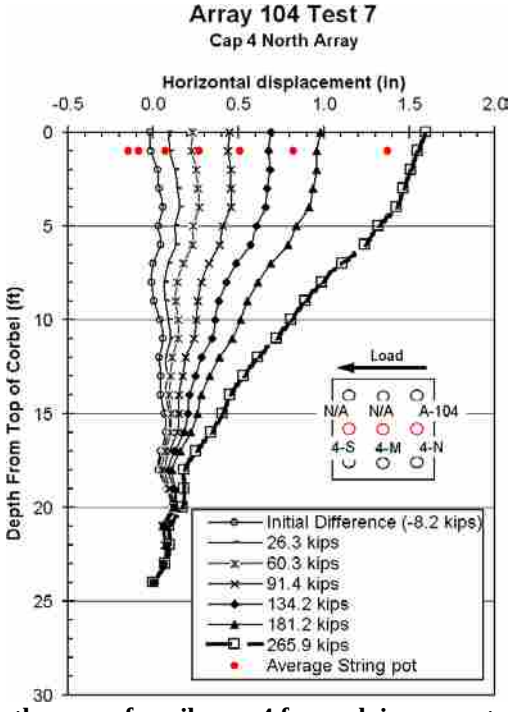

Figure 9-17 Deflection versus depth curves for pile cap 4 for each increment of the RAP test after excavation (Test 7), with pile head displacements from the string potentiometers also shown

9.2.4 Pile Bending Moment versus Depth

Bending moments were estimated from the depth versus displacement profiles from the center and north piles on pile cap 4 using the methods described in Section 6.2. Figure 9-18 and Figure 9-19 provide bending moment versus depth curves for the north and south piles in pile cap 4 at the six target displacement levels during Test 7. The curves in Figure 9-18 were obtained from the shape array while the individual points in Figure 9-18 and the curves in Figure 9-19 represent moments computed from strain gauges. The datum for these figures is the bottom of the pile cap. The maximum load at each target displacement is also listed in each figure's legend.

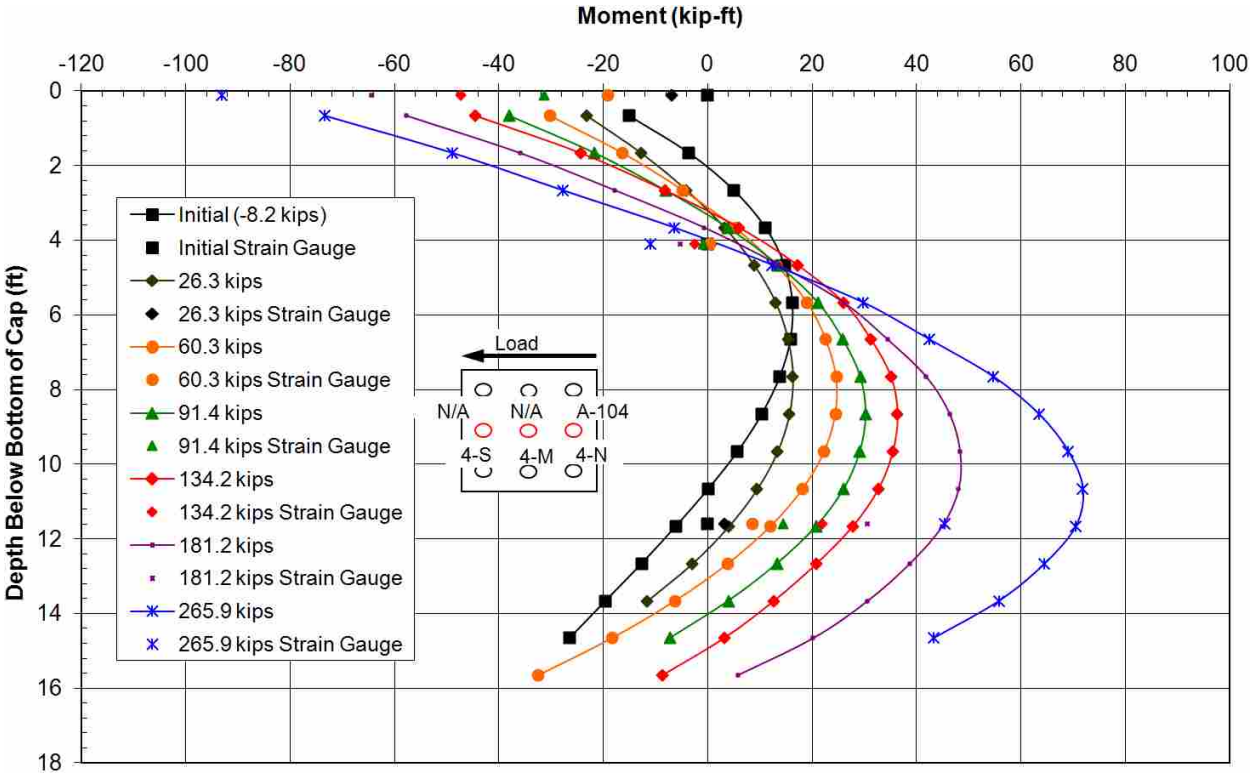

Figure 9-18 Moment versus depth curve for the north center pile of pile cap 4 (4-N) based on incremental deflection versus depth curves measured from shape array 104 during the RAP test after excavation (Test 7), with point moments measured from strain gauges at various depths also shown

The numerical method, in this case, shows a good correlation between shape array and strain gauges for the negative moments at greater displacements. The moment trends of the shape arrays in Figure 9-18 do not generally demonstrate good consistency when compared to the strain gauges. The shape array curves do, however, show good correlation with the strain gauge moments for the negative moments toward the top of the north pile for the larger displacements.

The maximum positive bending moments from the north pile array in Figure 9-18 tend to occur from about 8 ft to 10.7 ft below the bottom of the pile cap. The positive moments measured from the strain gauges do not match very well with the array moments. The maximum positive moments as measured by the strain gauges in the south pile (Figure 9-19) all occur at the 11 ft strain gauge (which is 9.2 ft below the base of the pile cap). The maximum positive

moments from the array are higher than the moments calculated from the strain gauges on both the north and south pile. The strain gauge data from the south pile does not look very realistic.

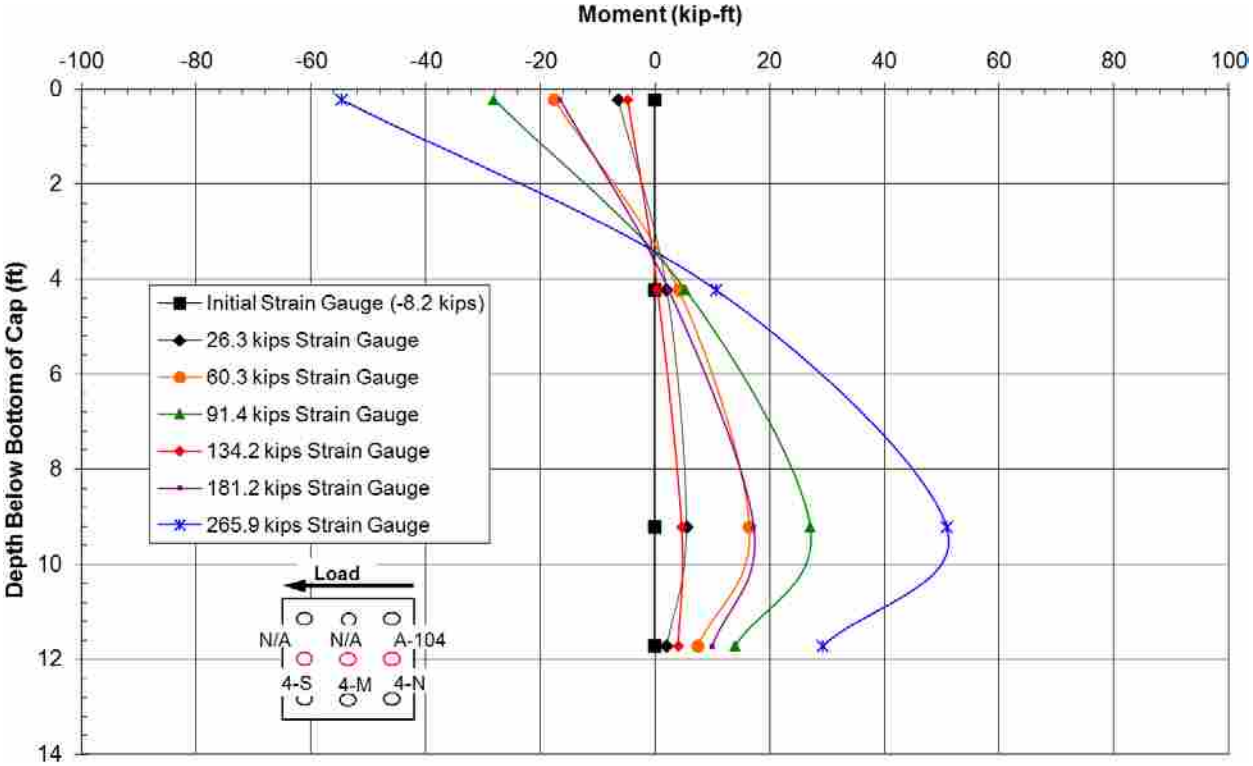

Figure 9-19 Moment versus depth curve for the south center pile of pile cap 4 (4-S) based on strain gauge readings at various depths for the RAP test after excavation (Test 7)

A comparison of the moments derived from array 104 and the inclinometers at the initial position and the maximum displacement is shown in Figure 9-20. There is reasonable agreement between the inclinometers and the array for the maximum displacement curves. The north inclinometer places the maximum positive bending moment at about 12.9 ft, the south inclinometer places it at about 12.4 ft, and array 104 places it higher at around 10.6 ft. When looking at the magnitude of the maximum positive moment, the north inclinometer measures about 62.8 kip-ft, the south inclinometer 64.9 kip-ft, and the north array 66.1 kip-ft. The maximum negative moment as measuring by the inclinometers and the shape array ranges from about 85 kip-ft from the north array to about 96 kip-ft from the south inclinometer, with the north

inclinometer falling between those values at around 94 kip-ft. The trends shown in the inclinometer comparison demonstrate what would be expected in showing a higher positive moment the farther south the readings are taken. Because the loading occurred toward the south, the southern piles should undergo a higher moment when compared to piles farther to the north.

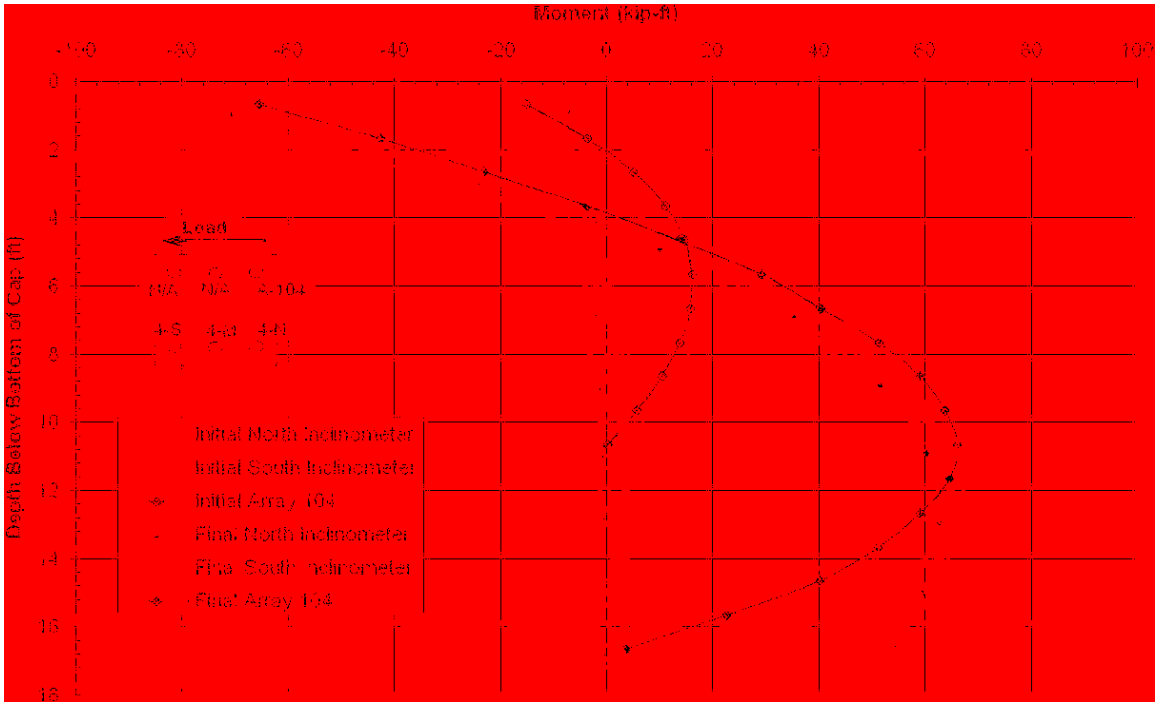

Figure 9-20 Moment versus depth comparison for the piles in pile cap 4 based on deflections measured from the north and south inclinometers and shape array 104 during the RAP test after excavation (Test 7)

9.2.1 Moment versus Load Results

Figure 9-21 and Figure 9-22 provide plots of the maximum positive and negative bending moments versus applied pile cap load respectively for cap 4 during Test 7. Moment data come from both shape array and strain gauge data when available. The curves are relatively linear as the load increases and the soil resistance is mobilized from the base of the pile cap downward. The curves from the strain gauges provide relatively consistent moment versus load curves with evidence of group interaction effects. The agreement between the curves computed by the strain

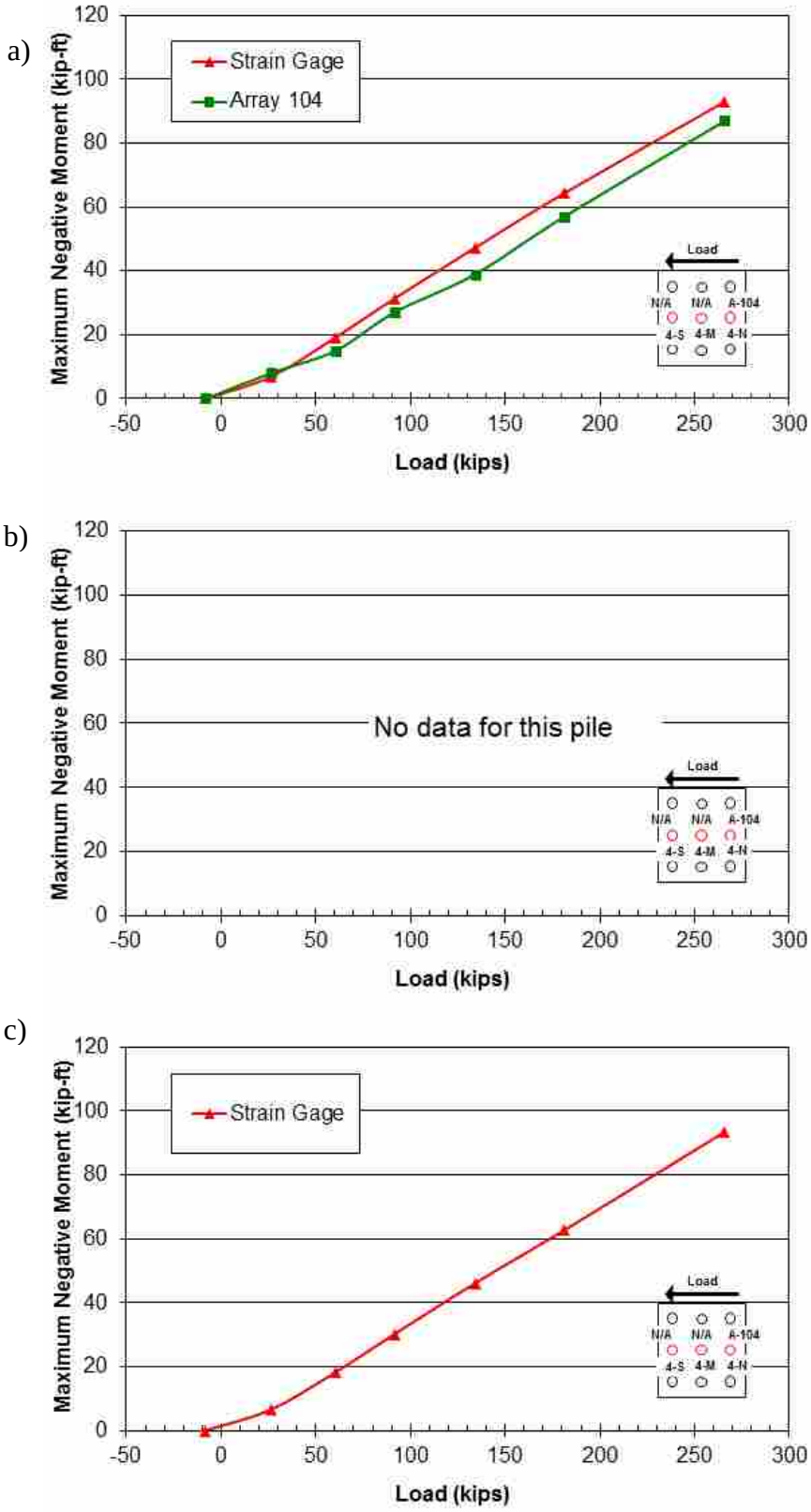

Figure 9-21 Maximum negative moment (base of cap) versus total pile cap load for piles (a) 4-N, (b) 4-M, and (c) 4-S in cap 4 during the RAP test after excavation (Test 7)

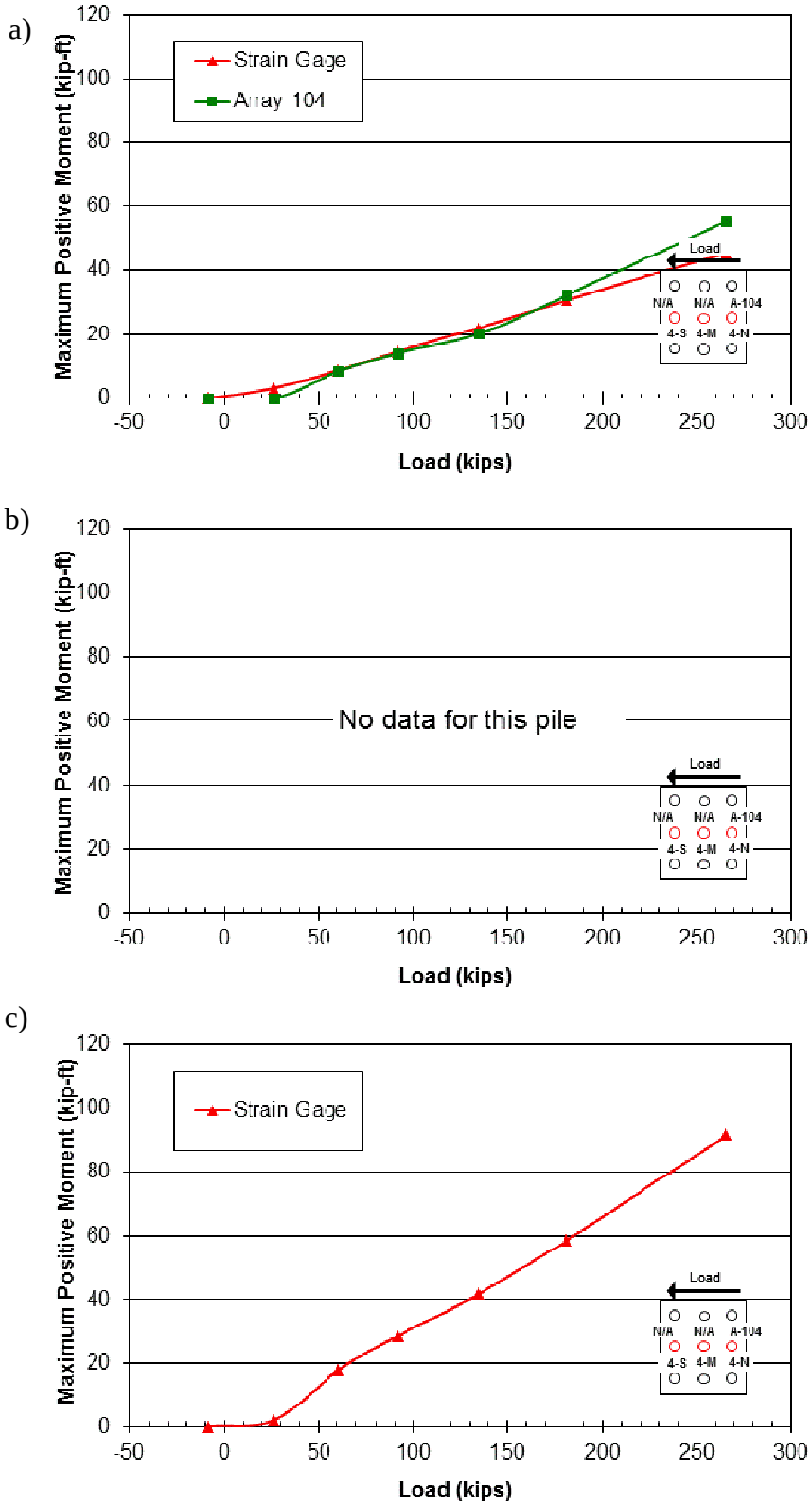

Figure 9-22 Maximum positive moment versus total pile cap load for piles (a) 4-N, (b) 4-M, and (c) 4-S in cap 1 during the RAP test after excavation (Test 7)

gauges and shape arrays is reasonable for the negative moments of the larger displacements, but not for the positive moments.

Comparisons of the test results from Test 7 and the other tests will be given in Chapter 0 along with a cost comparison of using a RAP retrofit versus a structural retrofit.

10 TEST COMPARISONS

This chapter will compare the results from the tests reported in the previous chapters. Tests 1 and 2 are compared to determine the amount of passive soil resistance acting directly on the pile cap during virgin clay loading. Test results from Test 5 are also compared to Tests 1 and 2 to determine the increase in capacity of a driven pile foundation underlain with compacted sand. The test results from Tests 3 through 7 are then compared to determine the increase in lateral resistance caused by treating the soil with compacted fill and RAPs. With results from these tests, the ultimate lateral resistance from the treated zones is calculated. Finally, a basic cost analysis will be presented to examine the relative cost of installing compacted fill or RAPs compared to a structural retrofit with additional piles and an expanded pile cap.

10.1 Virgin Test Comparisons

This section will compare the two tests performed to test the virgin clay: Tests 1 and 2. These comparisons will be used as a basis for comparisons of all of the other tests. The comparison of Tests 1 and 2 is used to set a baseline for comparison of the improvements gained from each of the retrofit approaches.

10.1.1 Pile Head Load versus Displacement

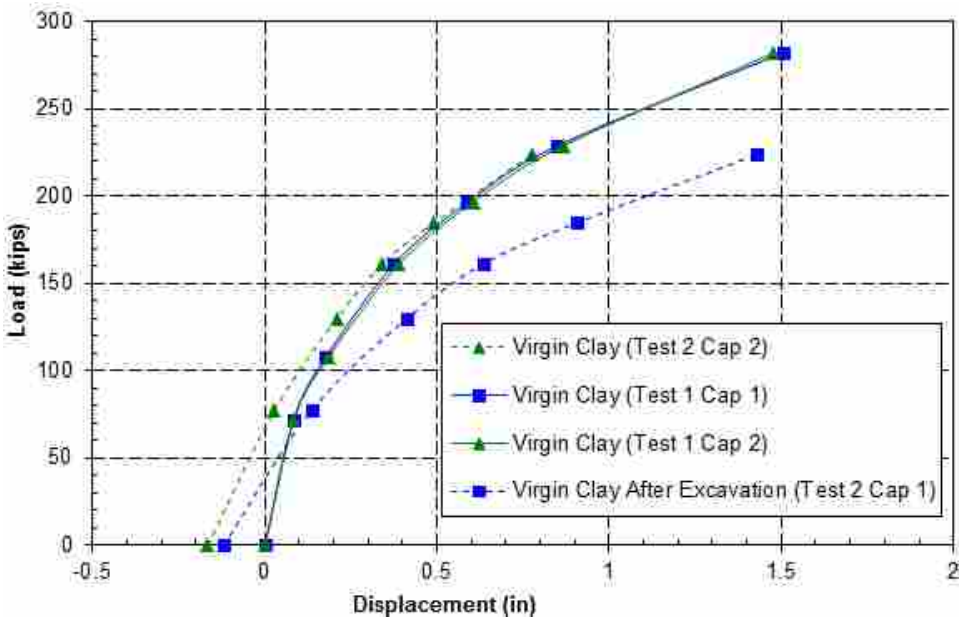

Figure 10-1 Comparison of peak pile cap load versus pile head displacement curves for pile caps 1 and 2 during virgin clay tests before (Test 1) and after excavation (Test 2).

Figure 10-1 provides a comparison between the pile head load-displacement curves for pile caps 1 and 2 during Tests 1 and 2. The load-displacement curves for Test 2 have been shifted to the right 0.15 inches to account for reloading effects. With this minor adjustment, the load-displacement curve for pile cap 2, with clay adjacent to the pile cap matches the curves for pile caps 1 and 2 during Test 1 at larger displacements, as would be expected. In contrast, the load-displacement curve for pile cap 1 in Test 2 is lower than that for pile cap 2 at a given displacement because the soil adjacent to the pile cap had been excavated.

The development of passive force on the pile cap was then determined by computing the difference in the lateral load as a function of displacement for the tests on pile cap 1 with and without soil against the pile cap. These calculations were performed at displacements of 0.25, 0.5, 0.75, 1.0, and 1.5 inches. The resulting passive force-displacement curve is displayed in Figure 10-2. The curve indicates that the ultimate passive force was approximately 54 kips, and

was fully developed at a displacement of about 0.75 inches or about 2.5 percent of the wall height. In this case, where the soil against the pile cap was largely stiff clay, the passive soil resistance behind the pile cap represents about 18 percent of the total lateral resistance of the pile group foundation.

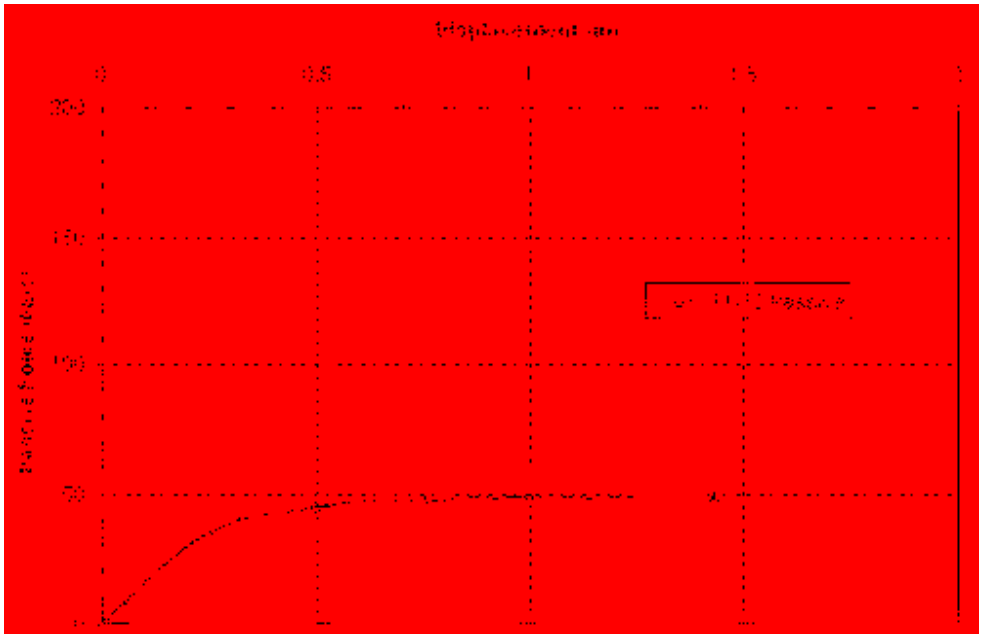

Figure 10-2 Development of passive force for virgin clay around pile cap 1

Based on the measured passive force, P_p, the average undrained shear strength of the upper 2.5 ft of the soil profile was back-calculated using the basic equation

$$P_p = 0.5\gamma z^2 B + 2c_u zB \qquad (10\text{-}1)$$

based on Rankine theory for undrained conditions where:

γ = total unit weight of the clay = 117 lb/ft^3

z = height of the pile cap = 2.5 ft

B = width of the pile cap = 9 ft

c_u= undrained shear strength (lb/ft^2).

Based on this back-analysis, the undrained shear strength in the upper 2.5 ft of the soil was found to be 1040 psf. This shear strength is higher than that measured by the unconfined compression testing (see Table 3-1), but within the range predicted by the correlation with the CPT cone tip resistance as shown in Figure 3-3. The shear strength in this zone is significantly higher than the underlying soft clay due to overconsolidation from desiccation. In addition, most of this zone was above the water table and thus may have only been partially saturated during the testing and/or subject to significant capillary stresses.

10.1.2 Load versus Pile Head Rotation Comparison

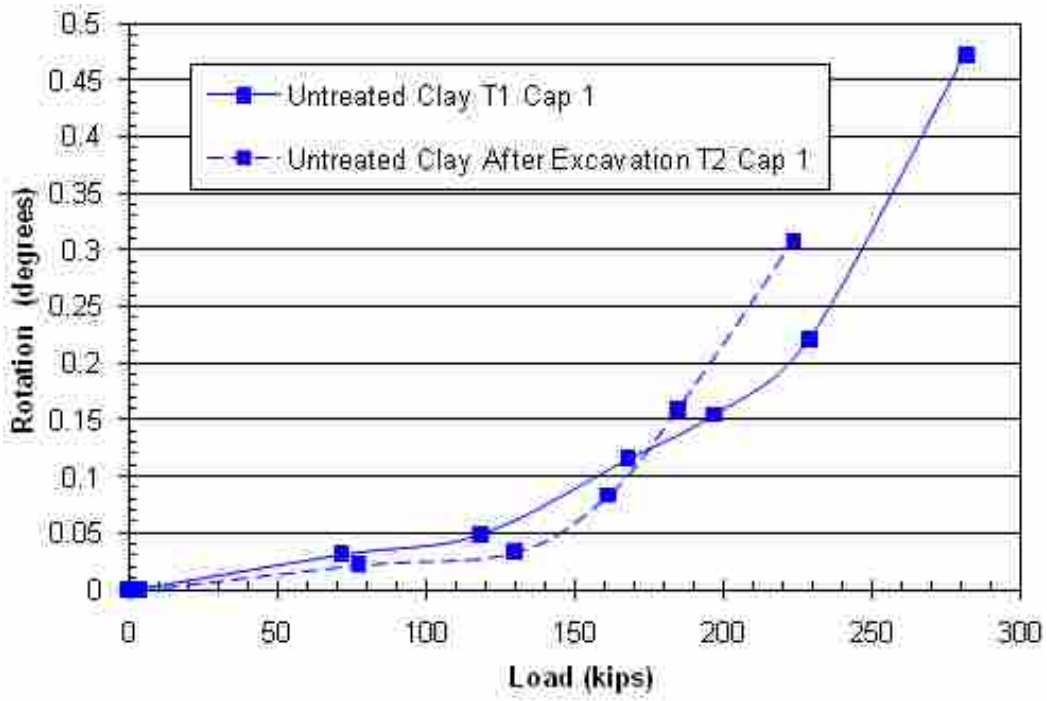

Figure 10-3 Load versus rotation curves for virgin clay tests before (Test 1) and after excavation (Test 2)

All rotation data for the virgin clay was zeroed to the start of testing. The curves for pile cap 1 in Figure 10-3 show a strange trend, with no passive resistance on the face of the pile cap it seemed to rotate less than when there was passive resistance on the cap. Generally, the

relationship between support and rotation is that the greater the support, the less rotation there should be at any given load. The inconsistencies in Figure 10-3 may be due to the difficulty of measuring such small angles accurately.

10.1.3 Moment versus Load Comparisons

Figure 10-4 illustrates the combined trends of selected maximum positive moment in the piles versus load curves for Tests 1 and 2 on pile cap 1. Curves that exhibit widely varying or irregular trends were excluded to facilitate identification of the general trend and to make comparisons. The curves from Test 1 are denoted with a square mark (blue) while those of Test 2 are denoted with a triangle mark (red). At a given load, the curves from Test 2 show a greater moment which is expected since Test 2 had no passive resistance behind the pile cap and thus experienced greater displacement or bending at the same load. Figure 10-5 shows similar plots for selected maximum negative moment versus load comparisons for Tests 1 and 2 on pile cap 1. Likewise, using the same marking convention, the curves for Test 2 also plot greater bending moments at the same loading than Test 1 curves. This is also what would be expected as Test 2 experienced greater displacements at the same load.

As was discussed in Section 7.2.5, the moment versus load curves show that when there is more support, the maximum negative moments in the piles generally decrease for a particular load. By plotting the maximum negative moments (Figure 10-6) and the maximum positive moments (Figure 10-7) from pile cap 1 in Tests 1 & 2 with the corresponding moments from pile cap 4 in Test 5, a similar trend can be seen in the case of the negative moments from Test 5, but not as much in the positive moments.

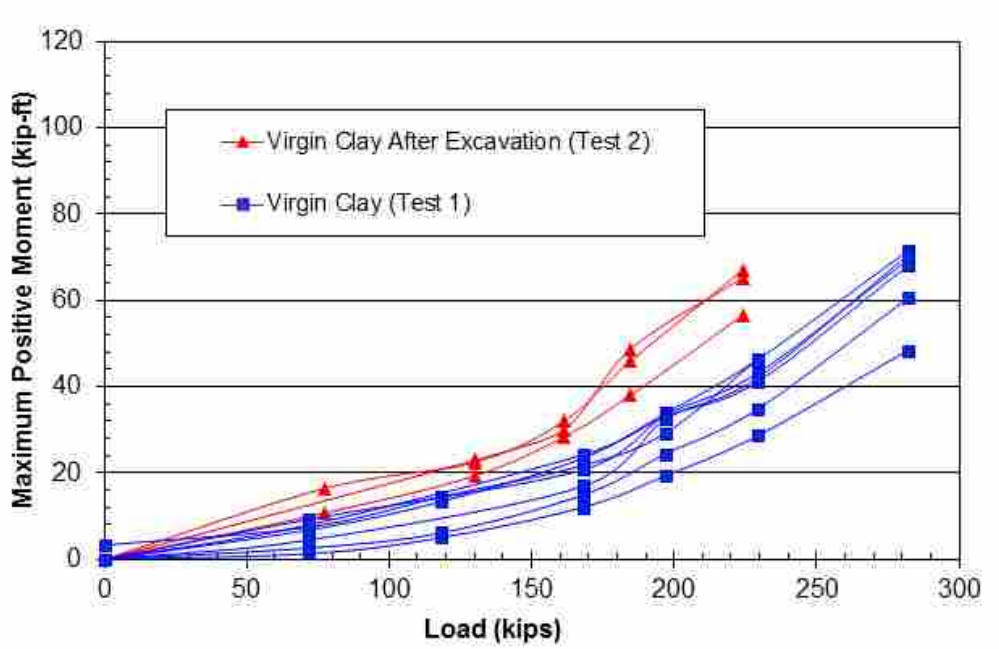

Figure 10-4 Selected maximum positive moment versus load plots from virgin clay tests (Tests 1 and 2) illustrating general trends experienced by pile cap 1.

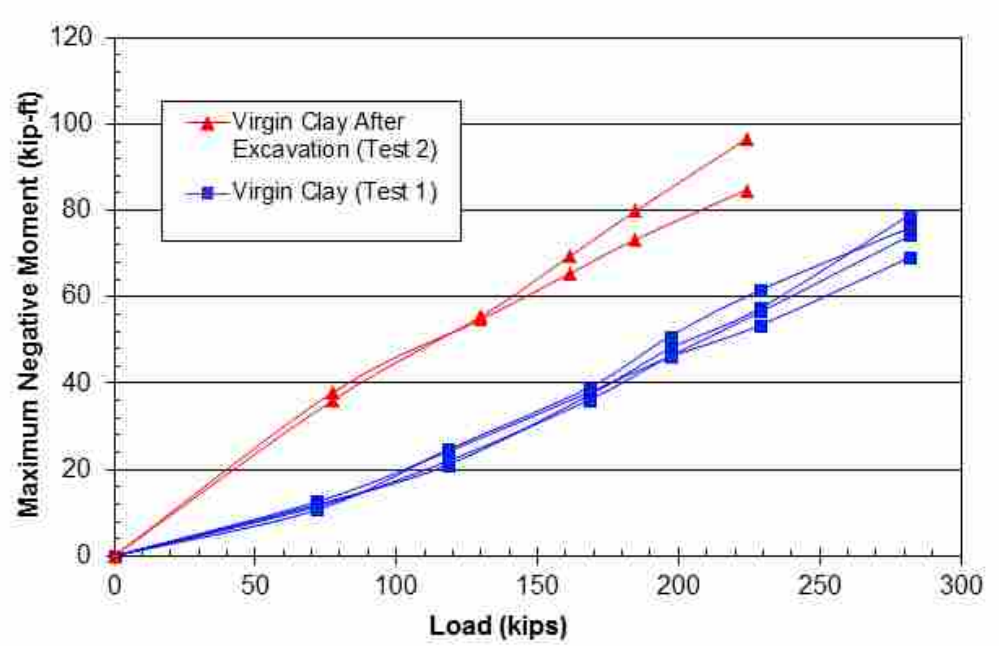

Figure 10-5 Selected maximum negative moment versus load plots from virgin clay tests (Test 1 and 2) illustrating general trends experienced by pile cap 1.

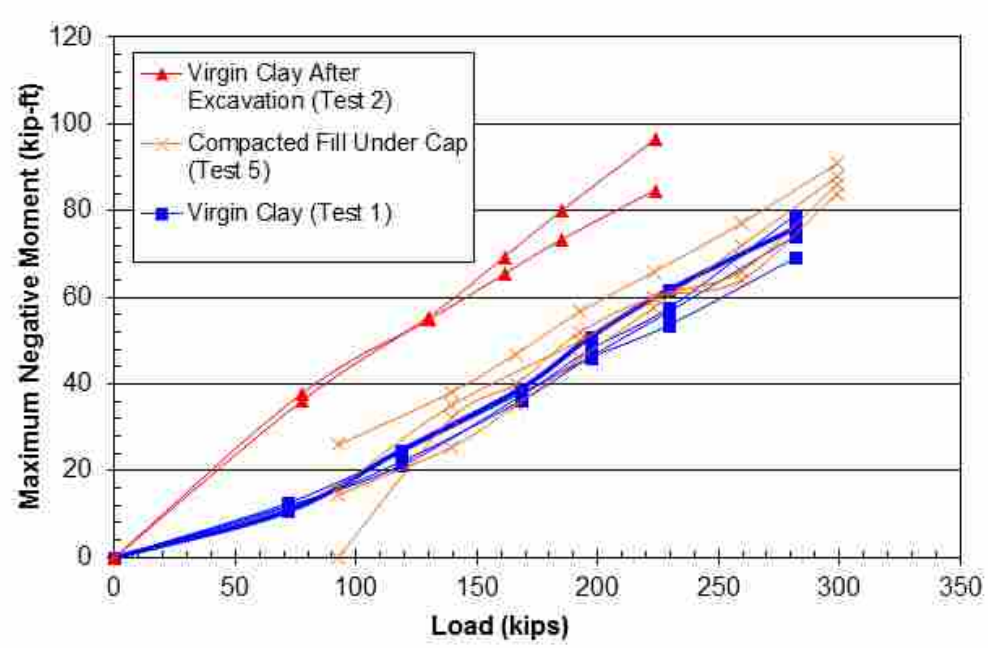

Figure 10-6 Selected maximum negative moment versus load plots of pile cap 1 from the virgin clay tests (Tests 1 and 2) compared to pile cap 4 from the test with compacted fill under the cap (Test 5) illustrating general trends.

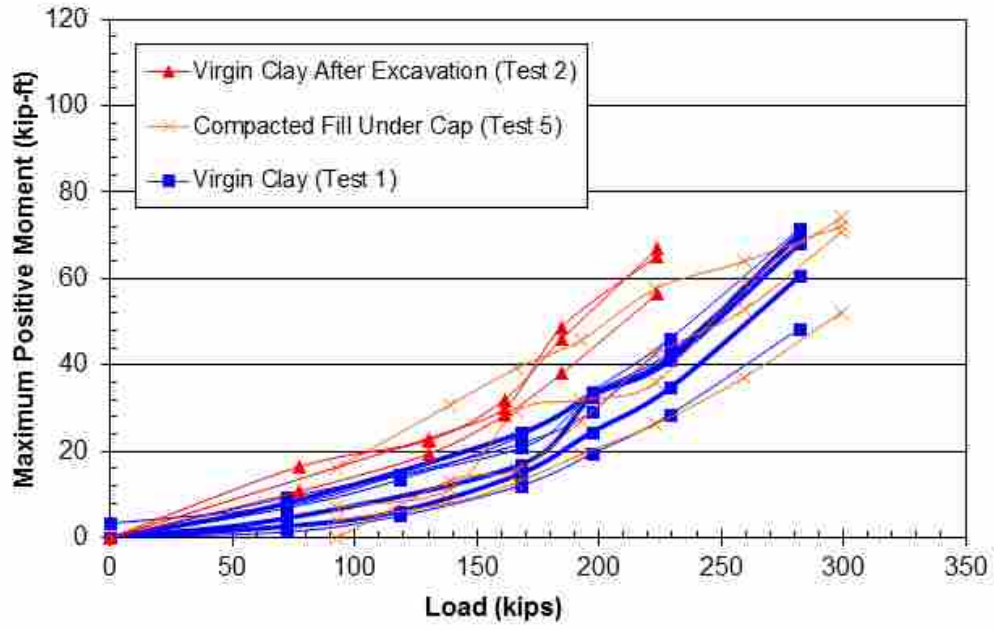

Figure 10-7 Selected maximum positive moment versus load plots of pile cap 1 from the virgin clay tests (Tests 1 and 2) compared to pile cap 4 from the test with compacted fill under the cap (Test 5) illustrating general trends.

10.2 Compacted Fill Test Comparisons

Excavation of soft, weak soils and replacement with compacted fill is likely the least expensive means of increasing the lateral resistance of a pile cap in soft clay. This series of tests provides an opportunity to quantify the increased resistance that can be achieved with this relatively simple improvement technique.

A comparison of the load-displacement curves for pile cap 4 during Test 5 and pile cap 1 during Test 1 is provided in Figure 10-8. Test 1 involves the pile cap in untreated clay, while compacted sand was placed directly below the pile cap for Test 5. Both pile caps had virgin clay adjacent to the face of the cap during the test. In order to appropriately compare the results, 0.2 inches of displacement needed to be added to the displacements of Test 5. This offset was chosen in order to make the comparisons consistent between the compacted fill tests and RAP tests and is reasonably consistent with the reloading adjustments developed previously due to

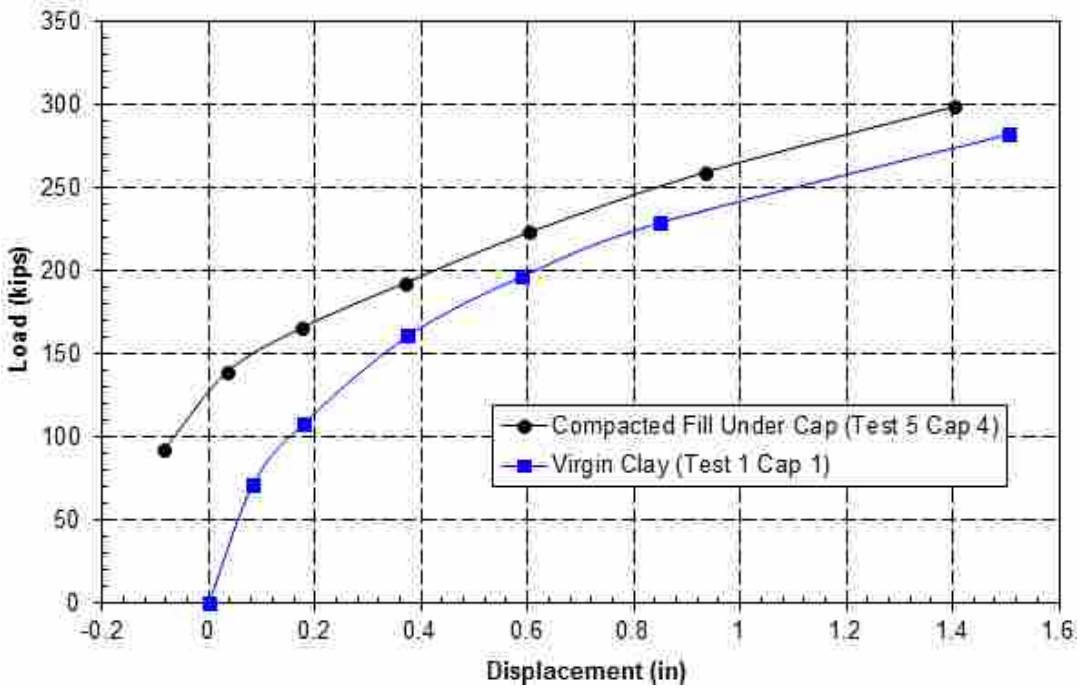

Figure 10-8 Load displacement comparison of virgin clay and compacted fill under the pile cap with clay against the cap face

soil flowing back into the gap formed adjacent to the pile during previous loading (see Section 10.3.1 for additional discussion of this rationale). The comparison of Test 5 with Test 1 shows an increase in lateral resistance of about 24 kips at a displacement of 1.5 inches resulting from placing compacted fill directly below the pile cap. This represents an 9 percent increase in resistance relative to the total resistance from soil-pile interaction and passive force. If the increased resistance of 24 kips is compared to the resistance provided by soil pile interaction only (229 kips after removing the passive force contribution of 54 kips), it still represents an increase of only 11 percent.

Figure 10-9 provides a comparison of the load-displacement curves for pile cap 1 during Test 2 and pile cap 4 during Test 3. As indicated previously, pile cap 1 was located in native clay, but the clay was excavated away from the pile cap face prior to Test 2. For pile cap 4, there was no soil against the cap face during Test 3 and the native clay below the cap had been excavated and replaced with compacted sand backfill. The sand backfill, which was 9 ft wide, extended to a depth of 2.5 ft below the base of the pile cap and 5 ft beyond the front face of the pile cap as shown in Figure 5-5.

The results in Figure 10-9 show that placement of the compacted sand increased the lateral soil-pile resistance by about 38 kips at a displacement of 1.5 inch. As expected, extending the compacted fill 5 ft beyond the cap increased the lateral resistance; however, the increase was relatively small. The increased resistance represents an increase of 16 percent relative to a comparable pile group in untreated clay. This increase in lateral resistance can only be attributed to increased soil-pile resistance or base shear because there was no soil adjacent to the pile cap. The increase of 16 percent is comparable to results reported by Brown et al (1986, 1987) when a stiff clay was replaced with compacted sand at a relative density of 50%.

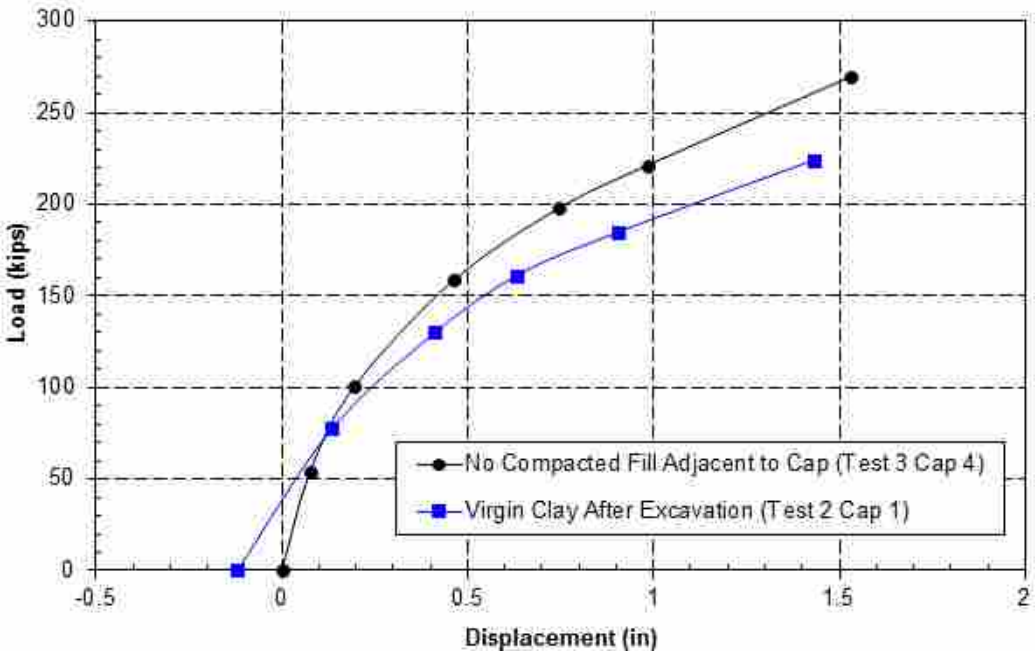

Figure 10-9 Comparison of load-displacement curves for compacted sand extending 5 ft beyond the cap and native clay without soil against the cap face

Greater improvement could potentially have been achieved if the compacted fill had extended deeper; however, this would have required flatter excavation slopes to prevent caving and more backfill material, which would increase the cost. Finite element studies conducted by Weaver and Chitoori (2007) suggest that most of the benefit from compacted fill around a pile occurs for fill materials extending five pile diameters below the ground surface. In this case, the fill extended about 2.5 pile diameters.

Figure 10-10 provides a comparison of the load-displacement curves for pile cap 4 during Tests 3 and 4. As indicated previously, no soil was adjacent to the pile cap during Test 3, but sand backfill was compacted against the pile cap prior to conducting Test 4. The sand backfill was 2.5 ft thick, 11 ft wide (extending 1 ft beyond the edges of the pile cap), and extended 5 ft beyond the front face of the pile cap as shown in Figure 5-5. Therefore, a comparison of the load-displacement curves from Tests 3 and 4 defines the increased passive resistance provided by a relatively narrow zone of compacted sand backfill adjacent to the pile cap. The residual

displacement of 0.40 inch prior to the start of Test 4 precludes a full evaluation of the development of passive force with displacement. Due to reloading, at displacements less than the previous maximum displacement, the load-displacement curve lies below the virgin curve; however, as displacement increases the curve once again joins the virgin curve. Nevertheless, the ultimate passive force can still be reasonably estimated because displacement of the pile cap exceeded 4.6% of the wall height and passive force is typically fully mobilized for displacements greater than 2 to 4% of the wall height (Rollins and Cole 2006).

A comparison between the load-displacement curves for Tests 3 and 4 (Figure 10-10) at the greatest displacements indicates that the ultimate passive force with the sand backfill was approximately 30 kips. This passive force is actually less than the 54 kip passive force measured when the native clay was left in place adjacent to the pile cap face, as discussed previously. This

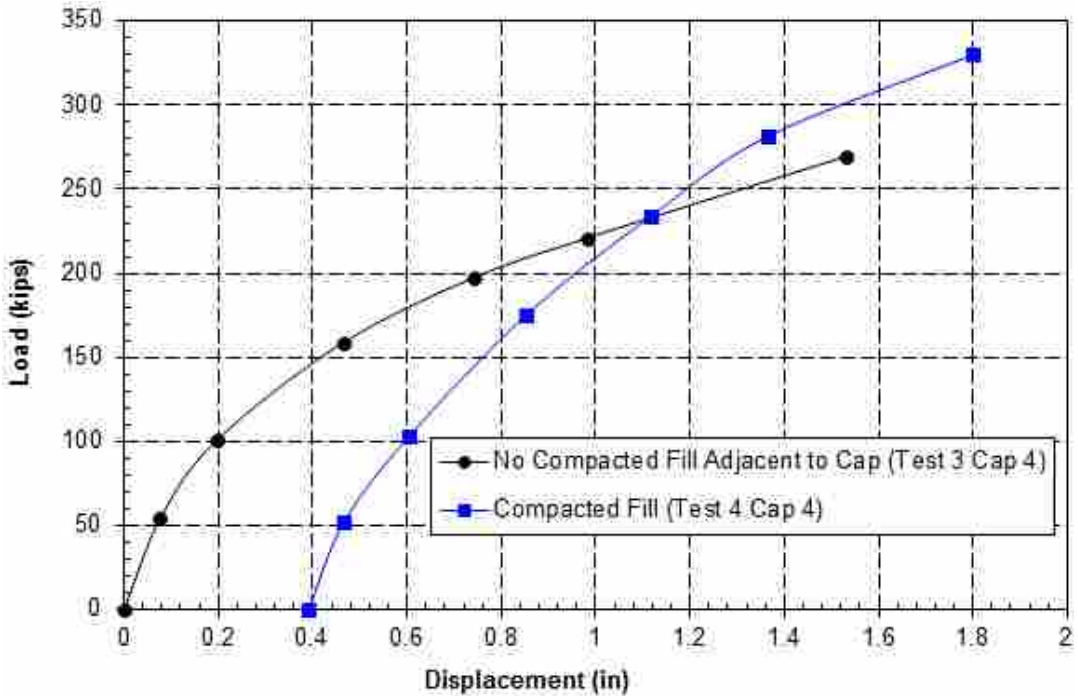

Figure 10-10 Comparison of load-displacement curves for pile cap 4 with and without fill adjacent to the pile cap

result highlights the fact that replacing clay with compacted sand is not always beneficial and must be analyzed. A similar decrease in resistance was noted in testing reported by Mokwa and Duncan (2001) when stiff clay was excavated and replaced with dense compacted gravel adjacent to a pile cap. This decrease occurs because the native clay in the upper 2.5 ft of the profile is desiccated and relatively stiff and the wall is relatively shallow so the effective stress on the sand is low. However, if the clay in the upper 2.5 ft of the profile was softer or the wall was taller, excavation and replacement with compacted sand could have potentially produced an increase in lateral resistance. For example, Table 10-1 shows the ultimate passive force which would be computed for the pile cap geometry in these tests using the Rankine theory [Equation (10-1)] for a range of undrained shear strengths. For undrained shear strengths less than about 600 psf, the ultimate passive force is less than that obtained using compacted sand backfill.

Table 10-1 Summary of ultimate passive resistance from clay adjacent to the pile cap assuming variable undrained shear strength

Unconfined Compressive Strength (psf)	Undrained Shear Strength or Undrained Cohesion (psf)	Ultimate Passive Force (kips)
400	200	12.3
600	300	16.8
800	400	21.3
1000	500	25.8
1200	600	30.3
1400	700	34.8
1600	800	39.3
1800	900	43.8
2000	1000	48.3
2400	1100	52.8

If the compacted fill had extended to a greater distance adjacent to the pile cap, the contribution from passive force might also have been larger. The largest potential passive force that could have been obtained would be when the failure surface was completely enclosed within

the sand backfill. To evaluate the ultimate passive force for this case, the force-displacement curve for the compacted sand was computed using the spreadsheet PYCAP developed by Duncan and Mokwa (2001). The spreadsheet computes the ultimate passive force using the log-spiral procedure and then uses a hyperbolic curve to compute the development of passive force with displacement.

Because the spreadsheet assumes that the shear surface occurs in a homogeneous material, compacted sand was used as the material and the value computed using the spreadsheet served as a maximum. A soil friction angle of 39°, a wall friction angle of 0.7ϕ (27.3°), an initial soil modulus of 900 ksf, Poisson's ratio of 0.2, and a moist unit weight of 115 pcf were used to calculate the ultimate passive load on a 9 ft by 2.5 ft pile cap face in compacted sand. PYCAP uses the Brinch-Hansen (1966) approach to account for 3D shear zones beyond the edge of the pile cap. The ultimate horizontal passive load computed by PYCAP for a dense sand backfill was 47.5 kips, which includes a 3D correction factor of 1.426. The value calculated by PYCAP is greater than the value determined from testing, thus showing that the value from testing is not unreasonably high. This result also indicates that at the greatest pile cap displacement (approximately 1.5 inches) the 5 ft zone of compacted sand produced only about 62 percent of the ultimate passive force that would have been developed if all the clay had been replaced by sand.

10.2.1 Load versus Pile Head Rotation Comparison

Load-rotation curves for pile cap 1 during Test 1 and pile cap 4 during Test 5 are compared in Figure 10-11. Because of the large starting load in Test 5, the rotation data from Test 5 was shifted 0.032° up to roughly match the rotation of Test 1 at 92.6 kips of load. Since

the two load-displacement curves were not dramatically different, the load-rotation curves should also exhibit similar trends. This is generally the case with the measured rotation for Test 1 being slightly greater than that for Test 5 because of the slightly higher resistance.

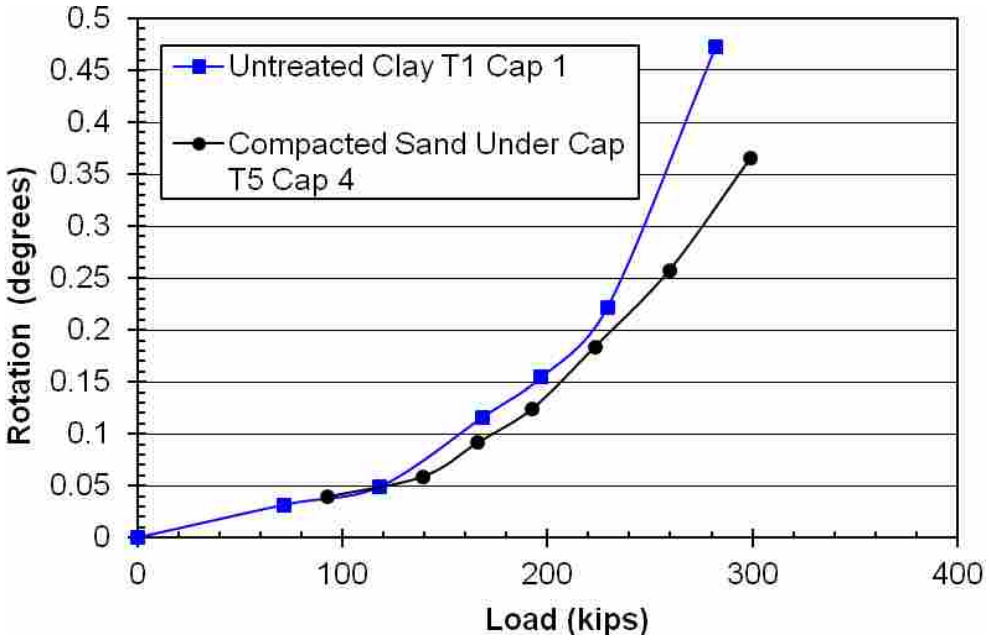

Figure 10-11 Load versus rotation curves for virgin clay and a layer of compacted fill under the pile cap with clay against the pile cap face

Figure 10-12 shows the rotation versus load curve for cap 1 during Test 1 and cap 4 during Test 5. The placement of the compacted fill under the cap increased the lateral resistance for cap 4 in Test 5 and the curves demonstrate the expected trend of decreased rotation with increased pile cap support. At 280 kips, the compacted fill offered a decrease in rotation of about 0.3° or 63 percent. Figure 10-13 compares the load-rotation curves for caps 1 and 4 during Tests 2 and 3 respectively. Compacted granular fill was placed against the pile cap during Test 3 but was not there during Test 2. With the exception of one data point on the curve for Test 2 in Figure 10-13, less rotation is observed for Test 3 as expected. At 225 kips, there was a decrease in rotation of 0.13° or 43 percent. In all the comparisons shown in Figure 10-11, Figure 10-12,

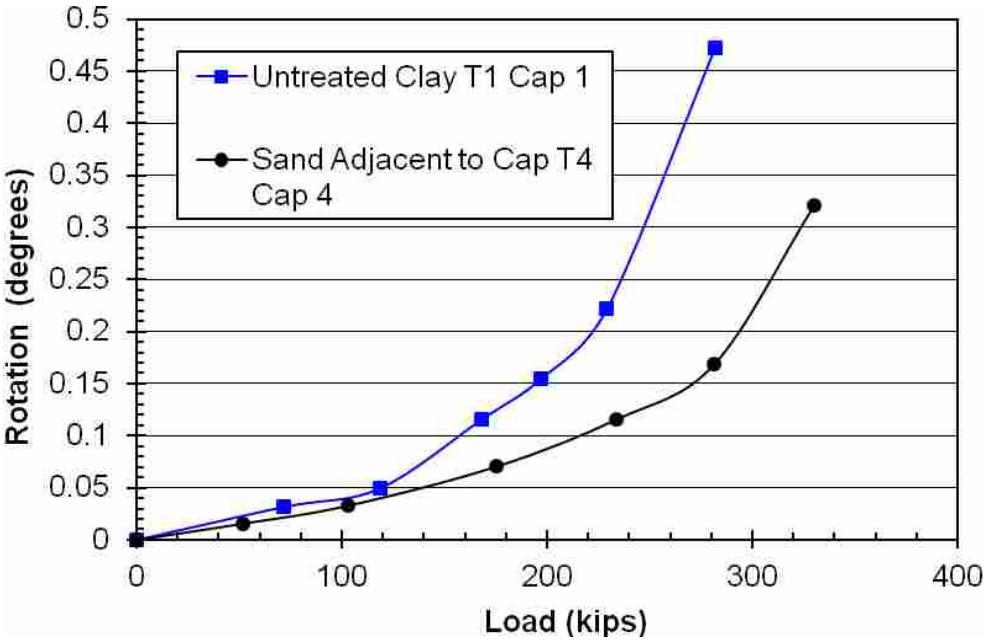

Figure 10-12 Load versus rotation comparison for virgin clay and compacted fill with soil against the pile cap

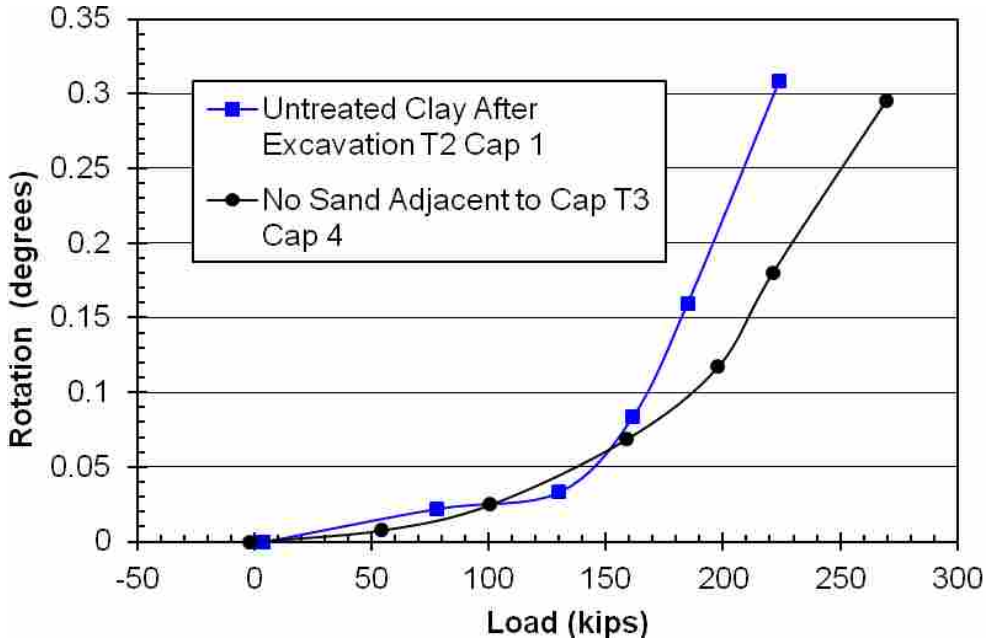

Figure 10-13 Load versus rotation comparison of virgin clay and compacted fill without soil against the pile cap face

and Figure 10-13, the differences in rotation are relatively small at small loads but become more substantial at higher load levels.

10.2.2 Moment versus Load Comparisons

Figure 10-14 and Figure 10-15 show selected moment versus load relationships for the virgin clay test and compacted fill test involving passive pressure. Figure 10-14 shows the maximum negative moments and Figure 10-15 shows the maximum positive moments. It does not appear, from the figure, that negative moments were affected greatly by the addition of compacted fill. This may be because the total increase in lateral resistance on the pile cap due to the compacted fill did not add sufficient resistance to affect the bending moments significantly.

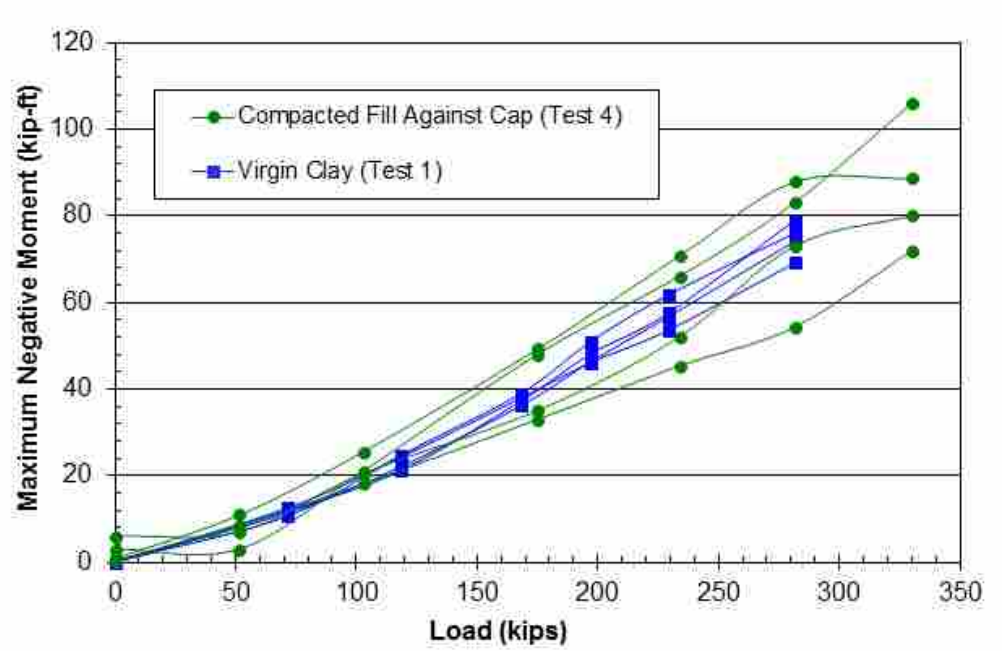

Figure 10-14 Selected load versus maximum negative moment comparisons for virgin clay and compacted fill against the pile cap face

The positive moments, however do show a definite grouping of moments for the different tests: Test 1 moments tend to be lower than moments from Test 4 for a given load.

Figure 10-16 and Figure 10-17 show the selected moment versus load relationships for the virgin clay test and compacted fill test that do not involve passive pressure on the pile cap. Figure 10-16 shows the maximum negative moments and Figure 10-17 shows the maximum positive moments. Unlike the comparisons of the tests with clay and compacted fill against the

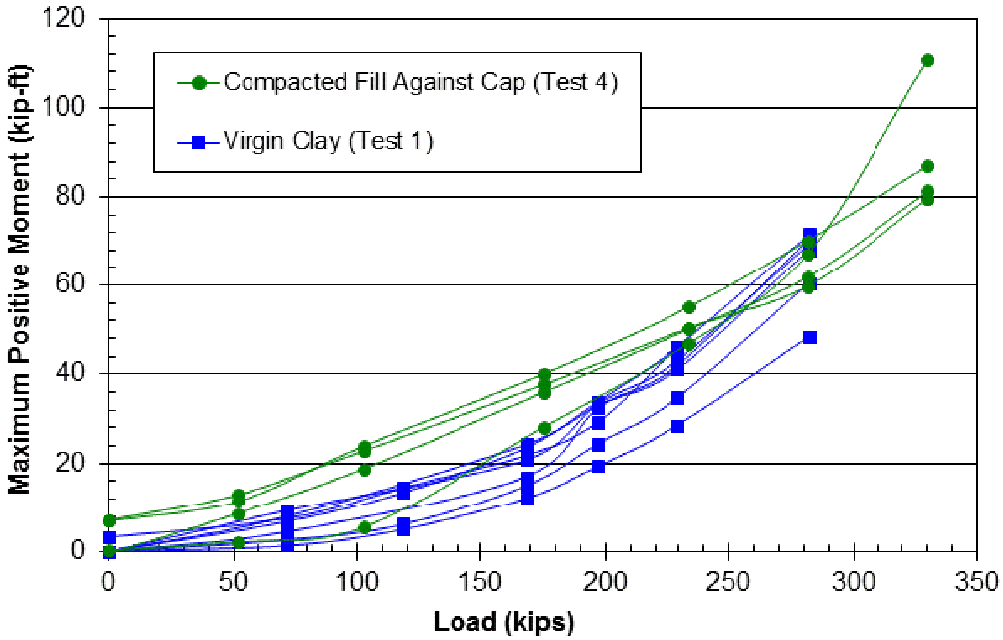

Figure 10-15 Selected load versus maximum positive moment comparisons for virgin clay and compacted fill against the pile cap face

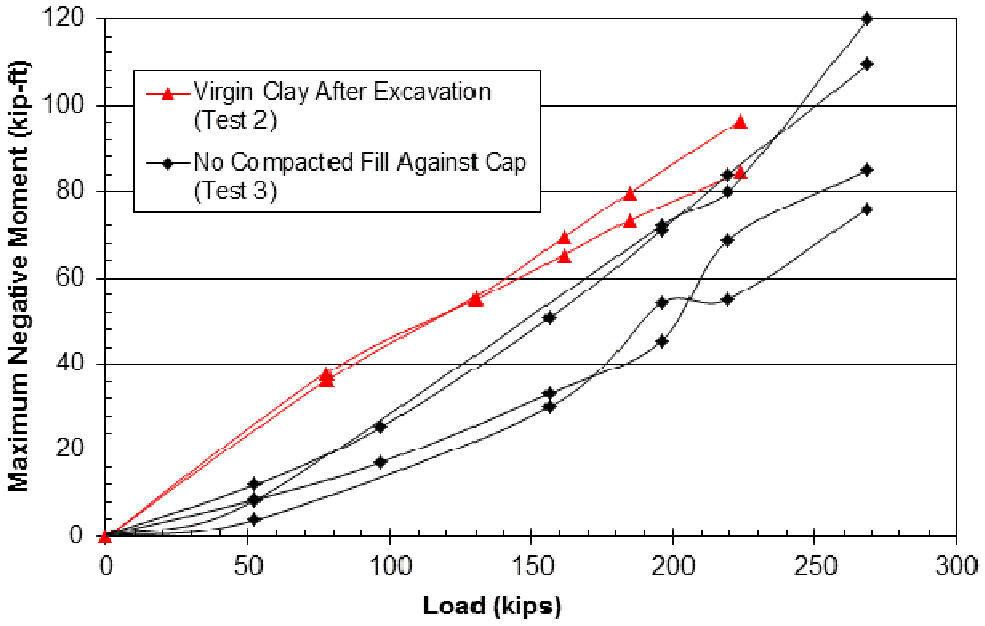

Figure 10-16 Selected load versus maximum negative moment comparisons for virgin clay and compacted fill without soil against the pile cap face

cap face, the negative moment curves for the clay test plot much higher than the test with the compacted fill installed up to the bottom of the pile cap. This trend indicates that the compacted fill which extended from the bottom of the pile cap to 2.5 ft below resisted more of the load than did the clay, causing lower moments to develop in the piles of the cap underlain with compacted fill. The effects of the increased resistance provided by the compacted fill seem to diminish before the depth of the maximum positive moments, so the curves from both tests indicate similar pile moments at depth.

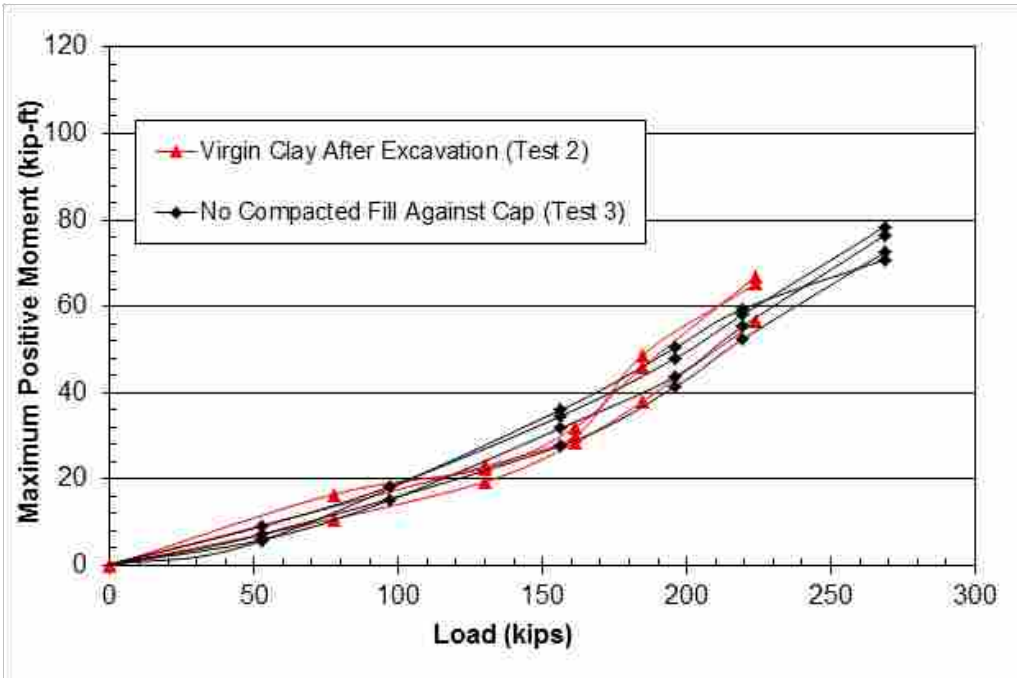

Figure 10-17 Selected load versus maximum positive moment comparisons for virgin clay and compacted fill without soil against the pile cap face

The maximum negative and positive moments from Tests 3 and 4 are compared in Figure 10-18 and Figure 10-19, respectively. Figure 10-18 shows that the negative moments from Test 4 generally plot lower than those from Test 3. This follows the trend that would be expected as the pile cap in Test 4 is supported by the passive resistance from the compacted fill

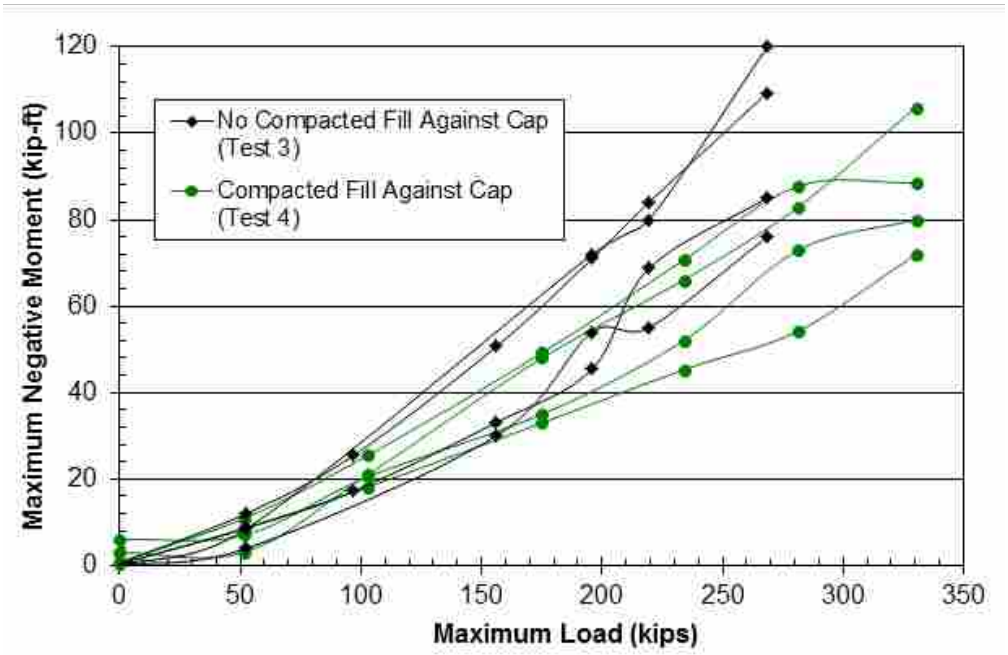

Figure 10-18 Selected load versus maximum negative moment comparisons for compacted fill with and without fill compacted against the face of the pile cap

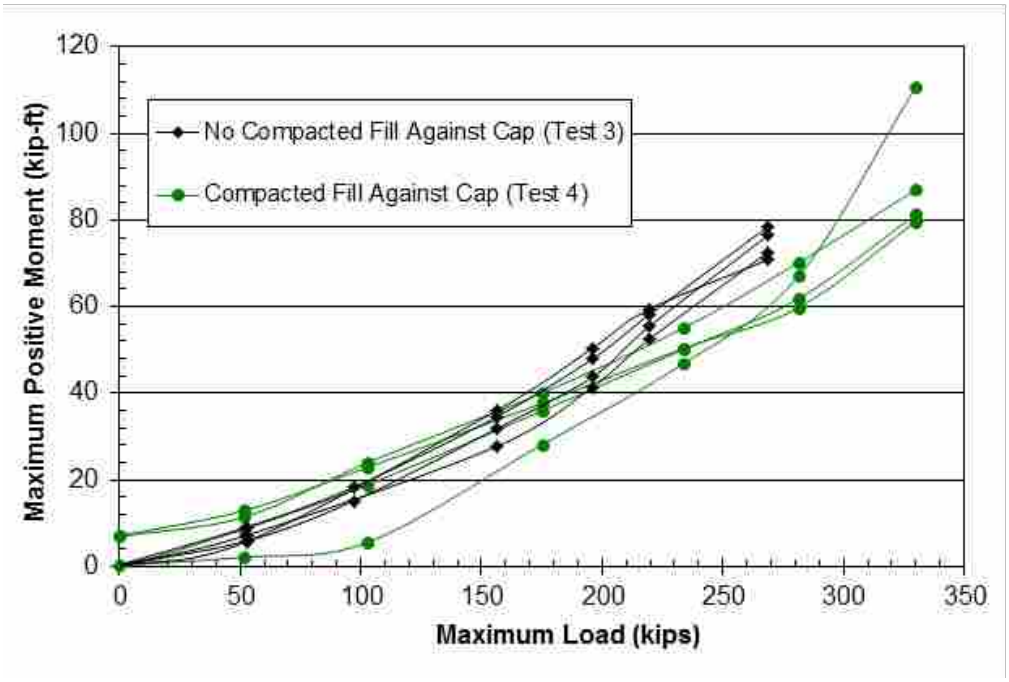

Figure 10-19 Selected load versus maximum positive moment comparisons for compacted fill with and without fill compacted against the face of the pile cap

while in Test 3 it is not. Figure 10-19 shows a very interesting trend between the positive moments from the two tests. At lower loads, the moments from Test 4 tend to plot higher than those of Test 3 and then at higher loads, the trend reverses.

10.3 Rammed Aggregate Piers Comparisons

Rammed Aggregate Piers (RAP) are a relatively inexpensive means of retrofitting a pile cap, but they are not designed specifically to increase lateral resistance. Nevertheless, comparison tests were performed to explore the potential for increasing lateral resistance using this approach. For comparison purposes in the RAP tests, virgin clay (Test 1) and RAPs (Test 6) with soil against the face of the pile cap will be plotted together and virgin clay (Test 2) and RAPs (Test 7) without soil against the face of the pile cap will be plotted together.

10.3.1 Load versus Pile Cap Displacement Comparisons

Figure 10-20 shows the load-displacement comparison between the tests with soil against the face of the pile cap (Tests 1 and 6). The curve from Test 6 shows the strength increase due to the installation of 13 RAPs adjacent to a pile cap to a depth of 12 ft. The datum for displacement of this test was the initial position of the pile cap at the beginning of Test 3 (no compacted fill against the cap). The zero-load point on the "RAP against cap" curve refers to the actual displacement measurement (compared to the "Test 3" datum) as was recorded in the test and for consistency with results from the compacted fill tests was not zero-set. The total strength increase at 1.5 inches of cap displacement is about 52 kips or 18 percent as compared to a virgin clay face with no fill compacted underneath. However, as discussed previously in section 1.1,

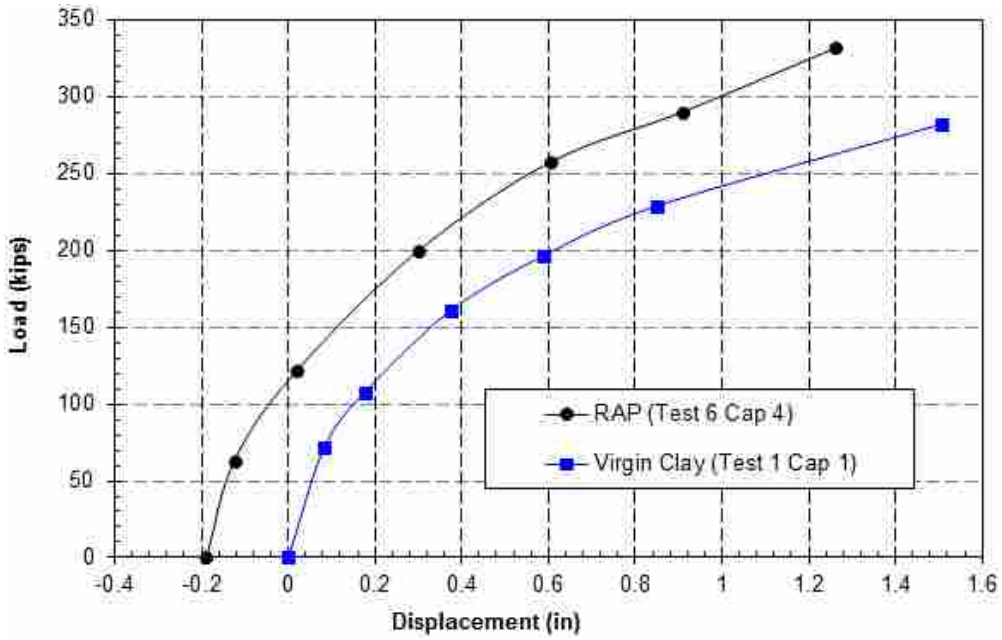

Figure 10-20 Load-Displacement comparison of virgin clay and RAP with soil against the pile cap face

the compacted sand below the cap contributed about 24 kips of this increase. Therefore, the strength increase of just the RAPs is about 28 kips or 10 percent higher than the capacity from Test 1.

Figure 10-21 shows the load-displacement comparisons between the tests without passive pressure due to soil against the cap (Tests 2 and 7). The curve for Test 7 exhibits reloading effects in that the curve is virtually linear from 1/8-inches of displacement until the end of testing. Without reloading effects, the curve for Test 7 would likely have plotted above the plot from Test 2 within this displacement range. This linear trend indicates that most of the load was being carried by the piles through structural stiffness rather than through soil resistance against the pile. The curves still show an increase of capacity of about 56 kips or 24 percent at 1.5 inches of pile cap displacement. Subtracting the effect of the compacted soil under the pile cap, the increase from just the RAPs was 32 kips or 14 percent relative to the capacity of the pile cap in virgin clay from Test 2.

Test 5 (underlain with compacted fill and pushed into virgin clay) was compared to Tests 6 and 7 (RAPs before and after excavation, respectively) as well to help confirm that the proper initial offset was selected. In Figure 10-22 and Figure 10-23 the same offset of 0.2 inches was used for Test 5 when compared with Tests 6 and 7 and with Tests 3 and 4 (compacted fill before and after placement of fill against the pile cap face respectively). Figure 10-22 provides a comparison of the lateral load-displacement curves for cap 4 after treatment with RAP columns (Test 6) in comparison with the same cap without the columns (Test 5). From the figure, at a displacement of about 1.3 inches, the addition of the RAP columns increased the total lateral resistance by about 40 kips. This represents an increase of roughly 15% relative to the cap without the RAP columns. This increase is quite consistent with the increase in resistance obtained from the comparison of Tests 1 and 6 and suggests that the offset is reasonable.

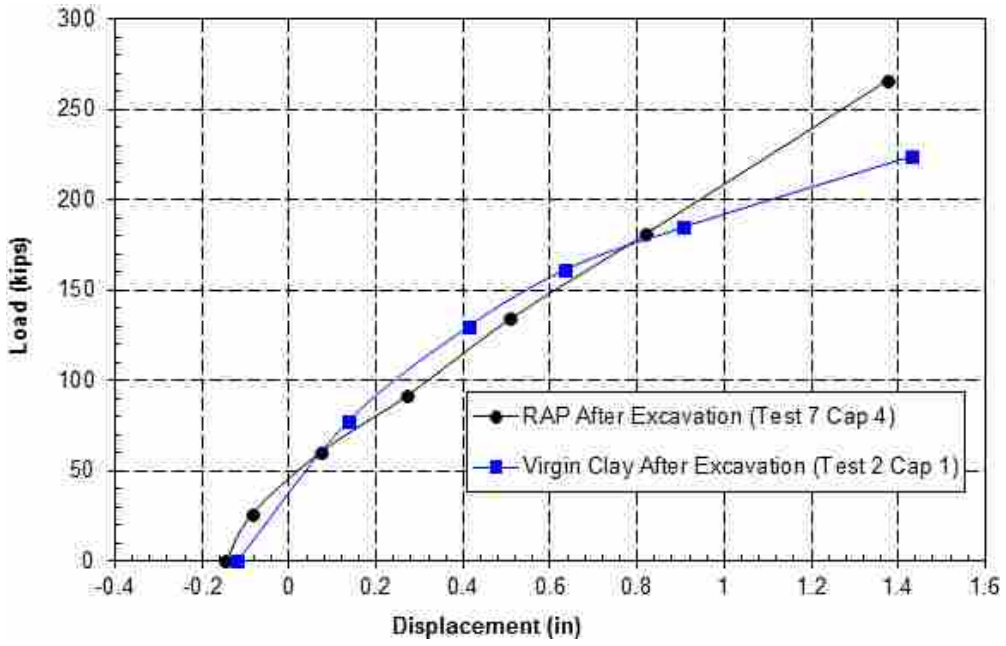

Figure 10-21 Load-Displacement comparison of virgin clay and RAP without soil against the pile cap face

Figure 10-24 plots the force-displacement curves for cap 4 after treatment with RAP columns before (Test 6) and after excavation (Test 7) of the soil adjacent to the pile cap along

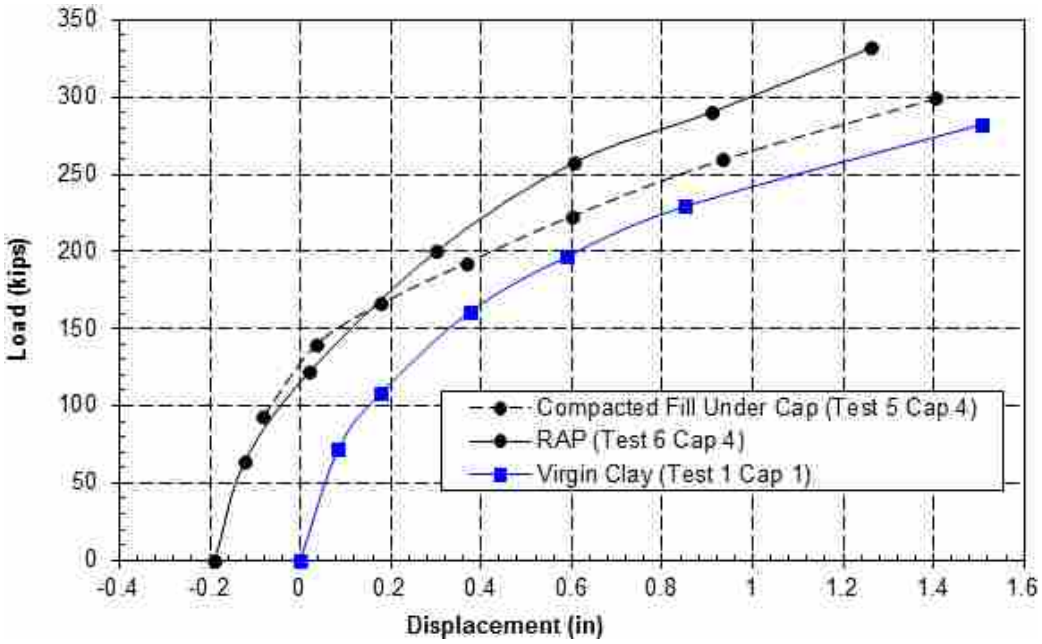

Figure 10-22 Load-displacement comparison of virgin clay and RAP with soil against the pile cap face, also showing compacted fill against pile cap face

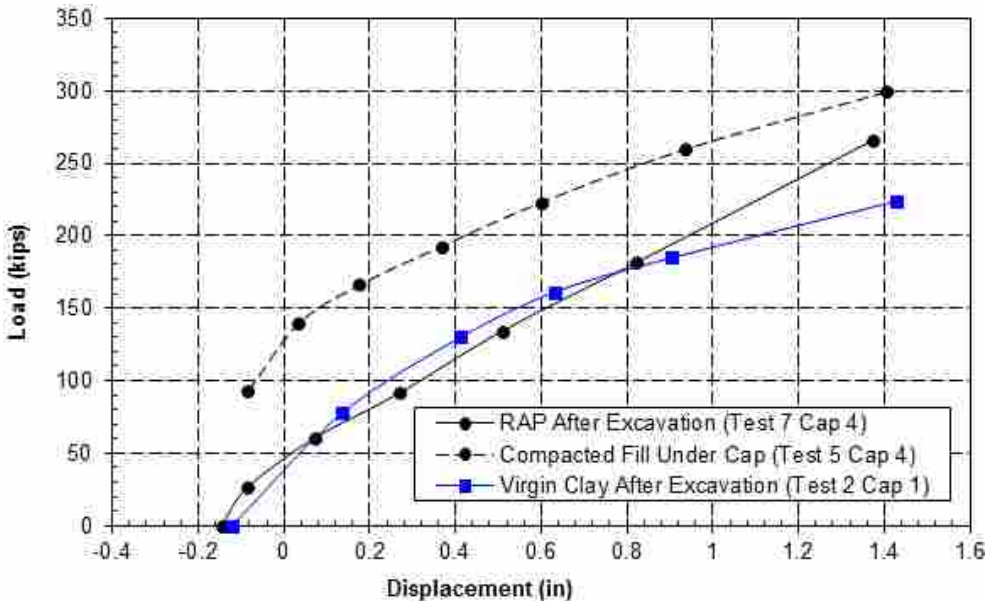

Figure 10-23 Load-displacement comparison of virgin clay and RAP without soil against the pile cap face, also showing compacted fill against pile cap face

with a plot of the virgin clay test after the excavation of soil from in front of the pile cap (Test 2). By comparing Test 6 and Test 7, the passive pressure increase can be determined for the installation of RAPs adjacent to the pile cap. Due to the effects of reloading, the passive

pressure can only be determined accurately toward the end of the displacement range by subtracting the ultimate capacity of the test with no passive pressure (Test 7) from the capacity of the test with soil against the face of the pile cap (Test 6). The curve for Test 7 should follow the shape of the curve from Test 2 (see Figure 10-24) in that displacement range, which would cause a lower passive pressure in that area. Because of reloading effects, the passive pressures are overestimated from 0.08 inches of displacement to about 0.72 inches. It is important to note that the passive pressure increases until a displacement of about 0.7 inch, after which it appears to remain constant or to decrease. This trend could denote a failure within the RAPs themselves.

Based on Figure 10-24, the interpreted passive force that will be used for comparison with other tests is about 85 kips at a displacement of 1.25 inches. This is about 31 kips higher

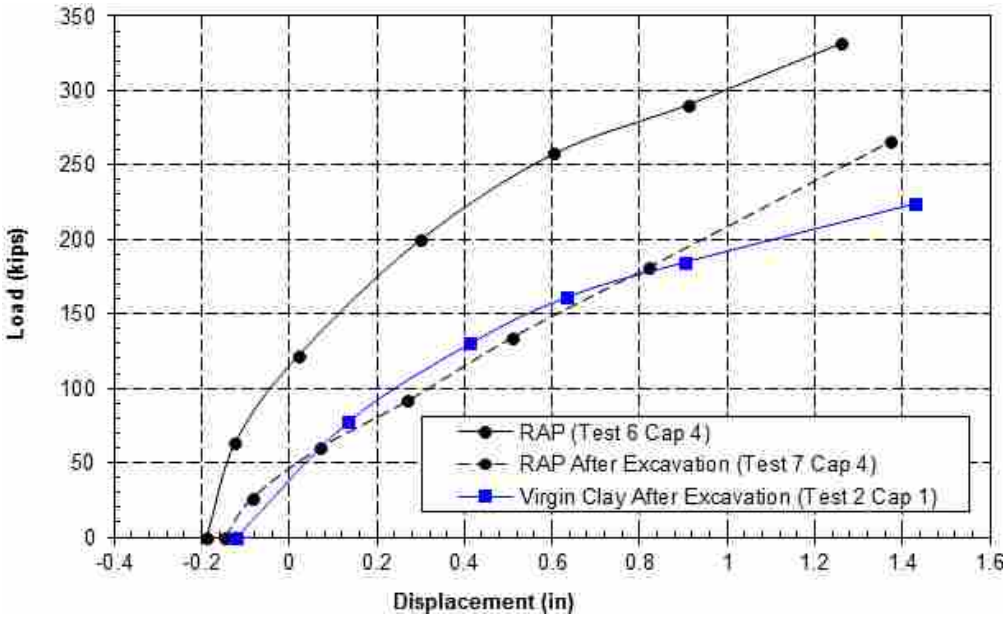

Figure 10-24 Load-Displacement comparison of RAP with and without soil against the face of the pile cap, also showing virgin clay without clay against the pile cap face

than the passive force (54 kips) obtained when clay alone was acting against the pile cap. This result indicates that most of the increased resistance provided by the RAP columns noted in previous comparisons was a result of increased passive force against the pile cap. This result

seems consistent based on the results of previous soil improvement tests in which little improvement in lateral pile resistance was achieved unless the soil improvement extended to the face of the piles (see Herbst 2008, Adsero 2008). The increase of 31 kips in the passive force alone represents about 57 percent of the passive resistance provided by the clay alone. By extrapolating the two RAP curves in Figure 10-24 to 1.5 inches of pile cap displacement, the passive resistance drops significantly to approximately 50 kips.

10.3.2 Load versus Pile Head Rotation Comparison

Figure 10-25 demonstrates the expected trend of decreased rotation with increased pile cap support. At 280 kips, the RAPs offered a decrease in rotation of about 0.3 degrees or 65

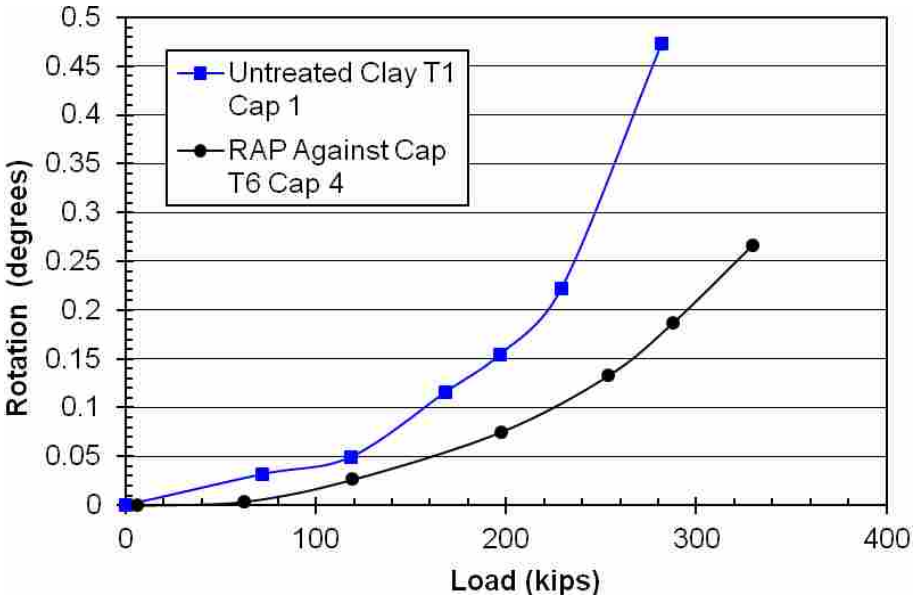

Figure 10-25 Load versus rotation comparison of virgin clay and RAP with soil against the face of the pile cap

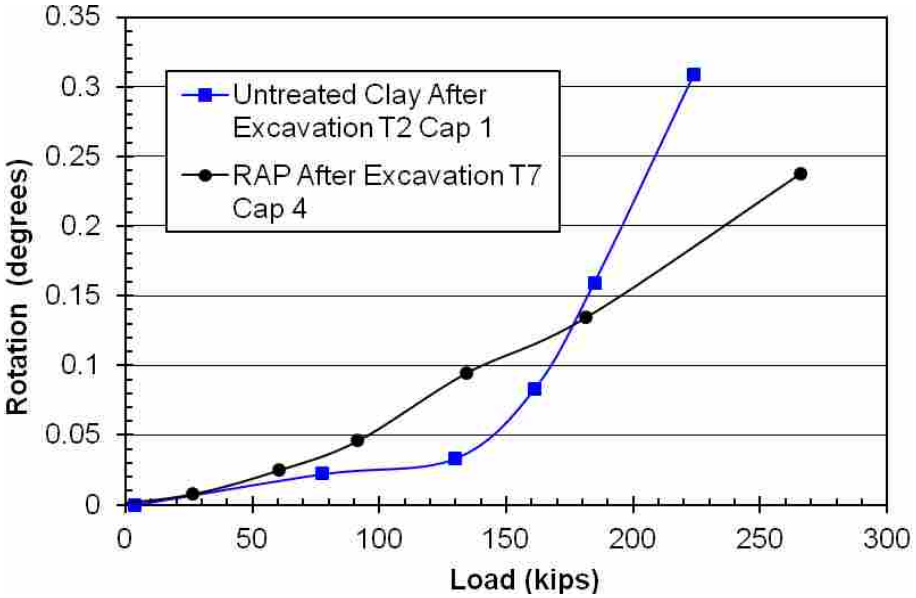

Figure 10-26 Load versus rotation comparison of virgin clay and RAP without soil against the face of the pile cap

percent. The curves in Figure 10-26 do not generally show the expected trend. However, at higher loads, Test 7 does decrease with respect to Test 2. The linear nature of the rotation curve denotes that the resistance to rotation was more pile based rather than soil based, possibly due to reloading effects. At 225 kips, there was a decrease in rotation of 0.13° or 41 percent.

10.3.3 Moment versus Load Comparisons

Figure 10-27 and Figure 10-28 show selected load versus moment relationships for the virgin clay test (Test 1) and RAP test (Test 6) involving passive pressure. Figure 10-27 shows the maximum negative moments and Figure 10-28 shows the maximum positive moments. The moment data from Test 6 appears to plot about equal to slightly lower than the moments from Test 1. The positive moments from Test 6 plot generally with the moments from Test 1, with the majority of the moments concentrated at the lower end. The negative moments show a rough trend toward the middle-to-low end of the moment from Test 1. As explained in section 10.3.1,

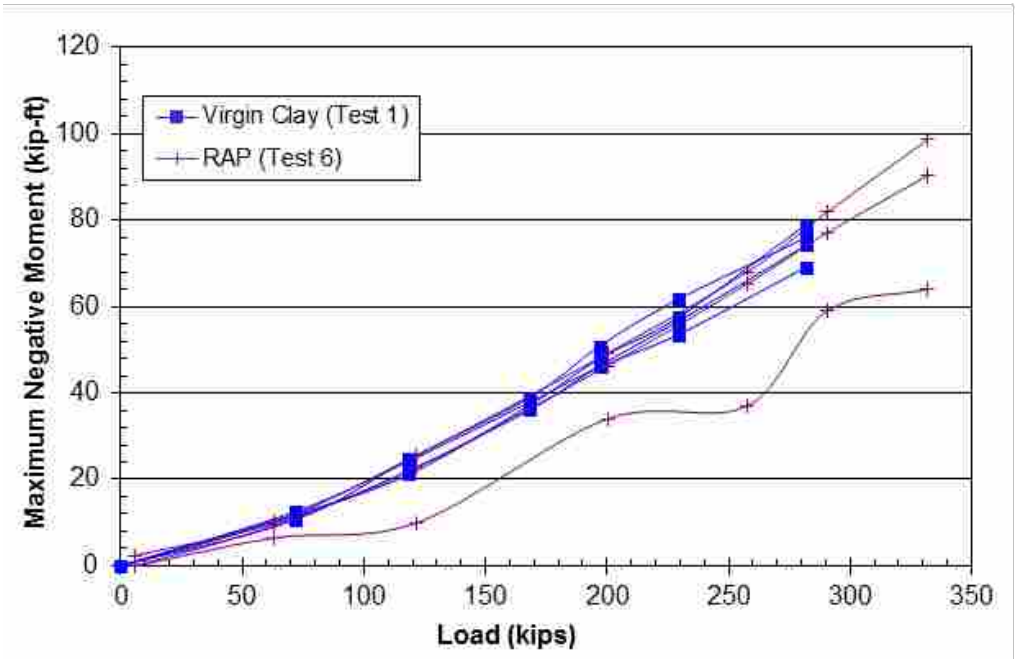

Figure 10-27 Selected load versus maximum negative moment comparison for virgin clay and RAPs with soil against the pile cap face

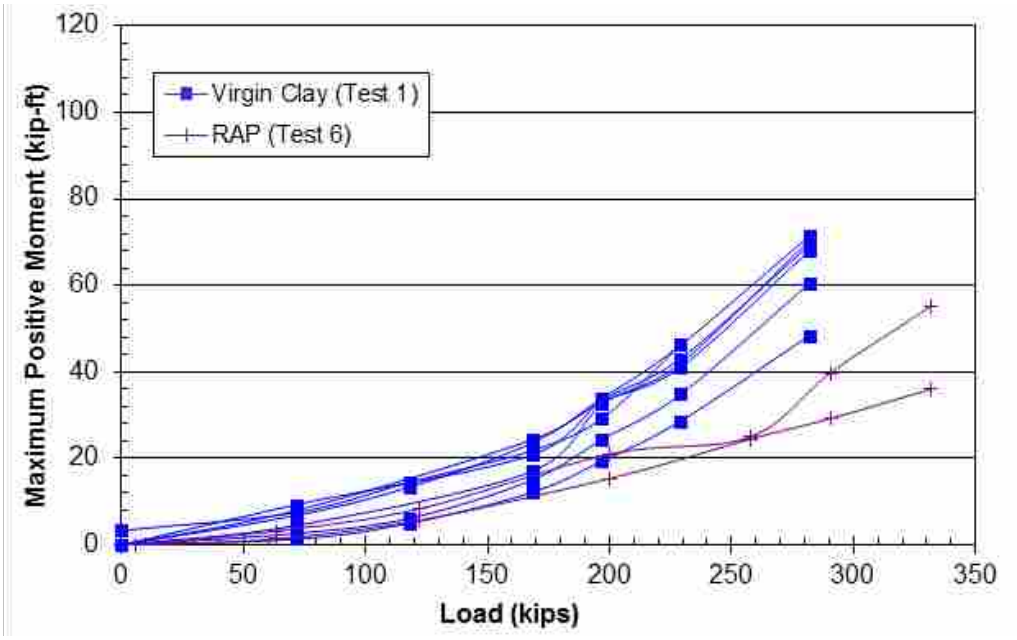

Figure 10-28 Selected load versus maximum positive moment comparison for virgin clay and RAPs with soil against the pile cap face

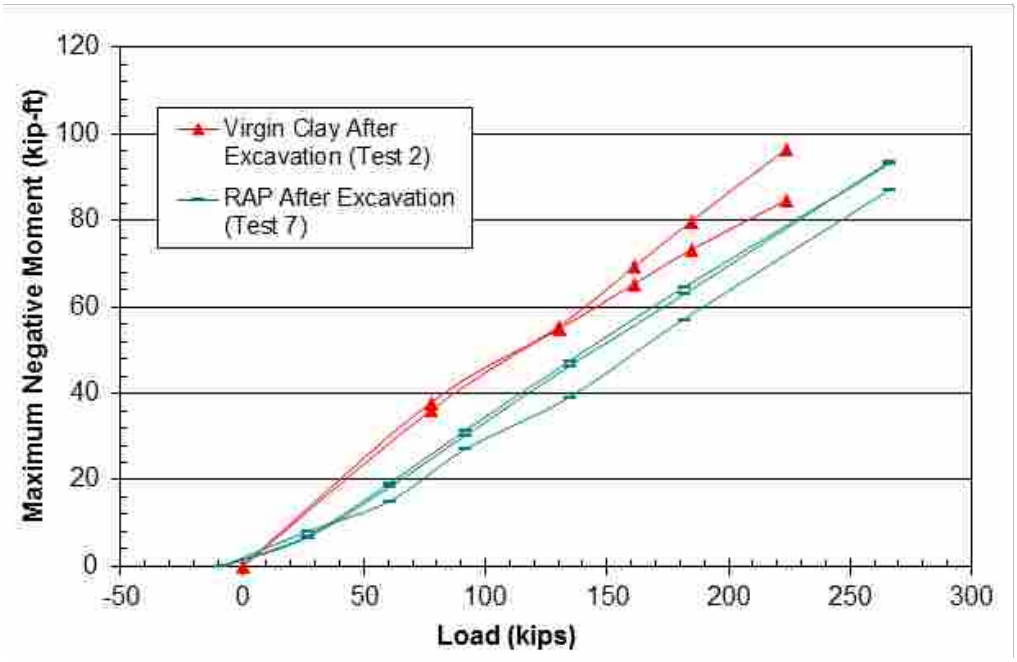

Figure 10-29 Selected load versus maximum negative moment comparisons for virgin clay and RAPs after excavation of soil from against the pile cap face

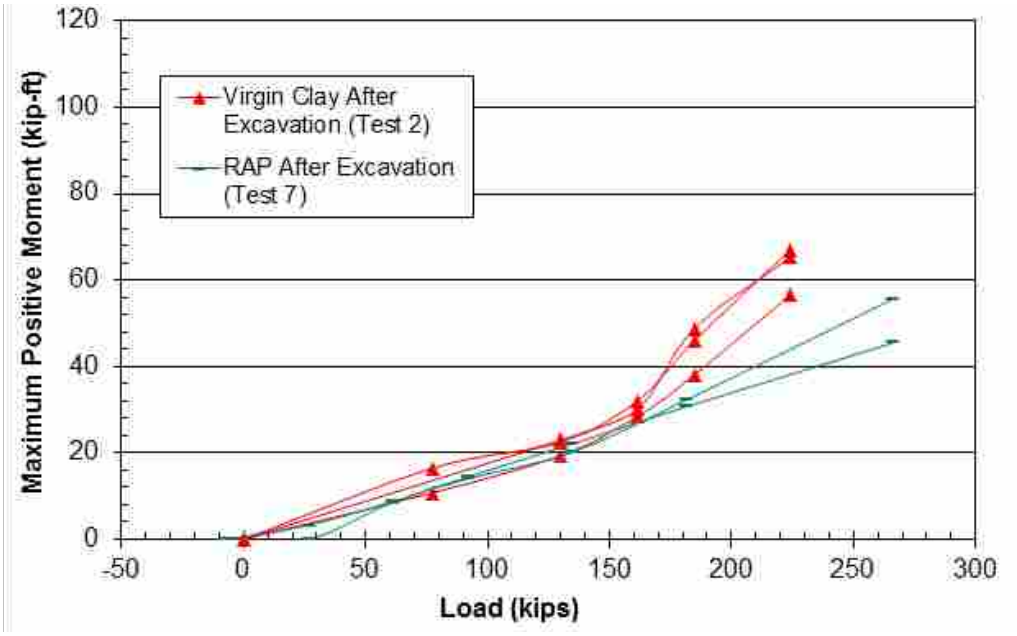

Figure 10-30 Selected load versus maximum positive moment comparisons for virgin clay and RAPs after excavation of soil from against the pile cap face

most of the increase in resistance shown in these curves is most likely due to the compacted fill under the pile cap.

Figure 10-29 and Figure 10-30 show selected load versus moment relationships for the virgin clay test (Test 2) and RAP test (Test 7) that do not involve passive pressure on the pile cap. Figure 10-29 shows the maximum negative moments and Figure 10-30 shows the maximum positive moments. The negative and positive moment curves for Test 2 tend to plot slightly higher than those from Test 7. As with the RAP test (Test 6) as compared to the virgin clay test (Test 1) with passive resistance on the pile cap, it appears that there is a slight increase in resistance in the RAP test without passive resistance as compared to the virgin clay test without passive resistance on the pile cap. The majority of the increase is most likely due to the compacted fill underneath cap 4.

The maximum negative and positive moments from RAPs before (Test 6) and after excavation of the soil from the face of the pile cap (Test 7) are compared in Figure 10-31 and Figure 10-32, respectively. Figure 10-31 shows that the negative moments from Test 6 generally

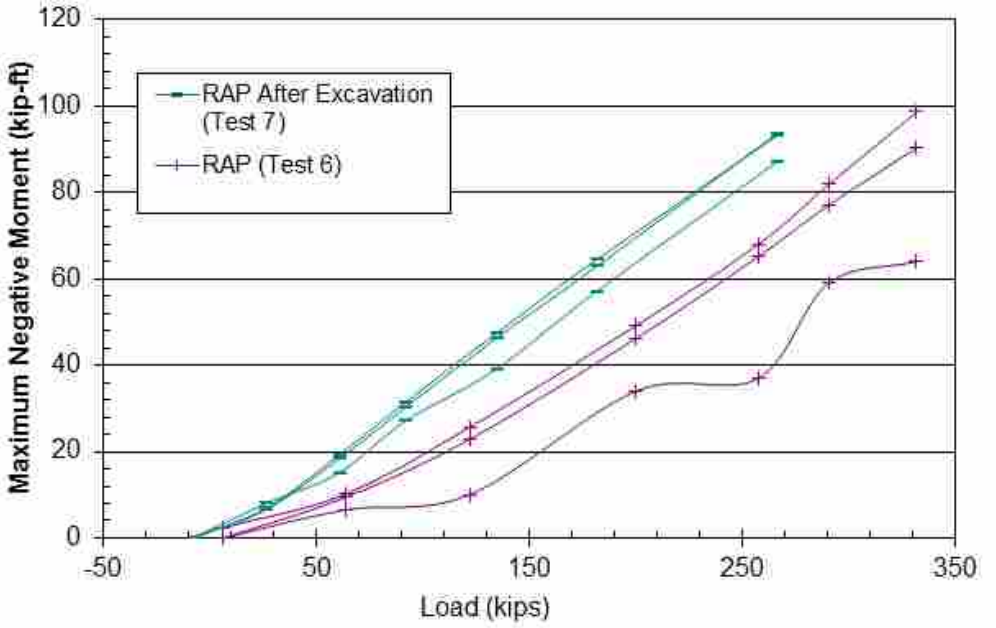

Figure 10-31 Selected load versus maximum negative moment comparisons for RAPs before and after excavation of soil from the face of the pile cap

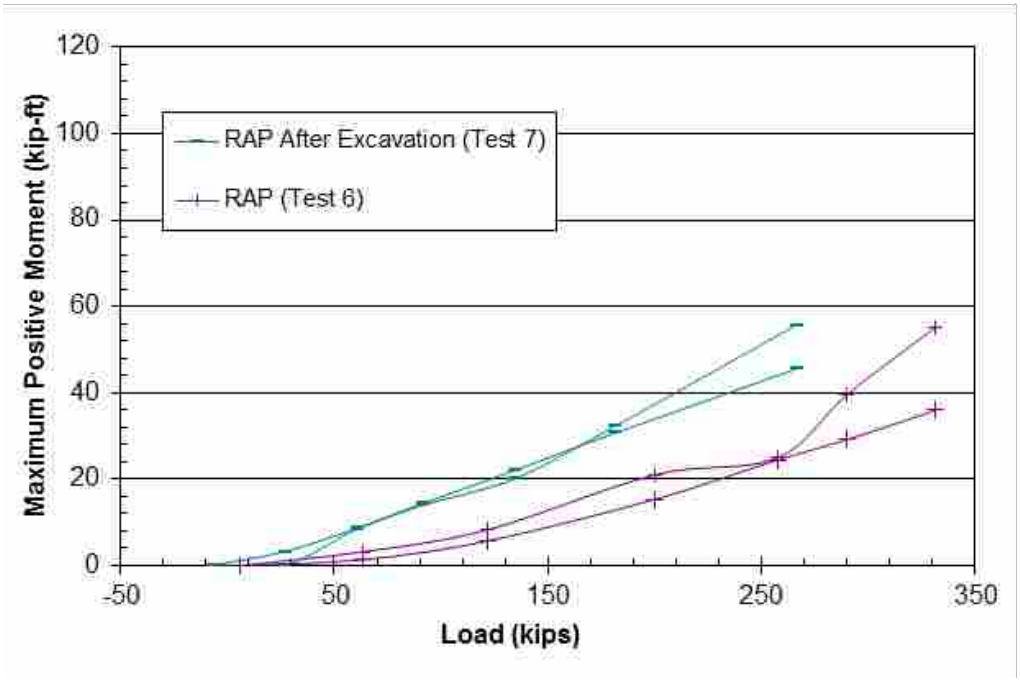

Figure 10-32 Selected load versus maximum positive moment comparisons for RAPs before and after excavation of soil from the face of the pile cap

plot lower than those from Test 7. This follows the trend that would be expected as the pile cap in Test 6 is supported by the passive resistance from the compacted fill while in Test 7 it is not.

10.4 Cost Comparisons

It was observed that compacting fill adjacent to a deep pile foundation increased the lateral resistance of the pile group by 50 kips, while installing RAPs adjacent to the pile cap increased the lateral resistance by about the same nominal amount. The cost of increasing the lateral resistance due to improving the soil as discussed in this document needs to be quantified to determine whether it is a cost-effective solution for increasing lateral resistance. To do this, an estimate of the cost of excavation and compaction of fill and of the installation of RAPs will be given along with an estimate of an equivalent structural retrofit.

Compacted fill retrofitting is typically the cheapest means of increasing the strength of an area of soil. The fill that was used in this research was washed concrete sand that sells for about

$15 to $20/ton with a delivery charge from $115 to $225 for 45 tons of material. This material is not a typical backfill material; typical materials would likely cost notably less. While this is not the least expensive backfill, it allowed for uniform compaction. Because the work of excavation and compaction was done by students, the cost was much lower than if the fill were being installed professionally. An estimate of the cost for excavation and compaction in actual costs is approximately $10 to $12/yd^3. For this project, an area of 9 ft wide by 14 ft long by 6 ft deep was filled with sand to an average dry unit weight of 111 pcf. This required a total of 45 tons of washed concrete sand. The material cost alone would be anywhere from $675 to $900. The excavation and compaction cost would range from $300 to $400. All of this considered, the total cost for compacted fill in a project like the one described herein would be in the range from $1100 to $1500. A summary of the costs involved in compacting fill as a soil retrofit is presented in Table 10-2.

Table 10-2 Summary of costs associated with retrofitting the existing foundation in this project with compacted fill

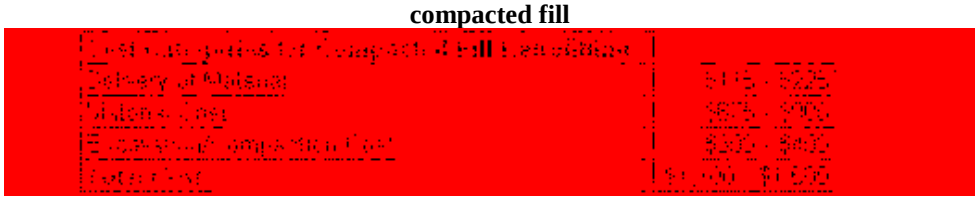

Rammed Aggregate Piers (RAPs) are a more expensive, but less labor-intensive means of retrofitting a pile group to increase lateral resistance. For small projects, the cost associated with mobilizing equipment and qualified operators to a particular site is the prohibiting factor. Included in these costs are mobilization and demobilization of equipment and operators to a site, as well as equipment set-up and tear-down. The cost involved in equipment mobilization to and from the site in this project was about $1,600. Drilling was contracted out to GeoDrill and the combined cost of drilling and equipment rental came to $3,900. The aggregate used in the RAPs

cost $1,300. One day of labor cost the project $2,400. The total cost for the RAP portion of this project was $9,200, but the cost would increase by 35 percent in a typical commercial project of this size. In most typical projects, more RAPs are installed, allowing for greater distribution of the mobilization costs. A summary of the costs involved in installing RAPs as a means of laterally retrofitting the existing pile cap from this project may be found in Table 10-3 (Plehn 2008).

One common method used to increase the lateral capacity of bridge abutment and bent foundations is to add more piles to the ones that are already installed and extend the pile cap to accommodate them. According to the results from pile cap 1 in Tests 2, the nine-pile group used

Table 10-3 Summary of costs associated with retrofitting the existing foundation in this project with Rammed Aggregate Piers

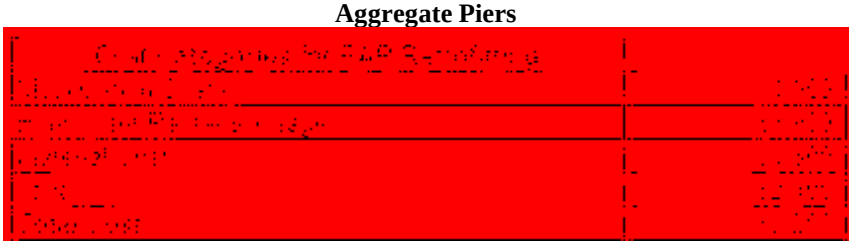

in this project was able to resist about 230 kips of lateral force with 1.5 inches of deflection. If each pile carried an evenly distributed amount of that load, each pile would carry about 26 kips. In order to reach the 269 to 297 kips of capacity attained using compacted fill, 2 or 3 additional piles would need to be driven and attached. In the case of the RAPs, in order to reach the 285 to 335 kips, 2 to 4 piles in addition to the nine existing piles would need to be driven and attached. These piles could be driven in a line in front of the existing 3x3 pile group.

During this study, the material cost for steel pipe piles was about $30/ft. Assuming 80 ft piles, 2-4 additional piles would cost $4,800 to $9,600. Mobilization cost for the pile driving equipment and to bring the piles to the site range from $15,000 to $20,000. Pile-driving costs in

the Utah area are approximately $45 per ft of driven pile (UDOT 2007), adding an additional $2000 to $4000 to the cost to drive the piles. Reinforced concrete (including the cost of steel and concrete) was approximately $300/yd^3 for this project. Approximately 5 to 10 yd^3 of concrete would be needed to fill the additional piles, which would cost about $1,500 to $3,000 in steel and concrete to reinforce inside the piles.

Assuming that the same 3 ft center-to-center spacing for the piles, the dimensions of the new pile caps would be 6 ft by 3 ft by 2.5 ft for the two piles and 12 ft by 3 ft by 2.5 ft for the four piles. This equates to pile cap volumes of between 2 yd^3 and 3.33 yd^{3}of additional concrete and steel. The cost of the reinforced concrete for the pile cap would be on the order of $600 for the two pile extension and $1,000 for the four pile extension. The total estimated cost for a structural retrofit to equal the increase in lateral pressure from using compacted fill or RAPs would be between $29,000 and $48,000 (Adsero 2008). A summary of the costs involved in driving additional piles is found in Table 10-4.

Table 10-4 Summary of costs associated with structurally retrofitting the existing foundation for this project to achieve a comparable strength gain with compacted fill or RAPs

Cost Categories for Structural Retrofit by Driving Additional Piles and Extending the Pile Cap	2 pile extension	3 pile extension	4 pile extension
Mobilization Costs	$15,000 - $20,000	$15,000 - $20,000	$15,000 - $20,000
Steel Cost for Piles	$4,800	$7,200	$9,600
Driving Cost for Piles	$1,920	$3,000	$3,900
Reinforcement Cost for Piles	$1,500	$2,000	$3,000
Pile Cap Extension Cost	$500	$750	$1,000
Total Cost	$29,000 - 34,000	$36,000 - $41,000	$43,000 - $48,000

Compared to a compacted fill retrofit using washed concrete sand, the addition of piles to the existing pile cap would be a more effective retrofit in the clay encountered at the test site. The great majority of the strength gain obtained from using compacted fill was due to increased soil-pile interactions or increased base shear due to the soil compacted underneath the pile cap. Other backfill material may give increased resistance to lateral loads, but with the backfill used

in this test, installation of compacted fill does not appear to be a very effective retrofit method. If a more competent material could be compacted in such a way that a significant increase in lateral resistance is measured, it may provide a very inexpensive alternative to driving additional piles. Compacted fill would cost on the order of $2,000 whereas driving additional piles would cost at least $41,000. If comparable capacity could be achieved, a savings of $39,000 could be realized. If greater strength gain is required, the structural retrofit would be a good alternative, but for the range described herein, compacted fill of a higher density and with a more well-graded composition is worth researching further simply based on the potential cost savings.

Compared to the installation of RAPs, the addition of piles to the existing pile cap would be a more expensive retrofit in soft clays. While very little to no increase in passive resistance was demonstrated in the tests, installing the RAPs may have slightly densified the fill under the pile cap, thereby increasing the lateral resistance. Installing RAPs is cheaper than retrofitting the through driving additional piles, which would cost from $29,000 to $48,000, whereas the RAP retrofit would only cost around $10,000. A savings of around $19,000 to $38,000 could be realized if the resulting strength increase due to installing the RAPs is sufficient to meet the potential demands on the structure. The minimal strength increase observed in this study does not justify the use of RAPs as a means to retrofit an existing pile cap for additional lateral capacity. Additional testing should be performed if RAPs are to be used to retrofit pile caps for increased lateral capacity.

11 CONCLUSIONS

In light of the findings in this thesis the following conclusions can be made with regards to using compacted fill and rammed aggregate piers (RAPs) as soil improvement methods to increase the lateral resistance of deep foundations in soft, cohesive soils. Table 11-1 summarizes the total load at 1.5 inches of pile cap displacement and the developed passive resistance for each of the tests performed. For those tests that did not reach 1.5 inches of displacement, the load trend of the load displacement curve was observed and extended to 1.5 inches to determine a reasonable comparison value.

Table 11-1 Summary of maximum resistance results and quantified improvements

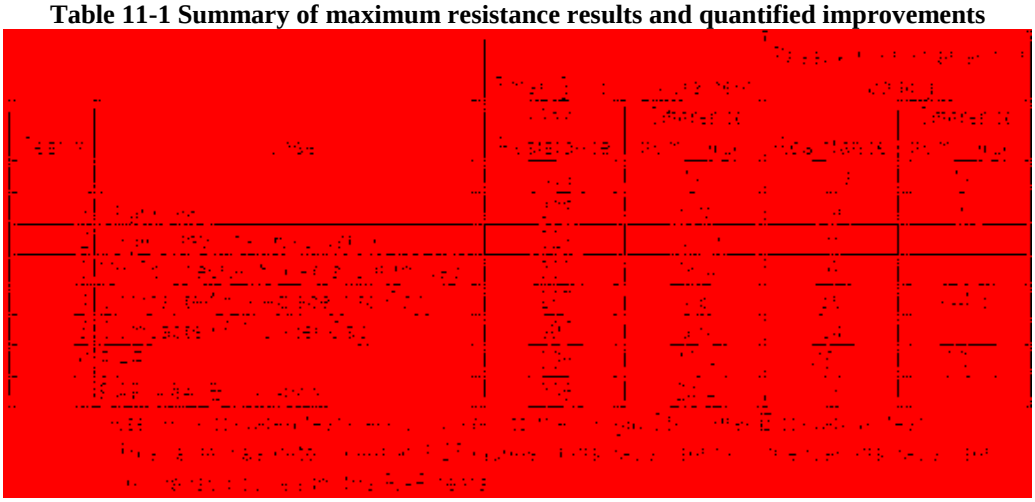

- Excavating soft clay to a depth of 2.5 ft (2.35 pile diameters) and replacing it with dense sand around a group of 9 piles provided relatively small increases in lateral resistance. For example the increase was only 24 kips or 11% when the dense

sand terminated at the edge of the pile cap and 38 kips or 16% when the dense sand extended 5 ft beyond the edge of the pile cap. These increases are in general agreement with results from available full-scale field tests (Rollins et al 2010, Brown et al 1987, and Brown et al 1988). Greater increases in resistance could be expected if the soil being replaced was softer and if excavation and replacement took place to a greater depth.

- Excavation of the clay adjacent to the pile cap (2.5 ft depth) and replacement with compacted sand to a distance of 5 ft beyond the cap actually reduced the passive force from a value of 54 kips for the clay to 30 kips for the sand backfill. This result occurred because the clay was relatively strong due to desiccation. If the entire surface clay layer had been excavated and replaced with sand, the passive force would still have only been 47.5 kips. Excavation and replacement would have been beneficial if the clay had been weaker (c_u < 600 psf) or if the pile cap and sand layer had been deeper so that effective stresses were higher. Furthermore, a compacted gravel backfill would likely have produced somewhat greater resistance due to its increased unit weight.
- Installation of a group of 13 Rammed Aggregate Piers adjacent to an existing pile cap (9 ft square and 2.5 ft deep) also provided a relatively small increase in lateral resistance. For example, the increased lateral resistance provided by the RAP columns alone (determined by removing the increased resistance from the compacted fill under the pile cap) was only about 28 kips or about 10 percent relative to the untreated virgin clay at a displacement of 1.5 inches.

- Subsequent testing of the RAPs, after excavation adjacent to the pile cap indicates that essentially all of the increased lateral resistance provided by the RAP columns was a result of increased passive resistance against the pile cap and that a smaller portion of the increase was produced by soil-pile interaction.
- Increased lateral resistance from placement of compacted fill and RAP columns also lead to increased rotational stiffness of the pile cap and reduced rotations for a given load. This increased rotational stiffness generally had the effect of reducing the maximum bending moments which developed in the piles. This effect was more pronounced for the maximum negative moment at the base of the pile cap than for the maximum positive moment which occurred at depth below the cap.
- Excavating soft clay and replacing it with compacted fill can provide a cost-effective means of increasing the lateral resistance of pile groups relative to installing additional piles. However, it should be noted that the cost savings are largely associated with mobilization costs for the pile driving equipment and this cost may become a smaller percentage of the overall cost for larger projects. In addition, it should be recognized that with using these ground improvement strategies the increased lateral resistance is limited to relatively small values. If substantial increases in lateral resistance are needed, it will likely be necessary to provide additional piles despite the higher costs associated with this alternative.

REFERENCES

Adsero, M. (2008). "Effect of Jet Grouting on the Lateral Resistance of Soil Surrounding Driven-Pile Foundations." M.S. Thesis, Civil & Environ. Engrg. Dept., Brigham Young University, Provo, Utah.

Briaud, J.L. and Miran, J. (1992). *The Cone Penetrometer Test, Report FHWA-SA-91043*, Federal Highway Administration, Washington, D.C, 166 p.

Brinch-Hansen, J. (1966). "Resistance of a rectangular anchor slab." *Bulletin No. 21*, Danish Geotechnical Institute, Copenhagen, 12–13.

Brown, D.A., Reese, L.C., and O'Neill, M.W. (1987). "Cyclic lateral loading of a large-scale pile group," J. of Geotech. Engrg. ASCE, 113(11), 1326-1343.

Brown, D.A., Morrison, C., and Reese, L.C., (1988). "Lateral load behavior of a pile group in sand." J. Geotech. Engrg., ASCE, 114(11), 1261-1276.

Duncan, J. M. and Mokwa, R. M. (2001). "Passive earth pressures: theories and tests." Journal of Geotechnical and Geoenvironmental Engineering, ASCE Vol. 127, No. 3, pp. 248-257.

Fitzpatrick, B.T. (2002). "Soil Reinforcement: 'The alternative to deep foundations.'" Brochure. <http://www.helicaldrilling.com/brochures/geopierbrochure.pdf> Accessed 20 May 2008.

Geopier Foundation Company (2010). "Rammed Aggregate Pier System: Vertical Ramming Makes the Difference: Project Summaries." <http://www.geopier.com/index.asp?id=29> Accessed 16 August.

Herbst, M. (2008). "Impact of Mass Mixing on the Lateral Resistance of Driven-pile Foundations". M.S. Thesis, Civil & Environ. Eng. Dept., Brigham Young University, Provo, Utah.

Higbee, J. (2007). Personal communication.

Lawton, E. C. (1999). "Performance of Geopier Foundations During Simulated Seismic Tests on I-15 Bridge Bents." 34th Symposium on Engineering Geology and Geotechnical Engineering, Logan, Utah, April, 25

Lawton, E. C. and Merry, S. M. (2000). “Performance of Geopier-Supported Foundations during Simulated Seismic Tests on Northbound Interstate 15 Bridge over South Temple, Salt Lake City, Utah”, Final Report, *Report No. UUCVEEN 00-03*, University of Utah, Salt Lake City, Utah, 73pp.

Miner, D.D. (2009). “The Effect of Flowable Fill on the Lateral Resistance of Soil Surrounding Driven-Pile Foundations” M.S. Thesis, Civil &Environ. Eng. Dept., Brigham young University, Provo, Utah.

Mokwa, R. L. and Duncan J. M. (2001). “Experimental evaluation of lateral-load resistance of Pile Caps.” J. Geotech. Geoenviron. Eng., ASCE, Vol. 127, No. 2, pp. 185-192.

Plehn, D. (2008) Personal communication. 14 May.

Rollins, K.M. and Anderson, J.K. (2004). “Performance of Vertical GeoComposite Drains Based on Full-Scale Testing at Massey Tunnel, Vancouver, B.C.”

Rollins, K.M. and Cole, R.T. (2006). “Cyclic Lateral Load Behavior of a Pile Cap and Backfill.” J. Geotechnical and Geoenvironmental Engrg., ASCE, Vol. 132, No. 9, 1143-1153.

Rollins, K.M., Hales, L., King, R.Y., Johnson, S.R., Snyder, J.L. (2005). “Lateral Load Testing of Drilled Shafts for Earthquake Conditions.” Proc. GEO Construction Quality Assurance/Quality Control, ADSC, Dallas, Texas, Ed. Bruce, D.A. and Cadden A.W. p. 540-548.

Rollins, K.M., Kwon, K.H., and Gerber, T.M. (2008). “Static and Dynamic Lateral Load Tests on a Pile Cap with Partial Gravel Backfill.” *Procs. Geotechnical Earthquake Engineering and Soil Dynamics Congress IV*, Sacramento, California, ASCE,10 p.

Rollins, K.M., Olsen, R.J., Egbert, J.J., Olsen, K.G., Jensen, D.H., Garrett, B.H. (2003). “Response, analysis, and design of pile groups subjected to static and dynamic lateral loads.” Report No. UT-03.03, Research Div., Utah Dept of Transportation, Salt Lake City, Utah, 523 p.

Utah Department of Transportation (UDOT). (2007) Statewide Average Bid Price Calculation for 2007. <http://www.dot.state.ut.us/main/f?p=100:pg:9479926774499246000:::: T,V:446> Accessed 7 April 2008

Walsh, J.M. (2005). “Full-scale lateral load test of a 3x5 pile group in sand”. M.S. Thesis, Civil & Environ. Engrg. Dept., Brigham Young University, Provo, Utah, 166 p.

Weaver, T.J. and Chitoori, B. (2007). “Influence of Limited Soil Improvement on Lateral Pile Stiffness.” Proc. Geo-Denver, Soil Improvement, (Geotechnical Special Publication 172), ASCE, Reston, VA, CD.

Wissmann, K.J. and N.S. Fox (2000). "Design and analysis of Short Aggregate Piers used to reinforce soils for foundation support." Proceedings, Geotechnical Colloquium, Technical University Darmstadt, Darmstadt, Germany, March 25, 2000.

APPENDIX A CORBEL DESIGN

Figures from Herbst (2008)

A.1 Corbel Specifications and Design Values

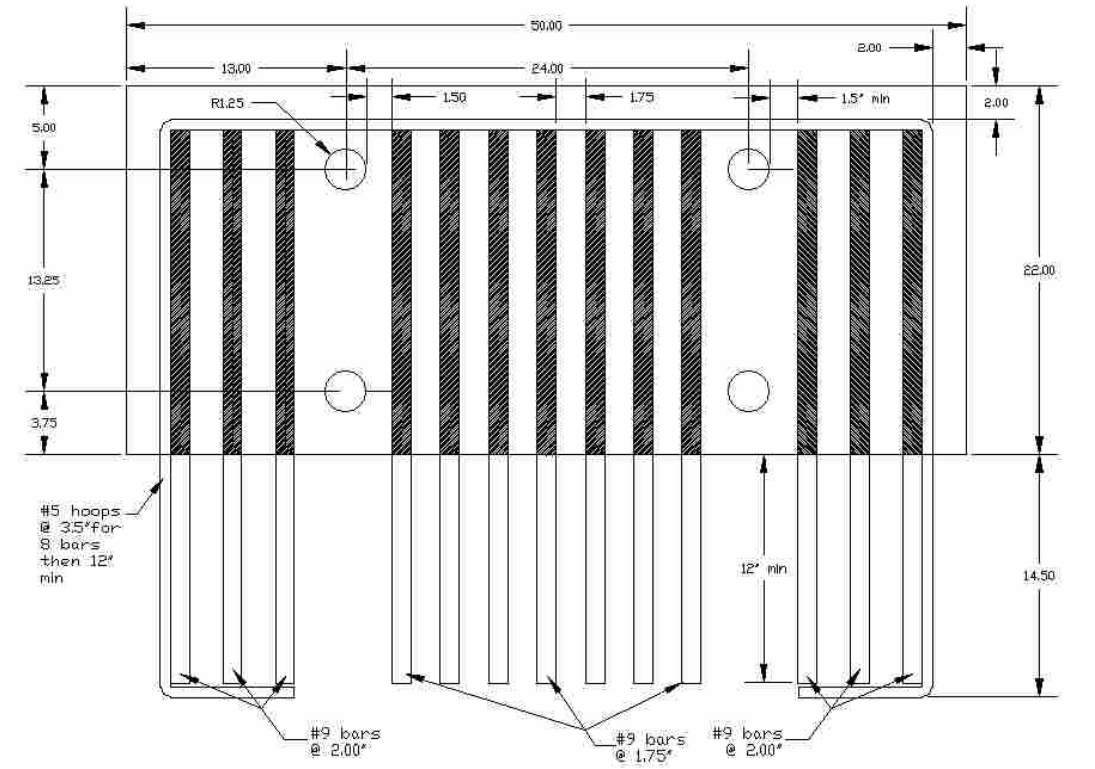

Figure A-1 Front view of the corbel steel where the actuator would connect to the corbel

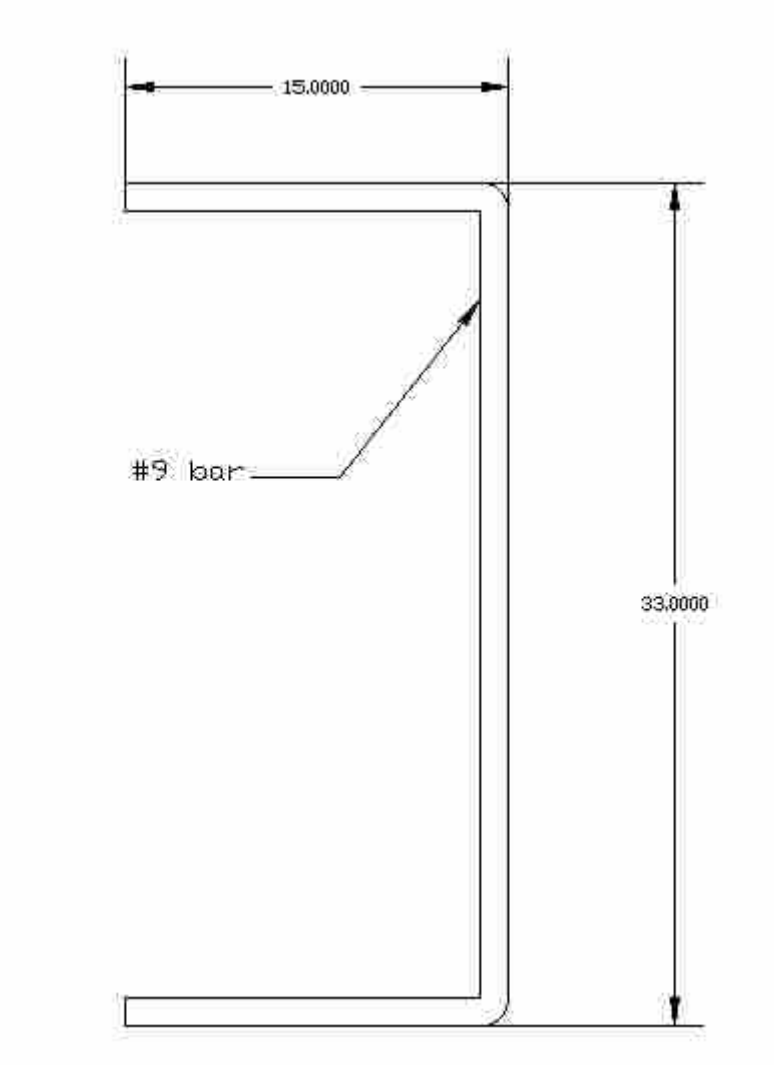

Figure A-2 The #9 bar main reinforcement for the corbel

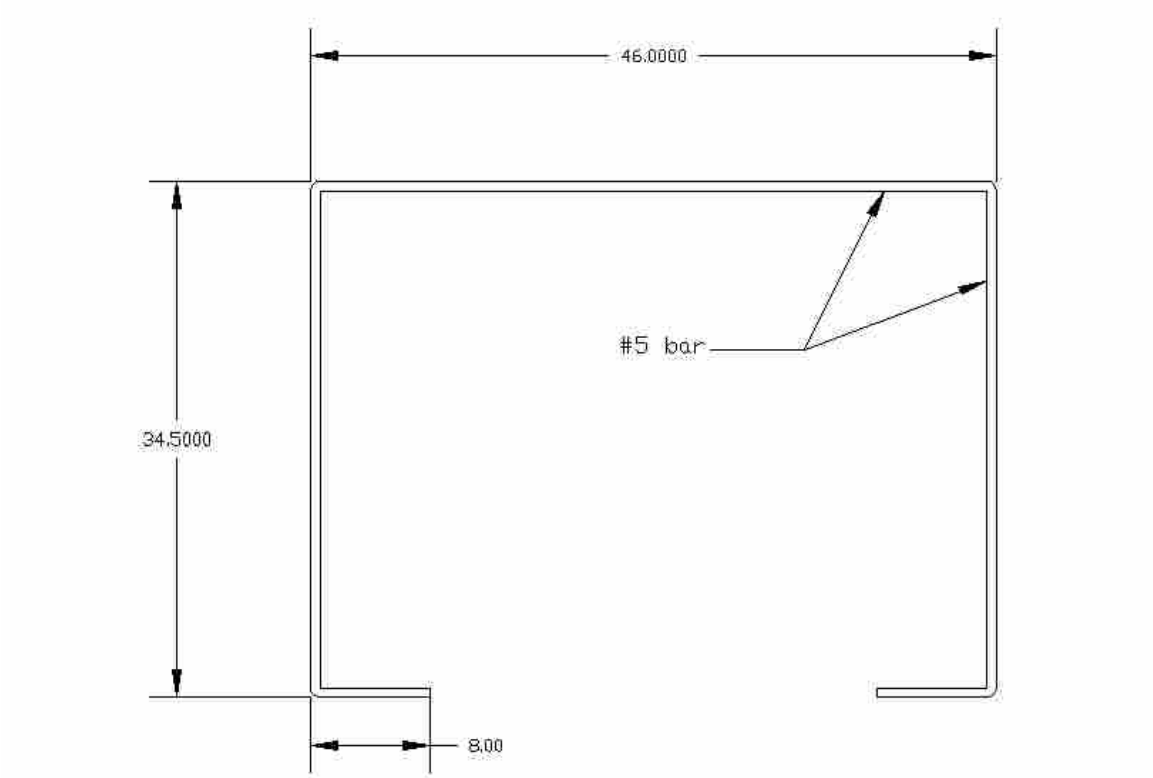

Figure A-3 The transverse or hoop reinforcement for the corbel

Mark Herbst
Corbel Design

Enter Value
Guess or Over Ride
Calculated Value

Parameters		
F'c	5000	psi
Vu (factored)	840	kips
Fy	60000	psi
Bw (guess)	50	inches

Bearing Plate Calcs			
b dim of plate	**30**		
Φ	0.65		
Bstress	2.7625	ksi	
Plate width	10.13574661	inches	try
L dim of plate	**20**	in min	30 x20x1.5 OK
L	**22**		

Depth of Corbel			
Vn(d)	50		
Vn(d)	40		
Used Vn(d)	40		Say
d min	28	inches	**48** in
Φ	0.75		

Forces		
Nuc	168	kips
Av	10.5	in
h	50	in
d	48	
Mu	9156	kip-in
Φ	0.75	

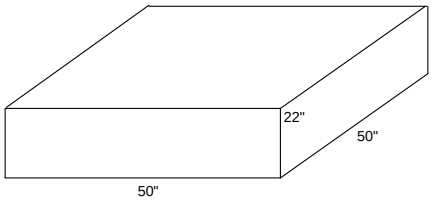

Shear Friction Steel		
λ	1	
Avf	13.33	in^2

Flexural Reinforcement		
Assume	d-a/2 = .9d	
Af	4.71	in^2
recompute a	1.33	
recompute Af	4.30	
An	3.733333333	in^2

Tension Tie Reinforcment	
Asc1	8.03
Asc2	12.62222222
Ascmin	8
	12.62

Bar Sizes	Area in^2	Diameter in	# Bars	Area	Total DofA: w/#4 stirup	Spacing Cl	1 row clearance
3	0.11	0.378	115	12.6500	44.47	117	-111.47
4	0.2	0.5	64	12.8000	33	66	-49
5	0.31	0.625	41	12.7100	26.625	43	-19.625
6	0.44	0.75	29	12.7600	22.75	31	-3.75
7	0.6	0.875	22	13.2000	20.25	24	5.75
8	0.79	1	16	12.6400	17	18	15
9	1	1.128	13	13.0000	15.664	16.536	17.8
10	1.27	1.27	10	12.7000	13.7	14.43	21.87
11	1.56	1.41	9	14.0400	13.69	14.28	22.03
14	2.25	1.693	6	13.5000	11.158	11.465	27.377
18	4	2.257	4	16.0000	10.028	9.771	30.201

Size	#Bars	As	Enough Steel
9	13	13	YEP!

Area of Horizontal Stirrups		
Ah	4.44	in^2

Bar Sizes	Area in^2	Diameter in	# Bars	Area	Total DofA: w/#4 stirup	Spacing Cl	1 row clearance
3	0.11	0.378	41	4.5100	16.498	43	-9.498
4	0.2	0.5	23	4.6000	12.5	25	12.5
5	0.31	0.625	15	4.6500	10.375	17	22.625

Size	#Bars	As	Enough Steel
5	8 Double leg	4.96	YEP!

Development Length			
Ldh	10.72	in	say 12
Db	1.128	in	
Reg Ld	62.21	in	5.1845069 ft
α	1.3		
β	1		
γ	1		
λ	1		
12*d	13.536		say 14

Figure A-4 Corbel design calculated values using ACI section 11.9.

APPENDIX B PYCAP ANALYSIS OF COMPACTED FILL

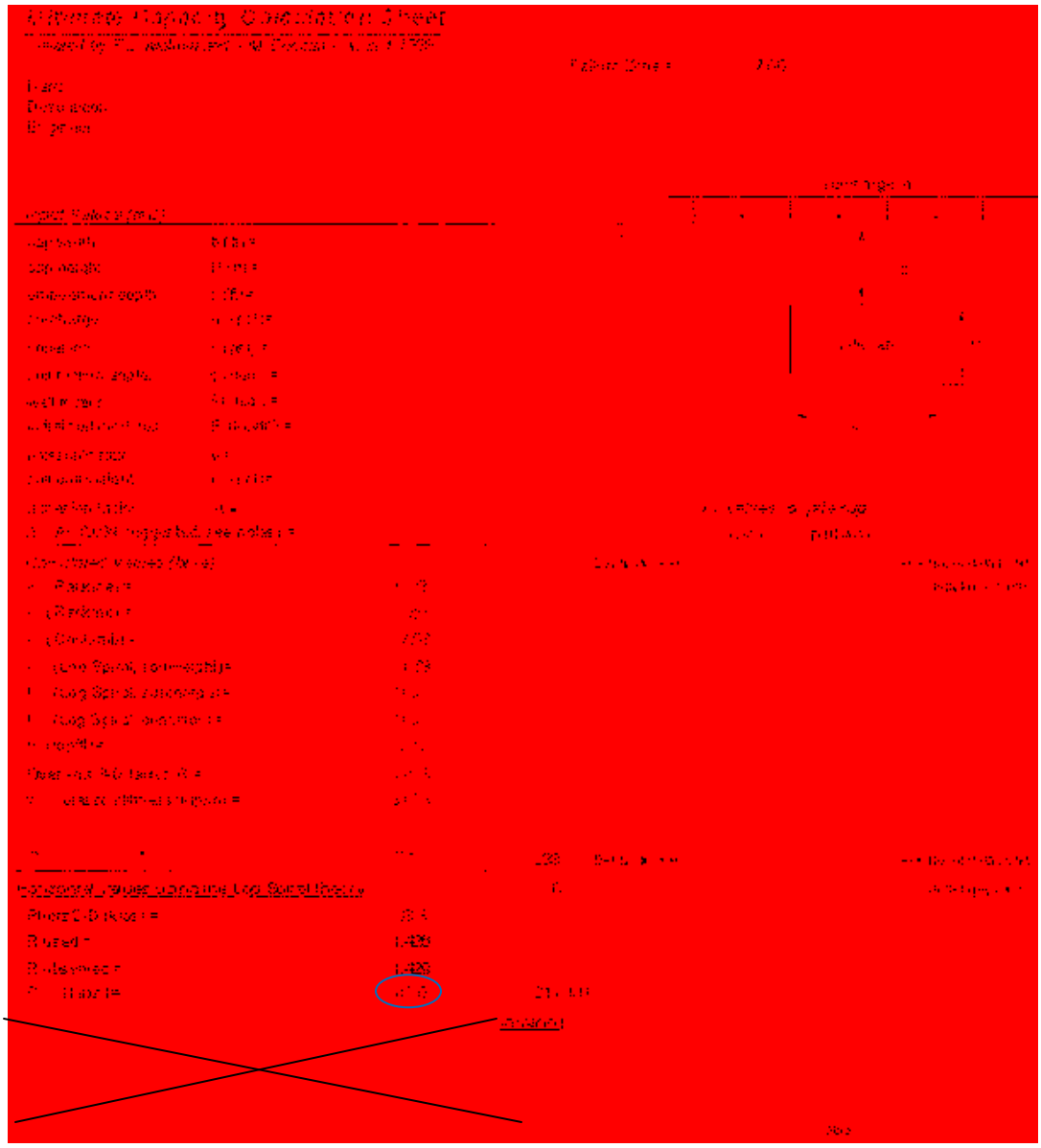

Figure B-1 PYCAP two-dimensional analysis summary for compacted fill